VOLUME: 17 NO: 5 YEAR: 2020

Indexed in PMC and Web of Science
ULAKBİM / TR Dizin, Scopus

ISSN: 1304-530X

TURKISH JOURNAL OF PHARMACEUTICAL SCIENCES

An Official Journal of the Turkish Pharmacists' Association, Academy of Pharmacy

TURKISH
JOURNAL OF PHARMACEUTICAL SCIENCES

TURKISH
JOURNAL OF PHARMACEUTICAL SCIENCES

TURKISH JOURNAL OF PHARMACEUTICAL SCIENCES

AIMS AND SCOPE

The Turkish Journal of Pharmaceutical Sciences is the only scientific periodical publication of the Turkish Pharmacists' Association and has been published since April 2004.
Turkish Journal of Pharmaceutical Sciences journal is regularly published 6 times in a year (February, April, June, August, October, December). The issuing body of the journal is Galenos Yayinevi/Publishing House level.
The aim of Turkish Journal of Pharmaceutical Sciences is to publish original research papers of the highest scientific and clinical value at an international level. The target audience includes specialists and professionals in all fields of pharmaceutical sciences.
The editorial policies are based on the "Recommendations for the Conduct, Reporting, Editing, and Publication of Scholarly Work in Medical Journals (ICMJE Recommendations)" by the International Committee of Medical Journal Editors (2013, archived at http://www.icmje.org/) rules.

Editorial Independence

Turkish Journal of Pharmaceutical Sciences is an independent journal with independent editors and principles and has no commerical relationship with the commercial product, drug or pharmaceutical company regarding decisions and review processes upon articles.

ABSTRACTED/INDEXED IN

PubMed Central
Web of Science-Emerging Sources Citation Index (ESCI)
SCOPUS SJR
TÜBİTAK/ULAKBİM TR Dizin
Directory of Open Access Journals (DOAJ)
ProQuest
Chemical Abstracts Service (CAS)
EBSCO
EMBASE
GALE
Index Copernicus
Analytical Abstracts
International Pharmaceutical Abstracts (IPA)
Medicinal & Aromatic Plants Abstracts (MAPA)
British Library
CSIR INDIA
GOALI
Hinari
OARE
ARDI
AGORA
Türkiye Atıf Dizini
Türk Medline
UDL-EDGE
J- Gate
Idealonline
ROOTINDEXING
CABI

OPEN ACCESS POLICY

This journal provides immediate open access to its content on the principle that making research freely available to the public supports a greater global exchange of knowledge.
Open Access Policy is based on the rules of the Budapest Open Access Initiative (BOAI) http://www.budapestopenaccessinitiative.org/. By "open access" to peer-reviewed research literature, we mean its free availability on the public internet, permitting any users to read, download, copy, distribute, print, search, or link to the full texts of these articles, crawl them for indexing, pass them as data to software, or use them for any other lawful purpose, without financial, legal, or technical barriers other than those inseparable from gaining access to the internet itself. The only constraint on reproduction and distribution, and the only role for copyright in this domain, should be to give authors control over the integrity of their work and the right to be properly acknowledged and cited.

CORRESPONDENCE ADDRESS

All correspondence should be directed to the Turkish Journal of Pharmaceutical Sciences editorial board;

Post Address: Turkish Pharmacists' Association, Mustafa Kemal Mah 2147.Sok No:3 06510 Çankaya/Ankara, TURKEY
Phone: +90 (312) 409 81 00
Fax: +90 (312) 409 81 09
Web Page: http://turkjps.org
E-mail: teb@teb.org.tr

PERMISSIONS

Requests for permission to reproduce published material should be sent to the publisher.
Publisher: Erkan Mor
Adress: Molla Gürani Mah. Kaçamak Sok. 21/1 Fındıkzade, Fatih, Istanbul, Turkey
Telephone: +90 212 621 99 25
Fax: +90 212 621 99 27
Web page: http://www.galenos.com.tr/en
E-mail: info@galenos.com.tr

ISSUING BODY CORRESPONDING ADDRESS

Issuing Body : Galenos Yayınevi
Address: Molla Gürani Mah. Kaçamak Sk. No: 21/1, 34093 İstanbul, Turkey
Phone: +90 212 621 99 25 Fax: +90 212 621 99 27
E-mail: info@galenos.com.tr

MATERIAL DISCLAIMER

The author(s) is (are) responsible for the articles published in the JOURNAL. The editor, editorial board and publisher do not accept any responsibility for the articles.

galenos yayınevi

Galenos Publishing House
Owner and Publisher
Derya Mor
Erkan Mor
Publication Coordinator
Burak Sever
Web Coordinators
Fuat Hocalar
Turgay Akpınar
Graphics Department
Ayda Alaca
Çiğdem Birinci
Gülşah Özgül
Finance Coordinator
Sevinç Çakmak

Project Coordinators
Proje Koordinatörü
Duygu Yıldırm
Gamze Aksoy
Gülay Akın
Hatice Sever
Melike Eren
Özlem Çelik
Pınar Akpınar
Rabia Palazoğlu
Saliha Tuğçe Evin
Research&Development
Mert Can Köse
Mevlüde Özlem Akgüney

Publisher Contact
Address: Molla Gürani Mah. Kaçamak Sk. No: 21/1
34093 İstanbul, Turkey
Phone: +90 (212) 621 99 25 **Fax:** +90 (212) 621 99 27
E-mail: info@galenos.com.tr/yayin@galenos.com.tr
Web: www.galenos.com.tr | Publisher Certificate Number: 14521
Printing at: Özgün Basım Tanıtım San. Tic. Ltd. Şti.
Yeşilce Mah. Aytekin Sok. Oto Sanayi Sitesi No: 21 Kat: 2
Seyrantepe Sanayi, Kağıthane, İstanbul, Türkiye
Telefon/Phone: +90 (212) 280 00 09 Sertifika No: 48150
Printing Date: October 2020
ISSN: 1304-530X
International scientific journal published quarterly.

TURKISH
JOURNAL OF PHARMACEUTICAL SCIENCES

INSTRUCTIONS TO AUTHORS

Turkish Journal of Pharmaceutical Sciences journal is published 6 times (February, April, June, August, October, December) per year and publishes the following articles:

• Research articles

• Reviews (only upon the request or consent of the Editorial Board)

• Preliminary results/Short communications/Technical notes/Letters to the Editor in every field of pharmaceutical sciences.

The publication language of the journal is English.

The Turkish Journal of Pharmaceutical Sciences does not charge any article submission or processing charges.

A manuscript will be considered only with the understanding that it is an original contribution that has not been published elsewhere.

The Journal should be abbreviated as "Turk J Pharm Sci" when referenced.

The scientific and ethical liability of the manuscripts belongs to the authors and the copyright of the manuscripts belongs to the Journal. Authors are responsible for the contents of the manuscript and accuracy of the references. All manuscripts submitted for publication must be accompanied by the Copyright Transfer Form [copyright transfer]. Once this form, signed by all the authors, has been submitted, it is understood that neither the manuscript nor the data it contains have been submitted elsewhere or previously published and authors declare the statement of scientific contributions and responsibilities of all authors.

Experimental, clinical and drug studies requiring approval by an ethics committee must be submitted to the JOURNAL with an ethics committee approval report including approval number confirming that the study was conducted in accordance with international agreements and the Declaration of Helsinki (revised 2013) (http://www.wma.net/en/30publications/10policies/b3/). The approval of the ethics committee and the fact that informed consent was given by the patients should be indicated in the Materials and Methods section. In experimental animal studies, the authors should indicate that the procedures followed were in accordance with animal rights as per the Guide for the Care and Use of Laboratory Animals (http://oacu.od.nih.gov/regs/guide/guide.pdf) and they should obtain animal ethics committee approval.

Authors must provide disclosure/acknowledgment of financial or material support, if any was received, for the current study.

If the article includes any direct or indirect commercial links or if any institution provided material support to the study, authors must state in the cover letter that they have no relationship with the commercial product, drug, pharmaceutical company, etc. concerned; or specify the type of relationship (consultant, other agreements), if any.

Authors must provide a statement on the absence of conflicts of interest among the authors and provide authorship contributions.

All manuscripts submitted to the journal are screened for plagiarism using the 'iThenticate' software. Results indicating plagiarism may result in manuscripts being returned or rejected.

The Review Process

This is an independent international journal based on double-blind peer-review principles. The manuscript is assigned to the Editor-in-Chief, who reviews the manuscript and makes an initial decision based on manuscript quality and editorial priorities. Manuscripts that pass initial evaluation are sent for external peer review, and the Editor-in-Chief assigns an Associate Editor. The Associate Editor sends the manuscript to at least two reviewers (internal and/or external reviewers). The Associate Editor recommends a decision based on the reviewers' recommendations and returns the manuscript to the Editor-in-Chief. The Editor-in-Chief makes a final decision based on editorial priorities, manuscript quality, and reviewer recommendations. If there are any conflicting recommendations from reviewers, the Editor-in-Chief can assign a new reviewer.

The scientific board guiding the selection of the papers to be published in the Journal consists of elected experts of the Journal and if necessary, selected from national and international authorities. The Editor-in-Chief, Associate Editors may make minor corrections to accepted manuscripts that do not change the main text of the paper.

In case of any suspicion or claim regarding scientific shortcomings or ethical infringement, the Journal reserves the right to submit the manuscript to the supporting institutions or other authorities for investigation. The Journal accepts the responsibility of initiating action but does not undertake any responsibility for an actual investigation or any power of decision.

The Editorial Policies and General Guidelines for manuscript preparation specified below are based on "Recommendations for the Conduct, Reporting, Editing, and Publication of Scholarly Work in Medical Journals (ICMJE Recommendations)" by the International Committee of Medical Journal Editors (2013, archived at http://www.icmje.org/).

Preparation of research articles, systematic reviews and meta-analyses must comply with study design guidelines:

CONSORT statement for randomized controlled trials (Moher D, Schultz KF, Altman D, for the CONSORT Group. The CONSORT statement revised recommendations for improving the quality of reports of parallel group randomized trials. JAMA 2001; 285: 1987-91) (http://www.consort-statement.org/);

PRISMA statement of preferred reporting items for systematic reviews and meta-analyses (Moher D, Liberati A, Tetzlaff J, Altman DG, The PRISMA Group. Preferred Reporting Items for Systematic Reviews and Meta-Analyses: The PRISMA Statement. PLoS Med 2009; 6(7): e1000097.) (http://www.prisma-statement.org/);

STARD checklist for the reporting of studies of diagnostic accuracy (Bossuyt PM, Reitsma JB, Bruns DE, Gatsonis CA, Glasziou PP, Irwig LM, et al., for the STARD Group. Towards complete and accurate reporting of studies of diagnostic accuracy: the STARD initiative. Ann Intern Med 2003;138:40-4.) (http://www.stard-statement.org/);

STROBE statement, a checklist of items that should be included in reports of observational studies (http://www.strobe-statement.org/);

MOOSE guidelines for meta-analysis and systemic reviews of observational studies (Stroup DF, Berlin JA, Morton SC, et al. Meta-analysis of observational studies in epidemiology: a proposal for reporting Meta-analysis of observational Studies in Epidemiology (MOOSE) group. JAMA 2000; 283: 2008-12).

GENERAL GUIDELINES

Manuscripts can only be submitted electronically through the Journal Agent website (http://journalagent.com/tjps/) after creating an account. This system allows online submission and review.

TURKISH
JOURNAL OF PHARMACEUTICAL SCIENCES

INSTRUCTIONS TO AUTHORS

Format: Manuscripts should be prepared using Microsoft Word, size A4 with 2.5 cm margins on all sides, 12 pt Arial font and 1.5 line spacing.

Abbreviations: Abbreviations should be defined at first mention and used consistently thereafter. Internationally accepted abbreviations should be used; refer to scientific writing guides as necessary.

Cover letter: The cover letter should include statements about manuscript type, single-Journal submission affirmation, conflict of interest statement, sources of outside funding, equipment (if applicable), for original research articles.

ETHICS COMMITTEE APPROVAL

The editorial board and our reviewers systematically ask for ethics committee approval from every research manuscript submitted to the Turkish Journal of Pharmaceutical Sciences. If a submitted manuscript does not have ethical approval, which is necessary for every human or animal experiment as stated in international ethical guidelines, it must be rejected on the first evaluation.

Research involving animals should be conducted with the same rigor as research in humans; the Turkish Journal of Pharmaceutical Sciences asks original approval document to show implements the 3Rs principles. If a study does not have ethics committee approval or authors claim that their study does not need approval, the study is consulted to and evaluated by the editorial board for approval.

SIMILARITY

The Turkish Journal of Pharmaceutical Sciences is routinely looking for similarity index score from every manuscript submitted before evaluation by the editorial board and reviewers. The journal uses iThenticate plagiarism checker software to verify the originality of written work. There is no acceptable similarity index; but, exceptions are made for similarities less than 15 %.

REFERENCES

Authors are solely responsible for the accuracy of all references.

In-text citations: References should be indicated as a superscript immediately after the period/full stop of the relevant sentence. If the author(s) of a reference is/are indicated at the beginning of the sentence, this reference should be written as a superscript immediately after the author's name. If relevant research has been conducted in Turkey or by Turkish investigators, these studies should be given priority while citing the literature.

Presentations presented in congresses, unpublished manuscripts, theses, Internet addresses, and personal interviews or experiences should not be indicated as references. If such references are used, they should be indicated in parentheses at the end of the relevant sentence in the text, without reference number and written in full, in order to clarify their nature.

References section: References should be numbered consecutively in the order in which they are first mentioned in the text. All authors should be listed regardless of number. The titles of Journals should be abbreviated according to the style used in the Index Medicus.

Reference Format

Journal: Last name(s) of the author(s) and initials, article title, publication title and its original abbreviation, publication date, volume, the inclusive page numbers. Example: Collin JR, Rathbun JE. Involutional entropion: a review with evaluation of a procedure. Arch Ophthalmol. 1978;96:1058-1064.

Book: Last name(s) of the author(s) and initials, book title, edition, place of publication, date of publication and inclusive page numbers of the extract cited.

Example: Herbert L. The Infectious Diseases (1st ed). Philadelphia; Mosby Harcourt; 1999:11;1-8.

Book Chapter: Last name(s) of the author(s) and initials, chapter title, book editors, book title, edition, place of publication, date of publication and inclusive page numbers of the cited piece.

Example: O'Brien TP, Green WR. Periocular Infections. In: Feigin RD, Cherry JD, eds. Textbook of Pediatric Infectious Diseases (4th ed). Philadelphia; W.B. Saunders Company;1998:1273-1278.

Books in which the editor and author are the same person: Last name(s) of the author(s) and initials, chapter title, book editors, book title, edition, place of publication, date of publication and inclusive page numbers of the cited piece. Example: Solcia E, Capella C, Kloppel G. Tumors of the exocrine pancreas. In: Solcia E, Capella C, Kloppel G, eds. Tumors of the Pancreas. 2nd ed. Washington: Armed Forces Institute of Pathology; 1997:145-210.

TABLES, GRAPHICS, FIGURES, AND IMAGES

All visual materials together with their legends should be located on separate pages that follow the main text.

Images: Images (pictures) should be numbered and include a brief title. Permission to reproduce pictures that were published elsewhere must be included. All pictures should be of the highest quality possible, in

JPEG format, and at a minimum resolution of 300 dpi.

Tables, Graphics, Figures: All tables, graphics or figures should be enumerated according to their sequence within the text and a brief descriptive caption should be written. Any abbreviations used should be defined in the accompanying legend. Tables in particular should be explanatory and facilitate readers' understanding of the manuscript, and should not repeat data presented in the main text.

MANUSCRIPT TYPES

Original Articles

Clinical research should comprise clinical observation, new techniques or laboratories studies. Original research articles should include title, structured abstract, key words relevant to the content of the article, introduction, materials and methods, results, discussion, study limitations, conclusion references, tables/figures/images and acknowledgement sections. Title, abstract and key words should be written in both Turkish and English. The manuscript should be formatted in accordance with the above-mentioned guidelines and should not exceed 16 A4 pages.

Title Page: This page should include the title of the manuscript, short title, name(s) of the authors and author information. The following descriptions should be stated in the given order:

TURKISH
JOURNAL OF PHARMACEUTICAL SCIENCES

INSTRUCTIONS TO AUTHORS

1. Title of the manuscript (Turkish and English), as concise and explanatory as possible, including no abbreviations, up to 135 characters

2. Short title (Turkish and English), up to 60 characters

3. Name(s) and surname(s) of the author(s) (without abbreviations and academic titles) and affiliations

4. Name, address, e-mail, phone and fax number of the corresponding author

5. The place and date of scientific meeting in which the manuscript was presented and its abstract published in the abstract book, if applicable

Abstract: A summary of the manuscript should be written in both Turkish and English. References should not be cited in the abstract. Use of abbreviations should be avoided as much as possible; if any abbreviations are used, they must be taken into consideration independently of the abbreviations used in the text. For original articles, the structured abstract should include the following sub-headings:

Objectives: The aim of the study should be clearly stated.

Materials and Methods: The study and standard criteria used should be defined; it should also be indicated whether the study is randomized or not, whether it is retrospective or prospective, and the statistical methods applied should be indicated, if applicable.

Results: The detailed results of the study should be given and the statistical significance level should be indicated.

Conclusion: Should summarize the results of the study, the clinical applicability of the results should be defined, and the favorable and unfavorable aspects should be declared.

Keywords: A list of minimum 3, but no more than 5 key words must follow the abstract. Key words in English should be consistent with "Medical Subject Headings (MESH)" (www.nlm.nih.gov/mesh/MBrowser.html). Turkish key words should be direct translations of the terms in MESH.

Original research articles should have the following sections:

Introduction: Should consist of a brief explanation of the topic and indicate the objective of the study, supported by information from the literature.

Materials and Methods: The study plan should be clearly described, indicating whether the study is randomized or not, whether it is retrospective or prospective, the number of trials, the characteristics, and the statistical methods used.

Results: The results of the study should be stated, with tables/figures given in numerical order; the results should be evaluated according to the statistical analysis methods applied. See General Guidelines for details about the preparation of visual material.

Discussion: The study results should be discussed in terms of their favorable and unfavorable aspects and they should be compared with the literature. The conclusion of the study should be highlighted.

Study Limitations: Limitations of the study should be discussed. In addition, an evaluation of the implications of the obtained findings/results for future research should be outlined.

Conclusion: The conclusion of the study should be highlighted.

Acknowledgements: Any technical or financial support or editorial contributions (statistical analysis, English/Turkish evaluation) towards the study should appear at the end of the article.

References: Authors are responsible for the accuracy of the references. See General Guidelines for details about the usage and formatting required.

Review Articles

Review articles can address any aspect of clinical or laboratory pharmaceuticals. Review articles must provide critical analyses of contemporary evidence and provide directions of or future research. Most review articles are commissioned, but other review submissions are also welcome. Before sending a review, discussion with the editor is recommended.

Reviews articles analyze topics in depth, independently and objectively. The first chapter should include the title in Turkish and English, an unstructured summary and key words. Source of all citations should be indicated. The entire text should not exceed 25 pages (A4, formatted as specified above).

TURKISH
JOURNAL OF PHARMACEUTICAL SCIENCES

CONTENTS

TURKISH
JOURNAL OF PHARMACEUTICAL SCIENCES

CONTENTS

PUBLICATION NAME	Turkish Journal of Pharmaceutical Sciences
TYPE OF PUBLICATION	Vernacular Publication
PERIOD AND LANGUAGE	Bimonthly-English
OWNER	Erdoğan ÇOLAK on behalf of the Turkish Pharmacists' Association
EDITOR-IN-CHIEF	Prof.Terken BAYDAR, Ph.D.
ADDRESS OF PUBLICATION	Turkish Pharmacists' Association, Mustafa Kemal Mah 2147.Sok No:3 06510 Çankaya/ Ankara, TURKEY

TURKISH
JOURNAL OF PHARMACEUTICAL
SCIENCES

Volume: 17, No: 5, Year: 2020

CONTENTS

Turk J Pharm Sci 2020;17(5):463-464
DOI: 10.4274/tjps.galenos.2020.13845

LETTER TO EDITOR

The Effect of Therapeutic Plasma Exchange on COVID-19 Therapy

Terapötik Plazma Değişiminin COVID-19 Tedavisine Etkisi

Cansu GÖNCÜOĞLU*, Fatma Nisa BALLI, Aygin BAYRAKTAR EKİNCİOĞLU

Hacettepe University Faculty of Pharmacy, Department of Clinical Pharmacy, Ankara, Turkey

Key words: COVID-19 treatment, therapeutic plasma exchange, drug removal, pharmacokinetic

Anahtar Kelimeler: COVID-19 tedavisi, terapötik plazma değişimi, ilaç itrahı, farmakokinetik

Dear Editor,

The global pandemic caused by the Severe Acute Respiratory syndrome-Coronavirus-2 started in Wuhan, China, in December 2019 and spread throughout the world. It is known that cytokine storms play an important role in acute respiratory distress syndrome and multiorgan dysfunction, which are among the main causes of mortality in Coronavirus Disease-2019 (COVID-19) patients. A cytokine storm is triggered by the secretion of proinflammatory cytokines such as tumor necrosis factor-α; interleukin (IL)-1b, IL-2, IL-6, IL-8, and IL-10; and interferon-γ. An excessive inflammatory response occurs as a result of this triggering, which leads to life-threatening clinical symptoms.[1] It has been shown that therapeutic plasma exchange (TPE) may be effective in suppressing cytokine storms.[2]

The main parameters in evaluating the effect of TPE on drug therapy are the volume of distribution and the affinity of drugs binding to plasma proteins. Drugs with low volumes of distribution (<0.2 L/kg) and high plasma protein binding (>80%) often remain in the intravascular compartment and are likely to be affected by TPE. However, not only those two parameters affect the processes of drug removal by TPE; the half-life (>2 h), endogenous drug clearance (<4 mL/min), hydrophilic/lipophilic properties of the drug, and the time between the onset of TPE and drug intake may also affect the rate of excretion. Drugs with a half-life longer than 2 h and that are slowly metabolized or have a low clearance rate are more likely to be excreted by TPE.[3]

TPE has been shown to increase interferon clearance in patients with hepatitis C-related vasculitis.[4] No studies on the effects of TPE on other drugs used in the treatment of COVID-19 have been found. The pharmacokinetic properties of the drugs used to treat COVID-19 are shown in Table 1. Accordingly, interferon, intravenous immunoglobulin, and lopinavir/ritonavir are likely to be affected by TPE. There are not enough data on favipiravir, oseltamivir, tocilizumab, and remdesivir to allow them to be evaluated; however, considering their low distribution volumes and long half-lives, it can be assumed that they are also removed by TPE. In cases when the drug is likely to be excreted with TPE, it is recommended to change the drug administration time to a time after TPE in order not to disrupt the regular blood concentration of the drug. Thus, with rational drug use, the blood level of the drug may be prevented from being affected by TPE and the patient obtains the maximum effect expected from the drug. Blood levels of drugs should be monitored if possible. Clinicians should always consider and evaluate the pharmacokinetic profiles of drugs when opting for co-administration with other therapeutic options.

*Correspondence: E-mail: cansugoncuoglu@gmail.com, Phone: +90 544 679 92 70 ORCID-ID: orcid.org/0000-0003-1415-4708
Received: 14.08.2020, Accepted: 30.08.2020

Table 1. Pharmacokinetic characteristics of drugs that are used to treat COVID-19

Drug	Volume of distribution	Plasma protein binding	Half-life	References
Hydroxychloroquine	47.257 L	40%	45±15 days	5
Chloroquine	65.000 L	55%	41±11 days	5
Azithromycin	31 L/kg	7-51%	68-72 hours	6
Ribavirin	2825 L	None	24-298 hours	6
Umifenovir	Data not available	Data not available	17-21 hours	7
Methylprednisolone	1.38 L/kg	78%	2.3 hours	8
Oseltamivir	23-26 L	3-42%	1-10 hours	6
Tocilizumab	6.4 L	Data not available	11-13 days	6
Favipiravir	15-20 L	54%	2-5.5 hours	9
Remdesivir	Data not available	Data not available	69 minutes	10
Ritonavir	0.41±0.25 L/kg	98-99%	3-5 hours	6
Lopinavir	Data not available	98-99%	5-6 hours	6
IVIG	0.05±0.13 L/kg	Data not available	14-24 days	6

Not expected to be affected by TPE Suspected to be affected by TPE Likely to be affected by TPE, TPE: Therapeutic plasma exchange

Conflicts of interest: No conflict of interest was declared by the authors. The authors alone are responsible for the content and writing of the paper.

REFERENCES

1. Liu B, Li M, Zhou Z, Guan X, Xiang Y. Can we use interleukin-6 (IL-6) blockade for coronavirus disease 2019 (COVID-19)-induced cytokine release syndrome (CRS)? J Autoimmun. 2020;111:102452.
2. Choi S, Kim MC, Kwon JS, Kim JY, Lee KH, Kim SH. Case Report: use of plasma exchange followed by convalescent plasma therapy in a critically ill patient with severe fever and thrombocytopenia syndrome-associated encephalopathy: cytokine/chemokine concentrations, viral loads, and antibody responses. Am J Trop Med Hyg. 2018;99:1466-1468.
3. Cheng CW, Hendrickson JE, Tormey CA, Sidhu D. Therapeutic Plasma Exchange and Its Impact on Drug Levels: An ACLPS Critical Review. Am J Clin Pathol. 2017;148:190-198.
4. Hausfater P, Cacoub P, Assogba U, Lebon P, Piette JC. Plasma exchange and interferon-alpha pharmacokinetics in patients with hepatitis C virus-associated systemic vasculitis. Nephron. 2002;91:627-630.
5. Schrezenmeier E, Dorner T. Mechanisms of action of hydroxychloroquine and chloroquine: implications for rheumatology. Nat Rev Rheumatol. 2020;16:155-166.
6. Wolters Kluwer UpToDate®. Last accessed date: 20.08.2020. Accessed 20/08/2020. Available from: https://www.uptodate.com/
7. Deng P, Zhong D, Yu K, Zhang Y, Wang T, Chen X. Pharmacokinetics, metabolism, and excretion of the antiviral drug arbidol in humans. Antimicrob Agents Chemother. 2013;57:1743-1755.
8. Szefler SJ, Ebling WF, Georgitis JW, Jusko WJ. Methylprednisolone versus prednisolone pharmacokinetics in relation to dose in adults. Eur J Clin Pharmacol. 1986;30:323-329.
9. Nguyen TH, Guedj J, Anglaret X, Laouenan C, Madelain V, Taburet AM, Baize S, Sissoko D, Pastorino B, Rodallec A, Piorkowski G, Carazo S, Conde MN, Gala JL, Bore JA, Carbonnelle C, Jacquot F, Raoul H, Malvy D, de Lamballerie X, Mentre F, JIKI study group. Favipiravir pharmacokinetics in Ebola-Infected patients of the JIKI trial reveals concentrations lower than targeted. Plos Negl Trop Dis. 017;11:e0005389.
10. Agency EM (2020) Summary on compassionate use: Remdesivir Gilead https://www.ema.europa.eu/en/documents/other/summary-compassionate-use-remdesivir-gilead_en.pdf

Turk J Pharm Sci 2020;17(5):465-473
DOI: 10.4274/tjps.galenos.2019.42243

ORIGINAL ARTICLE

Gas Chromatographic and Spectrophotometric Determination of Diclofenac Sodium, Ibuprofen, and Mefenamic Acid in Urine and Blood Samples

Gaz Kromatografisi ve Spektrofotometri Yöntemleriyle İdrar ve Kan Örneklerinde Diklofenak Sodyum, İbuprofen ve Mefenamik Asit Tayini

Nida S. JALBANI[1], Amber R. SOLANGI[1]*, Muhammad Yar KHUHAWAR[2], Shahabuddin MEMON[1], Ranjhan JUNEJO[1], Ayaz Ali MEMON[1]

[1]University of Sindh National Center of Excellence in Analytical Chemistry, Jamshoro, Pakistan
[2]University of Sindh Institute of Advanced Research Studies in Chemical Sciences, Jamshoro, Pakistan

ABSTRACT

Objectives: Non-steroidal anti-inflammatory drugs (NSAIDs) are widely used for the treatment of acute to chronic pain. A simple, fast, and reliable gas chromatographic (GC) method with flame ionization detection has been developed for the determination of NSAIDs such as diclofenac sodium, ibuprofen, and mefenamic acid after derivatization with ethyl chloroformate.

Materials and Methods: The GC conditions were optimized as elution from a DB-1 column (30 mx0.32 mm id) at column temperature 150 ˚C for 3 min, followed by a heating rate of 20 ˚C/min up to 280 ˚C and a hold time of 5 min. The nitrogen flow rate was 2.5 mL/min. For spectrophotometric studies, the absorbance was measured against methanol at a wavelength of 200-500 nm.

Results: The calibration curves were linear within 2-10 µg/mL with limits of detection of 0.4-0.6 µg/mL of each drug. The derivatization elution, separation, and quantitation were repeatable (n=3) with relative standard deviation (RSD) within 3.9%. The method was applied for the analysis of the drugs from pharmaceutical formulations and the results of the analysis agreed with labeled values with RSDs within 0.5-3.9%. The results were also confirmed by standard addition method. The percent recovery was calculated with spiked deproteinized human blood serum and urine samples and % recovery of the drugs was obtained within 96-98% with RSDs within 3.1%.

Conclusion: The validated method proved its ability for the assay of NSAIDs in bulk and dosage form in a short analysis time. The method was also useful for the analysis of biological samples.

Key words: NSAIDs, GC analysis, derivatization of NSAIDs

ÖZ

Amaç: Non-steroid anti-enflamatuvar ilaçlar (NSAID) akut ve kronik ağrı tedavisinde yaygın olarak kullanılmaktadır. Etil kloroformat ile türevlendirme işlemini takiben diklofenak sodyum, ibuprofen ve mefenamik asit gibi NSAID'lerin belirlenmesi için alev iyonizasyon dedektörlü basit, hızlı ve güvenilir bir gaz kromatografisi (GC) yöntemi geliştirilmiştir.

Gereç ve Yöntemler: GC koşulları, 3 dakika boyunca 150 ˚C kolon sıcaklığında DB-1 kolonundan (30 m x 0,32 mm id) elüsyon, ardından 280 ˚C'ye kadar 20 ˚C/dak olacak şekilde ısıtma ve 5 dakika bekleme olarak optimize edilmiştir. Azot akış hızı 2,5 mL/dk olarak ayarlanmıştır. Spektrofotometrik çalışmalar için absorbans, 200-500 nm dalga boyunda metanole karşı ölçülmüştür.

Bulgular: Kalibrasyon eğrilerinin, her ilacın 0,4-0,6 µg/mL saptama limitleri ile 2-10 µg/mL konsantrasyon aralığında doğrusal olduğu saptanmıştır. Türetme elüsyonunun, ayırmanın ve miktar tayininin, %3,9'luk bağıl standart sapma ile tekrarlanabilir (n=3) olduğu bulunmuştur. Yöntem, farmasötik formülasyonlardan elde edilen ilaçların analizi için uygulandı ve analiz sonuçları, RSD'ler ile %0,5-3,9 arasında etiketli değerlerle uyumluydu. Sonuçlar ayrıca standart ekleme yöntemi ile doğrulanmıştır. Geri kazanım yüzdesi, deproteinize edilmiş insan serumu ve idrar örnekleri ile hesaplandı ve ilaçların geri kazanım yüzdesi, %3,1 içindeki RSD'ler ile %96-98 içinde elde edildi.

Sonuç: Valide edilmiş bu yöntemin kısa analiz süresi içinde bulk ve dozaj formundaki NSAID'leri analiz edebildiği doğrulanmıştır. Yöntemin, biyolojik numunelerin analizi için de yararlı olduğu tespit edilmiştir.

Anahtar kelimeler: NSAID'ler, GC analizi, NSAID'lerin türevlendirilmesi

*Correspondence: E-mail: +923332760143, Phone: ambersolangi@gmail.com ORCID-ID: orcid.org/0000-0002-3852-1245
Received: 31.01.2019, Accepted: 21.03.2019

INTRODUCTION

Drugs such as diclofenac sodium, ibuprofen, and mefenamic acid are commonly used all over the world.[1] These drugs belong to the class of non-steroidal anti-inflammatory drugs (NSAIDs), which are used for antipyretic, analgesic, and anti-inflammatory purposes.[1,2] These types of drugs are generally used as pain killers. People use NSAIDs without a prescription from a doctor because of the low possibility of side effects. These types of drugs are also very effective for people with arthritis or rheumatic diseases. Pregnant women may use NSAIDs if prescribed by their physicians. NSAIDs can cause several side effects if used for a long time such as gastrointestinal bleeding, intestinal ulceration, aplastic anemia, agranulocytosis, kidney damage, and cardiovascular risk.[3] Diclofenac sodium [2-(2-6-diclorophenyl) aminophenyl benzoic acid], ibuprofen (Rs)-2[4-(2-methylpropyl phenyl) propanoic acid], and mefenamic acid [2-(2,3-dimethylphenyl) aminophenylbenzoic acid] are NSAIDs and are commonly used for antipyretic, analgesic, and anti-inflammatory purposes. They are also used for the treatment of rheumatic disorders, pain, and fever.[4,5]

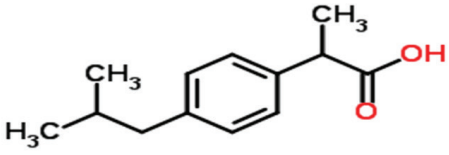

Ibuprofen

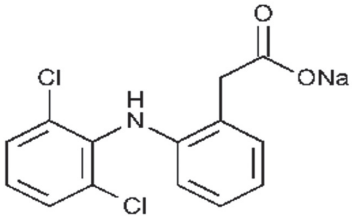

Diclofenac sodium

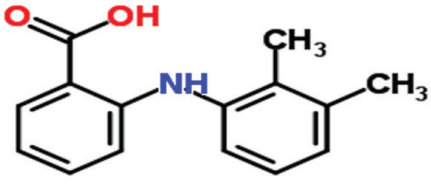

Mefenamic acid

Many methods have been reported for the determination of diclofenac sodium, ibuprofen, and mefenamic acid individually and in mixtures.[6] Diclofenac salts have been determined by spectrophotometry,[7] spectrofluorometry,[8] thin layer high performance liquid chromatography (HPLC),[9] and gas chromatography (GC)[10] in a wide variety of samples. Similarly, mefenamic acid has been analyzed by spectrophotometry,[11] spectrofluorometry,[12] electrophoresis,[13] and chromatography.[14] In pharmaceutical preparations and biological fluids for the simultaneous determination of NSAIDs chromatographic (GC, HPLC) procedures are used.[15] GC is easy to perform with high resolution efficiency and does not involve the problem of solvents used. The acidic compounds diclofenac sodium, mefenamic acid, and ibuprofen are difficult to elute from the GC column and require derivatization before their analysis.[16] GC derivatization can be defined as the procedure used to modify analyte functionality to make it suitable for GC separation. Derivatization enables an extremely polar substance to become quite volatile so that it can be easily eluted at sensible temperatures.[17] The compounds with attached functional groups, for instance -SH, -OH, -NH, and -COOH, have importance for GC analysis because these groups have a tendency to undergo hydrogen bonding.[18,19] These hydrogen bond formations have effects on the volatility, thermal stability, and interaction of the analyte with the column packing material.

The present work examineed the less expensive ethyl chloroformate (ECF) as a derivatizating reagent for GC-flame ionization detector (FID) determination of diclofenac sodium, ibuprofen, and mefenamic acid for an aqueous medium from a pharmaceutical preparation and biological fluids. In this study, we developed a new GC-FID method that is easy, cheap, fast, selective, and reliable for the determination of NSAIDs. Furthermore, spectrophotometric studies were also performed to optimize all the parameters with and without derivatization for all NSAIDs. The developed method shows better limits of detection (LOD) and limits of quantitation (LOQ) with a good regression coefficient and was applied to real blood and urine samples.

MATERIALS AND METHODS

Chemical and reagents

All the chemicals used were GR or AR grade. ECF (Fluka, Buchs, Switzerland), methanol, chloroform, acetonitrile (Fluka, Buchs, Switzerland), and pyridine (E-Merck, Darmstadt, Germany) were used. Pure standard of ibuprofen was obtained from Abbott Laboratories, Karachi, Pakistan, and mefenamic acid from Pfizer Laboratories Karachi, Pakistan, as a gift for the research. Diclofenac sodium was obtained from Sigma Aldrich (St. Louis, MO, USA). Ammonium chloride, potassium chloride, boric acid, sodium tetraborate, sodium carbonate, sodium bicarbonate, acetic acetate, ammonium acetate, ammonia solution, and hydrochloric acid (37%) for the preparation of buffer solutions were obtained from E-Merck, Darmstadt, Germany.

Buffer solutions (0.1 M) of pH 1-12 with 0.5 unit interval were prepared from the following: potassium chloride adjusted with hydrochloric acid (pH 1-2), acetic acid-sodium acetate (pH 3-6), ammonium acetate (pH 7), boric acid–sodium tetraborate (pH 7.5-8.5), ammonium chloride-ammonia (pH 10), and potassium chloride-potassium hydroxide (pH 11-12). Standard solutions of ibuprofen, diclofenac sodium, and mefenamic acid containing 1 mg/mL each were prepared separately in methanol:water (1:1 v/v). Further solutions were prepared by appropriate dilutions.

Instrumentation

All pH measurements were made with an Orion star pH meter (Orion Research Inc., Boston, MA, USA). The spectrophotometric studies were carried out on a Hitachi 220 double beam spectrophotometer [Hitachi (Pvt) Ltd, Tokyo, Japan] with dual quartz cuvettes. Gas chromatographic studies were carried out on an Agilent 6890 model gas chromatograph (Agilent Technologies, CA, USA) with a FID, split injector, hydrogen generator H_2-90 (Parker Hannifin, Haverhill, MA, USA), pure nitrogen (British Oxygen Company, Karachi, Pakistan), and a computer with Chemostation software. A capillary column, DB-1 (30 m x 0.32 mm id), with film thickness 0.25 µm (J.W. Scientific GC column, Willington, NC, USA) was used throughout the study.

Statistical analysis

All results were statistically analyzed and repeated 3 times. The % error, % relative standard deviation (RSD), and regression coefficient were calculated using SPSS 16.0.

Spectrophotometric procedure without derivatization

For the spectrophotometric study, stock solutions containing 1 mg/mL were prepared in methanol in a 25-mL volumetric flask. The solutions were appropriately diluted to 10 µg/mL for ibuprofen, mefenamic acid, and diclofenac sodium separately in a 10-mL volumetric flask. The solutions were well mixed, and the absorbance was measured against methanol on a spectrophotometer (Hitachi 220) at a wavelength of 200-400 nm. The maximum response was obtained at 240, 260, and 300 nm for ibuprofen, mefenamic acid, and diclofenac sodium, respectively.

Spectrophotometric procedure with derivatization

For the spectrophotometric study stock solutions containing 1 mg/mL were prepared for ibuprofen, mefenamic acid, and diclofenac sodium separately and were further diluted to 10 µg/mL in methanol. The solution of 1 mL each of 100 µg/mL ibuprofen, mefenamic acid, and diclofenac sodium was separately transferred into a 10-mL volumetric flask and (0.5 mL) solvent system of pyridine:methanol:acetonitrile:water (8:42:8:42 v/v) and (0.5 mL) buffer of solution pH 9 and (0.4 mL) ECF were added and the contents were sonicated for 20 min at 30 °C room temperature. Then methanol was added up to the mark in a 10-mL volumetric flask, the solutions were mixed, and the absorbance was measured against the reagent blank on a spectrophotometer at a wavelength of 200-400 nm. The maximum responses were obtained at 350, 310, and 350 nm for ibuprofen, diclofenac sodium, and mefenamic acid, respectively. The reagent blank was prepared with 1 mL of methanol and following the same procedure without addition of the analyte.

Gas chromatographic procedure

The solutions (0.2-1.0 mL) containing 10 µg/mL ibuprofen, mefenamic acid, and diclofenac sodium separately or in mixture were transferred to well stoppered test tubes. To the solution were added methanol:water:acetonitrile:pyridine (42:42:8:8 v/v) (0.5 mL) solvent, carbonate buffer solution of pH 9 (0.5 mL), and ECF (0.4 mL) and the contents were sonicated at room temperature (30 °C) for 15 min. Chloroform (0.5 mL) was added and the contents were mixed well. The layers were allowed to separate. The calculated volume of 0.5 mL from the organic layer was pipetted out into a screw capped sample vial. The solution (1 µL) was injected into the GC instrument at an initial column temperature of 150 °C for 3.0 min with a heating rate of 20 °C/min up to 280 °C. The nitrogen flow rate was 2.5 mL/min, while the rates for FID were fixed hydrogen 40 mL/min, nitrogen as makeup gas 40 mL/min, and air 250 mL/min.

Analysis of the pharmaceutical preparations

Five tablets of each pharmaceutical formulation, i.e. Brufen (Abbott Laboratories, Karachi), containing 200 mg/tablet ibuprofen; Ponstan (Pfizer Laboratories, Karachi), containing 25 mg/tablet mefenamic acid; and Qufen (High G. International, Karachi), containing 20 mg/tablet diclofenac sodium, were ground to fine powder separately. The powder corresponding to 1 tablet was dissolved in methanol:water (1:1 v/v). The solution was filtered and volume adjusted to 50 mL. The solution (0.2 mL and 0.4 mL) after appropriate dilution was analyzed following the GC analytical procedure. Quantitation was achieved from the external calibration curve using a linear regression equation: y=ax+b.

Analysis of the pharmaceutical preparations by standard addition

Five tablets of each pharmaceutical formulation, Brufen, Ponstan, and Qufen, were processed for the analysis of the pharmaceutical preparations. After appropriate dilution, two solutions of 0.2 mL and 0.4 mL from each of the pharmaceutical preparations were obtained in duplicate. To a solution was added 0.5 mL of standard drug solution containing 10 µg/mL. All the solutions were processed by GC analytical procedure. The quantitation was done from the linear regression equation and from the increase in response (peak height/peak area) with added standard.

Analysis of biological samples

Blood and urine samples were collected from healthy volunteers (students and employees) at the Institute of Advanced Research Studies in Chemical Sciences, University of Sindh. The blood samples were collected by vein puncture in ethylenediamine tetraacetic acid tubes and urine samples were collected in clean plastic bottles. The samples were processed as received. The volunteers were informed of the objective of the work and they gave verbal permission for their samples to be collected.

Each (5 mL) sample was kept at room temperature (30 °C) for 30 min and was centrifuged at 4000 rpm for 20 min. The supernatant layer was collected and 5 mL of methanol was added. The contents were mixed well and again centrifuged for 20 min at 4000 rpm. The two solutions of supernatant (1 mL each) were taken and a solution 0.5 mL of standard solution of ibuprofen, mefenamic acid, or diclofenac sodium was added containing 10 µg/mL. The solutions were processed by GC analytical procedure. The quantitation was done from the linear regression equation of the external calibration curve. The solution without addition of the standard was treated as blank.

RESULTS AND DISCUSSION

Spectrophotometric study without and with derivatization of ibuprofen

The solution of ibuprofen standard was examined on a double beam spectrophotometer within the range of 200-500 nm. The absorbance was measured at an interval of 5 nm. The absorption spectra were obtained with and without derivatization, which indicates the maximum absorbance at 260 nm for ibuprofen without derivatization when measured against the blank (methanol), while the absorption spectra after derivatization were obtained, which indicated maximum absorbance at 350 nm for ibuprofen (Figures 1a and 1b).

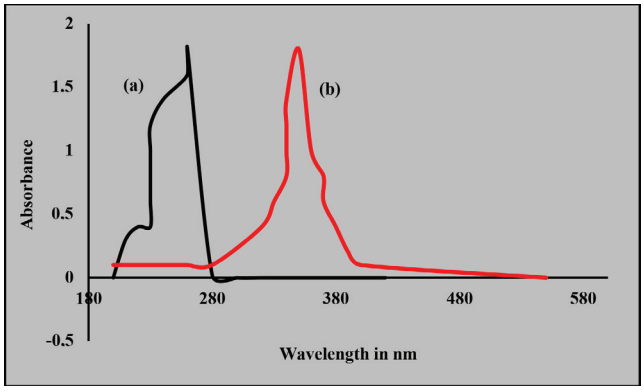

Figure 1. The absorption spectrum (a) shows ibuprofen without derivatization with a concentration of 10 µg/mL in methanol. The absorbance was measured within 200-500 nm (b) after derivatization ECF at a concentration of 10 µg/mL in methanol

ECF: Ethyl chloroformate

Spectrophotometric study without and with derivatization of mefenamic acid

The mefenamic acid in methanol standards was examined on a double beam spectrophotometer within the range of 200-500 nm. The absorption spectrum was obtained, which indicated maximum absorbance at 300 nm for mefenamic acid without derivatization when recorded against the reagent blank (methanol) (Figure 2a). The solution of mefenamic acid standard was also examined after derivatization with ECF within the range of 200-500 nm. The solution of mefenamic acid indicated maximum absorbance at 350 nm and was recorded against as the reagent blank (Figure 2b).

Spectrometric study without and with derivatization of diclofenac sodium

The diclofenac sodium solution in methanol was examined on a double beam spectrophotometer. The absorption spectra was obtained, which indicated maximum absorbance at 240 nm for diclofenac sodium when recorded against the blank (methanol) in Figure 3a, while the absorbance was measured after derivatization with ECF at 310 nm in Figure 3b.

Effect of pH

The effect of pH on the derivatization of ibuprofen, mefenamic acid, and diclofenac sodium was analyzed within

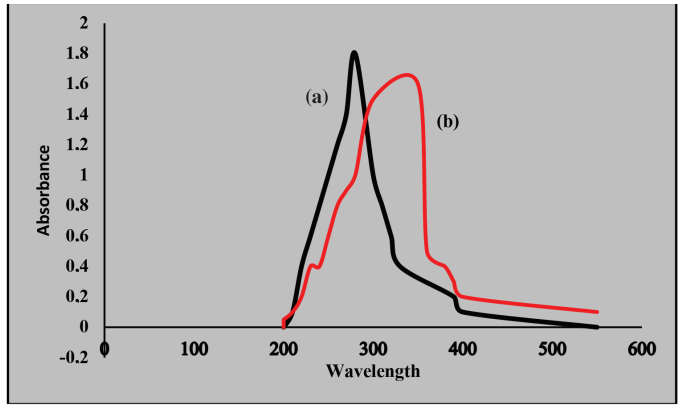

Figure 2. The absorption spectrum (a) shows mefenamic acid without derivatization with a concentration 10 µg/mL in methanol. The spectrum (b) is absorption spectrum of mefenamic acid after derivatization with an ECF concentration of 10 µg/mL in methanol

ECF: Ethyl chloroformate

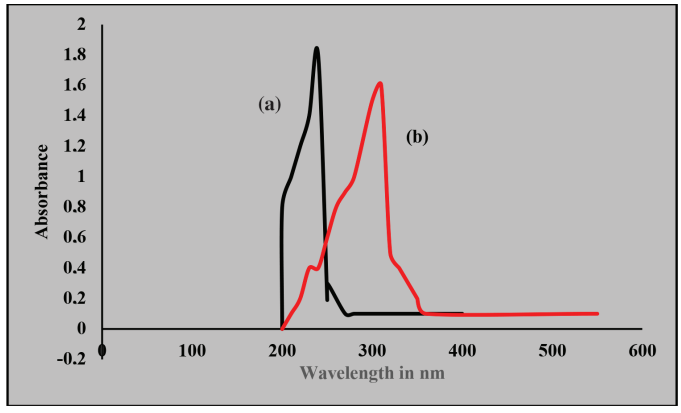

Figure 3. The absorption spectrum (a) of diclofenac sodium without derivatization at a concentration of 10 µg/mL in methanol. Spectrum (b) is after derivatization with ECF at a concentration of 10 µg/mL in methanol

ECF: Ethyl chloroformate

the pH range of 1-10. The reactions were monitored on a spectrophotometer against the reagent blank at appropriate pH. The absorbance was measured at the wavelength of maximum absorbance at 350 nm for ibuprofen and mefenamic acid, while diclofenac sodium showed absorbance at 310 nm. The maximum absorbance was observed at pH 9 for ibuprofen, mefenamic acid, and diclofenac sodium as shown in Figure 4.

Effect of ECF on derivatization

The effect of change in concentration of the derivatization reagent ECF was examined between 0.1 and 0.5 mL at an interval of 0.1 mL following the analytical procedure. Absorbance was measured at the wavelength of maximum absorbance at 350 nm for ibuprofen and mefenamic acid, while diclofenac sodium showed absorbance at 310 nm. The effect of concentration was not critical and a similar response was obtained from 0.2 to 0.5 mL, but for a quick response 0.4 mL was selected. The solvent system acetonitrile:water:pyridine:methanol (8:42:8:42 v/v) (0.5 mL) and carbonate buffer solution pH 9 (0.5 mL) were added during derivatization as mentioned in Figure 5.

Effect of sonication time on derivatization

The effect of sonication time on the derivatization of ibuprofen, mefenamic acid, and diclofenac sodium with ECF were examined within 5 to 30 min at an interval of 5 min from the absorbance of the analyte as shown in Figure 6. Following the analytical procedure, the absorbance was measured at 350 nm for ibuprofen and mefenamic acid and 310 nm for diclofenac sodium. The sonication time was critical and the same response was obtained from 5 to 30 min, but to get reproducible results a sonication time of 20 min was selected. The solvent system acetonitrile:water:pyridine:methanol (8:42:8:42 v/v) (0.5 mL) and carbonate buffer solution pH 9 (0.5 mL) were added.

Spectrophotometric calibration of ibuprofen with derivatization

The standard solution of different concentrations of ibuprofen was measured for absorbance at 350 nm. Linear calibration curves were obtained that obeyed Beer's law within the concentration range 20 to 160 µg/mL ibuprofen. The coefficient of determination (R^2) of ibuprofen was 0.999. The molar absorptivity calculated for ibuprofen at 350 nm was 43.733 L mol-cm^{-1}. The linear regression equation obtained for ibuprofen was y=0.007x+0.152.

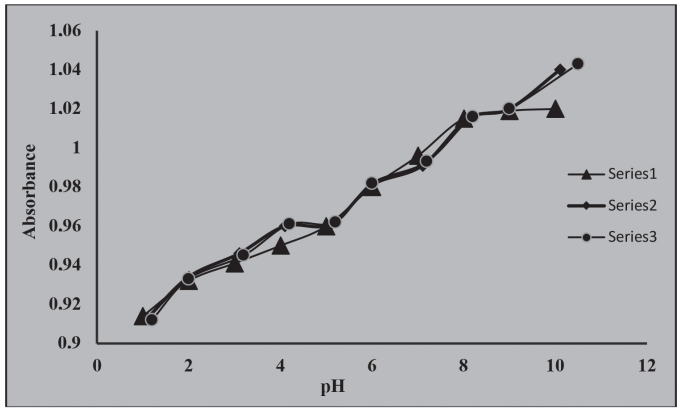

Figure 4. Effect of pH on the absorbance of ibuprofen, mefenamic acid, and diclofenac sodium derivative of ECF on a spectrophotometer at 350 and 310 nm

ECF: Ethyl chloroformate

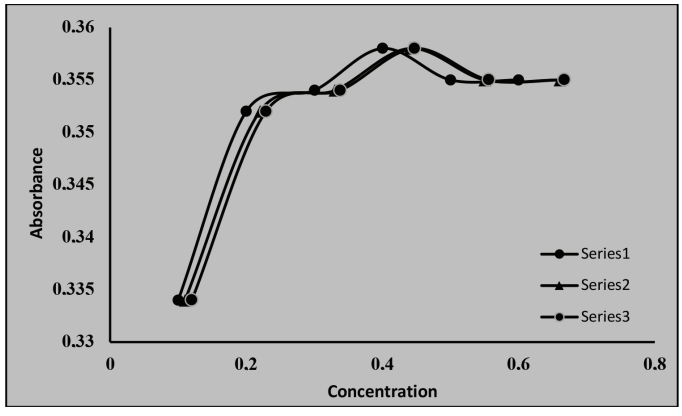

Figure 5. ECF concentration effect on the absorbance of ibuprofen, mefenamic acid, and diclofenac sodium

ECF: Ethyl chloroformate

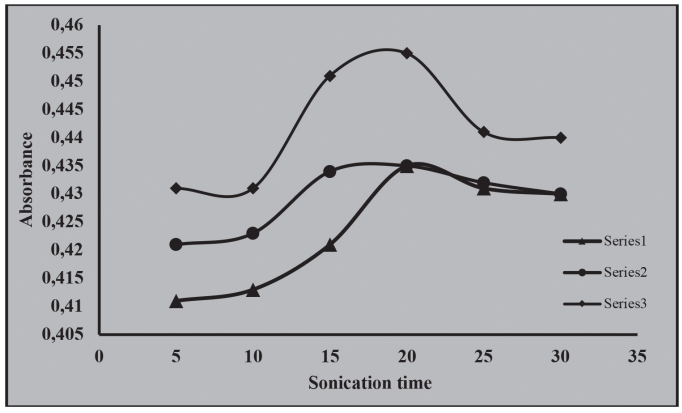

Figure 6. Effects of sonication time on the derivatization of ibuprofen, mefenamic acid, and diclofenac sodium

Spectrophotometric calibration of mefenamic acid with derivatization

The standard solution of different concentrations of mefenamic acid was measured for absorbance at 350 nm and linear calibration curves were obtained that obeyed Beer's law within the concentration range 10 to 200 µg/mL mefenamic acid. The coefficient of determination (R^2) of mefenamic acid was 0.998. The molar absorptivity calculated for mefenamic acid at 350 nm was 51.152 L mol-cm^{-1}. The linear regression equation obtained for mefenamic acid was y=0.020x+0.076.

Spectrophotometric calibration of diclofenac sodium with derivatization

The standard solution of different concentration of diclofenac sodium was measured for the absorbance at 310 nm and linear calibration curves were obtained that obeyed Beer's law within the concentration range 20 to 160 µg/mL diclofenac sodium. The coefficient of determination (R^2) of diclofenac sodium was 0.999. The molar absorptivity calculated for diclofenac sodium at 310 nm was 67,443,348 L mol-cm^{-1}. The linear regression equation obtained for diclofenac sodium was y=0.007x+0.134.

Quantitation of NSAIDs by gas chromatography

NSAIDs in GC elution occur after derivatization with ECF. Initially GC conditions were optimized for the elution as symmetrical peaks from the DB-1 column (30 m × 0.32 mm id). Different temperature programs were examined with nitrogen flow rates and reasonable peak shapes were observed at initial column temperature at 150 °C for 3.0 min, and with a heating rate of 20 °C/min up to 280 °C and a hold time of 5.0 min with a total run time 13.2 min and the flow rate of nitrogen was adjusted to 2.5 mL/min.

Solution (0.2-1.0 mL) of 10 µg/mL stock solution was taken of each of ibuprofen, mefenamic acid, and diclofenac sodium and 0.5 mL of acetonitrile:water:pyridine:methanol (8:42:8:42 v/v/v/v), 0.5 mL of sodium carbonate buffer solution (pH 9), and 0.4 mL of ECF were added. The contents were sonicated for 20 min at 30 °C and 0.5 mL of chloroform was added. The mixture was shaken well, and a separatory funnel was used to separate the layers. A portion of the extract (0.5 mL from 1 mL) was transferred to a vial with a screw cap and 1 µL of the solution was injected into the GC apparatus.

Quantitation of ibuprofen after derivatization

The linear calibration curve of ibuprofen was obtained by plotting concentration (µg/mL) of ibuprofen against peak height and was obtained within 2-10 µg/mL with the coefficient of determination (R^2=0.996). The linear regression equation was y=0.980x+1.789. The LOD and LOQ were calculated with 3:1 and 10:1 signal to noise ratios as 0.6 µg/mL and 1.8 µg/mL, respectively (Table 1).

Quantitation of mefenamic acid after derivatization

The linear calibration curve of mefenamic acid was obtained by plotting concentration (µg/mL) against peak height and was obtained within 2-10 µg/mL with the coefficient of determination (R^2=0.998). The linear regression equation was y=0.230x-0.174. The LOD and LOQ were calculated with 3:1 and 10:1 signal to noise ratios as 0.4 µg/mL and 1.2 µg/mL, respectively (Table 1).

Quantitation of diclofenac sodium after derivatization

The linear calibration curve of diclofenac sodium was obtained by plotting concentration (µg/mL) against peak height and was obtained within 2-10 µg/mL with the coefficient of determination (R^2=0.999). The linear regression equation was y=1.070x-1.301. The LOD and LOQ were calculated with 3:1 and 10:1 signal to noise ratios as 0.5 µg/mL and 1.5 µg/mL, respectively (Table 1).

GC analysis of ibuprofen

GC of ibuprofen after derivatization with ECF was performed. The GC was carried out with a DB-1 column (30 m×0.32 mm id). Temperatures were set at different values and the flow rate of nitrogen was examined and reasonable peak shapes were observed at column temperature initially set at 150 °C for 3 min, followed by a heating rate of 20 °C/min up to 280 °C and a hold time of 5 min with a whole run time of 13.2 min. The flow rate of nitrogen was adjusted to 2.5 mL/min.

GC analysis of mefenamic acid

GC of mefenamic acid after derivatization with ECF was performed. The column used was DB-1 (30 m×0.32 mm id). Temperatures were set and reasonable peak shapes were observed at column temperature initially set at 150 °C for 3 min, followed by a heating rate of 20 °C/min up to 280 °C and a hold time of 5 min with a whole run time of 13.2 min. The flow rate of nitrogen was adjusted to 2.5 mL/min.

GC analysis of diclofenac sodium

GC of diclofenac sodium after derivatization with ECF was performed. The column used was DB-1 (30 m×0.32 mm id). Temperatures were set and reasonable peak shapes were observed at column temperature initially set at 150 °C for 3 min, followed by a heating rate of 20 °C/min up to 280 °C and a hold time of 5 min with a whole run time of 13.2 min The flow rate of nitrogen was adjusted to 2.5 mL/min.

GC separation of ibuprofen, mefenamic acid, and diclofenac sodium

Gas chromatographic separation of ibuprofen, mefenamic acid, and diclofenac sodium was carried out after derivatization with ECF. Initially the GC conditions were optimized for the elution as symmetrical peaks from the DB-1 column (30 m×0.32 mm id). Temperature was set at different values and the flow rate of nitrogen was examined and reasonable peak shapes were observed at initial column temperature at 150 °C for 3.0 min, followed by a heating rate of 20 °C/min up to 280 °C and a hold time of 5.0 min with an entire run time of 13.2 min. The flow rate of nitrogen was adjusted to 2.5 mL/min (Figure 7).

Drug analysis of ibuprofen, mefenamic acid, and diclofenac sodium with derivatization

The method developed for the determination of ibuprofen, mefenamic acid, and diclofenac sodium after derivatization was applied for the analysis of the active ingredients in brufen (ibuprofen), ponstan (mefenamic acid), and qufen (diclofenac sodium) tablets. At least 5 tablets containing ibuprofen 200 mg/tablet, mefenamic acid 250 mg/tablet, and diclofenac sodium 20 mg/tablet were ground to a fine powder and dissolved in an appropriate amount in methanol. Then the solution was filtered and volume adjusted of 50 mL and an aliquot of solution after derivatization with ECF was injected into the DB-1 GC column (30 m × 0.32 mm id) and eluted with mobile phase optimized for GC separation and detection of ibuprofen, mefenamic acid, and diclofenac sodium. The quantitation was done from the linear regression equation and the amounts of ibuprofen,

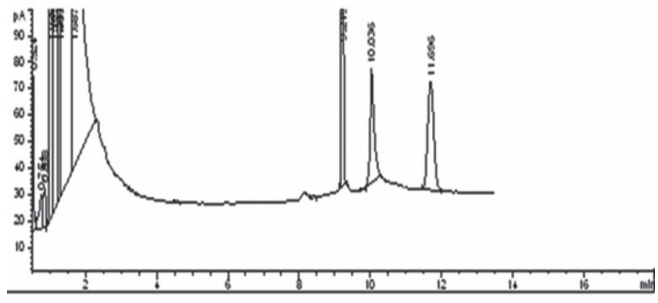

Figure 7. Gas chromatographic separation peaks of (1) ibuprofen, (2) mefenamic acid, and (3) diclofenac sodium after derivatization with ethyl chloroformate from a DB-1 column (30 m × 0.32 mm id)

Table 1. Quantitation results of ibuprofen, mefenamic acid, and diclofenac sodium using ethyl chloroformate as derivatizing reagent

Drug name	Limits of detection µg/mL	Limits of quantitation µg/mL	Calibration range µg/mL	Coefficient of determination (R^2)	Linear regression equation
Ibuprofen	0.6	1.8	2-10	0.9965	y=0.9809x+1.7892
Mefenamic acid	0.4	1.2	2-10	0.998	y=0.2303x-0.1743
Diclofenac sodium	0.5	1.5	2-10	0.999	y=1.0705x-1.3018

mefenamic acid, and diclofenac sodium were found to be 156.93 mg/mL, 193.14 mg/mL, and 19.48 mg/mL, respectively, which agreed with the amounts labeled, i.e. 160 mg/mL, 200 mg/mL, and 20 mg/mL, respectively. The % error was calculated as -1.9%, -3.4%, and -2.6%. The RSD calculated from replicated analysis (n=3) was within 0.5-3.0%. The percentage recovery of ibuprofen, mefenamic acid, and diclofenac sodium was 98%, 96%, and 97%, respectively (Table 2).

Determination of ibuprofen, mefenamic acid, and diclofenac sodium in spiked blood samples

Blood and urine samples (5 mL each) were collected from healthy volunteers on the condition that they had not taken any medicine over the previous week. The samples were centrifuged to remove blood cells and precipitate. The blood serum and urine were deprotonized with methanol. Samples (1 mL) were spiked with ibuprofen, mefenamic acid, and diclofenac sodium within the calibration range of each compound. The derivatization procedure with ECF was followed. The chloroform extract (1 µL) was then injected into the gas chromatograph equipped with a DB-1 column (30 m × 0.32 mm id). The elution was carried out under optimized conditions (Figures 8-13). The quantitation was done from the linear regression equation and all results are summarized in Tables 3 and 4.

GC determination of ibuprofen with standard addition

Five tablets of brufen (ibuprofen) containing 200 mg were processed as described above. The solution (0.2 mL) was taken in duplicate. To a solution was added 0.2 mL of ibuprofen containing 14.16 µg and both of the solutions were processed by GC. The quantitation was done from the linear regression equation of the external calibration curve and showed an increase in response with added standard (Table 5).

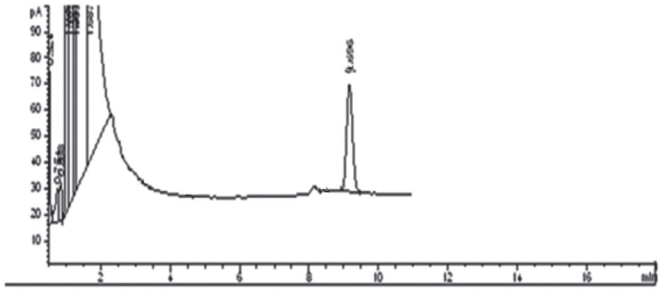

Figure 8. Gas chromatographic elution of ibuprofen in blood sample from a DB-1 column (30 m × 0.32 mm id)

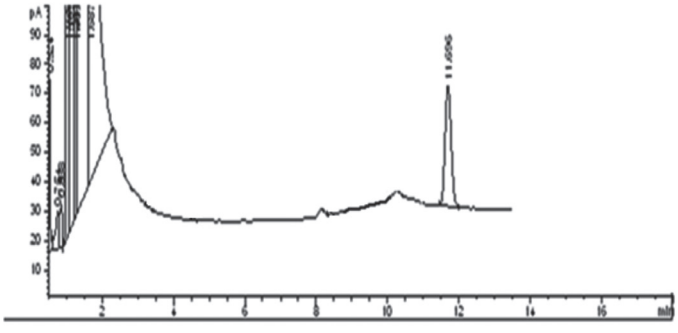

Figure 9. Gas chromatogram of mefenamic acid in blood sample from a DB-1 column (30 m × 0.32 mm id)

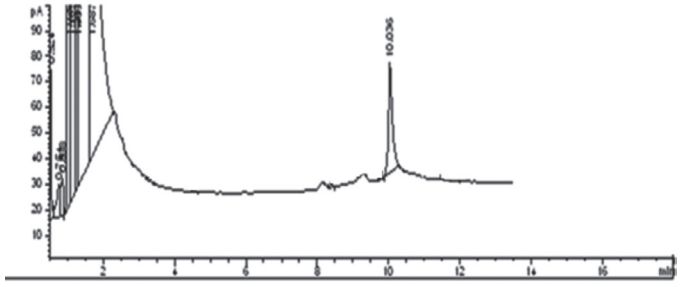

Figure 10. Gas chromatogram of diclofenac sodium in blood sample from a DB-1 column (30 m × 0.32 mm id)

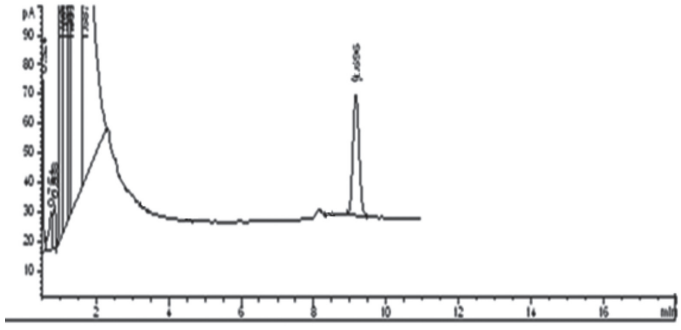

Figure 11. Gas chromatogram of mefenamic acid in urine sample from a DB-1 column (30 m × 0.32 mm id)

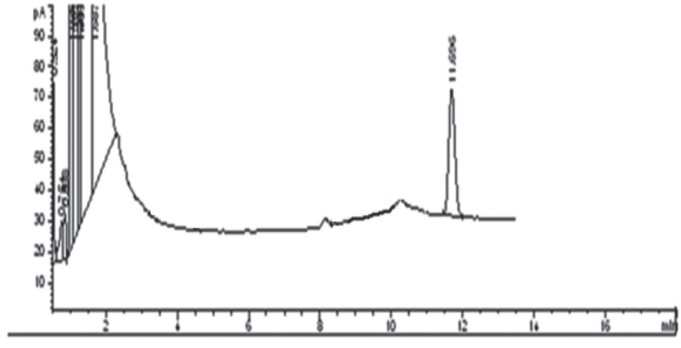

Figure 12. Gas chromatogram of mefenamic acid in urine sample from a DB-1 column (30 m × 0.32 mm id)

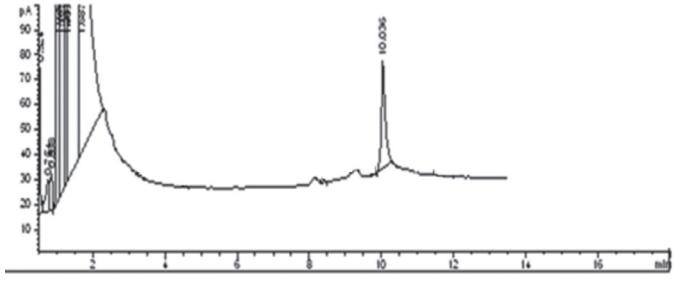

Figure 13. Gas chromatogram of diclofenac sodium in urine sample from a DB-1 column (30 m × 0.32 mm id)

GC determination of mefenamic acid with standard addition

Five tablet of ponstan (mefenamic acid) containing 250 mg were processed as described above. The solution (0.2 mL) was taken in duplicate. To a solution was added 0.2 mL of ibuprofen containing 17.76 µg and both solutions were processed by GC. The quantitation was done from the linear regression equation of the external calibration curve and showed an increase in response with added standard (Table 5).

GC determination of diclofenac sodium with standard addition

Five tablets of qufen (diclofenac sodium) containing 20 mg were processed as described above. The solution (0.2 mL) was taken in duplicate. To a solution was added 0.2 mL of ibuprofen containing 17.76 µg and both of the solutions were processed by GC. The quantitation was done from the linear regression equation of the external calibration curve and showed an increase in response with added standard (Table 5).

Intraday and interday studies

Inter- and intraday assays were performed by analyzing replicate injections of standard solution to study the repeatability of the method. The intraassay precision (n=5) was determined by the same analyst on the same day and under the same conditions with an interval of 2 h, whereas the interassay precision (n=3) was determined by the same analyst and under the same conditions on three consecutive days. The reproducibility of the separation was examined for all analytes in terms of peak area and the % RSD values of each are shown in Table 6.

CONCLUSION

A new analytical procedure has been developed for the gas chromatographic and spectrophotometric determination of ibuprofen, mefenamic acid, and diclofenac sodium after derivatization with ECF. The LOD and LOQ of ibuprofen were calculated with 3:1 and 10:1 signal to noise ratio as 0.6 µg/mL and 1.8 µg/mL, for mefenamic acid as 0.4 µg/mL and 1.2 µg/mL, and for diclofenac sodium as 0.5 µg/mL and 1.5 µg/mL, respectively. The method is repeatable and has been successfully applied for the analysis of pharmaceutical preparations and spiked deproteinized serum and urine samples.

Table 2. Drug analysis of ibuprofen, mefenamic acid, and diclofenac sodium with derivatization

No	Name of standard	Name of tablet	Amount added mg/mL	Amount found mg/mL	Error %	RSD %	Recovery %
1	Ibuprofen	Brufen	200 mg/mL	157.96 mg/mL	-1.9%	0.5%	98%
2	Mefenamic acid	Ponstan	250 mg/mL	193.14 mg/mL	-3.4%	3.6%	96%
3	Diclofenac sodium	Qufen	20 mg/mL	19.48 mg/mL	-2.6%	3.9%	97%

RSD: Relative standard deviation

Table 3. Gas chromatographic analysis results of ibuprofen, mefenamic acid and diclofenac sodium in blood samples using ethyl chloroformate

No	Age/gender	Name of standard	Amount added µg/mL	Amount found µg/mL	Error %	Recovery %
1	25/F	Ibuprofen	50 µg/mL	49.04 µg/mL	-1.95	98%
2	25/F	Mefenamic acid	40 µg/mL	39.66 µg/mL	-0.8	99%
3	25/F	Diclofenac sodium	50 µg/mL	49.0 µg/mL	-0.8	99%

F: Female

Table 4. Gas chromatographic analysis results of ibuprofen, mefenamic acid, and diclofenac sodium in urine samples using ethyl chloroformate

No	Age/gender	Name of standard	Amount added µg/mL	Amount found µg/mL	Error %	Recovery %
1	25/F	Ibuprofen	60 µg/mL	59.14 µg/mL	1.45	98%
2	25/F	Mefenamic acid	50 µg/mL	48.36 µg/mL	-2.9	98%
3	25/F	Diclofenac sodium	40 µg/mL	38.83 µg/mL	-3.0	97%

F: Female

Table 5. Gas chromatographic standard addition of ibuprofen, mefenamic acid, and diclofenac sodium

No	Name of standard	Name of tablet	Amount added µg/mL	Amount found µg/mL	Recovery %	Error %
1	Ibuprofen	Brufen	14.16 µg/mL	13.73 µg/mL	96%	-3.1%
2	Mefenamic acid	Ponstan	17.76 µg/mL	17.27 µg/mL	97%	-2.8%
3	Diclofenac sodium	Qufen	17.76 µg/mL	17.33 µg/mL	97%	-2.4%

Table 6. Intraday and interday study of nonsteroidal anti-inflammatory drugs

Concentration 10 (µg/mL)				
Ibuprofen	**Peak area**	**RSD %**	**Peak area**	**RSD %**
1	0.01644	0.33772	0.015473	0.362192
2	0.0399	0.1564	0.02957	0.224109
3	0.0544	0.35924	0.047067	0.39546
Mefenamic acid				
1	0.01511	0.21487	0.01511	0.214868
2	0.09147	0.03365	0.09147	0.033647
3	0.08417	0.05524	0.084167	0.055236
Diclofenac sodium				
1	0.02126	0.57062	0.019605	0.60538
2	0.01432	0.13947	0.013183	0.14222
3	0.08573	0.07509	0.075233	0.01291

RSD: Relative standard deviation

Conflicts of interest: No conflict of interest was declared by the authors. The authors alone are responsible for the content and writing of the paper.

REFERENCES

1. Bazregar M, Rajabi M, Yamini Y, Asghari A, Hemmati M. Tandem air-agitated liquid-liquid microextraction as an efficient method for determination of acidic drugs in complicated matrices. Anal Chim Acta. 2016;917:44-52.
2. Li N, Chen J, Shi YP. Magnetic polyethyleneimine functionalized reduced graphene oxide as a novel magnetic sorbent for the separation of polar non-steroidal anti-inflammatory drugs in waters. Talanta. 2019;191:526-534.
3. Borghi SM, Fattori V, Ruiz-Miyazawa K, Bertozzi W, Lourenco-Gonzalez Y, Tatakihara RL, Bussmann AJC, Mazzuco TL, Casagrande R, Verri WA Jr. Pyrrolidine dithiocarbamate inhibits mouse acute kidney injury induced by diclofenac by targeting oxidative damage, cytokines and NF-κB activity. Life Sci. 2018;208:221-231.
4. Davies NM, Anderson KE. Clinical pharmacokinetics of diclofenac. Clin Pharmacokinet. 1997;33:184-213.
5. Boynton CS, Dick CF, Mayor GH. NSAIDs: an overview. J Clin Pharmacol. 1988;28:512-517.
6. Fatta D, Achilleos A, Nikolaou A, Meric S. Analytical methods for tracing pharmaceutical residues in water and wastewater. Trends Anal Chem. 2007;26:515-533.
7. Sena MM, Chaudhry ZF, Collins CH, Poppi RJ. Direct determination of diclofenac in pharmaceutical formulations containing B vitamins by using UV spectrophotometry and partial least squares regression. J Pharm Biomed Anal. 2004;36:743-749.
8. Carreira L, Rizk M, El-Shabrawy Y, Zakhari N, Toubar S. Europium (III) ion probe spectrofluorometric determination of diclofenac sodium. J Pharm Biomed Anal. 1995;13:1331-1337.
9. Thongchai W, Liawruangrath B, Thongpoon C, Machan T. High performance thin layer chromatographic method for the determination of diclofenac sodium in pharmaceutical formulations. Chiang Mai J Sci. 2006;33:123-128.
10. Schneider W, Degen P. Simultaneous determination of diclofenac sodium and its hydroxy metabolites by capillary column gas chromatography with electron-capture detection. J. Chromatogr. 1981;217:263-271.
11. Dinç E, Yücesoy C, Onur F. Simultaneous spectrophotometric determination of mefenamic acid and paracetamol in a pharmaceutical preparation using ratio spectra derivative spectrophotometry and chemometric methods. J Pharm Biomed Anal. 2002;28:1091-1100.
12. Ruiz TP, Lozano CM, Tomás V, Carpena J. Analysis of binary mixtures of flufenamic, meclofenamic and mefenamic acids by derivative synchronous fluorescence spectrometry. Talanta. 1998;47:537-545.
13. Ahrer W, Scherwenk E, Buchberger W. Determination of drug residues in water by the combination of liquid chromatography or capillary electrophoresis with electrospray mass spectrometry. J Chromatogr. 2001;910:69-78.
14. Singh AK, Jang Y, Mishra U, Granley K. Simultaneous analysis of flunixin, naproxen, ethacrynic acid, indomethacin, phenylbutazone, mefenamic acid and thiosalicycic acid in plasma and urine by high-performance liquid chromatography and gas chromatography-mass spectrometry. J. Chromatogr. 1991;568:351-361.
15. Sun Y, Takaba K, Kido H, Nakashima MN, Nakashima K. Simultaneous determination of arylpropionic acidic non-steroidal anti-inflammatory drugs in pharmaceutical formulations and human plasma by HPLC with UV detection. J Pharm Biomed Anal. 2003;30:1611-1619.
16. Quintana, JB, Carpinteiro J, Rodríguez I. Chapter 2.5 Analysis of acidic drugs by gas chromatography. Trends Anal Chem. 2007;50:185-218.
17. Orata F. Derivatization reactions and reagents for gas chromatography analysis. In Advanced Gas Chromatography-Progress in Agricultural, Biomedical and Industrial Applications, In Tech: 2012.
18. Halket, J. M.; Zaikin, V. G., Derivatization in mass spectrometry-1. Silylation. Eur J Mass Spectrom. 2003;9:1-21.
19. Zaikin VG, Halket JM. Derivatization in mass spectrometry-2. Acylation. Eur J Mass Spectrom. 2003;9:421-434.

Turk J Pharm Sci 2020;17(5):474-479
DOI: 10.4274/tjps.galenos.2019.89719

ORIGINAL ARTICLE

Acetamiprid-induced Cyto- and Genotoxicity in the AR42J Pancreatic Cell Line

AR42J Pankreas Hücre Hattında Asetamiprid ile İndüklenen Sito- ve Genotoksisite

Mehtap KARA*, Ezgi ÖZTAŞ, Gül ÖZHAN

Istanbul University Faculty of Pharmacy, Department of Pharmaceutical Toxicology, İstanbul, Turkey

ABSTRACT

Objectives: Neonicotinoid insecticides, 30% of insecticides marketed worldwide, have selective toxicity on insects through α4p2 nicotinic acetylcholine receptors. Although it is known that acetamiprid exerts toxicity on several organ systems, its toxic effects on the pancreas and its mechanism of action have not been clarified yet. Therefore, in the present study, the cytotoxic and genotoxic potentials of acetamiprid on the AR42J pancreatic cell line were evaluated.

Materials and Methods: The (3-[4,5-dimethylthiazol-2-yl]-2,5 diphenyl tetrazolium bromide) (MTT) assay and comet assay were conducted for the cyto- and genotoxicity evaluations, respectively. Reactive oxygen species (ROS) production was assessed by flow cytometry and glutathione (GSH) levels were determined by ELISA for oxidative damage potential, which is thought to be an underlying mechanism of cyto-/genotoxic effects.

Results: To reveal the dose-response relationship the concentration range of 1-6 mM was selected for the assays. Cell viability decreased in a dose-dependent manner and the inhibitory concentration 50 value was calculated as 12.61 mM by the MTT assay. Acetamiprid induced DNA damage in all concentrations tested in a dose-depending manner. The mean tail intensity values were 3.84 and ≤32.96 for the control and exposure groups, respectively. There was no significant difference for ROS production; however, the GSH level was reduced at the highest concentration.

Conclusion: It is thought that the present study will contribute to the literature due to the lack of data on the potential toxic effects of acetamiprid on the pancreas. To better understand acetamiprid toxicity, further studies including a wide range of mechanistic parameters are needed.

Key words: Acetamiprid, AR42J pancreatic cell line, cytotoxicity, genotoxicity, oxidative damage

ÖZ

Amaç: Neonikotinoid insektisidler dünya piyasasındaki insektisidlerin %30'luk kısmını oluşturur ve etkilerini seçici olarak böceklerdeki α4p2 nikotinik asid reseptörünü inhibe ederek gösterirler. Asetamipridin çeşitli organ ve sistemler üzerine toksik etkileri biliniyor olmasına karşın, pankreas üzerindeki etkisi ve etki mekanizması bilinmemektedir. Bu çalışmada, asetamipridin AR42J pankreas hücre hattı üzerinde sitotoksik ve genotoksik etkileri araştırıldı.

Gereç ve Yöntemler: Sitotoksisite ve genotoksisite değerlendirmesi için (3-[4,5-dimetiltiyazol-2-il]-2,5 difenil tetrazolyum bromür) (MTT) ve comet analizi gerçekleştirildi. Reaktif oksijen türlerinin (ROS) oluşumu akış sitometresi ile, glutatyon (GSH) düzeyi ise ELISA yöntemi ile belirlenmiştir.

Bulgular: MTT sitotoksisite analizine gore, hücre canlılığının doza bağımlı olarak azaldığı gözlendi ve inhibitör konsantrasyon 50 değeri 12,61 mM olarak tespit edildi. Analizlerde doz yanıt ilişkisini gösterebilmek için 1-6 mM doz aralığı seçildi. Asetamiprid DNA hasarını doza bağımlı olarak artırdı ve ortalama kuyruk yoğunluğu değerleri kontrol ve çalışma grupları için sırasıyla 3,84 ve ≤32,96 olarak belirlendi. ROS üretimi açısından gruplar arasında anlamlı bir fark gözlenmemiş, GSH değerinin en yüksek doz grubunda anlamlı olarak çok düştüğü tespit edilmiştir.

Sonuç: Bu çalışma literatürde asetamipridin pankreas üzerine olası toksik etkisine yönelik eksik olan verilere katkı sağlamaktadır. Asetamipridin toksik etkisinin detaylandırılması için daha geniş çaplı mekanizma temelli çalışmalara ihtiyaç bulunmaktadır.

Anahtar kelimeler: Asetamiprid, AR42J pankreas hücre hattı, sitotoksisite, genotoksisite, oksidatif hasar

***Correspondence: E-mail:** matost@gmail.com, **Phone:** +90 507 349 24 78 **ORCID-ID:** orcid.org/0000-0001-7764-5593
Received: 04.03.2019, **Accepted:** 04.04.2019

INTRODUCTION

Many xenobiotics pose important threats for both human and environmental health. Pesticides, the most common pollutants, are harmful for biological structures via several mechanisms in acute and long-term exposure.[1-3] Neonicotinoid pesticides as a new class of insecticides that are commonly used instead of organophosphate, and carbamate pesticides have selectively neurotoxic effects on nicotinic acetylcholine receptor. Neonicotinoid pesticides are highly effective insecticides that can disperse in all parts of plants, plant fluids, and fruits that grow on plants. Recent studies revealed that neonicotinoid pesticides can be associated with several adverse effects including decreased sperm production and function, decreased pregnancy rates, increased embryo death, stillbirth, and premature birth in vertebrate and invertebrate species.[4-6]

Acetamiprid [(E)-N-[(6-chloro-3- pyridyl) methyl]-N-cyano-N-methylacetamidine] is one of the most commonly used neonicotinoid class insecticides in many countries for crop pests on agricultural products. In general, acetamiprid has been considered a safe insecticide; however, several different adverse health effects may occur after exposure to acetamiprid as well as other neonicotinoids.[3] In previous studies, it has been reported that acetamiprid showed teratogenic, mutagenic, and genotoxic effects via induction of oxidative stress. However, the data about its cyto- and genotoxic potentials are contradictory.[7-12] As is well known, the worldwide rate of diabetes continues to rise, and the major molecular mechanisms underlying diabetes are increased oxidative stress and altered enzyme functions in pancreatic tissue.[13] Indeed, no association between diabetes risk and neonicotinoid pesticides has been reported. Furthermore, there has been no study on the toxic effects of acetamiprid on the pancreas. Therefore, for the first time, we aimed to investigate the cytotoxic and genotoxic effects of acetamiprid on the AR42J pancreatic cell line and evaluated its oxidative damage potential as an underlying molecular mechanism.

MATERIALS AND METHODS

Chemicals

Acetamiprid, dimethyl sulfoxide (DMSO), sodium dodecyl sulfate (SDS), 3-[4,5-dimethylthiazol-2-yl]-2,5-diphenyl-tetrazolium bromide (MTT), and 2′,7′-dichlorodihydrofluorescein diacetate (H_2DCF-DA) were purchased from Sigma Chemical Co. Ltd. (St. Louis, Missouri, USA). The cell culture medium [Roswell Park Memorial Institute (RPMI 1640)] and other chemicals were purchased from Multicell Wisent (Quebec, Canada), while the disposable materials were purchased from Corning (Amsterdam, the Netherlands). All other chemicals at required biological grade were purchased from Merck (New Jersey, USA).

Cell culture and treatments

The AR42J (CRL1492) cell line was obtained from the American Type Culture Collection (ATCC, Virginia, USA), and for all cell applications incubation was carried out according to the manufacturer's instructions. The cells were grown with 1640 cell culture medium including 10% fetal bovine serum, 100 U/mL penicillin, and 100 mg/mL streptomycin in a humidified incubator in 5% CO_2 at 37 °C. Subculturing was performed every 2-3 days when the cells reached confluence. Prior to exposure cells were seeded into appropriate plasticware and incubated overnight to ensure cell attachment.

Acetamiprid stock solution was prepared by dissolving in 100% DMSO, and stored at -20 °C until the day the assays were conducted. Before the cell treatments acetamiprid was diluted with culture medium to the desired concentrations, and DMSO concentration finalized as 1%. Treatments were performed at a concentration range for 24 h to evaluate dose-dependent effects. All experiments were performed in triplicate on three separate days.

MTT cytotoxicity test

The AR42J cells were placed into 96-well plates ($1x10^4$ cells/100 µL cell culture medium/well). The cells were treated with acetamiprid following overnight incubation at the concentration range of 1-50 mM for 24 h. After 5 mg/mL MTT was added to each well, the cells were again kept for 3 h at 37 °C in the dark. Cell culture medium was used as a growth control, 1% DMSO was used as a solvent control, and 10% SDS was used as a positive control. The wells were washed with poly (butylene succinate) (PBS) twice after 3 h. Following the washing step, 100 µL of DMSO was added, followed by incubation for 5 min on an orbital shaker (150 rpm) for evenly dissolved formazan crystals and optical densities were measured using a microplate reader (Biotek, Epoch, Vermont, USA) at 570 nm. The percentage of inhibition of cell viability for each concentration and the inhibitory concentration 50 (IC_{50}) value were determined.

Comet genotoxicity assay

AR42J cells were placed into 6-well plate as $5x10^5$ cells/2 mL cell culture medium/well and kept overnight for incubation. The cells were exposed to acetamiprid at 1, 2, 4, and 6 mM concentrations and 1% DMSO as a negative control for 24 h. After the cells were detached with trypsin-ethylenediaminetetraacetic acid (EDTA) and washed with PBS twice, the viability of cells was evaluated with the trypan blue test, and cell viability was determined as ≥80% for all concentrations. Next 100 µL of single cell suspension was mixed with 100 µL of prewarmed 0.65% low-melting agarose and then layered on microscope slides coated with 1.5% normal-melting point agarose. After lysing for 1 h at 4 °C, the slides were incubated in cold fresh electrophoresis buffer (0.3 M NaOH, 1 mM EDTA, pH 13) at 4 °C for 20 min for DNA unwinding. The electrophoresis conditions were 4 °C for 20 min (20 V/300 mA). The slides were neutralized in 0.4 M tris-HCl buffer (pH 7.5). DNA staining was performed with 20 mg/mL ethidium bromide dye and evaluated under a fluorescent microscope (Olympus BX53, Olympus, Tokyo, Japan) at 40x10 magnification by Comet Assay IV, Perceptive software (Suffolk, UK). One hundred cells were counted and scored for each concentration and %TDNA and tail intensity were evaluated.[14]

Oxidative stress parameters

A total reactive oxygen species (ROS) assay was performed via (2'-7'-dichlorodihydrofluorescein diacetate) analysis by flow

cytometry. Next 5x10^5 cells/2 mL cell culture medium/well were placed into a 6-well plate. After one day of incubation, the cells were exposed to acetamiprid at 1, 2, 4, and 6 mM concentrations and 1% DMSO as a negative control for 24 h. After 24 h the plates were washed with PBS twice. The cells were incubated with 20 µM H_2DCF-DA at 37 °C for 30 min on a shaker in the dark. They were detached from the plates via trypsinization and resuspended in 150 µL of PBS with 1% bovine serum albumin. Fluorescence intensity was measured by FITC channel with excitation 488 nm and emission 530 nm via an ACEA NovoCyte flow cytometer (San Diego, California, USA). The results were shown as median fluorescence intensity.

Glutathione (GSH) levels were determined by [5,50-dithiobis-2-nitrobenzoic acid) (DTNB)] reagent method described by Beutler.[15] This method is based on DTNB reduction by free SH groups of GSH to 5-mercapto-2-nitrobenzoate. After treatment with acetamiprid, 1 mL of cell lysates was deproteinated with 1.67 g of metaphosphoric acid, 0.2 g of Na_2 EDTA, and 30 g of NaCl solved in distilled water. After that, 2.4 mL of Na_2HPO_4 and 0.3 mL of DTNB were added, followed by centrifugation for 10 min at 3000x *g*. 5-Thio-2-nitrobenzoic acid formation was measured at 412 nm by spectrophotometer. GSH results were expressed as µmol/g protein.[15]

Statistical analysis

The experimental results were analyzed by One-Way ANOVA post hoc Dunnett's t-test and given as mean ± standard deviation. The level of statistical significance was set as p≤0.05. All analyses were performed using SPSS version 20.0 (SPSS Inc., Chicago, Illinois, USA).

RESULTS

Cell viability

The MTT assay is one of the most frequently used, simple, and rapid colorimetric cell viability/cytotoxicity assays and yields quantitative data. This assay is based on reduction of water-soluble yellow tetrazolium salt by the mitochondrial succinate dehydrogenase enzyme in metabolically active/live cells dehydrogenase and quantified color intensity of dissolved formazan crystals by spectrophotometer.[16]

The cytotoxicity of acetamiprid on the AR42J cell line was evaluated with the MTT assay in the dose range of 1-50 mM after 24 h exposure and the IC_{50} value was determined as 12.61 mM (Figure 1).

Comet assay

The alkaline comet assay is a very common method for measuring DNA damage in a single cell suspension via migration of DNA under electrophoresis conditions. It has been reported that the tail intensity value is the most recommended end point for an alkaline comet assay in a dose-dependent manner.[17]

According to the results of the comet assay in the concentration range of 1-6 mM, acetamiprid significantly increased DNA damage in a dose-dependent manner. The mean tail intensity values were significantly increased in all exposure groups compared to the control group (Figure 2).

Oxidative stress parameters

Oxidative damage via ROS plays a key role in different human diseases such as cancer, cardiovascular diseases, diabetes, and neurodegeneration. Dichlorodihydrofluorescein diacetate (DCFH-DA) is a widely used assay that enables direct measurement of the redox state in the cells. This method is very sensitive, easy to use, and cheap and can be used to follow changes in ROS over time.[18]

There were no significant differences between the control and exposure groups according to total ROS levels, which were evaluated by H_2DCF-DA with a flow cytometer. However, the GSH level was significantly reduced in the 6 mM group compared to the control group. It was observed that 6 mM of acetamiprid dramatically reduced GSH level by 98.07% (Figure 3).

DISCUSSION

Widespread use of acetamiprid in agriculture alone or in combination with other insecticides may cause pesticide spread into the environment and the food chain, resulting in toxicity in humans and animals. An increased risk of pancreatic

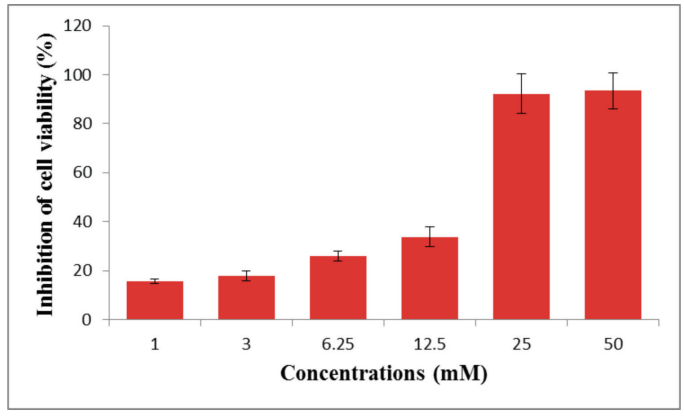

Figure 1. The inhibition of the cell viability values by MTT test in the AR42J cell line

MTT: 3-[4,5-dimethylthiazol-2-yl]-2,5 diphenyl tetrazolium bromide

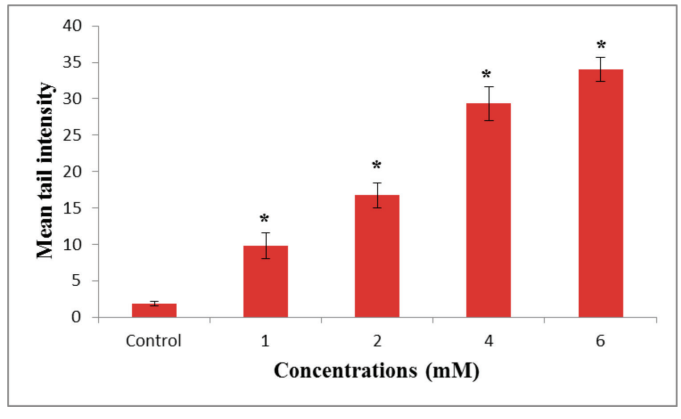

Figure 2. Acetamiprid-induced DNA damage in AR42J cell line at a concentration range of 1-6 mM as observed by comet assay. Representative single cell images clearly indicated that tail intensity was increasing while head of the cell was decreasing in a dose-dependent manner. The error bar represents ± standard deviation and *p<0.05 compared to other groups

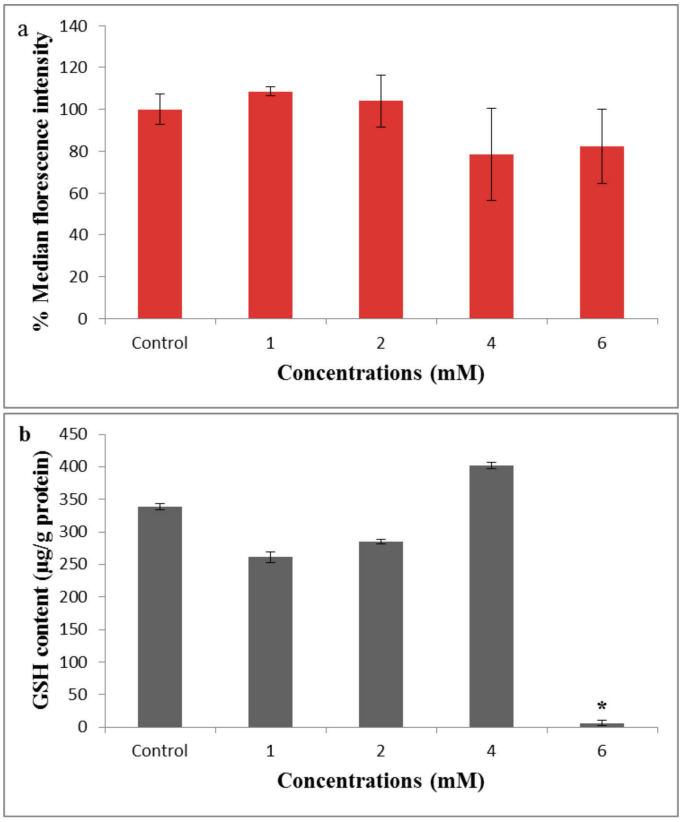

Figure 3. Oxidative damage potential of acetamiprid (1, 2, 4, or 6 mM) evaluated by H_2DCF-DA (a) and GSH (b) assays. The ROS production was expressed as mean fluorescence intensity and GSH levels were expressed as µg/g protein. The error bar represents ± standard deviation and *p<0.05 compared to other groups

GSH: Glutathione, ROS: Reactive oxygen species, H_2DCF-DA: 2′,7′-dichlorodihydrofluorescein diacetate

cancer is found in those in agricultural occupations; however, pesticides' effects on oncogenesis mechanisms have not been extensively evaluated yet.[19,20] There are limited data about the effects of neonicotinoids on pancreatic tissue; moreover, there are no data about acetamiprid's effects on the pancreas. Khalil et al.[13] reported that 0.5 and 1.0 mg/kg bw imidacloprid over 60 days disrupted glucose homeostasis in male rats. In treated groups, the GLUT4 mRNA expression level was decreased and pancreatic islets shrinkage and infiltration of round cells, interlobular congestion, and hemorrhage were observed with histopathologic examination, and also decreased insulin expression in the pancreatic β cells was detected in the imidacloprid-treated groups.

To further examine the potential associations between their usage and toxic profiles for neonicotinoid pesticides, we conducted a study on *in vitro* acetamiprid exposure in a pancreatic cell line. Although there are a few studies on acetamiprid's cyto- and genotoxicity potentials in the literature, there is no *in vitro*/*in vivo* study focusing on the pancreas. It has been reported that the LD_{50} value is the range of 140-417 mg/kg b.w. in rodents and the NOAEL level is 400 ppm in 13 week old mice for acetamiprid.[21] It has been reported in another study that IC_{50} values of acetamiprid on SH-SY5Y and HepG2 cell lines were 2.16 and 3.61 mM, respectively.[22] In our study, the cytotoxicity was evaluated by MTT assay in acetamiprid (1-50 mM) treated AR42J cells after 24 h exposure. The IC_{50} value was calculated as 12.61 mM.

In the same study, significantly increased DNA damage was shown at 500 µM in SH-SY5Y cells.[22] In another study, >50 µM acetamiprid significantly increased micronuclei formation and DNA breaks in IMR-90 human lung cells.[8] Genotoxic effects of acetamiprid on sister chromatid exchange, micronucleus, and chromosomal aberration analysis with 25, 30, 35, and 40 µg/mL doses for 24 and 48 h were shown in human peripheral blood lymphocytes. Micronucleus formation was significantly induced compared to the control group while the proliferation index was decreased.[12] It has been reported that acetamiprid increased micronuclei per cell and chromosomal aberrations in Swiss albino male mice bone marrow depending on concentration with acetamiprid treatment over 60 and 90 days at 4.6 and 2.3 mg/kg/day i.p.[23] According to the results of the comet assay performed with the concentration range of 1-6 mM, acetamiprid significantly induced DNA damage depending on concentration. The different results obtained from several studies can be related to cell types, study duration, and/or method selection.

Oxidative stress mechanisms could underlie the cyto- and genotoxic potentials of neonicotinoid pesticides.[7,8,12] It has been reported that pesticides may impair the redox balance effects in different cells. However, the mechanisms underlying oxidative stress are still not fully understood.[16] There are several studies about the effects of acetamiprid on oxidative stress parameters in different species such as rodents, bacteria, plants, and fish.[24-30] In Wistar rat brain tissue 3.14 mg/kg acetamiprid exposure resulted in increased mitochondrial oxidative stress status that was significant. Decreased oxidative stress parameters were GSH level, GSH peroxidase, and catalase activities. Increased parameters determined were malondialdehyde level, GSH s-transferase, and superoxide dismutase activities.[31] In our study, no significant difference was found between the control and exposure groups according to total ROS levels. However, the GSH levels were significantly different compared to the control at the highest concentration. It was observed that 6 mM acetamiprid dose dramatically reduced GSH level by 98.07%. In earthworms, it has been demonstrated that different concentrations of acetamiprid (0, 0.05, 0.10, 0.25, and 0.50 mg/kg of soil) with different exposure periods (7, 14, 21, and 28 days) increased the ROS levels to varying degrees. Olive tail moment, which indicates DNA damage in the comet assay, increased in a dose-dependent manner, indicating that subchronic acetamiprid exposure might cause oxidative stress and induce DNA damage in earthworms.[24]

Acetamiprid is classified as an "unlikely" human carcinogen according to EPA guidelines and its target organ toxicity data are not clear yet. Acetamiprid's acute oral toxicity category is "II" for rats and its acute inhalation toxicity category is "III" for rabbits. Its NOAEL value for rats is 12.4/14.6 mg/kg/day (M/F) and its LOAEL value for rat is 50.8/56.0 mg/kg/day (M/F). The chronic carcinogenicity NOAEL value for rats is 7.1/8.8 mg/

kg/day (M/F). According to the EPA acetamiprid is not yet classified as genotoxic.[32] A target organ toxicity assessment for further subchronic and chronic *in vivo* studies may clarify the risk caused by acetamiprid for pancreas tissue-based diseases.

CONCLUSION

Under different durations in the pancreatic cell line acetamiprid may affect these oxidative stress parameters significantly. To clarify the oncogenic potential of acetamiprid on pancreatic tissue it is necessary to perform further *in vivo* studies with subchronic or chronic studies with molecular mechanistic observations.

Conflicts of interest: No conflict of interest was declared by the authors. The authors alone are responsible for the content and writing of the paper.

REFERENCES

1. Hamadache M, Benkortbi O, Hanini S, Amrane A, Khaouane L, SI Moussa C. A quantitative structure activity relationship for acute oral toxicity of pesticides on rats: validation, domain of applicationandprediction. J Hazard Mater. 2016;303:28-40.
2. Speck-Planche A, Kleandrova VV, Luan F, Cordeiro MND. Predicting multiple ecotoxicological profiles in agrochemical fungicides: a multi-species chemo informatic approach. Ecotoxicol Environ Saf. 2012;80:308-313.
3. Chakroun S, Ezzi L, Grissa I, Kerkeni E, Neffati F, Bhouri R, Sallem A, Najjar MF, Hassine M, Mehdi M, Haouas Z, Cheikh HB. Hematological, biochemical, and toxicopathic effects of subchronic acetamiprid toxicity in Wistar rats Environ Sci Pollut Res Int 2016;23:25191-25199.
4. Çavaş T, Çinkılıç N, Vatan Ö, Yılmaz D. Effects of fullerenol nanoparticles on acetamiprid induced cytoxicity and genotoxicity in cultured human lung fibroblasts. Pestic Biochem Physiol. 2014;114:1-7.
5. Cimino AM, Boyles AL, Thayer KA, Perry MJ. Effects of neonicotinoid pesticide exposure on human health: a systematic review. Environ Health Perspect. 2017;125:155-162.
6. Mikolić A, Karačonji IB. Imidacloprid as reproductive toxicant and endocrine disruptor: investigations in laboratory animals. Arh Hig Rada Toksikol. 2018;69:103-108.
7. Al-Sarar AS, Abobakr Y, Bayoumi AE, Hussein HI. Cytotoxic and genotoxic effects of abamectin, chlorfenapyr, and imidacloprid on CHOK1 cells. Environ Sci Pollut Res. 2015;22:17041-17052.
8. Çavaş T, Çinkılıç N, Vatan Ö, Yılmaz D, Coşkun M. *In vitro* genotoxicity evaluation of acetamiprid in CaCo-2 cell susing the micronucleus, cometand γH2AX fociassays. Pestic Biochem Physiol 2012;104:212-217.
9. Caldero´n-Segura ME, Go´mez-Arroyo S, Villalobos-Pietrini R, Martínez-Valenzuela C, Carbajal-López Y, del Carmen Calderón-Ezquerro M, Cortés-Eslava J, García-Martínez R, Flores-Ramírez D, Rodríguez-Romero MI, Méndez-Pérez P, Bañuelos-Ruíz E. Evaluation of genotoxic and cytotoxic effects in human peripheral blood lymphocytes exposed *in vitro* to neonicotinoid ınsecticides news. J Toxicol. 2012:612647.
10. Demsia G, Vlastos D, Goumenou M, Matthopoulos DP. Assessment of the genotoxicity of imidacloprid and metalaxyl in cultured human lymphocytesandrat bone-marrow. Mutat Res Genet Toxicol Environ. 2007;634:32-39.
11. Feng S, Kong Z, Wang X, Peng P, Zeng EY. Assessing the genotoxicity of imidacloprid and RH-5849 in human peripheral blood lymphocytes in vitro with comet assay and cytogenetic tests. Ecotoxicol Environ Saf. 2005;61:239-246.
12. Kocaman AY, Topaktaş M. *In vitro* evaluation of the genotoxicity of acetamiprid in human peripheral blood lymphocytes. Environ Mol Mutagen. 2007;48:483-90.
13. Khalil SR, Awad A, Mohammed HH, Nassan MA. Imidacloprid insecticide exposure induces stress and disrupts glucose homeostasis in male rats. Environ Toxicol Pharmacol. 2017;55:165-174.
14. Singh NP, McCoy MT, Tice RR, Schneider EL. A simple technique for quantitation of low levels of DNA damage in individual cells. Exp Cell Res. 1988;175:184-191.
15. Beutler E. Red Cell Metabolism. In: A manual of Biochemical Methods. 2nd ed. New York, NY: Grunneand Stratton: 1975;71-73.
16. Karakaş D, Ari F, Ulukaya E. The MTT viability assay yields strikingly false-positive viabilities although the cells are killed by some plant extracts. Turk J Biol. 2017;41:919-925.
17. Kennedy EK, McNamee JP, Lalonde LP, Jones T, Wilkinson D. Acellular comet assay: a tool for assessing variables influencing the alkaline comet assay. Radiat Prot Dosimetry. 2012;148:155-161.
18. Eruslanov E, Kusmartsev S. Identification of ROS using oxidized DCFDA and flow-cytometry. Methods Mol Biol. 2010;594:57-72.
19. Andreotti G, Freeman LE, Hou L, Coble J, Rusiecki J, Hoppin JA, Silverman DT, Alavanja MCR. Agricultural pesticide use and pancreatic cancer risk in the Agricultural Health Study Cohort. Int J Cancer. 2009; 15:124:2495-2500.
20. Caron-Beaudoin É, Denison MS, Sanderson JT. Effects of neonicotinoids on promoter-specificexpressionand activity of aromatase (CYP19) in human adrenocortical carcinoma (H295R) and primary umbilical vein endothelial (HUVEC) Cells Toxicol Sci. 2016;149:134-144.
21. FAO, Food and Agriculture Organization of the United Nations. Last Accessed Date: 6.12.2018 Available from: http://www.fao.org/fileadmin/templates/agphome/documents/Pests_Pesticides/JMPR/Report11/Acetamiprid.pdf
22. Şenyildiz M, Kilinc A, Ozden S. Investigation of the genotoxic and cytotoxic effects of widely used neonicotinoid insecticides in HepG2 and SH-SY5Y cells. Toxicol Ind Health. 2018:1-9.
23. Bagri P, Jain SK. Assessment of acetamiprid-induced genotoxic effects in bone marrowcells of Swiss albino malemice. Drug Chem Toxicol. 2018;6:1-7.
24. Li B, Xia X, Wang J, Zhu L, Wang J, Wang G. Evaluation of acetamiprid-induced genotoxic and oxidative responses in Eiseniafetida. Ecotoxicol Environ Saf. 2018;19:610-615.
25. Quintana MM, Rivero Osimani V, Magnarelli G, Rovedatti MG, Guiñazú N. The insecticides chlorpyrifos and acetamiprid induce redox imbalance in umbilical cord blood erythrocytes *in vitro*. Pestic Biochem Physiol. 2018;148:87-92.
26. Wang Y, Wu S, Chen J, Zhang C, Xu Z, Li G, Cai L, Shen W, Wang Q. Single and joint toxicity assessment of four currently used pesticides to zebrafish (Danio rerio) using traditional and molecular endpoints. Chemosphere. 2018;192:14-23.
27. Dhouib IB, Annabi A, Doghri R, Rejeb I, Dallagi Y, Bdiri Y, Lasram MM, Elgaaied A, Marrakchi R, Fazaa S, Gati A. Neuroprotective effects of

curcumin against acetamiprid-induced neurotoxicity and oxidative stress in the developing male rat cerebellum: biochemical, histological, and behavioral changes. Environ Sci Pollut Res Int. 2017;24:27515-27524.

28. Yu X, Lu W, Sun R, Guo X, Xu B. Identification and characterization of a novel calcyclinbinding protein (CacyBP) gene from Apisceranacerana. Mol Biol Rep. 2012;39:8053-80563.
29. Ford KA, Gulevich AG, Swenson TL, Casida JE Neonicotinoid insecticides: oxidative stress in planta and metallo-oxidase inhibition J Agric Food Chem. 2011;59:4860-4867.
30. Yao XH, Min H, Lv ZM. Response of superoxide dismutase, catalase, and ATPase activity in bacteria exposed to acetamiprid. Biomed Environ Sci. 2006;19:309-314.
31. Gasmi S, Kebieche M, Rouabhi R, Touahria C, Lahouel A, Lakroun Z, Henine S, Soulimani R. Alteration of membrane integrity and respiratory function of brain mitochondria in the rats chronically exposed to a low dose of acetamiprid. Environ Sci Pollut Res Int. 2017;24:22258-22264.
32. EPA, United States Environmental Protection Agency. Pesticide Fact Sheet, Acetamiprid. Last Accessed Date: 20.01.2019 Available from: https://www3.epa.gov/pesticides/chem_search/reg_actions/registration/fs_PC-099050_15-Mar-02.pdf

Turk J Pharm Sci 2020;17(5):480-485
DOI: 10.4274/tjps.galenos.2018.24572

ORIGINAL ARTICLE

Determination of the Genetic Relationships Among *Salvia* Species by RAPD and ISSR Analyses

Salvia Türleri Arasındaki Genetik İlişkilerin RAPD ve ISSR Analizleriyle Belirlenmesi

Serap SUNAR[1]*, Mustafa KORKMAZ[2], Burcu SIĞMAZ[3], Güleray AĞAR[3]

[1]Erzincan University Faculty of Pharmacy, Department of Pharmaceutical Botany, Erzincan, Turkey
[2]Erzincan University Faculty of Science and Arts, Department of Biology, Erzincan, Turkey
[3]Atatürk University Faculty of Science, Department of Biology, Erzurum, Turkey

ABSTRACT

Objectives: *Salvia* L. is the largest genus of the family Lamiaceae, which includes approximately 1000 species. According to recent studies, 100 *Salvia* species in total grow in Turkey. At the same time, 53% of them are endemic. The purpose of this study was to investigate the genetic relationships among 15 *Salvia* species that grow in wild conditions in Turkey's Eastern Anatolia region.

Materials and Methods: The genetic relationships among 15 *Salvia* species were investigated using inter-simple sequence repeat (ISSR) and random amplified polymorphic-DNA (RAPD) profiles in the present study. Thirteen ISSR primers and 11 RAPD primers were utilized. The ISSR and RAPD data were combined to construct the unweighted pair group method using arithmetic average cluster.

Results: Based on the RAPD and ISSR data, the *Salvia* species were classified into six groups. As a result of the combined analysis, it was shown that similarities between the species varied between 0.54 (*S. rosifolia-S. sclarea, S. rosifolia-S. limbata, and S. staminea-S. verticillata*) and 0.93 (*S. sclera-S. divaricata*).

Conclusion: The findings show that the two markers represent powerful instruments for assessing the genetic diversity and relationships among *Salvia* species.

Key words: *Salvia* species, genetic diversity, ISSR, RAPD

ÖZ

Amaç: *Salvia* L., yaklaşık 1000 tür içeren Lamiaceae familyasının en büyük cinsidir. Son çalışmalara göre, Türkiye'de toplam 100 *Salvia* türü yetişmektedir. Aynı zamanda, türlerin %53'ü endemiktir. Bu çalışmada, Türkiye'nin Doğu Anadolu Bölgesi'nde doğal olarak yetişen 15 *Salvia* türü arasındaki genetik çeşitliliğin değerlendirilmesi amaçlanmıştır.

Gereç ve Yöntemler: On beş *Salvia* türü arasındaki genetik çeşitlilik, random amplifiye polimorfik DNA (RAPD) ve ISSR DNA profilleri kullanılarak araştırıldı. On üç ISSR primeri ve on bir RAPD primeri kullanıldı. Aritmetik ortalamayı kullanan ağırlıksız çift grup metodu kümelenmesi ISSR ve RAPD verilerinin kombinasyonu ile gerçekleştirildi.

Bulgular: RAPD ve ISSR verilerinin sonuçlarına göre, *Salvia* türleri altı gruba ayrılmıştır. Kombine analiz sonucunda türlerin benzerliklerinin 0,54 (*S. rosifolia-S. sclarea, S. rosifolia-S.limbata ve S. staminea-S. verticillata*) ve 0,93 (*S. sclera-S. divaricata*) arasında değiştiği görülmüştür.

Sonuç: Bu çalışmada, hem RAPD hem de ISSR belirteçlerinin *Salvia* türleri arasındaki genetik çeşitliliği incelemek için kullanılabileceği gösterilmiştir.

Anahtar kelimeler: *Salvia* türleri, genetik çeşitlilik, ISSR, RAPD

***Correspondence: E-mail:** ssunar@erzincan.edu.tr, **Phone:** +90 506 533 57 26 **ORCID-ID:** orcid.org/0000-0002-2011-1117
Received: 31.08.2018, **Accepted:** 15.11.2018

INTRODUCTION

Salvia L. is the largest genus of the family Lamiaceae. Central and South America, Western Asia (Iran, Afghanistan, Turkey, and Russia), Eastern Asia, Africa, and Europe are the main distribution regions of *Salvia* species. Western Asia is the second richest region with ca. 200 species of the genus after America with ca. 500 species.[1,2] Turkey is among the important diversity centers of *Salvia*.[1] According to the Flora of Turkey there are 86 species.[3] According to recent studies, 100 *Salvia* species in total grow in Turkey. At the same time, 53% of them are endemic.[2]

Species have been utilized as traditional medication for the mild sickness of the stomach and the common cold since ancient times.[4] Moreover, their volatile oils are utilized as an anti-inflammatory agent and antiseptic and, at the same time, a pleasurable sensory feeling is produced by them in the mouth and throat.[5,6] *Salvia* species have antibacterial, antifungal, antimycobacterial, cytotoxic, antitumor, cardiovascular, antifeedant, and insecticidal effects.[7] *Salvia* species have the following essential oil composition: α-pinene, β-pinene, 1.8-cineole, camphor, borneol, b-thujone, thymol, caryophyllene, caryophyllene oxide, and 1-octadecanol.[5,8] Several *Salvia* species were also studied to investigate their antioxidant and antibacterial properties.[5,7,9,10] Different properties of *Salvia* species growing around Erzincan Province were investigated in previous studies. Polat et al.[11] investigated the micromorphological and anatomical characteristics of three endemic *Salvia* species. The ethnobotanical uses of some *Salvia* species were investigated in and around Erzincan by Korkmaz and Karakuş.[12]

It has been confirmed that molecular markers are highly estimable for judicial, biodiversity, and mapping practices. Sufficiently high polymorphism enables the component bands of the fingerprints to function as genetic markers, with the distinction and recombination of the markers, which are utilized for the building of genetic maps.[13]

Various kinds of molecular markers, for example, random amplified polymorphic DNA (RAPD),[14] inter-simple sequence repeats (ISSRs),[15] and amplified fragment length polymorphism (AFLP),[16] have been improved and utilized widely in the investigation of genetic relationships, germplasm management, and genetic diversity, together with the developments achieved in plant molecular biology. Scientists extensively utilize ISSRs, which take place among the above-mentioned molecular markers, in different spheres of plant improvement due to their being simple and cost effective.[17] Variation in species is also studied by RAPD.[14]

The aim of the present study was to evaluate the genetic diversity present in 15 *Salvia* species, employing two marker systems.

MATERIALS AND METHODS

The material used

Leaf specimens of 15 *Salvia* taxa from Turkey were examined. The following species were analyzed: *S. cryptantha* Montbret and Aucher, *S. caespitosa*, *S. candidissima*, *S. nemorosa* L., *S. sclarea* L., *S. verticillata* L., *S. verticillata* L. subsp. *amasiaca* (Freyn & Bornm.) Bornm., *S. staminea* Montbret and Aucher ex Benth., *S. multicaulis* Vahl, *S. limbata* C.A.Mey., *S. aethiopis* L., *S. rosifolia* Sm., *S. virgata* Jacq., *S. pachhystachya* Trauv., and *S. divaricata* Montbret and Aucher ex Benth. Eleven examples of Irano-Turanian elements, 1 Euro-Siberian, and 3 of unknown region were among the samples examined. Table 1 includes information on the phytogeographical regions, endemism, and record numbers of *Salvia* taxa.

In field studies, plant specimens gathered from various regions of Turkey represent the species. Scientific names of the plant specimens were determined with the help of Davis[18] and Guner[19] after herbarium studies had been carried out. All of the taxon names were checked in the literature.[20,21] Furthermore, identification of the phytogeographical regions and endemic taxa was performed. Irano-Turanian elements constitute the majority of the taxa (11 taxa). There were 4 endemic taxa (27%). Herbarium samples of all taxa were deposited at the Herbarium of Erzincan University.

Chemicals

The DNA isolation of *Salvia* species was performed by the combination of cetyltrimethyl ammonium bromide isolation methods with minor changes.[22] Nanodrop (QIAGEN) was used for the determination of the quantity and purity of genomic DNA and 0.8% agarose gel electrophoresis was utilized against the known concentrations to prove this.

Random amplified polymorphic DNA

Eleven primers out of 23 were amplified polymorphic amplicons and used for the analyses of genetic diversity in RAPD-polymerase chain reactions (PCR) (Table 2). PCR amplifications were performed in SENSEQUEST Thermal Cycle in a total volume of 20 µL, 1X PCR buffer (without $MgCl_2$) 0.25-µM deoxyribonucleoside triphosphate (dNTP), 0.5 mM primer, 2.5 mM $MgCl_2$, and 1.5 U Taq DNA polymerase (BioLab M0267S). Initial denaturation at 95 ˚C for 5 min with the following 46 cycles at 94 ˚C for 1 min at various annealing temperatures for all primers for 1 min, 72 ˚C for 2 min, a penultimate step of 15 min at 72 ˚C, and a final extension of 10 min at 4 ˚C constituted the amplification profile. The PCR products (20 mL) were blended with 6X gel loading buffer (3 mL) and exposed to agarose. Then electrophoresis was applied to separate them by means of 1% agarose gel in 0.5X tris, borate, and EDTA (TBE) buffer with 80 V constant voltages for 150 min. The gels were dyed with Etd-Br visualized under ultraviolet light and the gel visualization system was used to take photographs of them.

Inter-simple sequence repeats

Fifteen primers were used for ISSR amplifications. Two primers of these (ISSR UBC844B and ISSR UBC822) did not give amplification in PCR reactions. The other 13 primers were amplified polymorphic amplicons (Table 3). The PCR mixture (20 µL) was prepared as follows: 2.0 µL of 10X PCR buffer, 0.5 µL of dNTPs (10 mM), 2 µL of magnesium chloride (25 mM), 1.0 µL of primer (5 mM), 0.5 µL of polymerase enzyme (Taq)

Table 1. Taxonomic information about the *Salvia* species studied

No	Taxon name	Record no	Locality	Phytogeographical region	Endemic
1	***S. cryptantha*** Montbret & Aucher ex Benth.	Korkmaz 3649	Erzincan, Çayırlı	Ir.-Tur.	+
2	***S. caespitosa*** Montbret & Aucher ex Benth.	Korkmaz 3891	Erzincan, Çayırlı	Ir.-Tur.	+
3	***S. candidissima*** Vahl	Korkmaz 2887; 3896	Erzincan, Çayırlı	Ir.-Tur.	-
4	***S. nemorosa*** L.	Korkmaz 2805	Erzincan, Çayırlı	-	-
5	***S. sclarea*** L.	Korkmaz 2795	Erzincan, Çayırlı	-	-
6	***S. verticillata*** L.	Korkmaz 2994; 2792	Erzincan, Çayırlı	Eur.-Sib.	-
7	***S. verticillata*** L. subsp. ***amasiaca*** (Freyn & Bornm.)	Korkmaz 107	Erzincan, Çayırlı	Ir.-Tur.	-
8	***S. staminea*** Montbret & Aucher ex Benth.	Korkmaz 3858	Erzincan, Çayırlı	Ir.-Tur.	-
9	***S. multicaulis*** Vahl	Korkmaz 3516	Erzincan, Çayırlı	Ir.-Tur.	-
10	***S. limbata*** C.A.Mey.	Korkmaz 2992	Erzincan, Çayırlı	Ir.-Tur.	-
11	***S. aethiopis*** L.	Korkmaz 3221	Erzincan, Çayırlı	-	-
12	***S. rosifolia*** Sm.	Korkmaz 3268	Erzincan, Çayırlı	Ir.-Tur.	+
13	***S. virgata*** Jacq.	Korkmaz 3217	Erzincan, Çayırlı	Ir.-Tur.	-
14	***S. pachhystachya*** Trautv.	Korkmaz 2228	Erzincan, Ergan Mountain	Ir.-Tur.	-
15	***S. divaricata*** Montbret & Aucher ex Benth	Korkmaz 2641	Erzincan, Ergan Mountain	Ir.-Tur.	+

Ir.: Iran, Tur.: Turkey, Sib.: Siberian, Eur.: Europe

Table 2. Primers and sequences used in RAPD amplification

RAPD primers	Sequence (5'-3')	Length of amplified bands	No of bands	No of monomorphic bands	No. of polymorphic bands	Polymorphism ratio (%)
OPA-1	CAGGCCCTTC	2238-444	15	0	15	100
OPA-2	TGCCGAGCTG	2941-433	16	0	16	100
OPA-4	TGCCGAGCTG	1649-400	12	0	12	100
OPA-6	AATCGGGCTG	2088-600	11	0	11	100
OPB-8	CTGCTGGGAC	2439-419	18	0	18	100
OPB-10	GGTCCCTGAC	1500-232	11	0	11	100
OPH-18	GTCCACACGG	958-183	8	0	8	100
OPW-8	GAATCGGCCA	1945-566	13	0	13	100
OPY-6	GACTGCCTCT	1873-353	15	0	15	100
OPY-16	AAGGCTCACC	1174-200	10	0	10	100
OPH-17	CACTCTCTCTC	1790-351	14	0	14	100

RAPD: Random amplified polymorphic DNA

(250 units), 13 µL of distilled water, and 1.0 µL of genomic DNA sample (100 ng/µL). Initial denaturation at 94 °C for 4 min with the following 35 cycles at 94 °C for 0.30 min, at various annealing temperatures for all primers for 0.35 min, 72 °C for 1 min, a penultimate step of 5 min at 72 °C, and a final extension of 10 min at 4 °C constituted the amplification profile. The PCR products (20 mL) were blended with 6X gel loading buffer (3 mL) and exposed to agarose. Then electrophoresis was applied to separate them by means of 2% agarose gel in 0.5X TBE buffer with 80 V constant voltage for 150 min. The gels were dyed with Etd-Br visualized under UV light and the gel visualization system was used to take photographs of them.

Table 3. Primers and sequences used in ISSR amplification

ISSR primers	Sequence (5'-3')	Length of amplified bands	No. of bands	No. of. monomorphic bands	No. of polymorphic bands	Polymorphism ratio (%)
ISSR UBC811	GAGAGAGAGAGAGAGAC	1935-276	15	0	15	100
ISSR UBC815	CTCTCTCTCTCTCTCTG	1246-408	11	0	11	100
ISSR UBC826	ACACACACACACACACC	936-362	7	0	7	100
ISSR UBC840	GAGAGAGAGAGAGAGATT	1303-241	12	0	12	100
ISSR UBC844A	CTCTCTCTCTCTCTCTGC	1592-378	13	0	13	100
ISSR UBC845	CTCTCTCTCTCTCTCTTT	2878-391	18	0	18	100
ISSR UBC852	TCTTCTTCTCTCTCTCAA	1432-592	7	0	7	100
ISSR 8081	GAGAGAGAGAGAGAGAGAC	2040-303	14	0	14	100
ISSR 8082	CTCTCTCTCTCTCTCTCTG	3483-441	14	0	14	100
ISSR 17889A	GTGTGTGTGTGTCC	1268-337	17	0	17	100
ISSR HB12	CAGCAGCAGGC	1392-408	10	0	10	100
ISSR HBS10	GAGAGAGAGAGACC	1362-344	11	0	11	100
ISSR UBC834	AGAGAGAGAGAGAGAGTT	1442-458	11	0	11	100

ISSR: Inter-simple sequence repeat

Statistical analysis

The Total Lab TL120 program was utilized for the assessment of the ISSR and RAPD patterns. The scoring of PCR products was performed as presence (1) and absence (0) of bands. The Jaccard (1908) similarity index was calculated by using the data, and a dendrogram was created based on the unweighted pair group method using arithmetic average.

RESULTS AND DISCUSSION

First, screening of 23 RAPD primers was performed against *Salvia* species, and 143 distinct reproducible bands in total with 10.2 bands on average per primer were produced by 11 primers. The products amplified varied between 183 and 2941 bp in size. All (100%) of the 143 bands acquired were polymorphic. Their division into four clusters was enabled by the construction of a dendrogram in accordance with the RAPD data of *Salvia* species (Figure 1).

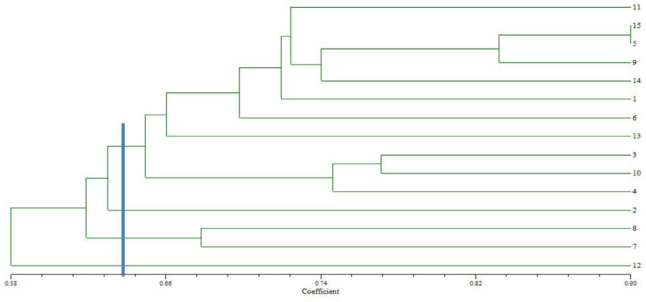

Figure 1. RAPD marker-based UPGMA clustering for *Salvia* species

1. *Salvia cryptantha*, 2. *S. caespitosa*, 3. *S. candidissima*, 4. *S. nemorosa*, 5. *S. sclarea*, 6. *S. verticillata*, 7. *S. verticillata subsp. amasiaca*, 8. *S. staminea*, 9. *S. multicaulis*, 10. *S. limbata*, 11. *S. aethiopis*, 12. *S. rosifolia*, 13. *S. virgata*, 14. *S. pachhystachya*, 15. *S. divaricata*

RAPD: Random amplified polymorphic DNA, UPGMA: Unweighted pair group method using arithmetic averag

The first cluster included *S. cryptantha*, *S. candidissima*, *S. nemorosa*, *S. sclarea*, *S. verticillata*, *S. multicaulis*, *S. limbata*, *S. aethiopis*, *S. virgata*, *S. pachhystachya*, and *S. divaricata*.

The second one included *S. caespitosa*.

The third one included *S. verticillata* subsp. *amasiaca* and *S. staminea*.

The fourth cluster included *S. rosifolia*.

The most significant likeness was identified between *S. rosifolia* and *S. caespitosa* (0.50), while the most significant difference was determined between *S. divaricata* and *S. sclarea* (0.90).

According to the RAPD data, most of the species (seven from 11 species) in the first cluster were Irano-Turanian phytogeographical region elements of Turkey (Table 1; Figure 1). Both of the most similar species (*S. rosifolia* and *S. caespitosa*) are Irano-Turanian phytogeographical region elements and endemic species.

To perform cultivar identification, 13 ISSR primers that demonstrated reproducible and polymorphic patterns were selected and produced 160 bands (polymorphic) in total, with 12.3 bands on average per primer. There was a variation from 241 to 3483 base pairs in size. The ISSR data of *Salvia* species were used to construct a dendrogram, which enabled their division into six clusters (Figure 2).

The first cluster included *S. cryptantha*, *S. candidissima*, *S. sclarea*, *S. multicaulis*, *S. limbata*, *S. aethiopis*, *S. virgata*, *S. pachhystachya*, and *S. divaricata*.

The second one included *S. verticillata*.

The third cluster included *S. nemorosa*.

The fourth cluster included *S. verticillata* subsp. *amasiaca* and *S. staminea*.

The fifth cluster included *S. rosifolia*.

The sixth cluster included *S. caespitosa*.

The most significant likeness was identified between *S. caespitosa* and *S. divaricata* (0.47), while the most significant difference was determined between *S. divaricata* and *S. sclera* (0.95).

According to the ISSR data, most of the species (seven from nine species) in the first cluster were Irano-Turanian phytogeographical region elements of Turkey (Table 1; Figure 2). Both of the most similar species (*S. divaricata* and *S. caespitosa*) are Irano- Turanian phytogeographical region elements and endemic species.

The construction of a dendrogram was performed according to the combined data acquired from the RAPD and ISSR marker analyses (Figure 3).

The first cluster included *S. cryptantha*, *S. candidissima*, *S. sclarea*, *S. multicaulis*, *S. limbata*, *S. aethiopis*, *S. virgate*, *S. pachhystachya*, and *S. divaricata*.

The second cluster included *S. verticillata*.

The third cluster included *S. nemorosa*.

The fourth cluster included *S. staminea* and *S. verticillata* subsp. *amasiaca*.

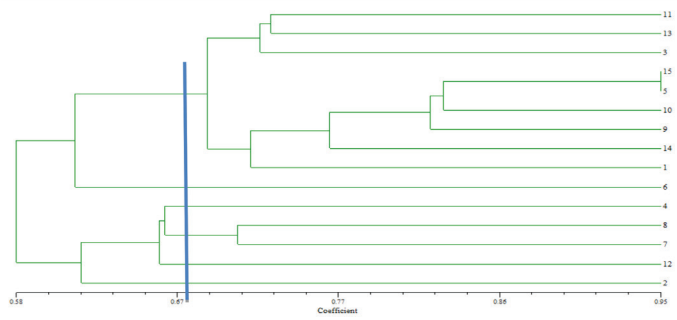

Figure 2. ISSR marker-based UPGMA clustering for *Salvia* species

1. *Salvia cryptantha*, 2. *S. caespitosa*, 3. *S. candidissima*, 4. *S. nemorosa*, 5. *S. sclarea*, 6. *S. verticillata*, 7. *S. verticillata subsp. amasiaca*, 8. *S. staminea*, 9. *S. multicaulis*, 10. *S. limbata*, 11. *S. aethiopis*, 12. *S. rosifolia*, 13. *S. virgata*, 14. *S. pachhystachya*, 15. *S. divaricata*

ISSR: Inter-simple sequence repeat, UPGMA: Unweighted pair group method using arithmetic averag

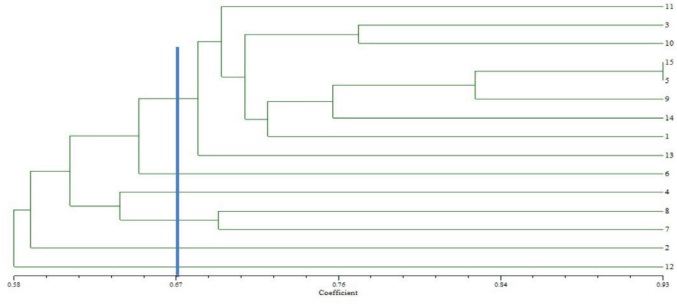

Figure 3. RAPD-ISSR marker-based UPGMA clustering for Salvia species

1. *Salvia cryptantha*, 2. *S. caespitosa*, 3. *S. candidissima*, 4. *S. nemorosa*, 5. *S. sclarea*, 6. *S. verticillata*, 7. *S. verticillata subsp. amasiaca*, 8. *S. staminea*, 9. *S. multicaulis*, 10. *S. limbata*, 11. *S. aethiopis*, 12. *S. rosifolia*, 13. *S. virgata*, 14. *S. pachhystachya*, 15. *S. divaricata*

RAPD: Random amplified polymorphic DNA, ISSR: Inter-simple sequence repeat, UPGMA: Unweighted pair group method using arithmetic averag

The fifth cluster included *S. caespitosa*.

The sixth cluster included *S. rosifolia*.

As a result of the combined analysis, it was determined that similarities of the species varied between 0.54 (*S. rosifolia-S. sclarea*, *S. rosifolia-S. limbata*, and *S. staminea-S. verticillata*) and 0.93 (*S. sclera-S. divaricata*).

The most significant difference was determined between *S. sclera* and *S. divaricata* in RAPD, ISSR, and the combined data produced from RAPD and ISSR. Differently from *S. sclera*, *S. divaricata* is an Irano-Turanian phytogeographical region element and endemic species of Turkey.

The descriptions of morphological and agronomic properties and isozyme examination were constituted for evaluating the relationship among *Salvia* species. Morphological examinations have a number of limitations, which can be eliminated by the use of molecular markers with good reproducibility and high sensitivity.[23] Molecular markers showing polymorphism at the level of DNA have been regarded as an important instrument used to assess plant genetic diversity characterization.[24,25]

To characterize *Salvia* species, different types of molecular markers, for example, RAPD, ISSR,[26,27] AFLP,[28,29] SSR,[28] and sequence-related amplified polymorphism (SRAP),[27] have been employed with great success. Agar et al.[26] used RAPD profiles to study genetic relationships in eight *Salvia* taxa. They showed that RAPD profiles were useful for the determination of genetic profiles that can be used to identify *Salvia* species. In another study, Song et al.[27] used ISSR and SRAP markers to assess the level of genetic diversity in *S. miltiorrhiza*. The results showed that these markers were effective and reliable in evaluating the degree of genetic variation in *S. miltiorrhiza*.

RAPD and ISSR represent an easy and effective marker system used to assess and determine genetic diversity among plant species. The ISSR technique has a number of benefits, such as combining the majority of the advantages of AFLP and SSR markers, providing higher reproducibility when compared to RAPD, identifying a higher rate of genomic polymorphisms when compared to RFLP, and being more cost-efficient when compared to AFLP.[29-31]

RAPD and ISSR markers were used to measure the genetic diversity among eight species of *Salvia* collected from different locations in Iran.[32] In our study, RAPD and ISSR combined data obtained from marker assays showed that *S. limbata* and *S. aethiopis* were in the same group just like in that study. *S. verticillata* and *S. nemorosa* species were also observed in separate groups.

ISSR and RAPD markers revealed findings that were almost independent of each other among *Salvia* species. Therefore, an especially positive correlation was determined for the ISSR and RAPD analysis of genetic relations among *Salvia* species.

CONCLUSION

The findings show that these two markers represent powerful instruments used to assess the genetic diversity and relations among *Salvia* species.

ACKNOWLEDGEMENTS

The authors would like to thank the Office of Scientific Research Projects of Erzincan University (EUBAP-SAGE-080715-0166) for its financial support.

Conflicts of interest: No conflict of interest was declared by the authors. The authors alone are responsible for the content and writing of the paper.

REFERENCES

1. Walker JB, Sytsma KJ. Staminal evolution in the genus *Salvia* (Lamiaceae): Molecular phylogenetic evidence for multiple origins of the staminal lever, Annals of Botany. 2007;100:375-391.
2. Celep F, Karabacak O, Malekmohammadi M, Fidan M, Dogan M. First record of Psylliostachys spicata (Plumbaginaceae) and confirmation of Salvia pratensis (Lamiaceae) from Turkey and taxonomic status of *Salvia* ertekinii, Turkish Journal of Botany. 2015;40:226-230.
3. Hedge IC, Salvia L. In: Davis PH (ed) Flora of Turkey and East Aegean Islands, Edinburgh; University of Edinburgh Press; 1982:400-461.
4. Altun A, Unal M, Kocagoz T, Goren C. Essential oil compositions and antimicrobial activity of *Salvia* species, JEOBP. 2007;10:251-258.
5. Baytop T. Therapy with Medicinal Plants in Turkey (Past and Present), İstanbul; Nobel Tıp Kitapevleri; 1999.
6. Ulubelen A. III. Chemical constituents terpenoids in the genus *Salvia*. In Medicinal and Aromatic Plants Book from C.H.I.P.S. SAGE Kintzios SE (ed) The Genus Salvia, Harwood Academic Publishers: 2000:55.
7. Topçu G, Gören AC. Biological activity of diterpenoids isolated from Anatolian Lamiaceae plants, Rec Nat Prod. 2007;1:1.
8. Demirci B, Baser KHC, Yildiz B, Bahcecioglu Z. Composition of the essential oils of six endemic *Salvia* spp. from Turkey, Flavour Fragr J. 2003;18:116.
9. Öksüz S, Kolak U, Johansson CB, Çelik C, Voelter W. Antibacterial diterpenes from the roots of Salvia viridis, Planta Med. 2000;66:458-462.
10. Kabouche A, Kabouche Z, Öztürk M, Kolak U, Topçu G. Antioxidant abietane diterpenoids from *Salvia* barrelieri, Food Chem. 2207;102:1281-1287.
11. Polat R, Cakilcioglu U, Selvi S, Turkmen Z, Kandemir A. The anatomical and micromorphological properties of three endemic and medicinal *Salvia* species (Lamiaceae) in Erzincan (Turkey), Plant Biosystems - An International Journal Dealing with all Aspects of Plant Biology. 2015;151:63-73.
12. Korkmaz M, Karakuş S. Traditional uses of medicinal plants of Uzumlu district Erzincan Turkey, Pakistan Journal of Botany. 2015;47:125-134.
13. Botstein D, White RL, Skolnick M, Davis RW Construction of a genetic linkage map using restriction fragment length polymorphisms, Am J Hum Genet. 1980;32;314-331.
14. Vos P, Hogers R, Bleeker M, Reijans M, van der Lee T, Hornes M, Frijters A, Pot J, Peleman J, Kuiper M, Zabeau M. AFLP:A new technique for DNA ingerprinting, Nucleic Acids Res. 1995;21:4407-4414.
15. Williams JG, Kubelik AR, Livak KJ, Rafalski JA, Tingey SV, DNA polymorphisms amplified by arbitrary primers are useful as genetic markers, Nucleic Acids Res. 1990;18;6531-6535.
16. Meyer W, Mitchell TG, Freedman EZ, Vilgays R. Hybridization probes for conventional DNA fingerprinting used as single primers in the polymerase chain reaction to distinguish strains of Cryptococcus neoformans, J Clin Microbiol. 1993;31:2274-2280.
17. Reddy MP, Sarla N, Siddiq EA. Inter simple sequence repeat (ISSR) polymorphism and its application in plant breeding, Euphytica. 2002;128:9-17.
18. Davis PH. Flora of Turkey and the East Aegion Islands, Edinburg; Edinburg University Press; 1982.
19. Guner A. A check list of the flora of Turkey (Vascular plants), Flora Dizisi 1, İstanbul; Nezahat Gökyiğit Botanical Garden Publications; 2012.
20. The Plant List. Last Accessed Date: 2015. Available from:http://www.theplantlist.org
21. Turkish Plants Data Service (TUBİVES) Last Accessed Date: 2015. Available from: http://www.tubives.com 2015
22. Baris O. Determination of genetic profiles and biological activities of some Salvia species in East Anatolia, Ataturk University, Turkey. 2004.
23. Sarwat M, Nabi G, Das S, Srivastava PS. Molecular markers in medicinal plant biotechnology: past and present. Crit Rev Biotechnol. 2012;32:74-92.
24. Li J, Schulz B, Stich B. Population structure and genetic diversity in elite sugar beet germplasm investigated with SSR markers. Euphytica. 2010;175:35-42.
25. Keneni G, Bekele E, Imtiaz M, Dagne K, Getu E, Assefa F. Genetic diversity and population structure of Ethiopian chickpea (*Cicer arietinum L.*) germplasm accessions from different geographical origins as revealed by microsatellite markers. Plant Mol Biol Report. 2011;30:654-665.
26. Agar G, Adiguzel A, Baris O, Gulluce M and Sahin F. Phenotypic and genetic variation of some *Salvia* species grown in eastern anatolia region of Turkey. Asian Journal of Chemistry. 2008;20:3935-3944.
27. Song Z, Li X, Wang H, Wang J. Genetic diversity and population structure of *Salvia* miltiorrhiza Bge. in China revealed by ISSR and SRAP, Genetica 138, 241-249, 2010.
28. Guo BL, Feng YX, Zhao YJ. Review of germplasm resources studies on Salvia miltiorrhiza. China Journal of Chinese Materia Medica. 2002;27:492-495.
29. Yang D, Ma P, Liang X, Liang Z, Zhang M, Shen S, Liu H, Liu Y. Metabolic profiles and cDNA-AFLP, Analysis of *Salvia* miltiorrhiza and Salvia castanea Diel f. tomentosa stib. PloS One 2012;7:e29678.
30. Deng KJ, Zhang Y, Xiong BQ, Peng JH, Zhang T, Zhao XN, Ren ZL. Identification characterization and utilization of simple sequence repeat markers derived from *Salvia* miltiorrhiza expressed sequence tags. Acta Pharmaceutica Sinica. 2009;44:1165-1172.
31. Culley TM, Sbita SJ, Wick A. Population genetic effects of urban habitat fragmentation in the perennial herb Viola pubescens (Violaceae) using ISSR markers. Ann Bot. 2007;100:91-100.
32. Javan ZS, Rahmani F, Heidari R. Assessment of genetic variation of genus *Salvia* by RAPD and ISSR markers. Aust J Crop Sci. 2012;6:1068-1073.

Turk J Pharm Sci 2020;17(5):486-491
DOI: 10.4274/tjps.galenos.2019.24445

ORIGINAL ARTICLE

Design and *In Vitro* Characterization of Orally Disintegrating Modified Release Tablets of Naproxen Sodium

Naproksen Sodyumun Ağızda Dağılan Değiştirilmiş Salım Tabletlerinin Tasarımı ve *İn Vitro* Karakterizasyonu

Amjad HUSSAIN[1]*, Maham MISBAH[1], Nasir ABBAS[1], Muhammad IRFAN[2], Muhammad Sohail ARSHAD[3], Rahat SHAMIM[1], Nadeem Irfan BUKHARI[1], Faisal MAHMOOD[1]

[1]University College of Pharmacy, University of the Punjab, Lahore, Pakistan
[2]Department of Pharmaceutics, Faculty of Pharmaceutical Sciences, GC University Faisalabad, Pakistan
[3]Faculty of Pharmacy, Bahauddin Zakariya University, Multan, Pakistan

ABSTRACT

Objectives: The aim of this study was to prepare orally disintegrating, slow release tablets of naproxen sodium for prompt onset and sustained action required in many types of acute pain.

Materials and Methods: Tablet formulations containing varying concentrations of croscarmellose sodium (a superdisintegrant) and Soluplus® (as release modifier) were prepared by wet granulation method using a single punch tablet machine. The prepared granules were evaluated for their bulk properties and the tablets were evaluated for hardness, disintegration time, and drug release profiles.

Results: The results showed that the granules so prepared have good flow and compressional properties. A disintegration time of tablets <30 s was achieved by selecting an optimum concentration of croscarmellose sodium. The drug release from the tablets was sustained for 2 h by incorporating a suitable amount of Soluplus®.

Conclusion: This study examined the use of Soluplus® (a novel solubilizer) for the first time as a release modifier of API from tablets.

Key words: Orally disintegrating tablets, modified release tablets, naproxen sodium, Soluplus®

ÖZ

Amaç: Bu çalışmanın amacı, birçok akut ağrı tipinde gerekli olan hızlı ve sürekli etki için ağızda dağılan, yavaş salımlı naproksen sodyum tabletlerinin hazırlanmasıdır.

Gereç ve Yöntemler: Farklı konsantrasyonlarda kroskarmeloz sodyum (bir süper dağıtıcı) ve Soluplus® (salım değiştirici olarak) içeren tablet formülasyonları, tek zımbalı tablet makinesi kullanılarak ıslak granülasyon yöntemi ile hazırlandı. Hazırlanan granüller, yığın özellikleri açısından değerlendirildi ve tabletler, sertlik, parçalanma süresi ve ilaç salım profilleri açısından değerlendirildi.

Bulgular: Bu şekilde hazırlanan granüllerin iyi akış ve sıkıştırma özelliklerine sahip olduğu tespit edildi. Optimum kroskarmeloz sodyum konsantrasyonu seçilerek <30 saniyelik bir tablet parçalanma süresine ulaşıldı. Tabletlerden ilaç salımı, uygun miktarda Soluplus® eklenerek 2 saat süreyle sürdürüldü.

Sonuç: Bu çalışmada, Soluplus®'un (yeni bir çözücü) ilk kez tabletlerden API'nın salım değiştiricisi olarak kullanımını araştırıldı.

Anahtar kelimeler: Ağızda dağılan tabletler, değiştirilmiş salım tabletleri, naproksen sodyum, Soluplus®

*Correspondence: **E-mail:** +924299211616, **Phone:** amjad_husein@hotmail.com **ORCID-ID:** orcid.org/0000-0002-9427-2677
Received: 08.05.2019, **Accepted:** 22.07.2019

INTRODUCTION

The design and manufacture of solid oral dosage forms (tablets and capsules) are widespread as the oral route is preferred by both healthcare professionals[1] and patients.[2,3] The main advantages include: easy for self-administration,[4] cost-effective[5] highly stable dosage forms, and dispensing in more ready to administer forms.[4] On the other hand, some problems are also associated with the use of solid oral dosage forms in conventional or immediate release tablets such as the frequent administration and small residence time of the drug in the plasma due to its short half-life, leading to fluctuation in plasma level and noncompliance by the patients due to frequent administration. The development of modified release tablets is an advancement in the design of tablets that overcomes these problems associated with the conventional tablet design and promotes a constant plasma level and improves patient compliance.[6,7]

Although these modified release tablets overcome several problems associated with conventional tablets, they also possess the drawback of being larger than the immediate release tablets of the same drug. This makes them difficult to swallow, particularly for geriatric patients and those suffering from dysphagia, a condition marked by difficulty in swallowing, which is reported in about 35% of the general population, 30-40% of elderly in-patients, and 18-22% of all people in long-term care facilities. This difficulty reduces patient compliance but can be overcome[4] by producing orally disintegrating tablets (ODTs). An ODT is one that disintegrates into small granules within 30 s of its placement in the oral cavity.[8] The small granules produced thereby can easily be swallowed as compared to swallowing the whole tablet.[9] ODTs are also advantageous for travelers, who can take their medicine without the requirement of water. According to a survey, the majority of patients prefer to have an ODT than conventional forms of tablets.[8] Therefore, an ODT improves patient compliance.

Recently, researchers have become increasingly interested in developing modified release ODTs that combine the above-mentioned benefits of both modified release dosage forms and ODTs.[10,11]

Naproxen sodium is the drug of choice for rheumatoid arthritis-associated joint pain and early morning stiffness. Hence, a modified release preparation of naproxen sodium would be useful for maintaining a sustained level of naproxen sodium at the required time. The half-life of naproxen sodium is 14 h; therefore, its effect is long lasting but repeated administration of an immediate release formulation will lead to spikes in plasma concentration of the drug, thus making the pain-relieving effect erratic and remitting, as well as leading to gastro-intestinal irritation due to the high drug concentration at one time. In order to maintain a sustained level of drug plasma concentration with minimum variations, a sustained release formulation is required that will lead to sustained pain relief action and a more optimal therapeutic response with minimal side effects. Moreover, due to the high protein binding of naproxen sodium (99.7%), it may be more efficient to deliver this drug as a sustained release dosage form.[12]

Additionally, an orally disintegrating formulation with sustained release characteristics will certainly benefit the patient with quick onset of action. Naproxen sodium has been declared an ideal candidate for development into an ODT.[13] In the present study, an orally disintegrating modified release matrix tablet of naproxen sodium was prepared by incorporating Soluplus®, a novel amphiphilic graft copolymer. In parallel, the potential of Soluplus® as a tablet binder and as a release modifier for water-soluble drug was investigated.

MATERIALS AND METHODS

Naproxen sodium was obtained as a gift sample from Pacific Pharmaceuticals Pvt. Ltd, Lahore, Pakistan; Soluplus® was purchased from BASF, UK; and croscarmellose sodium, starch, and all other excipients (pharmaceutical grade) were purchased from the local market of Lahore, Pakistan, and were used as received.

Preparation of ODTs

The design of the tablet formulations was accomplished in two phases. The target of the first phase was to achieve fast disintegration of tablets, i.e. within 30 s. Eight trial tablet formulations (F1-F8) were prepared (see Table 1) by wet granulation method by varying the concentration (2-20%) and distribution (extragranular/intragranular) of superdisintegrant, i.e. croscarmellose sodium. For this purpose, a dry mixture of naproxen sodium (API), starch (disintegrant), and lactose monohydrate (diluent) was prepared in a tumbler mixture. This mixture was then moistened by using 2.5% Soluplus® solution

Table 1. Composition of trial formulations F1-F8

Formulation	Naproxen sodium (mg)	CSS (% w/w) Extra-gran	CSS (mg) Intra-gran	Starch (mg)	Magnesium stearate (mg)	Lactose Qs (mg)
F1	200	10	-	10	3	400
F2	200	20	-	10	3	400
F3	200	30	-	10	3	400
F4	200	40	-	10	3	400
F5	200	5	5	10	3	400
F6	200	10	10	10	3	400
F7	200	15	15	10	3	400
F8	200	20	20	10	3	400

as binder and the wet mass was screened through sieve 8 to produce granules. The granules were then dried in a hot air oven for 24 h. Croscarmellose sodium as superdisintegrant[14] and magnesium stearate (1.5%) as lubricant were mixed with these granules and the mixtures were compressed in a single punch tablet machine (locally manufactured, Lahore, Pakistan).

In the next phase, sustaining the release of naproxen sodium was the target. For this purpose, eight test formulations (F9-F16) were prepared having same composition of API, diluent, superdisintegrant (optimum concentration), and binder, except for the incorporation of varying concentrations of Soluplus® (5% to 50% w/w of drug), as release modifier. A control tablet formulation of naproxen sodium (F0) was also prepared containing superdisintegrant but no release modifier for comparison purposes.

Characterization of granules

In order to determine the compaction and flowability, bulk and tapped densities and angle of repose of prepared granules of each formulation were measured. Porosity, compressibility index, and Hausner's ratio were calculated using the tapped and bulk densities data.

Characterization of tablets

Tablets of each formulation were tested for their hardness, disintegration time, and drug release characteristics. Tablet hardness/crushing strength was measured in triplicate by applying a force until the tablet was crushed using a digital hardness tester (Curio/2020+, Pakistan) and the average value was reported for each formulation.

The disintegration of each formulation was tested by using the method described in the literature.[11] For this purpose, a tablet from each formulation was placed in a petri dish containing distilled water maintained at ~37 °C. The time taken by the tablet to disintegrate completely was recorded by stopwatch. The measurements were performed in triplicate and the average disintegration time for each test formulation was reported. The disintegration pattern of tablets was also photographed by stereo-zoom microscope (model SZ2-ILST/Olympus Corporation, Japan).

In vitro drug release studies

In vitro drug release of naproxen sodium from the test formulations was carried out in a USP type II (paddle) dissolution apparatus (Curio, Pakistan). Phosphate buffer (pH 7.4) was selected as dissolution medium and 900 mL of this was added to each flask of the test apparatus and the temperature of the medium was maintained at 37±0.5 °C. One tablet was placed in each dissolution flask and the paddle was rotated at 50 rpm. Aliquots of 5 mL were withdrawn at various intervals and replaced with equal amounts of fresh dissolution medium to maintain the sink conditions. The samples were diluted adequately and analyzed spectrophotometrically for their naproxen sodium content.

For the purpose of the ultraviolet assay, the absorbance of each sample was recorded in triplicate at 271 nm (i.e. λ_{max} of naproxen sodium determined in this study). From the average value of this absorbance, the corresponding value of concentration was calculated from the calibration curve. The calibration curve (absorbance vs concentration) was plotted by measuring the absorbance of stock solution and its dilutions. The plot was linear between the concentration range of 10 µg/mL and 50 µg/mL naproxen sodium with the coefficient of regression approaching unity, i.e. 0.998. The values of the intercept and gradient were 0.0093 and 0.0131, respectively.

Statistical analysis

The drug release data are presented as mean ± standard deviation and were analyzed by One-Way ANOVA. The statistical differences were set at $p<0.05$.

RESULTS AND DISCUSSION

Bulk properties of granules

The values of bulk and tapped density of the granules of all formulations are summarized in Table 2. The values of bulk density ranged between 0.234 and 0.341 g/mL and of tapped density between 0.250 and 0.357 g/mL. From these values the respective Carr's index and Hausner's ratio were obtained.

The values of Carr's index were in the range of 3.23% to 12.5%, whereas the values of Hausner's ratio were between 1.03 and 1.13, which shows excellent flow properties of all formulations (F1-F16) except for one (F3), which showed good flow properties. Carr's index corresponds to powder bridge strength and stability, while Hausner's ratio depicts interparticulate friction. Therefore, given the low values of both these parameters for all formulations, one can expect good die fill and proper compressible tablets from all formulations.[15]

Hardness of prepared tablets

The tablet hardness of trial formulations F1-F4 was between 2.9 and 3.3 kg/cm^2 (Table 3). However, incorporation of disintegrant into the granules (formulation F5-F8) increased the overall hardness of the tablets (average hardness ~3.4 kg/cm^2). The test formulations F9-F16 also showed hardness of ~3.4 kg/cm^2. These hardness values are lower than those of regular tablets, i.e. 4-6 kg/(cm^2),[16] however, they are still sufficient to tolerate any stress during manufacturing and processing.[17]

Disintegration time

The results show that the disintegration time was inversely proportional to the concentration of superdisintegrant as it decreased from 68 min for F1 containing 5% of disintegrant to 7.5 min for F4 containing 20% of it. The mode of addition of disintegrant also influences the disintegration time. The formulations containing only extragranular disintegrants (F1-F4) showed disintegration times >35 min. However, in formulations where the disintegrant was also added intragranularly (F5-F8), the disintegration time was much lower, i.e. between 0.45 and 7.5 min (Table 3). Out of these formulations, F6 showed rapid disintegration, i.e. 0.45 min (27.3 s), satisfying the limits set for ODTs. This indicated that not only the addition of superdisintegrant but also the mode of addition (intragranular or extragranular or both) affects the disintegration time.[18] The

Table 2. Values of bulk density, tapped density, Hausner's ratio, porosity, and Carr's index and corresponding flow properties of granules of different formulations

Formulation	Bulk volume	Tapped volume	Bulk density (g/mL)	Tapped density (g/mL)	Carr's index	Hausner Ratio	Porosity	Flow properties
F1	5.2	5.0	0.288	0.300	4.0	1.04	3.8	Excellent
F2	5.4	5.2	0.278	0.288	3.85	1.04	3.7	Excellent
F3	5.4	4.8	0.278	0.313	12.5	1.13	11.11	Good
F4	6.2	5.6	0.242	0.268	10.7	1.11	9.6	Excellent
F5	6.0	5.4	0.250	0.278	11.1	1.11	10	Excellent
F6	6.4	6.2	0.234	0.242	3.23	1.03	3.12	Excellent
F7	6.2	5.6	0.241	0.268	10.7	1.11	9.6	Excellent
F8	6.4	5.8	0.234	0.259	10.3	1.1	9.37	Excellent
F9	4.8	4.6	0.313	0.326	4.3	1.04	4.16	Excellent
F10	4.4	4.2	0.341	0.357	4.8	1.05	4.54	Excellent
F11	5.2	5.0	0.288	0.3	4	1.04	3.84	Excellent
F12	5.4	5.0	0.277	0.3	8	1.08	7.40	Excellent
F13	6.2	6.0	0.242	0.25	3.3	1.03	3.22	Excellent
F14	6.4	6.0	0.234	0.25	6.7	1.06	6.25	Excellent
F15	6.0	5.4	0.25	0.278	11.1	1.11	10	Excellent
F16	6.0	5.6	0.25	0.268	7.1	1.07	6.66	Excellent

Table 3. Values of hardness and disintegration of trial and test tablet formulations

Trial formulation			Test formulation		
Formulation	Hardness (kg/cm^2)	Disintegration time (min)	Formulation	Hardness (kg/cm^2)	Disintegration time (s)
F1	2.87±0.06	68.0±1.0	F9	3.4±0.1	27.1±0.1
F2	3.30±0.20	49.5±0.5	F10	3.2±0.1	27.3±0.1
F3	3.07±0.06	36.5±0.5	F11	3.4±0.1	27.3±0.1
F4	3.1±0.1	7.5±0.5	F12	3.3±0.1	27.5±0.1
F5	3.6±0.2	2.4±0.4	F13	3.4±0.1	27.1±0.1
F6	3.5±0.25	0.45±0.06	F14	3.2±0.1	28.2±0.1
F7	3.4±0.15	0.85±0.06	F 15	3.1±0.1	27.5±0.1
F8	3.4±0.2	0.73±0.08	F16	3.1±0.1	28.2±0.1
			F0	3.3±0.1	26.3±0.1

min: Minute

formulation F6 had the fastest dissolution rate as it contained both intra- and extragranular disintegrant and the optimum concentration of superdisintegrants was 10% each.

The disintegration time of all orally disintegrating test formulations (F9-F16) and blank formulation F0 was almost the same as that of the trial formulations, i.e. <30 s, as shown in Table 3. This indicates that the different concentrations of Soluplus® have no influence on disintegration time, probably due to its highly water soluble nature.[19]

The rapid disintegration of tablets can be attributed to the wicking and swelling capability of starch and croscarmellose sodium.[20] This was witnessed in microscopic images of tablets taken during the disintegration test. Figure 1 shows that the tablets were swollen at 15 s as the water was taken up by the disintegrants, which ultimately led to erosion of the tablets after 20 s.

In vitro drug release

The release profiles of naproxen sodium from test formulations F9-F16 are shown in Figure 2. It is evident that in the first 10 min the drug release was almost complete (100%) from F0 and F9, while it was ~95% from F10, ~90% from F11, ~90% from F12,

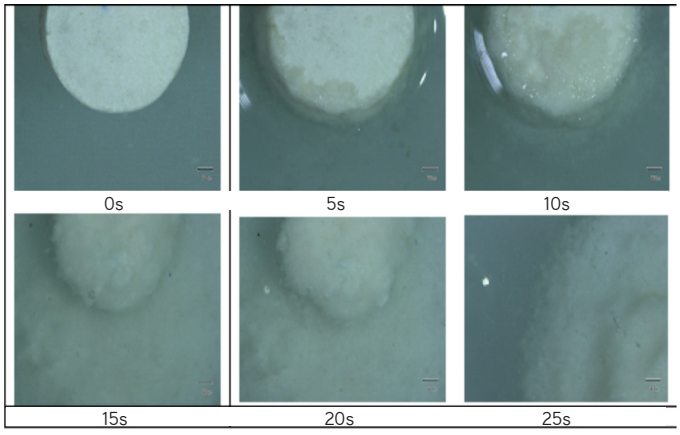

Figure 1. Stages of tablet disintegration, showing swelling and erosion of a tablet of formulation F12 at 0 s, 5 s, 10 s, 15 s, 20 s, and 25 s

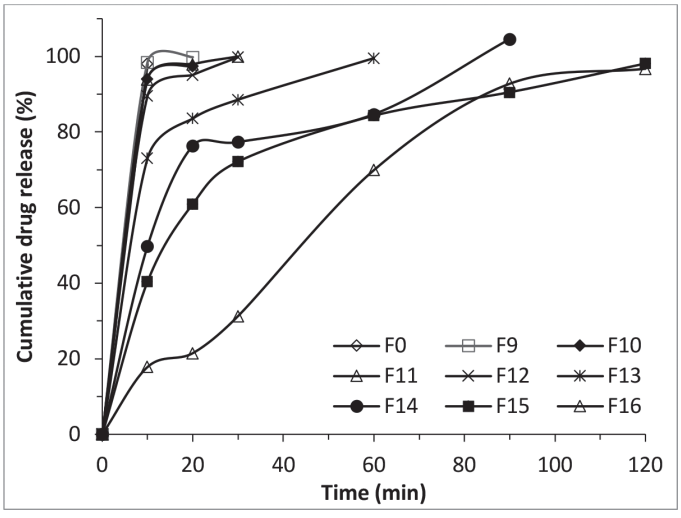

Figure 2. Dissolution profiles of orally disintegrating tablet formulations (F0 and F9-F16) having no Soluplus® or containing different concentrations of Soluplus® as release modifier

~75% from F13, ~50% from F14, ~40% from F15, and ~20% from F16. This trend remained similar after 30 min, where the drug release was almost complete from formulations F10-F12, while F13 showed ~90%, F14 ~80%, F15 ~70%, and F16 ~30% drug release. The results indicate that drug release was sustained by the incorporation of Soluplus® in ODTs and increasing the concentration of Soluplus® in the formulations from F9 (containing 5% w/w) to F16 (50% w/w with drug) enhanced the release-modifying effect of this copolymer. Statistical analysis showed a significant difference in drug release ($p<0.05$) from all nine formulations. This indicated the significant role of Soluplus® in drug release.

This shows that Soluplus® has the ability to retard the drug release of naproxen sodium, a water-soluble drug. This effect of Soluplus® has been shown in some previous studies.[21] In order to find the pattern of drug release from the tablet formulations, the release data were subjected to different release models. It was shown from the results that the Korsmeyer-Peppas model best fitted with the release profile with R^2 values 0.971. The value of release coefficient "n" was 0.748, i.e. >0.5, indicating non-Fickian or anomalous release from the tablet formulations.[22]

CONCLUSION

Orally disintegrating sustained release tablets of naproxen sodium, a water-soluble drug, were successfully prepared using an optimum concentration of croscarmellose sodium as disintegrant and Soluplus® as release modifier. The study highlighted the drug release modifying role of Soluplus® for the first time from tablet formulations.

ACKNOWLEDGEMENTS

The authors would like to thank the University of the Punjab, Lahore, Pakistan, for funding this project.

Conflicts of interest: No conflict of interest was declared by the authors. The authors alone are responsible for the content and writing of the paper.

REFERENCES

1. Shojaei, AH. Buccal mucosa as a route for systemic drug delivery: a review. J Pharm Pharm Sci. 1998;1:15-30.
2. Abdelbary G, Prinderre P, Eouani C, Joachim J, Reynier JP, Piccerelle P. The preparation of orally disintegrating tablets using a hydrophilic waxy binder Int. J Pharm. 2004;278:423-433.
3. Hirani JJ, Rathod DA, Vadalia KR. Orally disintegrating tablets: a review trop. J Pharm Res. 2009;8:61-172.
4. Mahal RK, Dr. Samein LH, Shehab M. Formulation and *in-vitro* evaluation of orodispersible tablet. Int J Pharm Sci Res. 2015;4:689-696.
5. Sharma D, Kumar D, Singh M, Singh G, Rathore M. Fast disintegrating tablets: a new era in novel drug delivery system and new market opportunities. JDDT. 2012;1:74-86.
6. Reddy KR, Mutalik S, Reddy S. Once-daily sustained-release matrix tablets of nicorandil: formulation and *in vitro* evaluation. AAPS Pharm Sci Tech. 2003;4:480-488.
7. Tiwari SB, Murthy TK, Pai MR, Mehta PR, Chowdary PB. Controlled release formulation of tramadol hydrochloride using hydrophilic and hydrophobic matrix system. AAPS Pharm Sci Tech. 2003;4:18-23.
8. Sagar N, Goswami L, Kothiyal P. Orally disintegrating tablets: a review. Int J Apl Res. 2012;3:1222-1228.
9. Chang RK, Xiaodi G, Burnside BA, Couch RA. Fast-dissolving tablets. Pharm tech. 2000;24:52-58.
10. Fini A, Bergamante V, Ceschel GC, Ronchi C, de Moraes CAF. Fast dispersible/slow releasing ibuprofen tablets. Eur J Pharm Biopharm. 2008;69:335-341.
11. Wei Q, Yang F, Luan L. Preparation and *in vitro/in vivo* evaluation of a Ketoprofen orally disintegrating/sustained release tablet. Drug Dev Ind Pharm. 2013;39:928-934.
12. Amaral MH, Lobo JS, Ferreira D. Effect of hydroxypropyl methylcellulose and hydrogenated castor oil on naproxen release from sustained-release tablets. AAPS Pharm Sci Tech. 2001;2:14-21.
13. Badgujar B, Mundada AS. The technologies used for developing orally disintegrating tablets: a review. Acta Pharm. 2011;61:117-139.

14. Setty CM, Prasad DVK, Gupta VRM, Sa B. Development of fast dispersible aceclofenac tablets: effect of functionality of superdisintegrants. Ind. J Pharm Sci. 2008;70:180.

15. Shah RB, Tawakkul MA, Khan MA. Comparative evaluation of flow for pharmaceutical powders and granules. AAPS Pharm Sci Tech. 2008;9:250-258.

16. Elkhodairy KA, Hassan MA, Afifi SA. Formulation and optimization of orodispersible tablets of flutamide. Saudi Pharma J. 2014;22:53-61.

17. Siddiqui MN, Garg G, Sharma PK. Fast dissolving tablets: preparation, characterization and evaluation: an overview. IJPSRR. 2010;4:87-96.

18. Gohel MC, Parikh RK, Brahmbhatt BK, Shah AR. Preparation and assessment of novel coprocessed superdisintegrant consisting of crospovidone and sodium starch glycolate: a technical note. AAPS Pharm Sci Tech. 2007;8:E63-E69.

19. Djuric D. Solubility enhancement with BASF pharma polymers: Solubilizer compendium. BASF SE Pharma Ingredients & Services, Germany: 2011;67-72.

20. Khairnar DA, Anantwar SP, Chaudhari CS, Shelke PA. Superdisintegrants: an emerging paradigm in orodispersible tablets. Int J Biopharm. 2014;5:119-128.

21. Naelapää K, Boetker JP, Müllertz A, Rades T, Rantanen J, Bar-Shalom D. Soluplus® for modifying the release of highly water soluble APIs. AAPS Annual meeting and exposition, Chicago, USA 2012.

22. Ford JL, Rubinstein MH, McCaul F, Hogan JE, Edgar PJ. Importance of drug type, tablet shape and added diluents on drug release kinetics from hydroxypropylmethylcellulose matrix tablets. Int J Pharm. 1987;40:223-234.

Turk J Pharm Sci 2020;17(5):492-499
DOI: 10.4274/tjps.galenos.2019.76402

ORIGINAL ARTICLE

Formulation and *In Vitro* Evaluation of Telmisartan Nanoparticles Prepared by Emulsion-Solvent Evaporation Technique

Emülsiyon-Çözücü Buharlaştırma Tekniği ile Hazırlanan Telmisartan Nanopartiküllerinin Formülasyonu ve *İn Vitro* Değerlendirilmesi

Naile ÖZTÜRK[1], Aslı KARA[2], İmran VURAL[3]*

[1]İnönü University Faculty of Pharmacy, Department of Pharmaceutical Technology, Malatya, Turkey
[2]Hitit University Sungurlu Vocational High School, Department of Medical Services and Techniques, Çorum, Turkey
[3]Hacettepe University Faculty of Pharmacy, Department of Pharmaceutical Technology, Ankara, Turkey

ABSTRACT

Objectives: Telmisartan (TLM) is an antihypertensive drug that has been shown to have antiproliferative effects on cancer cells. It has low solubility and suboptimal oral bioavailability. To investigate the potential anticancer effect of TLM on breast cancer cells, poly (D, L-lactide) (PLA) nanoparticles were formulated with the benefit of improving its solubility.

Materials and Methods: TLM-loaded PLA nanoparticles were prepared by emulsion solvent evaporation. The effects of sonication time and polymer:drug ratio on nanoparticle size and drug encapsulation were investigated. TLM-loaded nanoparticles were tested against MCF-7 and MDA-MB-231 breast cancer cell lines for antiproliferative effects.

Results: Nanoparticles with mean particle size 272 nm and 79% encapsulation efficiency were obtained. Sustained release TLM nanoparticles (40% in 24 h) decreased cell viability to 45% for MCF-7 cells at 72 h, even at the lowest TLM concentration, indicating better anticancer efficiency than TLM solution.

Conclusion: TLM nanoparticles could be potential anticancer agents for breast cancer and deserve further studies.

Key words: Telmisartan, nanoparticles, anticancer effect, drug repositioning

ÖZ

Amaç: Telmisartan (TLM), kanser hücreleri üzerinde antiproliferatif etkisi olduğu gösterilmiş antihipertansif bir ilaçtır. Düşük çözünürlüğe, suboptimal oral biyoyararlanıma sahiptir. TLM'nin meme kanseri hücreleri üzerindeki potansiyel antikanser etkisini araştırmak için, TLM'nin çözünürlüğünü iyileştiren poli (D, L-laktid) PLA nanopartikülleri formüle edilmiştir.

Gereç ve Yöntemler: TLM yüklü PLA nanopartikülleri emülsiyon hazırlama-çözücü buharlaştırma yöntemiyle hazırlanmıştır. Sonikasyon süresi ve polimer: ilaç oranının nanopartikül büyüklüğü ve ilaç enkapsülasyonu üzerindeki etkisi araştırılmıştır. TLM yüklü nanopartiküllerin, antiproliferatif etkileri MCF-7 ve MDA-MB-231 meme kanseri hücre hatları kullanılarak test edilmiştir.

Bulgular: Ortalama partikül büyüklüğü 272 nm ve %79 enkapsülasyon etkinliğine sahip nanopartiküller elde edilmiştir. Sürekli salım gösteren TLM nanopartikülleri (24 saatte %40) MCF-7 hücrelerinde, TLM çözeltisinden daha iyi antikanser aktivite göstererek, en düşük TLM konsantrasyonunda bile hücre canlılığını 72 saatte %45'e düşürmüştür.

Sonuç: TLM nanopartiküllerinin, meme kanseri için potansiyel antikanser ajanlar olabileceği ve daha ileri çalışmalarda araştırılmaya değer olduğu sonucuna varılmıştır.

Anahtar kelimeler: Telmisartan, nanopartiküller, antikanser etki, ilaç yeniden konumlandırma

*Correspondence: E-mail: +90 312 305 12 41, Phone: imranvural23@gmail.com ORCID-ID: orcid.org/0000-0002-1627-3834
Received: 17.07.2019, Accepted: 30.07.2019

INTRODUCTION

Drugs are developed by a long and costly development process. However, finding new uses for existing drugs is an alternative strategy that shortens the time to market and lowers the cost for developers. By employing this strategy new anticancer agents could be discovered and more accessible treatments could be presented to patients. Angiotensin II receptor blockers (ARBs) are an example for old drugs that are investigated for potential new activities. Telmisartan (TLM), which is an ARB used for the treatment of hypertension, has been investigated in this context and antiproliferative activity of TLM against various cancer cells such as lung adenocarcinoma cells, urological cancer cells, and endometrial cancer cells has been discovered.[1-3] It was reported that TLM has an antiproliferative effect on leukemia cell lines and *ex vivo* peripheral blood monocytes, and TLM causes autophagy and apoptosis by caspase activation.[4] Besides being an ARB, TLM is also described as a peroxisome proliferator-activated receptor (PPAR)-gamma activator and in some studies its antitumor activity is linked to PPAR-gamma activation.[1-3] Intraperitoneal administration of TLM to human endometrial tumor-bearing nude mice showed that treatment with TLM inhibited tumor growth significantly.[2] In a transgenic rat model for prostate cancer, TLM was administered orally in drinking water (2 or 10 mg/kg/day) for 12 weeks and it was found that TLM suppressed prostate cancer by activation of caspases, inactivation of p38 MAPK, and downregulation of the androgen receptor.[5]

Considering the potential anticancer application of TLM, it is also important to design an optimal formulation for effective therapy. TLM has poor aqueous solubility (0.6 µg/mL) and its solubility is pH-dependent.[6] According to the Biopharmaceutics Classification System (BCS), it is classified as a BCS II drug[7] (low solubility, high permeability) and its oral bioavailability is ~43%.[8] To improve its oral bioavailability, nanoparticle systems are one of the methods that are being investigated.[7,9] Moreover, for effective cancer therapy, accumulation of anticancer agent at the tumor site with minimum distribution in healthy tissues is a major goal. For TLM, its side-effect profile is reported as comparable to that of a placebo;[10] however, using nanoparticles (NPS) to achieve TLM accumulation at the tumor site can enhance the interaction of TLM with cancer cells, which leads to improved cancer therapy.

In the present work TLM was encapsulated with NPS that were formed by biodegradable poly (D, L-lactide) (PLA) polymer. The NPS were prepared by emulsion-solvent evaporation and studies were carried out to optimize particle size. The anticancer effect of TLM-loaded NPS was investigated against MCF-7 and MDA-MB-231 breast cancer cells.

MATERIALS AND METHODS

Materials

TLM was a kind gift from Nobel Pharmaceutical Industry and Trade Inc. Co., Turkey. Dichloromethane, dimethyl sulfoxide (DMSO), PLA (average Mw 75,000-120,000), and poly (vinyl alcohol) (PVA) (average mol wt 30,000-70,000) were purchased from Sigma-Aldrich Co., USA. MCF-7 and MDA-MB-231 cell lines were obtained from the American Type Culture Collection. Fetal bovine serum (FBS) and penicillin/streptomycin, Dulbecco's Modified Eagle Medium (DMEM), and 3-(4,5-dimethylthiazol-2-yl)-2,5-diphenyltetrazolium bromide (MTT) were purchased from Biochrom (Germany). All other reagents were analytical grade.

Preparation of nanoparticles

NPS were prepared by a modified emulsion solvent evaporation method.[11] PLA was dissolved in 1 mL of dichloromethane and 10 mL of PVA aqueous solution (0.3% w/v) was added to it. The mixture was vortexed for 1 min and then immediately was sonicated using a probe-type sonicator (Bandelin Sonopuls HD2200). After sonication the dichloromethane was evaporated by a rotary evaporator (IKA RV10). Then the NPS were centrifuged at 15.000 rpm for 15 min (23.656 x g, Hermle Z323K). The precipitated NPS were suspended in ultrapure water and centrifuged twice more for the washing steps. For TLM-loaded NPS (TLM-NP) the same procedure was performed with addition of TLM to dichloromethane. The effect of sonication time on blank and TLM-loaded NP size (polymer:drug ratio, 25:1 mg/mg) was investigated using different sonication times (5, 10, 20 min). After determining the optimal sonication time for obtaining the smallest NPS, two more polymer:drug ratios (25:2, 25:0.5, mg:mg) were studied to obtain TLM-NP and to observe the effect of drug amount on nanoparticle size and encapsulation efficiency (EE).

Characterization studies

Particle size and zeta potential measurements

The particle size, polydispersity index (PDI), and zeta potential values of blank and TLM-NP were measured by dynamic light scattering method using a Malvern Zeta Sizer Nano Series ZS instrument (UK). Measurements were performed for both freshly prepared and lyophilized NPS. The initial experiments showed that NPS lyophilized without any additive were not dispersible. Thus they were freeze-dried using 5% trehalose as cryoprotectant to prevent aggregation.

Encapsulation efficiency and drug loading capacity

Suspended NPS were frozen at -20 °C for 16 h and then were lyophilized for 48 h (Labconco, Freezone 4.5). The lyophilized NPS were dissolved in DMSO and were analyzed by ultraviolet-visible (UV-Vis) spectrophotometry at 309 nm to determine the encapsulated TLM amount. Spectrums in DMSO were used to show insignificant absorbance of PLA polymer at 309 nm. The concentration range of the calibration curve was 1-20 µg/mL. The regression equation was y=0.048x-0.006 (standard error (SE) of slope was $8x10^{-5}$, SE of intercept was $2x10^{-3}$, and R^2 was 1) and the limit of detection (LOD) was 0.3 µg/mL and limit of quantification (LOQ) was 0.8 µg/mL.

EE and drug loading capacity (DLC) were calculated using equations 1 and 2, respectively.

EE=mass of the drug in NPS/mass of drug used initially
Equation 1

DLC=mass of the drug in NPS/total mass of the NPS Equation 2

In vitro drug release

In vitro drug release experiments were carried out using the dialysis membrane method in a shaking water bath. NPS were dispersed in phosphate buffered saline (PBS) containing 0.5% (w/v) sodium lauryl sulfate (SLS) and 1 mL of this suspension was placed into a dialysis bag (molecular weight cutoff 8000 Da). The dialysis bag was placed in 50 mL of 0.5% SLS containing PBS and at specific time points 1 mL of release medium was withdrawn to determine the amount of TLM released. At each time point, 1 mL of fresh medium was added to the release medium after sampling. In addition, coarse TLM powder was dispersed in PBS containing 0.5% SLS and TLM dissolution was determined under the same conditions as for NPS.

Samples were analyzed by UV-Vis spectrophotometry using a calibration curve obtained from TLM solutions in 0.5% SLS containing PBS at 300 nm. The calibration curve was obtained in the concentration range of 0.5-10 µg/mL. The regression equation was y=0.048x-0.002 (SE of slope was 0.0002, SE of intercept was 0.0008, and R^2 was 1) and the LOD and LOQ were 0.1 µg/mL and 0.4 µg/mL, respectively.

Scanning electron microscopy (SEM)

NP morphology was observed with SEM. A NP suspension (10 µL) was placed on aluminum foil and was air dried. Then the foil was placed onto an SEM stub and was coated with gold/palladium using a BAL-TEC SCD 050 (Liechtenstein). The coated sample was visualized with a LEO-EVO 40 (UK) SEM unit.

Cell culture studies

MCF-7 and MDA-MB-231 cell lines were grown in DMEM containing penicillin (IU/mL), streptomycin (50 µg/mL), and 10% FBS and were maintained in a humidified atmosphere of 95% air and 5% CO_2 at 37 ˚C. Cells were seeded at a density 5000 cells/well in 100 µL of complete culture medium in a 96-well plate. After overnight incubation, the medium was removed from the wells and serial dilutions of TLM solution (in complete medium containing 1% DMSO), blank-NP (B-NP), and TLM-NP in complete culture medium were applied to the cells. As the control, cells were treated with complete medium alone and complete medium containing 1% DMSO. Following 24, 48, and 72 h of incubation 25 µL of MTT solution (5 mg/mL in PBS) was added to the wells. After 4 h of incubation the medium was removed from the wells and 200 µL of DMSO was added to them to dissolve the formazan crystals. The optical densities of plates were measured using a microplate reader (Molecular Devices, USA) at 570 nm. Cell viability was calculated as the percentage of control cells.

Statistics analysis

The results were presented as the mean and standard deviation/SE. Statistical analysis was performed by GraphPad Prism using One and Two-Way ANOVA and $p<0.05$ was considered statistically significant.

RESULTS

Particle size and zeta potential of nanoparticles

NPS were prepared by emulsion solvent evaporation and their particle size and zeta potential were measured directly after preparation. In addition, to investigate the effect of freeze-drying on particle size, the particle size of lyophilized NPS (freeze-dried with 5% trehalose) was measured. Firstly, three different sonication times were used to investigate the effect of sonication time on the size and EE of NPS. Particle size and zeta potential data of the freshly prepared and lyophilized B-NP, TLM-NP with different sonication times are given in Table 1. Particle size and zeta potential data of the blank and freshly prepared and lyophilized B-NP, TLM-NP with different sonication times are given in Table 1. Zeta potential values were negative and between -10 and -20 mV for all formulations and NP size was between 218 and 238 nm for blank formulations and between 273 and 333 nm for the TLM-NP formulations. The smallest NP size was obtained with 10 min sonication; therefore, formulations of different polymer:drug ratios were prepared by performing 10 min sonication. After the freeze-drying process nanoparticle size was decreased for both blank and TLM formulations, which indicates the stabilizing effect of trehalose. Zeta potential values of freeze-dried formulations were slightly lower than those of freshly prepared NPS and were between -7.0 and -9.5 mV.

Particle size and zeta potential values of TLM-NP, which were prepared using different drug amounts, are given in

Table 1. Effect of sonication time on the particle size, polydispersity index, and zeta potential of freshly prepared and freeze-dried formulations (n=3, mean ± standard deviation)

Sonication time (minute)		B-NP			TLM-NP		
		Particle size (nm)	PDI	Zeta potential (mV)	Particle size (nm)	PDI	Zeta potential (mV)
5	Fresh	237.8±1.1	0.1±0.0	-15.2±1.3	332.6±3.8	0.3±0.0	-10.5±2.1
10		218.1±3.6	0.1±0.0	-18.8±0.5	272.6±1.6	0.2±0.0	-15.0±2.6
20		223.6±1.5	0.1±0.0	-15.7±2.0	302.2±3.1	0.3±0.0	-15.7±0.4
5	Freeze-dried	210.1±1.7	0.1±0.0	-7.0±0.2	227.1±8.2	0.2±0.0	-7.9±0.2
10		205.9±3.9	0.1±0.0	-9.5±0.4	215.5±3.7	0.1±0.0	-8.1±0.2
20		212.4±1.6	0.1±0.0	-8.5±0.5	286.7±9.1	0.2±0.0	-7.4±0.2

PDI: Polydispersity index, TLM-NP: Telmisartan-loaded nanoparticles, B-NP: Blank-nanoparticles

Table 2. Particle size of the formulations with 25:2 and 25:0.5 polymer:drug ratios was smaller than that of the formulation with 25:1 polymer:drug ratio for freshly prepared NPS. Freeze-dried formulations showed different behavior in terms of particle size. While for the formulations of 25:1 and 25:0.5 polymer:drug ratios particle size decreased with freeze-drying, for the formulation of 25:2 polymer:drug ratio the opposite was true. The heterogeneity of the particle size distribution of this formulation (25:2 polymer:drug ratio) is thought to be the reason behind the further aggregation during lyophilization.

Encapsulation efficiency and drug loading capacity

Three different polymer:drug ratios were studied to investigate the effect on NP EE. The EE and DLC of TLM-NP are presented in Table 3. The highest drug loading was obtained with the formulation of 25:1 polymer:drug ratio.

In vitro drug release

The NP formulation with the highest EE (polymer:drug ratio, 25:1, mg:mg) was selected for *in vitro* drug release experiments. The release profiles of TLM-NP and TLM in PBS with 0.5% SLS are given in Figure 1. It was clear from the TLM release profile (around 40% release at the end of 24 h) that the NPS showed controlled release. Moreover, the TLM NPS displayed higher dissolution, compared to 17.2% release of TLM in 24 h.

Scanning electron microscopy

Freshly prepared NP suspension (polymer:drug ratio, 25:1, mg:mg) was placed on aluminum foil and after drying in atmospheric conditions the NPS were visualized by SEM as presented in Figure 2.

Table 2. Effect of polymer:drug ratio on the particle size, polydispersity index, and zeta potential of telmisartan-loaded nanoparticles (n=3, mean ± standard deviation)

Polymer:drug ratio (mg/mg)		Particle size (nm)	PDI	Zeta potential (mV)
25:0.5	Fresh NP	233.8±2.0	0.2±0.0	-15.2±0.4
25:1		272.6±1.6	0.2±0.0	-15.0±2.6
25:2		226.2±9.4	0.3±0.1	-11.1±0.5
25:0.5	Freeze-dried NP	228.0±4.6	0.2±0.0	-12.2±0.2
25:1		215.5±3.7	0.1±0.0	-8.1±0.2
25:2		267.8±3.3	0.3±0.0	-7.5±0.2

PDI: Polydispersity index, NP: Nanoparticles

Table 3. Encapsulation efficiency and drug loading capacity of telmisartan-loaded nanoparticles (n=3, mean ± standard deviation)

Polymer:drug ratio (mg/mg)	Sonication time (min)	EE (%)	DLC (%)
25:0.5	10	40.0±1.2	1.1±0.1
25:1	5	79.1±3.5	5.4±0.1
25:1	10	37.7±0.2	1.7±0.1
25:1	20	97.4±0.9	4.8±0.1
25:2	10	60.3±2.1	5.3±0.3

EE: Encapsulation efficiency, DLC: Drug loading capacity

Cell culture studies

MCF-7 and MDA-MB-231 cells were used as model cell lines to investigate whether there is an antiproliferative effect of TLM and TLM-NP on breast cancer cells. The cell viability results for 24, 48, and 72 h incubation periods are given in Figures 3-5, respectively.

For MCF-7 cells, B-NP did not reduce cell viability below 80% at 24 h incubation period and at 48 and 72 h the highest concentration resulted in 73% and 67% cell viability, respectively (Figures 3a, 4a, and 5a). TLM solution reduced cell viability to 75% at 24 h, to 61% at 48 h, and to 60% at 72 h (Figures 3a, 4a, and 5a). However, there was not a dramatic difference between the viability results of different concentrations of TLM treatments at each time period. The TLM-NP formulation decreased cell viability in a concentration-dependent manner and at the highest TLM concentration viability decreased to 45% at 24 h and 72 h (Figures 3a and 5a). As the incubation time increased lower TLM concentrations caused lower cell viability results.

For MDA-MB-231 cells, B-NP did not reduce cell viability below 76% even at 72 h incubation (Figures 3b, 4b, and 5b). TLM solution reduced cell viability in a dose-dependent manner;

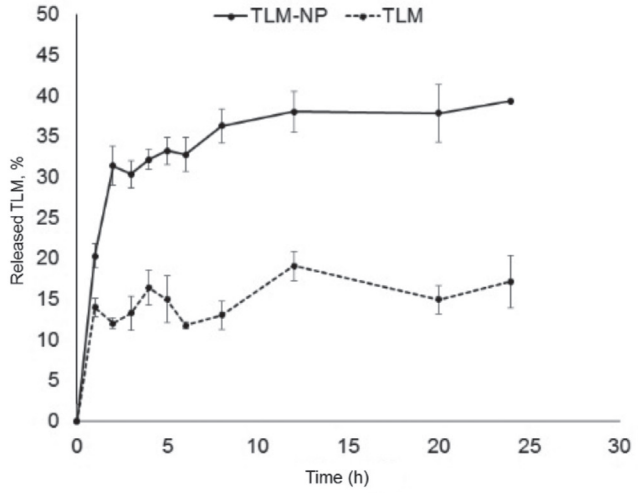

Figure 1. In vitro release profile of TLM-loaded nanoparticles and TLM (n=3, mean ± SE)
TLM-NP: Telmisartan-loaded nanoparticles, SE: Standard error

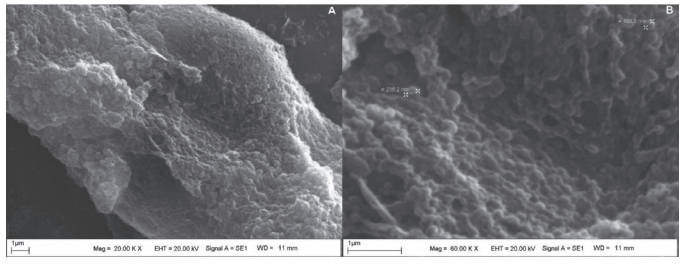

Figure 2. SEM images of TLM-loaded nanoparticles at A: 20K magnification B: 60K magnification
SEM: Scanning electron microscopy, TLM: Telmisartan

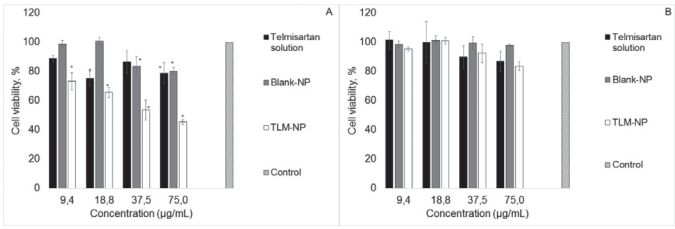

Figure 3. Cell viability of formulations after 24 h incubation. A: MCF-7 cells, B: MDA-MB-231 cells (n=3, mean ± SE). *Indicates significantly different from control ($p<0.05$)

SE: Standard error, TLM-NP: Telmisartan-loaded nanoparticles

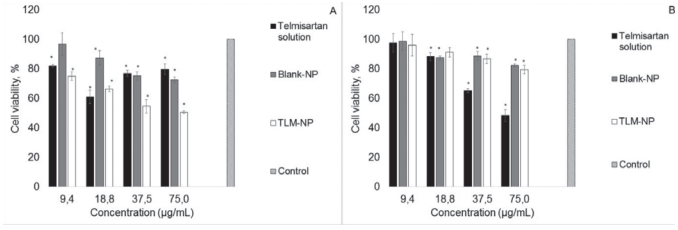

Figure 4. Cell viability of formulations after 48 h incubation. A: MCF-7 cells, B: MDA-MB-231 cells (n=3, mean ± SE). *Indicates significantly different from control ($p<0.05$)

SE: Standard error, TLM-NP: Telmisartan-loaded nanoparticles

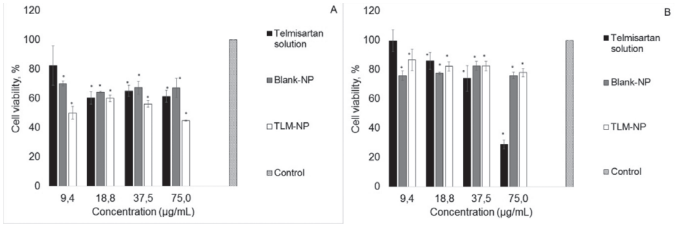

Figure 5. Cell viability of formulations after 72 h incubation. A: MCF-7 cells, B: MDA-MB-231 cells (n=3, mean ± SE). *Indicates significantly different from control ($p<0.05$)

SE: Standard error, TLM-NP: Telmisartan-loaded nanoparticles

it was especially pronounced at 48 and 72 h (Figures 4b and 5b). Interestingly the TLM-NP formulation did not cause any significant loss of viability; 78% was the lowest viability, obtained with the TLM-NP formulation at 72 h.

DISCUSSION

Novel strategies are being investigated for cancer therapy by repositioning various drugs that have different action mechanisms. Recently, these strategies have become extremely popular for the development of new potential cancer treatment modalities. Angiotensin II receptor antagonists are widely used for the treatment of hypertension and their anticancer activity was reported in various scientific papers.[12,13] Several tumor cells were reported to express angiotensin II receptors;[12-14] therefore, the anticancer effect of ARBs has been associated with inhibition of tumor angiogenesis.[15-17] One of the ARBs, TLM, is generally used for treatment of cardiovascular diseases including hypertension and coronary artery diseases.[18] However, recent studies have drawn attention to the anticancer effect of TLM. As indicated in different studies, TLM showed antitumoral activities in various cancer types such as lung,[1] prostate,[19] and endometrium.[2] Researchers have revealed that TLM has the potential to inhibit the proliferation of cancer cells through apoptosis by PPAR-gamma activation.[1,3,20] PPAR-gamma activation by using TLM as a PPAR-gamma ligand may serve as an anticancer therapy model.[21]

Due to properties mentioned above, TLM has the potential to be used in cancer therapy as a part of drug repositioning studies. However, TLM is a BCS class II model drug and has some limitations like poor solubility influencing its bioavailability.[22] Therefore, to improve the solubility of TLM and to deliver it to the target site specifically, it is important to design an effective drug delivery system. TLM encapsulation within polymeric carriers is an alternative way to protect the drug from degradation, to ensure controlled release, and to increase bioavailability because of increased solubility.

Based on this idea, in the present study we prepared a polymeric nanoparticulate system by encapsulating TLM in PLA NPS by a modified emulsion solvent evaporation method to improve drug solubility. In addition, we aimed to investigate the anticancer efficiency of an antihypertensive drug nanoparticulate system as a potential, novel treatment modality for breast cancer. To the best of our knowledge this is the first study in which a novel drug delivery system was developed using PLA NPS to deliver the poorly soluble drug TLM as a model anticancer drug for breast cancer therapy.

In the present study, TLM-loaded and B-NP were prepared with biodegradable PLA polymer. As indicated in the literature, PLA is a biocompatible, biodegradable polymer that shows low toxicity and high mechanic strength, and so in the present study PLA polymer was chosen for these advantages.[23,24] NPS were prepared by emulsion solvent evaporation, which involves emulsification of polymer solution and then evaporation of solvent, which precipitates the polymer as NPS. In order to obtain an optimized formulation, sonication time and polymer:drug ratio were evaluated in terms of particle size, PDI, EE, DLC. The particle size and PDI were measured by dynamic light scattering. Several parameters like sonication time and polymer:drug ratio highly affect the physicochemical properties of NPS, including particle size, EE, and drug loading ratio. Therefore, these parameters were studied to determine the optimum formulation. Different sonication times were tested to determine particle size as the first parameter and the results indicated that while the size of B-NP was in the range of 218-238 nm, the size of TLM-NP formulations was in the range of 273-333 nm. During the emulsification process sonication leads to dispersion of the organic phase into small nanodroplets, and so it is expected that by increasing sonication time more energy will be released and smaller droplets will be dispersed; consequently smaller NPS will be obtained.[25] Increasing sonication time from 5 min to 10 min reduced particle size but nanoparticle size was higher when 20 min sonication was performed, compared to 10 min sonication. The decrease in particle size as the sonication

time increases is expected, but several scientific papers report that there is a threshold value.[26,27] After that threshold value is reached, increasing sonication time does not reduce particle size significantly. Furthermore, it should be noted that sonication is a very dynamic process; while sonication energy disrupts droplets into smaller droplets, some of the droplets may collide due to this energy and form larger droplets, which may explain why 20 min sonication caused a slight increase in particle size. The difference between the size of TLM-NP (formulations prepared with different sonication times and drug amounts) was statistically significant ($p<0.05$). As expected, encapsulating drug into PLA NPS caused an increase in particle size. The PDI results of the blank and TLM-NP were in the range of 0.1-0.3, indicating a narrow and homogeneous size distribution. As well as the sonication time, the second important parameter, different drug:polymer ratios, was tested. Increasing drug amount from 0.5 to 1 mg in the formulation caused an increase in particle size. In contrast, by using 2 mg of drug in the formulation, a smaller mean particle size was obtained. However, PDI was increased for this formulation, indicating that size distribution was not as narrow as in other formulations in which 0.5 and 1 mg TLM were used. The effect of freeze-drying on the particle size of NPS was also investigated. Addition of trehalose as cryoprotectant to the NP suspension before the freeze-drying process resulted in decreased particle size generally. Similarly, Fonte et al.[28] reported that the particle size of polymeric NPS lyophilized with trehalose was decreased and this may be related to adsorption of cryoprotectants on the nanoparticle surface and their particular behavior during freeze-drying. The negative zeta potential values of blank and TLM-NP decreased after lyophilization. This is attributed to the rearrangement of surfactants on the NP surface. Moreover, trehalose may mask the surface of NP due to hydrogen bonding between nanoparticle and cryoprotectant.[29]

EE was increased as higher drug amounts were used and the highest drug loading was achieved with 25:1 polymer:drug ratio. *In vitro* drug release experiments showed that TLM was released from the NPS slowly and in a sustained manner (40% drug release at 24 h). The drug's partitioning between polymer and aqueous release medium influences the release rate.[30] Slow TLM (a hydrophobic drug) release from hydrophobic PLA NPS is explained by the solubility of drug in the polymer and its lower partitioning to the aqueous phase. Furthermore, coarse TLM powder dissolution (17.2% in 24 h) was significantly slower than the TLM-NP formulation ($p<0.05$), indicating increased solubility of TLM. The release medium was 50 mL of PBS with 0.5% SLS (pH 7.4) and coarse TLM powder and TLM-NP equivalent to 0.15 mg TLM were dispersed in PBS with 0.5% SLS and were placed in a dialysis membrane. As solubility of TLM in PBS with 0.5% SLS (pH 7.4) was reported as 0.108±0.04 mg/mL,[31] sink conditions were maintained during the experiment.

SEM images of NPS (Figure 2) show that they were clustered together during the drying process but individual spherical NPS were easily distinguished in images obtained at higher magnifications as expected.

The cell viability results indicate that although TLM solution decreased the cell viability of MCF-7 cells as the incubation time increased, the concentration viability relationship was erratic. TLM-NP decreased cell viability in a concentration-dependent manner to 45%, even at the lowest concentrations at 72 h incubation. By using NPS, solubility can be increased and cellular uptake of drugs can be modified. The superior antiproliferative results of the TLM-NP formulation compared to TLM solution is thought to be linked to these properties of TLM-NP formulations. TLM solution decreased the cell viability of MDA-MB-231 cells as the incubation time increased in a dose-dependent manner. However, the TLM-NP formulation did not cause the same dramatic loss of viability. It is clear for MDA-MB-231 cells that there should be a certain drug dose present in solution to see a significant loss of viability. Considering the slow drug release from TLM NPS, the reason for the high viability results obtained with them is attributed to the low amount of drug released. MCF-7 is an estrogen-dependent cell line and MDA-MB-231 is a triple negative cell line (cells that do not express estrogen receptor or progesterone receptor, and do not have HER-2/Neu amplification). It was reported that TLM induced the stimulation of collagen biosynthesis (which may influence cell growth and metabolism) in MCF-7 cells cultured in the absence of estrogen and there was crosstalk between PPAR-gamma and estrogen receptor. However, collagen biosynthesis was not influenced by TLM in estrogen-independent MDA-MB-231 cells when cultured in the same conditions.[32] As Kociecka et al.[32] reported, the different responses of cells to TLM could be receptor related and need to be investigated further.

Study limitations

TLM NP formulations were prepared and their antiproliferative effect was investigated, but investigation of anticancer effect mechanisms was not within the scope of this study.

CONCLUSION

In our study TLM-loaded biodegradable PLA NPS were prepared and it was observed that sonication time and drug amount could impact NP size. It was demonstrated that sustained release TLM-NP inhibit proliferation of MCF-7 breast cancer cells better than TLM solution, indicating their potential use as an anticancer system. Further studies should be conducted to elucidate the anticancer mechanisms of TLM NPS on breast cancer cells.

ACKNOWLEDGEMENTS

The authors acknowledge İnönü University IBTAM for the SEM analysis.

Conflicts of interest: No conflict of interest was declared by the authors. The authors alone are responsible for the content and writing of the paper.

REFERENCES

1. Li J, Chen L, Yu P, Liu B, Zhu J, Yang Y. Telmisartan exerts anti-tumor effects by activating peroxisome proliferator-activated receptor-gamma in human lung adenocarcinoma A549 cells. Molecules. 2014;19:2862-2876.
2. Koyama N, Nishida Y, Ishii T, Yoshida T, Furukawa Y, Narahara H. Telmisartan induces growth inhibition, DNA double-strand breaks and apoptosis in human endometrial cancer cells. PLoS One. 2014;9:e93050.
3. Matsuyama M, Funao K, Kuratsukuri K, Tanaka T, Kawahito Y, Sano H, Chargui J, Touraine JL, Yoshimura N, Yoshimura R. Telmisartan inhibits human urological cancer cell growth through early apoptosis. Exp Ther Med. 2010;1:301-306.
4. Kozako T, Soeda S, Yoshimitsu M, Arima N, Kuroki A, Hirata S, Tanaka H, Imakyure O, Tone N, Honda S-I, Soeda S. Angiotensin II type 1 receptor blocker telmisartan induces apoptosis and autophagy in adult T-cell leukemia cells. FEBS Open Bio. 2016;6:442-460.
5. Takahashi S, Uemura H, Seeni A, Tang M, Komiya M, Long N, Ishiguro H, Kubota Y, Shirai T. Therapeutic targeting of angiotensin II receptor type 1 to regulate androgen receptor in prostate cancer. Prostate. 2012;72:1559-1572.
6. Marasini N, Tran TH, Poudel BK, Cho HJ, Choi YK, Chi SC, Choi HG, Yong CS, Kim JO. Fabrication and evaluation of pH-modulated solid dispersion for telmisartan by spray-drying technique. Int J Pharm. 2013;441:424-432.
7. Zhong L, Zhu X, Luo X, Su W. Dissolution properties and physical characterization of telmisartan-chitosan solid dispersions prepared by mechanochemical activation. AAPS PharmSciTech. 2013;14:541-550.
8. Stangier J, Schmid J, Turck D, Switek H, Verhagen A, Peeters PA, van Marle SP, Tamminga WJ, Sollie FA, Jonkman JH. Absorption, metabolism, and excretion of intravenously and orally administered [14C] telmisartan in healthy volunteers. J Clin Pharmacol. 2000;40:1312-1322.
9. Patel J, Dhingani A, Garala K, Raval M, Sheth N. Design and development of solid nanoparticulate dosage forms of telmisartan for bioavailability enhancement by integration of experimental design and principal component analysis. Powder Technology. 2014;258:331-343.
10. Meredith PA. Optimal dosing characteristics of the angiotensin II receptor antagonist telmisartan. The American Journal of Cardiology. 1999;84:7-12.
11. McCall RL, Sirianni RW. PLGA nanoparticles formed by single- or double-emulsion with vitamin E-TPGS. J Vis Exp. 2013:51015.
12. Fujimoto Y, Sasaki T, Tsuchida A, Chayama K. Angiotensin II type 1 receptor expression in human pancreatic cancer and growth inhibition by angiotensin II type 1 receptor antagonist. FEBS Letters. 2001;495:197-200.
13. Miyajima A, Kosaka T, Asano T, Asano T, Seta K, Kawai T, Hayakawa M. Angiotensin II type I antagonist prevents pulmonary metastasis of murine renal cancer by inhibiting tumor angiogenesis. Cancer Research. 2002;62:4176-4179.
14. Inwang ER, Puddefoot JR, Brown CL, Goode AW, Marsigliante S, Ho MM, Payne JG, Vinson GP. Angiotensin II type 1 receptor expression in human breast tissues. Br J Cancer. 1997;75:1279-1283.
15. Kosaka T, Miyajima A, Takayama E, Kikuchi E, Nakashima J, Ohigashi T, Asano T, Sakamoto M, Okita H, Murai M, Hayakawa M. Angiotensin II type 1 receptor antagonist as an angiogenic inhibitor in prostate cancer. Prostate. 2007;67:41-49.
16. Kosugi M, Miyajima A, Kikuchi E, Horiguchi Y, Murai M. Angiotensin II type 1 receptor antagonist candesartan as an angiogenic inhibitor in a xenograft model of bladder cancer. Clin Cancer Res. 2006;12:2888-2893.
17. Huang W, Wu YL, Zhong J, Jiang FX, Tian XL, Yu LF. Angiotensin II type 1 receptor antagonist suppress angiogenesis and growth of gastric cancer xenografts. Dig Dis Sci. 2008;53:1206-1210.
18. Asmar R. Telmisartan in High Cardiovascular Risk Patients. European Cardiology Review. 2012;8:10-16.
19. Puri R, Kaur Bhatia R, Shankar Pandey R, Kumar Jain U, Katare OP, Madan J. Sigma-2 receptor ligand anchored telmisartan loaded nanostructured lipid particles augmented drug delivery, cytotoxicity, apoptosis and cellular uptake in prostate cancer cells. Drug Dev Ind Pharm. 2016;42:2020-2030.
20. Funao K, Matsuyama M, Kawahito Y, Sano H, Chargui J, Touraine JL, Nakatani T, Yoshimura R. Telmisartan as a peroxisome proliferator-activated receptor-gamma ligand is a new target in the treatment of human renal cell carcinoma. Mol Med Rep. 2009;2:193-198.
21. Tyagi S, Gupta P, Saini AS, Kaushal C, Sharma S. The peroxisome proliferator-activated receptor: A family of nuclear receptors role in various diseases. J Adv Pharm Technol Res. 2011;2:236-240.
22. Isaac J, Ganguly S, Ghosh A. Co-milling of telmisartan with poly(vinyl alcohol)--An alkalinizer free green approach to ensure its bioavailability. Eur J Pharm Biopharm. 2016;101:43-52.
23. Mokale V, Naik J, Verma U, Yadava S. Preparation and Characterization of Biodegradable Glimepiride Loaded PLA Nanoparticles by o/w Solvent Evaporation Method Using High Pressure Homogenizer A Factorial Design Approach. SAJ Pharmacy and Pharmacology. 2014;1:1.
24. Feng C, Yuan X, Chu K, Zhang H, Ji W, Rui M. Preparation and optimization of poly (lactic acid) nanoparticles loaded with fisetin to improve anti-cancer therapy. Int J Biol Macromol. 2019;125:700-710.
25. Mainardes RM, Evangelista RC. PLGA nanoparticles containing praziquantel: effect of formulation variables on size distribution. Int J Pharm. 2005;290:137-144.
26. Bilati U, Allémann E, Doelker E. Sonication parameters for the preparation of biodegradable nanocapsules of controlled size by the double emulsion method. Pharmaceutical development and technology. 2003;8:1-9.
27. Cun D, Foged C, Yang M, Frøkjær S, Nielsen HM. Preparation and characterization of poly (DL-lactide-co-glycolide) nanoparticles for siRNA delivery. International journal of pharmaceutics. 2010;390:70-75.
28. Fonte P, Soares S, Costa A, Andrade JC, Seabra V, Reis S, Sarmento B. Effect of cryoprotectants on the porosity and stability of insulin-loaded PLGA nanoparticles after freeze-drying. Biomatter. 2012;2:329-339.
29. De Chasteigner S, Cavé G, Fessi H, Devissaguet JP, Puisieux F. Freeze-drying of itraconazole-loaded nanosphere suspensions: a feasibility study. Drug Development Research. 1996;38:116-124.

30. Panyam J, Williams D, Dash A, Leslie-Pelecky D, Labhasetwar V. Solid-state solubility influences encapsulation and release of hydrophobic drugs from PLGA/PLA nanoparticles. J Pharm Sci. 2004;93:1804-1814.

31. Chella N, Narra N, Rama Rao T. Preparation and characterization of liquisolid compacts for improved dissolution of telmisartan. Journal of drug delivery. 2014;2014:692793.

32. Kociecka B., Surazynski A., Miltyk W., Palka J. The effect of Telmisartan on collagen biosynthesis depends on the status of estrogen activation in breast cancer cells. Eur J Pharmacol. 2010;628:51-56.

Turk J Pharm Sci 2020;17(5):500-505
DOI: 10.4274/tjps.galenos.2019.42650

ORIGINAL ARTICLE

Antimicrobial Activities of Some Pyrazoline and Hydrazone Derivatives

Bazı Pirazolin ve Hidrazon Türevlerinin Antimikrobiyal Aktiviteleri

Begüm EVRANOS AKSÖZ[1]*, Suna Sibel GÜRPINAR[2], Müjde ERYILMAZ[2]

[1]Süleyman Demirel University Faculty of Pharmacy, Department of Pharmaceutical Chemistry, Isparta, Turkey
[2]Ankara University Faculty of Pharmacy, Department of Pharmaceutical Microbiology, Ankara, Turkey

ABSTRACT

Objectives: Resistance to antibiotics is recognized as one of the biggest threats to human health worldwide. Frequent and unnecessary use of antibiotics has caused infectious agents to adapt to antibiotics and thus drugs have become less effective. The resistance to many antibiotics necessitates the discovery of new antibiotics. In this study, two new and 23 previously reported 2-pyrazoline derivatives and one hydrazone derivative were evaluated for their in vitro antibacterial and antifungal activities.

Materials and Methods: For the determination of the minimum inhibitory concentration (MIC) values of compounds, microbroth dilution was used.

Results: The antimicrobial activities of the compounds were found in a wide range with MIC values of 32-512 µg/mL.

Conclusion: The synthesized compounds showed moderate antimicrobial activity compared with the standards. They can be used as lead molecules for the synthesis of more effective compounds.

Key words: Synthesis, antimicrobial activity, pyrazoline derivatives, hydrazone derivatives

ÖZ

Amaç: Antibiyotik direnci, dünya çapında insan sağlığına yönelik en büyük tehditlerden biri olarak kabul edilmektedir. Sık ve gereksiz antibiyotik kullanımı, bulaşıcı organizmaların antibiyotiklere adapte olmasına neden olarak ilaçların daha az etkili hale gelmesine yol açmıştır. Birçok antibiyotiğe karşı gelişen direnç, yeni antibiyotiklerin keşfini gerektirmektedir. Bu çalışmada, daha önce başka etkileri nedeni ile yayınlanmış 23 2-pirazolin ve bir hidrazon türevi ile iki yeni 2-pirazolin türevi bileşiğin, *in vitro* antibakteriyel ve antifungal aktiviteleri incelenmiştir.

Gereç ve Yöntemler: Bileşiklerin minimum inhibitör konsantrasyon (MİK) değerlerinin belirlenmesi için mikrobroth dilüsyon yöntemi kullanıldı.

Bulgular: Bileşiklerin antimikrobiyal aktiviteleri, 32-512 µg/mL MİK değerleri ile geniş bir aralıkta bulunmuştur.

Sonuç: Sentezlenen bileşikler, standartlarla karşılaştırıldıklarında orta düzeyde antimikrobiyal aktivite göstermiştir ve daha etkili bileşiklerin sentezi için öncü moleküller olarak kullanılabilecekleri sonucuna varılmıştır.

Anahtar kelimeler: Sentez, antimikrobiyal aktivite, pirazolin türevleri, hidrazon türevleri

***Correspondence: E-mail:** begumevranos@gmail.com, **Phone:** +90 530 285 17 73 **ORCID-ID:** orcid.org/0000-0002-1029-6998
Received: 29.04.2019, **Accepted:** 22.08.2019

INTRODUCTION

Antimicrobials are drugs that kill or inhibit the growth of microorganisms. Resistance to antimicrobials occurs when microorganisms change in a way that reduces the effectiveness of drugs. Antibiotic resistance has become a major clinical and public health problem worldwide today. Resistance rates are rising dangerously in the world. New resistance mechanisms are emerging, making it difficult to treat infectious diseases.[1-4] In order to control this global problem, all government sectors and societies should take the necessary precautions and should support investigations on developing new antimicrobial drugs.

Hydrazones are formed as intermediates in the reaction of hydrazine and its derivatives with β-unsaturated carbonyl compounds but they are often not isolated due to their low stability and give pyrazolines with ring closure.[5,6] These compounds have interesting biological properties, such as antimicrobial, antituberculous, antidepressant, analgesic, anticonvulsant, antitumor, antiviral, and antiinflammatory activities.[7] Pyrazolines are five-membered and two neighboring nitrogen-containing heterocyclic compounds. They can be synthesized by the reaction of chalcones and hydrazines/hydrazides.[8-10] Pyrazoline derivatives are electron-rich compounds that are thought to cause a wide variety of biological activities. Pyrazolines are important compounds because of their antimicrobial, analgesic, antiinflammatory, and antidepressant activities.[11-13] According to the literature above, both pyrazoline and hydrazone compounds have antimicrobial activity. Therefore, we tested our compounds for their antimicrobial activity. In the present study, two new and 23 previously reported 2-pyrazoline derivatives and one hydrazone derivative were tested for their antibacterial and antifungal activity.

MATERIALS AND METHODS

Antimicrobial activity tests

In the antibacterial activity tests, *Staphylococcus aureus* ATCC 29213, *Bacillus subtilis* ATCC 6633, *Enterococcus faecalis* ATCC 29212, *Escherichia coli* ATCC 25922, and *Pseudomonas aeruginosa* ATCC 27853 were used as test bacteria. For antifungal activity testing, *Candida albicans* ATCC 10231 was used. The cultures were prepared in Mueller Hinton Broth (Difco, Difco Laboratories, Detroit, MI, USA). For determination of minimum inhibitory concentration (MIC) values, microbroth dilution was used.[14,15] Serial two-fold dilutions ranging from 1024 µg/mL to 8 µg/mL were made in the medium. The incubation conditions for the bacteria were 18-24 h at 35±1 °C and for the fungi were 48 h at 35±1 °C; the last well with no microbial growth was noted as the MIC value (mg/mL). Ampicillin, ofloxacin, and fluconazole were used as the positive control and 10% dimethyl sulfoxide (DMSO) was used as the negative control. All experiments were repeated three times. There was no statistical data analysis.

Chemistry

All compounds except compounds 20 and 24 have been reported earlier.[10,13]

Synthesis of chalcone derivatives (A, B)

2'-Hydroxy-4'-methoxy acetophenone/5'-chloro-2'-hydroxy acetophenone (4.99 mmol) and 4-bromobenzaldehyde/4-benzyloxybenzaldehyde (4.99 mmol) were reacted in ethanol (20 mL) using KOH solution (50% w/v) in water (5 mL) as catalyzer at room temperature overnight. Ice was added to the mixture and pH was set to 3-4 with 1 M HCl. Then the mixture was filtered and crystallized from ethanol.[16-18]

(E)-3-(4-bromophenyl)-1-(2-hydroxy-4-methoxyphenyl)prop-2-en-1-one (A): Yellow product. 61.14% yield. M.p. 141.0 °C. [lit. 138.0-140.0 °C].[19] $C_{16}H_{13}BrO_3$.

(E)-3-(4-(benzyloxy)phenyl)-1-(5-chloro-2-hydroxyphenyl) prop-2-en-1-one (B): Orange product. 93.70% yield. M.p. 138.0 °C. [lit. 100.0-102.0 °C].[20] $C_{22}H_{17}ClO_3$.

Synthesis of compounds 20 and 24

First, 1 equiv of compound A/compound B and 1 equiv of isoniazid were heated and stirred in ethanol (20 mL) for 4-25 h. Then the filtered products recrystallized from ethanol to give 20 and 24.[21-23]

(5-(4-(benzyloxy)phenyl)-3-(5-chloro-2-hydroxyphenyl)-4,5-dihydropyrazol-1-yl)(pyridin-4-yl)methanone (20): Beige product. Yield: 24.8%. M.p. 237.1 °C. IR (ν, cm^{-1}): 3167 (OH), 1641 (amide C=O), 1585 (C=N). ^{1}H NMR (DMSO-d_6, 400 MHz): 2.91 (dd, 1H, J_1=16.4 Hz, J_2=12.4 Hz, H_A), 3.46 (dd, 1H, J_1=3.2 Hz, J_2=3.2 Hz H_B), 5.14 (s, 2H, -OCH_2Ph), 5.22 (dd, 1H, J_1=2.4 Hz, J_2=2.8 Hz, H_x), 7.02-8.74 (16H, aromatic-H), 11.11 (s, 1H, OH). MS (ESI): m/z=484 [M+H] (100%). $C_{28}H_{22}ClN_3O_3$. 1.25 H_2O: C 66.36, H 4.44, N 8.05; calcd. C 66.14, H 4.72, N 8.26.

(5-(4-bromophenyl)-3-(2-hydroxy-4-methoxyphenyl)-4,5-dihydropyrazol-1-yl) (pyridin-4-yl)methanone (24): Cream colored product. Yield 29.5%. M.p. 225.5 °C. IR (ν, cm^{-1}): 3174 (OH), 1641 (amide C=O), 1576 (C=N). ^{1}H NMR (DMSO-d_6, 400 MHz): 2.82 (dd, 1H, J_1=12.4 Hz, J_2=12.8 Hz, H_A), 3.41 (dd, 1H, J_1=2.8 Hz, J_2=3.2 Hz, H_B), 3.79 (s, 3H, -OCH_3), 5.29 (dd, 1H, J_1=2.8 Hz, J_2=2.4 Hz, H_x), 6.59-8.73 (11H, aromatic-H), 11.02 (s, 1H, OH). MS (ESI): m/z=452 [M+H], 454 [M+H+2] (100%). $C_{22}H_{18}BrN_3O_3$. 0.5 H_2O: C 57.15, H 4.38, N 9.36; calcd. C 57.23, H 4.12, N 9.10.

RESULTS AND DISCUSSION

A number of pyrazoline derivatives (compounds 2-26) and one hydrazone derivative (compound 1) were prepared. The structures of the target compounds are outlined in Figure 1.

Twenty-six compounds were tested for their antibacterial and antifungal activities. Antimicrobial activity was screened against two Gram-negative (*E. coli* ATCC 25922 and *P. aeruginosa* ATCC 27853*)* and three Gram-positive (*S. aureus* ATCC 29213, *E. faecalis* ATCC 29212, and *B. subtilis* ATCC 6633*)* bacteria and a fungus (*C. albicans* ATCC 10231) using ampicillin, ofloxacin, and fluconazole as the standard drugs. The results are given in Table 1.

Compound 1, the hydrazone, showed moderate activity against all the bacteria and the fungus. Pyrazoline derivatives were found to possess moderate activity against the bacteria and fungus. Whether the ring was open (hydrazone) or closed

Table 1. ***In vitro*** **antimicrobial activities of hydrazone (1) and 2-pyrazoline (2-26) derivatives**

	MIC values of test microorganisms (µg/mL)					
Compound	Gram-negative bacteria		Gram-positive bacteria			Fungus
	Escherichia coli ATCC 25922	*Pseudomonas aeruginosa* ATCC 27853	*Staphylococcus aureus* ATCC 29213	*Enterococcus faecalis* ATCC 29212	*Bacillus subtilis* ATCC 6633	*Candida albicans* ATCC 10231
1	256	128	128	128	128	128
2	256	128	256	128	128	128
3	256	128	128	64	128	128
4	512	256	256	256	256	256
5	256	128	64	64	128	64
6	256	128	256	128	128	128
7	256	128	128	64	128	128
8	256	128	128	128	128	128
9	256	128	256	256	256	128
10	256	128	128	128	128	128
11	256	128	512	256	256	128
12	512	128	256	128	128	128
13	512	128	256	256	128	128
14	512	256	512	256	256	256
15	512	256	512	256	128	256
16	512	256	512	256	256	128
17	512	128	512	256	256	256
18	256	128	256	256	128	128
19	256	64	64	256	128	128
20	256	128	128	128	128	128
21	256	128	256	256	128	128
22	512	64	128	32	64	128
23	512	256	256	64	256	128
24	512	256	64	32	256	128
25	-	512	-	256	-	256
26	-	512	512	64	64	128
Ampicillin	NT	NT	0.3	1	6	NT
Ofloxacin	1	8	NT	NT	NT	NT
Fluconazole	NT	NT	NT	NT	NT	1

NT: Not tested, MIC: Minimum inhibitory concentration, -: Represents no activity

(pyrazolines) generally did not appear to make a large difference in antimicrobial effect. Compounds 5, 19, and 24 exhibited the highest antibacterial activity against *S. aureus*, with a MIC value of 64 µg/mL among the tested bacteria. Compounds 19 and 22 were found to have the best activity against *P. aeruginosa.* Compounds 22 and 26 showed the best activity against *B. subtilis*, with a MIC value of 64 µg/mL. Compounds 22 and 24 exhibited the highest antimicrobial activity against *E. faecalis*, with a MIC value of 32 µg/mL. Compound 5 was found the most active compound against *C. albicans*, with a MIC value of 64 µg/mL.

Karad et al.[24] synthesized (2-morpholinoquinolin-3-yl)-4,5-dihydro-1H-pyrazol-1-yl) derivatives and studied their antibacterial activity. They found that the existence of -OCH_3 substituent at position-4 in the phenyl ring at the C-3 position in the pyrazoline scaffold enhanced the antibacterial activity and antimalarial potency. For our compounds, a methoxy substituent in this position increased the antibacterial activity against *S. aureus* and *E. faecalis*, when it had bromo at the R^7 position and pyridin-4-yl at the R^8 position (compound 24).

Replacement of 4-methyl with 4-bromo substitution on the B ring in the pyrazoline nucleus enhanced the activity against *S. aureus* and *E. faecalis* (compounds 23 and 24).

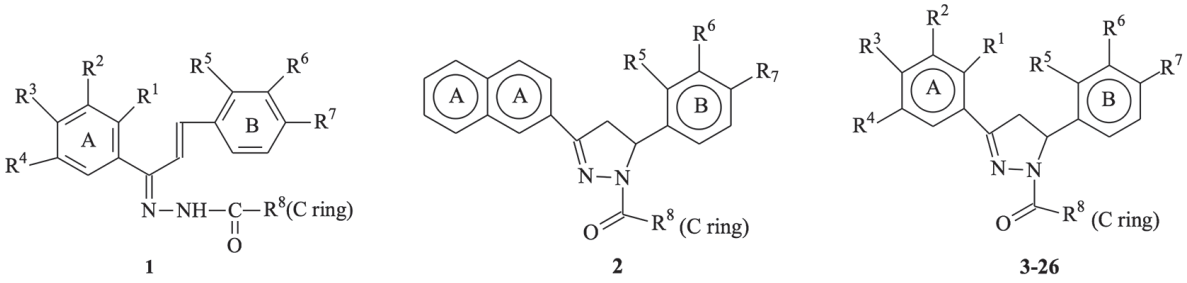

Figure 1. Structures of compounds 1-26

Compound	R^1	R^2	R^3	R^4	R^5	R^6	R^7	R^8 (C ring)
1	-H	-H	-F	-H	-H	-H	-CH_3	Furan-2-yl
2	-	-	-	-	-H	-H	-OCH_3	Pyridin-4-yl
3	-OH	-H	-H	-CH_3	-H	-H	-OCH_3	Phenyl
4	-OH	-Cl	-H	-Cl	-OCH_3	-H	-H	Pyridin-4-yl
5	-OH	-Cl	-H	-Cl	-H	-H	-CH_3	Furan-2-yl
6	-OH	-H	-H	-CH_3	-H	-H	-CH_3	Phenyl
7	-OH	-H	-H	-Cl	-OCH_3	-H	-H	Phenyl
8	-OH	-H	-H	-Br	-OCH_3	-H	-H	Pyridin-4-yl
9	-OH	-H	-H	-CH_3	-H	-H	-CH_3	Furan-2-yl
10	-H	-OH	-H	-H	-OCH_3	-H	-H	Phenyl
11	-H	-OH	-H	-H	-OCH_3	-H	-H	Furan-2-yl
12	-OH	-H	-H	-Br	-OCH_3	-H	-H	Phenyl
13	-OH	-H	-H	-Cl	-H	-OCH_3	-H	Phenyl
14	-OH	-H	-H	-H	-OCH_3	-H	-H	Phenyl
15	-OH	-H	-OCH_3	-H	-H	-H	- CH_3	Phenyl
16	-OH	-H	-H	-Cl	-OCH_3	-H	-H	Furan-2-yl
17	-OH	-H	-H	-Cl	-H	-OCH_3	-H	Furan-2-yl
18	-OH	-H	-H	-Br	-H	-H	-OCH_3	Phenyl
19	-OH	-H	-H	-Cl	-H	-OCH_3	-H	Pyridin-4-yl
20	-OH	-H	-H	-Cl	-H	-H	-OCH_2Ph	Pyridin-4-yl
21	-OH	-H	-H	-Cl	-OCH_3	-H	-H	Pyridin-4-yl
22	-OH	-H	-H	-Br	-H	-H	-OCH_3	Pyridin-4-yl
23	-OH	-H	-OCH_3	-H	-H	-H	-CH_3	Pyridin-4-yl
24	-OH	-H	-OCH_3	-H	-H	-H	-Br	Pyridin-4-yl
25	-OH	-H	-H	-H	-H	-CH_3	-H	Pyridin-4-yl
26	-OH	-H	-H	-Cl	-H	-H	-OCH_3	Furan-2-yl

According to Hamada and Abdo,[9] the addition of pharmacophores such as chloro and bromo substituents with lipophilic properties increased the antimicrobial activity. For our compounds 7, 12, and 14, the substitution of chloro and bromo atoms at the 5-position of the A ring tended to increase the biological activity.

When the C ring had a phenyl scaffold, replacement of the 2-hydroxy-5-bromo phenyl (A ring) by 2-hydroxy-5-chloro phenyl increased the antibacterial activity against *E. coli*, *S. aureus*, and *E. faecalis* (compounds 7 and 12). When the compound carried a pyridine as the C ring, the substitution of 2-hydroxy-3,5-dichloro phenyl decreased the antimicrobial and antifungal activity. Replacement of this group by 2-hydroxy-5-bromo phenyl enhanced the antimicrobial activity against all bacteria and the fungus (compounds 4 and 8). Replacement of 2-hydroxy-3,5-dichloro phenyl by 2-hydroxy-5-chloro phenyl increased the activity against *E. coli*, *P. aeruginosa*, *B. subtilis*, and *C. albicans* (compounds 4 and 21).

The addition of the naphthyl group instead of phenyl on the A ring in compound 2 resulted in increased efficacy against *E. coli*. It reduced the activity against *S. aureus*, *P. aeruginosa*, *E. faecalis*, and *B. subtilis.* Compound 25 showed no antimicrobial activity against *E. coli*, *S. aureus*, or *B. subtilis.* Compound 26 showed no antimicrobial activity against *E. coli*.

Addition of phenyl instead of 2-furyl as the C ring increased the activity (compounds 6 and 9; compounds 10 and 11; compounds 13 and 17; compounds 7 and 16). The presence of phenyl instead of pyridine as the C ring increased the antimicrobial activity against *E. coli*. However, addition of pyridine instead of phenyl as the C ring enhanced the antibacterial activity against *S. aureus*, *P. aeruginosa*, *E. faecalis*, and *B. subtilis* (compounds 18 and 22). The substitution by a methoxy group at the fourth position on the B ring produced comparable antimicrobial activity against *S. aureus* and *E. faecalis* to the substitution by a methyl group (compounds 3 and 9).

Meta methoxy substitution on the B ring increased the activity against *P. aeruginosa* and *S. aureus* in the presence of pyridine as the C ring (compounds 19 and 21). Para methoxy substitution on the B ring enhanced the antimicrobial activity against *P. aeruginosa*, *E. faecalis*, and *B. subtilis* in the case of a pyridine substituent at the R^8 position (compounds 8 and 22). Orto methoxy substitution on the B ring is not preferable, especially when the C ring is pyridine. According to Manna and Agrawal[25] ortho substitution in the phenyl ring with a methoxy group at the 5th position of the pyrazoline ring caused less or inactive antibacterial activity against Gram-negative bacteria.

Replacement of 5-bromo with 5-methyl substitution on the A ring enhanced the activity against *S. aureus* and *E. faecalis* (compounds 3 and 18*)*.

The presence of a methyl group at the fifth position of the A ring instead of a methoxy group at the fourth position of the A ring increased the antifungal activity and antimicrobial activity against *E. coli*, *S. aureus*, *E. faecalis, P. aeruginosa*, and *C. albicans* (compounds 6 and 15).

CONCLUSION

In this work, several pyrazoline derivatives and one hydrazone derivative were synthesized and screened for their antibacterial and antifungal activities. We noted that the pyridine ring as the C ring and methoxy and bromo substitutions on the B ring are preferable for a good antibacterial effect. 2-hydroxy-5-chloro substitution and 2-hydroxy-4-methoxy substitution substituents are favorable as the A ring. Further studies are necessary in order to understand the relation between the substitutions and activity, which could guide the design of more potent antimicrobial agents for therapeutic use.

ACKNOWLEDGEMENTS

I would like to thank to the staff of the Central Laboratory of the Pharmacy Faculty of Ankara University for the acquisition of the nuclear magnetic resonance mass spectrometer, and elemental analyzer of this work.

Conflicts of interest: No conflict of interest was declared by the authors. The authors alone are responsible for the content and writing of the paper.

REFERENCES

1. Ventola CL. The antibiotic resistance crisis, part 1: causes and threats, PT. 2015;40:277-283.
2. Wernli D, Jørgensen PS, Harbarth S, Carroll SP, Laxminarayan R, Levrat N, Rottingen JA, Pittet D. Antimicrobial resistance: The complex challenge of measurement to inform policy and the public. PLoS Med. 2017;14:e1002378.
3. He J, Jia X, Yang S, Xu X, Sun K, Li C, Yang T, Zhang L. Heteroresistance to carbapenems in invasive Pseudomonas aeruginosa infections. Int J Antimicrob Agents. 2018;51:413-421.
4. Luo K, Shao F, Kamara KN, Chen S, Zhang R, Duan G, Yang H. Molecular characteristics of antimicrobial resistance and virulence determinants of Staphylococcus aureus isolates derived from clinical infection and food. J Clin Lab Anal. 2018;e22456.
5. Raiford LC, Davis HL. Condensation products of benzalacetophenone and some of its derivatives. J Am Chem Soc. 1928;50:156-162.
6. Pimenov AA, Makarova NV, Moiseev IK, Zemtsova MN. Interaction of α,β-unsaturated ketones of the adamantane series with N,N'-binucleophiles. Chem Heterocycl Compd. 2004;40:575-581.
7. Rollas S, Küçükgüzel ŞG. Biological activities of hydrazone derivatives. Molecules. 2007;12:1910-1939.
8. Gökhan-Kelekçi N, Koyunoglu S, Yabanoglu S, Yelekçi K, Özgen Ö, Uçar G, Erol K, Kendi E, Yesilada A. New pyrazoline bearing 4(3H)-quinazolinone inhibitors of monoamine oxidase: synthesis, biological evaluation, and structural determinants of MAO-A and MAO-B selectivity. Bioorg Med Chem. 2009;17:675-689.
9. Hamada NM, Abdo NY. Synthesis, characterization, antimicrobial screening and free-radical scavenging activity of some novel substituted pyrazoles. Molecules. 2015;20:10468-10486.
10. Evranos Aksoz B, Ucar G, Yelekçi K. Design, synthesis and hMAO inhibitory screening of novel 2-pyrazoline analogues hMAO inhibitory screening of novel 2-pyrazolines. Comb Chem High Throughput Screen. 2017;20:510-521.

11. Sahu SK, Banerjee M, Samantray A, Behera C, Azam MA. Synthesis, analgesic, anti-inflammatory and antimicrobial activities of some novel pyrazoline derivatives. Trop J Pharm Res. 2008;7:961-968.

12. Yusuf M, Jain P. Synthetic and biological studies of pyrazolines and related heterocyclic compounds. Arab J Chem. 2014;7:553-596.

13. Evranos Aksoz B, Ucar G, Taş ST, Aksoz E, Yelekci K, Erikci A, Sara Y, Iskit AB. New hMAO-A inhibitors with potential antidepressant activity: design, synthesis, biological screening and evaluation of pharmacological activity. Comb Chem High Throughput Screen. 2017;20:461-473.

14. Clinical and Laboratory Standards Institute. Methods for dilution antimicrobial susceptibility tests for bacteria that grow aerobically. Approved Standard. In: CLSI Publication M 07-A8, 8th ed., CLSI; Wayne, PA, USA, 2009.

15. European Committe on Antimicrobial Susceptibility Testing (EUCAST). Breakpoint tablets for interpretation of MICs and zone diameters. Version 3.1., Last Accessed Date: 11.02.2013 Available from: https://eucast.org/

16. Zhao LM, Jin HS, Sun LP, Piao HR, Quan ZS. Synthesis and evaluation of antiplatelet activity of trihydroxychalcone derivatives. Bioorg Med Chem Lett. 2005;15:5027-5029.

17. Boeck P, Falcao CAB, Leal PC, Yunes RA, Filho VC, Torres-Santos EC, Rossi-Bergmann B. Synthesis of chalcone analogues with increased antileishmanial activity. Bioorg Med Chem. 2006;14:1538-1545.

18. Jun N, Hong G, Jun K. Synthesis and evalution of 2',4',6'-trihydroxychalcones as a new class of tyrosine inhibitors. Trihydroxychalcones as a new class of tyrosine inhibitors. Bioorg Med Chem. 2007;15:2396-2402.

19. Forghieri M, Laggner C, Paoli P, Langer T, Manao G, Camici G, Bondioli L, Prati F, Costantino L. Synthesis, activity and molecular modeling of a new series of chromones as low molecular weight protein tyrosine phosphatase inhibitors. Bioorg Med Chem. 2009;17:2658-2672.

20. De Meyer ND, Haemers A, Mishra L, Pandey HK, Pieters LAC, Berghe DAV, Vlietinck AJ. 4'-Hydroxy-3-methoxyflavones with potent antipicornavirus activity. J Med Chem. 1991;34:736-746.

21. Hozien ZA. Synthesis of some new heterocyclic systems derived from 2- acetylbenzimidazole. J Chem Tech Biotechnol. 1993;57:335-341.

22. Prasad YR, Rao AL, Prasoona L, Murali K, Kumar PR. Synthesis and antidepressant activity of some 1,3,5-triphenyl-2-yrazolines and 3-(2''-hydroxy naphthalen-1''-yl)-1,5-diphenyl-2-pyrazolines. Bioorg Med Chem Lett. 2005;15:5030-5034.

23. Ali MA, Shaharyar M, Siddiqui AA. Synthesis, structural activity relationship and anti-tubercular activity of novel pyrazoline derivatives. Eur J Med Chem. 2007;42:268-275.

24. Karad SC, Purohit VB, Thakor P, Thakkar VR, Raval DK. Novel morpholinoquinoline nucleus clubbed with pyrazoline scaffolds: synthesis, antibacterial, antitubercular and antimalarial activities. Eur J Med Chem. 2016;112:270-279.

25. Manna K, Agrawal YK. Microwave assisted synthesis of new indophenazine 1,3,5-trisubstiuted pyrazoline derivatives of benzofuran and their antimicrobial activity. Bioorg Med Chem Lett. 2009;19:2688-2692.

Turk J Pharm Sci 2020;17(5):506-510
DOI: 10.4274/tjps.galenos.2019.15807

ORIGINAL ARTICLE

In Vitro Investigation of the Effects of Imidacloprid on AChE, LDH, and GSH Levels in the L-929 Fibroblast Cell Line

L929 Fibroblast Hücre Hattında İmidoklorit Etkisinin *İn Vitro* Araştırılması

Çiğdem SEVİM[1], Ali TAGHİZADEHGHALEHJOUGHİ[2], Mehtap KARA[2]*

[1]İstanbul University Faculty of Pharmacy, Department of Pharmaceutical Toxicology, İstanbul, Turkey
[2]Atatürk University Veterinary Faculty, Department of Pharmacology and Toxicology, Erzurum, Turkey

ABSTRACT

Objectives: There are several types of pesticides to control pests and several new types coming into use that could be less toxic compared to the old ones. Pesticide-induced oxidative stress, which is one of the main mechanisms of toxicity, is the research area focused most on over the last decade. There are several different studies in the literature on whether pesticide exposure induces oxidative stress parameter-mediated toxicity. Pesticide-induced oxidative stress level depends on the biochemical features of mammalian systems. Imidacloprid is a neonicotinoid pesticide in wide use that is considered safe; however, it has been reported in different studies that it may cause changes in oxidative stress parameters.

Materials and Methods: We investigated the dose- and time-dependent effects of imidacloprid on acetylcholinesterase (AChE), lactate dehydrogenase (LDH), and glutathione (GSH) levels in the L-929 fibroblast cell line. The effects of 1-500 µg imidacloprid dose range on AChE, GSH, and LDH were investigated.

Results: LDH levels were significantly increased dose dependently in the 250 and 500 ng imidacloprid groups compared to the control group. GSH levels nonsignificantly decreased dose dependently and GSH levels were lower in the 500 ng imidacloprid group compared to the control group. There were no significant differences between the groups in AChE levels.

Conclusion: These results indicated that high doses of imidacloprid may induce oxidative stress in fibroblast cells.

Key words: Imidacloprid, L-929 cell line, oxidative stress, AChE

ÖZ

Amaç: Haşereleri kontrol altına almak için çeşitli pestisit türleri ve eskilere kıyasla daha az toksik olan yeni tür pestisitler kullanıma giriyor. Toksisitenin ana mekanizmalarından biri olan pestisit kaynaklı oksidatif stres, son on yılda en çok odaklanan araştırma alanıdır. Literatürde pestisit maruziyetinin oksidatif stres parametresi aracılı toksisiteyi indüklemesine ilişkin farklı çalışmalar mevcuttur. Pestisit kaynaklı oksidatif stres seviyesi, memeli sistemlerinin biyokimyasal özelliklerine bağlıdır. İmidakloprid, güvenli olduğu düşünülen, yaygın olarak kullanılan bir neonikotinoid pestisittir; ancak oksidatif stres parametrelerinde değişikliklere neden olabileceği farklı çalışmalarda bildirilmiştir.

Gereç ve Yöntemler: Bu çalışmada doza ve zamana bağımlı olarak imidaklopridin L-929 fibroblast hücrelerinde AChE, laktat dehidrogenaz (LDH) ve glutatyon (GSH) düzeyleri üzerine etkisini inceledik. 1-500 µg imidakloprid dozlarının asetilkolinesteraz, glutatyon ve laktat dehidrojenaz düzeyleri üzerine etkileri araştırıldı.

Bulgular: 250 ve 500 ng dozda imidaklopridin LDH seviyelerini, kontrol grubuna kıyasla anlamlı olarak artırdığı tespit edildi. GSH seviyelesinin dozdan bağımsız olarak 500 ng imidakloprid dozunda kontrol grubuna kıyasla anlamlı olarak azaldığı tespit edildi. Asetilkolinesteraz seviyeleri arasında anlamlı bir fark gözlenmedi.

Sonuç: Bu sonuçlara göre yüksek doz imidakloprid maruziyeti fibroblast hücrelerinde oksidatif stres parametrelerini uyarabileceği gözlemlenmiştir.

Anahtar kelimeler: İmidakloprid, L-929 hücre hattı, oksidatif hasar, AChE

*Correspondence: **E-mail:** matost@gmail.com, **Phone:** +90 507 349 24 78 **ORCID-ID:** orcid.org/0000-0001-7764-5593
Received: 30.05.2019, **Accepted:** 29.08.2019

INTRODUCTION

Pesticides are mixtures of substances used to prevent, control, or reduce harmful organisms. Pesticides include active substances and filling material that facilitate usage and increase the effect of their active substances. Commercially available drugs are manufactured and launched to market in mixed form with filling material. In Turkey 2,500 tons of pesticides are used every year.[1-3]

It has been speculated that neonicotinoid pesticides exhibit much lower toxic effects on mammals than on insects and therefore can replace organophosphates and carbamate insecticides. Neonicotinoid pesticides are a high risk for humans as they are often used not only in agricultural applications but also in the removal of domestic pests. Neonicotinoid pesticides show their selective toxic effects on insects via nicotinic acetylcholine receptors. Imidacloprid, which is a member of a new neuroactive neonicotinoid insecticide class, is a commonly used insecticide around the world as well as in Turkey. It has been reported that 120 countries have commonly used imidacloprid since 1990, when it was first introduced commercially. It has been reported that imidacloprid's oral LD50 values for rats were 380-650 mg/kg body weight and for mice 130-170 mg/kg body weight. Under aerobic conditions, imidacloprid is an environmentally persistent chemical with a 3-year half-life, which increases its risk.[4-7]

Pesticide-induced oxidative stress has been the focus of toxicological research over the last decade as a possible mechanism of toxicity. Several studies have been conducted to determine whether oxidative stress in humans or animals is caused by various agents in this group and is related to their toxic effects.[8,9] It has been reported in different studies that imidacloprid induced oxidative stress parameters' imbalance in different organisms *in vitro* and *in vivo*;[10-17] however, there are no studies on imidacloprid's oxidative imbalance effects on fibroblast tissue in the literature.

In the present study we aimed to investigate the *in vitro* effects of imidacloprid on acetylcholinesterase (AChE), lactate dehydrogenase (LDH), and glutathione (GSH) levels in the L929 fibroblast cell line.

MATERIALS AND METHODS

Chemicals

Dulbecco's Modified Eagle's Medium (DMEM), fetal bovine serum (FBS), phosphate-buffered saline (PBS), penicillin streptomycin solution, and trypsin-EDTA solution were purchased from Sigma-Aldrich Co. (St. Louis, MO, USA). The AChE assay kit (Fluorometric Red, ab138873), LDH assay kit (Fluorometric, ab197000), and GSH assay kit (Fluorometric, ab65322) were purchased from Abcam (Cambridge, UK). The L929 cell line (CRL-6364) was purchased from the American Type Culture Collection (ATCC, VA, USA). The imidacloprid-based herbicide (GORTCA FS 600) was purchased from Safa Tarım Ltd. (Turkey) and contained pure imidacloprid (CAS number: 138261-41-3, product code: 0210-207).

Cell culture and treatments

All experiments on L929 were performed within 20 passages. The cells were grown with DMEM containing 10% FBS and 1% penicillin-streptomycin-amphotericin B in a humidified incubator supplied with 5% of CO_2 at 37 ˚C. Before the treatments were conducted, the cells were cultured for 24 h to ensure attachment.

The L-929 cells were incubated with imidacloprid dissolved in 100% of dimethyl sulfoxide (DMSO) and diluted with medium to the desired concentrations as 500 µg, 250 µg, 125 µg, 50 µg, 25 µg, 5 µg, and 1 µg. Studies reported that cytotoxicity is observed at concentrations higher than 500 µg/mL. In the present study a high concentration of imidacloprid was determined as 500.[18] Vehicle control cells received equal volumes of DMSO (0.5%) as the treatment for 24 h. LDH, GSH, and AChE assays were performed after 24 h of exposure.

Lactate dehydrogenase and glutathione parameters

LDH is a cytosolic enzyme and the measurement of its leakage to the extracellular matrix due to cell membrane damage is an indicator of cell membrane integrity loss and oxidative stress.[19]

For this purpose, the L-929 cells were plated in 96-well plates at $1x10^4$ cells/well and grown for 24 h. Following the cell treatments, the LDH release in supernatants due to membrane damage was quantified using a rat LDH ELISA kit (Cat. number: E-EL-R2547) in accordance with the manufacturer's protocol. To each well was added 100 µL of standard or sample, followed by incubation for 90 min at 37 ˚C. After the liquid was removed, 100 µL of Biotinylated detection Ab was added, followed by incubation for 1 h at 37 ˚C. After aspiration and washing 3 times, 100 µL of horseradish peroxidase (HRP) conjugate was added, followed by incubation for 15 min at 37 ˚C. After more aspiration and washing 5 times, 90 µL of substrate reagent was added, followed by incubation for 15 min at 37 ˚C. When 50 µL of stop solution was added, it was read at 450 nm using a micro-plate reader (Biotek Epoch, USA).

GSH is an important molecule for the cellular antioxidant system and under oxidative stress conditions GSH level decreases. The L-929 cells were cultured in 25-cm^2 flasks to determine GSH levels. Following exposure of cells to imidacloprid, $1x10^6$ cells were harvested in 1 mL of PBS and were homogenized by sonication, and the GSH content of the L-929 cells was determined using the GSH ELISA kit (Cat. number: E-EL-0026) to assay human GSH following the manufacturer's procedure and referred to as µmol/g protein. To each well was added 50 µL of standard or sample and then immediately 50 µL of Biotinylated detection Ab was added, followed by incubation for 45 min at 37 ˚C. After aspiration and washing 3 times, 100 µL of HRP conjugate was added, followed by incubation for 30 min at 37 ˚C. After aspiration and washing 5 times, 90 µL of substrate reagent was added, followed by incubation for 15 min at 37 ˚C. When 50 µL stop solution was added, it was read at 450 nm using a micro-plate reader (Biotek Epoch, USA).

Acetylcholinesterase assay

AChE is strikingly distributed in the cell-substrate interface of radiated and migrating fibroblasts (morphoregulation by AChE in fibroblasts and astrocytes) and it helps us to understand how the nervous system works. The L-929 cells were cultured in 25-cm^2 flasks to determine AChE levels. Following exposure of cells to imidacloprid, 1x10^6 cells were harvested in 1 mL of PBS and were homogenized by sonication, and the AChE content of L-929 cells was determined using the AChE assay kit (colorimetric, Cat. number: ab138871). To each well of AChE standard, blank control, and test samples was added 50 µL of AChE reaction mixture to make the total AChE assay volume 100 µL/well, followed by incubation for 30 min at room temperature. Increased fluorescence monitored absorbance optical density at 140 nm with a micro-plate reader (Biotek Epoch, USA).

Statistical analysis

All the experiments were performed as three replicates and the results were presented as the mean ± standard deviation. The statistical comparisons were evaluated using One-Way ANOVA followed by Tukey's test for post hoc analysis, and the statistical significance was set at $p<0.05$ (SPSS, version 21.0, USA).

RESULTS

The LDH results of imidacloprid exposure on L929 cells are shown in Figure 1. We observed that LDH levels increased dose dependently, and 250 and 500 ng imidacloprid increased LDH levels significantly compared to the control group. GSH results of imidacloprid exposure on L929 cells are shown in Figure 2. GSH levels nonsignificantly decreased dose dependently and GSH levels decreased in the 500 ng imidacloprid group compared to the control group. AChE results of imidacloprid exposure on L929 cells are shown in Figure 3. There were no significant differences between the groups, but the AChE level nonsignificantly decreased in the 125 ng group.

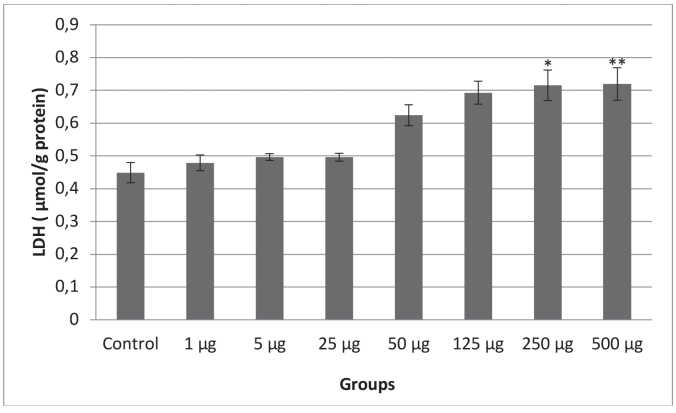

Figure 1. LDH level in L-929 cells with imidacloprid exposure
LDH: Lactate dehydrogenase

DISCUSSION

Neonicotinoids are pesticides popular worldwide whose use has increased since 2000. Neonicotinoids exert their effects on insects by cellular nAChR mechanism.[20,21] In recent years, neonicotinoids have taken the place of pyrethroid, organophosphorus, and carbamate insecticides.[22] It is thought that they are a safe pesticide group for nontarget species; however, there are several recent studies in the literature about different toxic effects of neonicotinoids on nontarget organisms.[23,24]

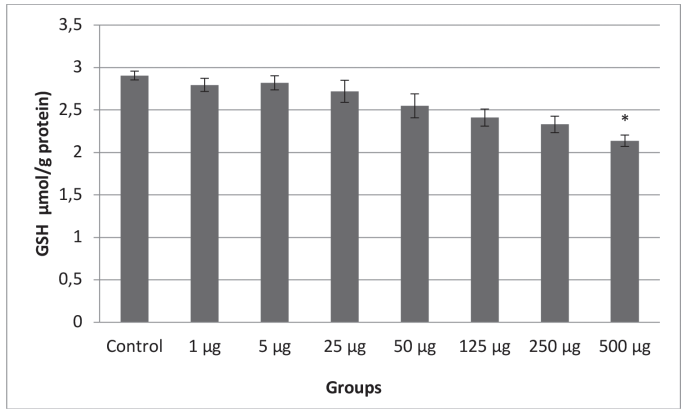

Figure 2. GSH level in L-929 cells with imidacloprid exposure
GSH: Glutathione

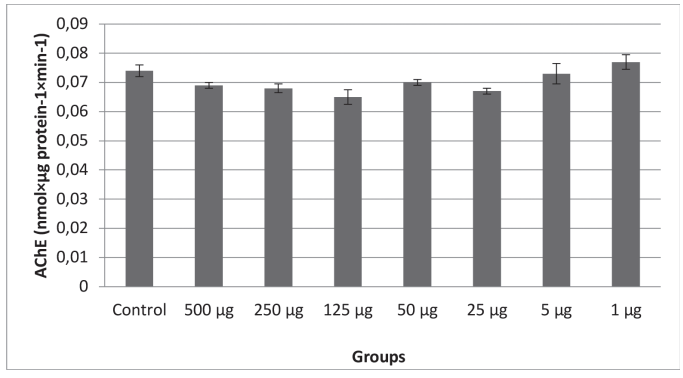

Figure 3. AChE level in L-929 cells with imidacloprid exposure
AChE: Acetylcholinesterase

The stable cytoplasmic enzyme LDH is an important biomarker for oxidative stress, apoptosis, necrosis, and other forms of cellular damage, expressed in all cells and rapidly released when the plasma membrane is damaged. In a study conducted in 2018, Kumar et al. [25,26] showed that LDH level increased with cellular damage, in accordance with our study. Abu Zeid et al.[27] reported that imidacloprid exposure in the Rock pigeon (*Columba livia domestica*) resulted in a significant increase in plasma LDH levels in high dose (6 mg/kg) and median dose (3 mg/kg) imidacloprid groups; however, there were no significant increase in the low dose (2 mg/kg) group compared to the control group. Plasma AChE's enzyme activities in all imidacloprid dose groups significantly increased compared to the control group. Lonare et al.[28] demonstrated that, 45 and 90 mg/kg body weight oral exposure of imidacloprid for 28 days significantly decreased AChE level in rats' erythrocytes. In addition, the brain AChE activity in rats in the imidacloprid treatment groups was decreased in a dose dependant manner compared to the control group. They also demonstrated that LDH levels increased and

GSH levels decreased significantly imidacloprid treated groups in different tissues of rats. Imidacloprid exposure increased the GSH and AChE activities in Chinese rare minnows' brain. This result indicates that imidacloprid has no effect on Chinese rare minnows.[11] It has been demonstrated that imidacloprid has neurotoxic effects through AChE inhibition and induces oxidative stress in rainbow trout brain tissue.[29] Moreover, imidacloprid exposure significantly decreased AChE levels in the plasma and brain of 10 and 20 mg/kg treated female rats.[30] In another study 24-h 20 mg/kg imidacloprid administration decreased AChE activity approximately 22% in the brain and 28% in red blood cells.[31]

CONCLUSION

Studies about imidacloprid's effects on AChE, LDH, and GSH express controversial results, which may be related to different study conditions such as species variety, exposure time variety, *in vitro* and *in vivo* conditions, and different doses. There are studies that include oxidative stress inducing effects of imidacloprid with different species in the literature; however, the underlying mechanism is not elucidated yet. Further studies are needed to clarify the toxic effects of neonicotinoids, especially imidacloprid, in different species and in different tissues.

Conflicts of interest: No conflict of interest was declared by the authors. The authors alone are responsible for the content and writing of the paper.

REFERENCES

1. Cha YS, Kim H, Lee Y, Choi EH, Kim HI, Kim OH, Cha KC, Lee KH, Hwong SO. The relationship between serum ammonia level and neurologic complications in patients with acute glufosinate ammonium poisoning: A prospective observational study. Hum Exp Toxicol. 2018;37:571-579.
2. Park S, Kim DE, Park SY, Gil HW and Hong SY. Seizures in patients with acute pesticide intoxication, with a focus on glufosinate ammonium. Hum Exp Toxicol. 2018;37:331-337.
3. Calas AG, Perche O, Richard O, Perche A, Pâris A, Lauga F, Herzine A, Palomo J. Ardourel MY, Menuet A, Mortaud S, Pichon J, Montécot-Dubourg C. Characterization of seizures induced by acute exposure to an organophosphate herbicide, glufosinate-ammonium. Neuroreport. 2016;27:532-541.
4. Kavvalakis MP, Tzatzarakis MN, Theodoropoulou EP, Barbounis EG, Tsakalof AK, Tsatsakis AM. Development and application of LC-APCI-MS method for biomonitoring of animal and human exposure to imidacloprid. Chemosphere. 2013;93:2612-2620.
5. Kim J, Park Y, Yoon KS, Clark JM, Park Y. Imidacloprid, a neonicotinoid insecticide, induces insulin resistance. J Toxicol Sci. 2013;38:655-660.
6. Park Y, Kim Y, Kim J, Yoon KS, Clark J, Lee J, Park Y. Imidacloprid, a neonicotinoid insecticide, potentiates adipogenesis in 3T3-L1 adipocytes. J Agric Food Chem. 2013;61:255-259.
7. Tomizawa M, Casida JE. Imidacloprid, thiacloprid, and their imine derivatives up-regulate the alpha 4 beta 2 nicotinic acetylcholine receptor in M10 cells. Toxicol Appl Pharmacol. 2010;169:114-120.
8. Etemadi-Aleagha A, Akhgari M, Abdollahi M. A brief review on oxidative stress and cardiac diseases. Mid East Pharm. 2002;10:8-9.
9. Abdollahi M, Ranjbar A, Shadnia S, Nikfar S, Rezaie A. Pesticides and oxidative stress: a review. Med. Sci. Monit. 2004;10:141-147.
10. Wang Y, Han Y, Xu P, Guo B, Li W, Wang X. The metabolism distribution and effect of imidacloprid in chinese lizards (Eremias argus) following oral exposure. Ecotoxicol Environ Saf. 2018;165:476-483.
11. Tian X, Yang W, Wang D, Zhao Y, Yao R, Ma L, Ge C, Li X, Huang Z, He L, Jiao W, Lin A. Chronic brain toxicity response of juvenile Chinese rare minnows (Gobiocypris rarus) to the neonicotinoid insecticides imidacloprid and nitenpyram. Chemosphere. 2018;210:1006-1012.
12. Njattuvetty Chandran N, Fojtova D, Blahova L, Rozmankova E, Blaha L. Acute and (sub) chronic toxicity of the neonicotinoid imidacloprid on Chironomus riparius. Chemosphere. 2018;209:568-577.
13. Shakir SK, Irfan S, Akhtar B, Rehman SU, Daud MK, Taimur N, Azizullah A. Pesticide-induced oxidative stress and antioxidant responses in tomato (Solanum lycopersicum) seedlings. Ecotoxicology. 2018;27:919-935.
14. Özdemir S, Altun S and Arslan H. Imidacloprid exposure cause the histopathological changes, activation of TNF-α, iNOS, 8-OHdG biomarkers, and alteration of caspase 3, iNOS, CYP1A, MT1 gene expression levels in common carp (Cyprinus carpio L.). Toxicol Rep. 2017;27:125-133.
15. Wang X, Anadón A, Wu Q, Qiao F, Ares I, Martínez-Larrañaga MR, Yuan Z, Martínez MA. Mechanism of neonicotinoid toxicity: impact on oxidative stress and metabolism. Annu Rev Pharmacol Toxicol. 2018;6:471-507.
16. Kapoor U, Srivastava MK, Bhardwaj S, Srivastava LP. Effect of imidacloprid on antioxidant enzymes and lipid peroxidation in female rats to derive its No Observed Effect Level (NOEL). J Toxicol Sci. 2010;35:577-581.
17. International Programme on Chemical Safety Toxicological evaluations: Imidacloprid, 2001; http://www.inchem.org/documents/jmpr/jmpmono/2001pr07.htm, 2011.
18. California Environmental Protection Agency/Department of Pesticide Regulation; Summary of Toxicology Data, Imidacloprid (138261-41-3) p. 5-6 (May 24, 1993, Revised November 18, 2013). Available from, as of January 15, 2016.
19. Jovanovic P, Zoric L, Stefanovic I, Dzunic B, Djordjevic-Jocic J, Radenkovic M, Jovanovic M. Lactate dehydrogenase and oxidative stress activity in primary open-angle glaucoma aqueous humour. Bosn J Basic Med Sci. 2010;10:83-88.
20. Casida JE and Durkin KA Neuroactive insecticides: targets, selectivity, resistance, and secondary effects. Annu Rev Entomol. 2013;58:99-117.
21. Wood TJ, Goulson D. The environmental risks of neonicotinoid pesticides: a review of the evidence post Environ Sci Pollut Res Int. 2017;24:17285-17325.
22. Tankiewicz M, Fenik J and Biziuk M. Determination of organophosphorus and organonitrogen pesticides in water samples. Trac Trends Anal Chem. 2010;29:1050-1063.
23. Tennekes HA, Sanchez-Bayo F. Time-dependent toxicity of neonicotinoids and other toxicants: implications for a new approach to risk assessment J Environ Anal Toxicol. 2011;S4:1-8.
24. Whitehorn PR, O'connor S, Wackers FL, Goulson D. Neonicotinoid pesticide reduces bumble bee colony growth and queen production. Science. 2012;336:351-352.

25. Shi DY, Xie FZ, Zhai C, Stern JS, Liu Y and Liu SL.The role of cellular oxidative stress in regulating glycolysis energy metabolism in hepatoma cells. Mol Cancer. 2003;5:32.

26. Kumar P, Nagarajan A and Uchil PD 2018 Analysis of Cell Viability by the Lactate Dehydrogenase Assay. Cold Spring Harb Protoc. 6 pdb. prot095497.

27. Abu Zeid EH, Alam RTM, Ali SA, Hendawi MY. Dose-related impacts of imidacloprid oral intoxication on brain and liver of rock pigeon (Columba livia domestica), residues analysis in different organs. Ecotoxicol Environ Saf. 2018;5:60-68.

28. Lonare M, Kumar M, Raut S, Badgujar P, Doltade S, Telang A. Evaluation of imidacloprid-induced neurotoxicity in male rats: a protective effect of curcumin. Neurochem. 2014;78:122-129.

29. Topal A, Alak G, Ozkaraca M, Yeltekin AC, Comaklı S, Acıl G, Kokturk M, Atamanalp M. Neurotoxic responses in brain tissues of rainbow trout exposed to imidacloprid pesticide: Assessment of 8-hydroxy-2-deoxyguanosine activity, oxidative stress and acetylcholinesterase activity. Chemosphere. 2017;175:186-191.

30. Vohra P, Khera KS, Sangha GK. Physiological, biochemical and histological alterations induced by administration of imidacloprid in female albino rats. Pestic Biochem Physiol. 2014;110:50-56.

31. Kapoor U, Srivastava MK, Trivedi P, Garg V, Srivastava LP. Disposition and acute toxicity of imidacloprid in female rats after single exposure. Food Chem Toxicol. 2014;68:190-195.

Turk J Pharm Sci 2020;17(5):511-522
DOI: 10.4274/tjps.galenos.2019.46548

ORIGINAL ARTICLE

Antimicrobial Potential of Bioactive Metabolites and Silver Nanoparticles from *Bacillus* spp. and of Some Antibiotics Against Multidrug Resistant *Salmonella* spp.

Bacillus spp.'nin Biyoaktif Metabolitleri ile Gümüş Nanopartikülleri ve Çoklu İlaç Direncine Karşı Bazı Antibiyotiklerin Antimikrobiyal Potansiyelleri

Bukola Christianah ADEBAYO-TAYO*, Oluwadara EKUNDAYO-OBABA, Olutayo Israel FALODUN

Ibadan University, Department of Microbiology, Ibadan, Oyo State, Nigeria

ABSTRACT

Objectives: The synthesis of nanoparticles using microorganisms and their metabolites is of increasing interest because they are potential producers of biocompatible and environmental friendly nanoparticles. Their nanoparticles can serve as potent alternatives to antibiotics against multidrug resistant (MDR) bacteria. The antibacterial potential of *Bacillus* spp. metabolites, their silver nanoparticles (SNPs), and some antibiotics against MDR *Salmonella* spp. was evaluated.

Materials and Methods: The antimicrobial potential of metabolites and SNPs biosynthesized from *Bacillus* spp. was characterized, the effect of physicochemical parameters on SNP biosynthesis, the antimicrobial activity of the SNPs, and combination of SNPs and antibiotics against MDR *Salmonella* strains were evaluated.

Results: The bioactive metabolites of the *Bacillus* spp. exhibited varied antimicrobial potential against the tested MDR *Salmonella* spp. The metabolites were able to bioreduce silver nitrate ($AgNO_3$) to Ag+ for SNP biosynthesis. Change in color from whitish to darkish brown and a surface plasma resonance peak of 600-800 nm were observed. The SNPs were aggregated, rods, and crystalline in shape and their sizes were 15 µm, 16 µm, and 13 µm. Carboxylic acid, amino acid, alcohol, esters, and aldehydes were the functional groups found in the biosynthesized SNPs. The antibacterial activity of BAC1-SNPs, BAC7-SNPs, and BAC20-SNPs against MDR *Staphylococcus aureus* 9 (MDRSA9) and MDRSA18 was 6.0-22 mm and 11-20 mm. SNPs biosynthesized at pH 7 and 10 mM $AgNO_3$ had the highest antagonistic activity. Combination of SNPs and antibiotics exhibited the best antagonistic potential.

Conclusion: The metabolites and SNPs from *Bacillus* spp. exhibited antagonistic effects against MDR *Salmonella* spp. The combined SNPs and antibiotics had better antimicrobial activity.

Key words: *Bacillus* strains, metabolites, antimicrobial, silver nanoparticles, MDR *Salmonella* species, synergistic effect

ÖZ

Amaç: Biyouyumlu ve çevre dostu nanopartiküllerin potansiyel üreticileri olan mikroorganizmalar ve bunların metabolitleri kullanılarak hazırlanan nanopartiküllere olan ilgi son yıllarda artmıştır. Bu nanopartiküller, çoklu ilaç direnci (MDR) olan bakterilere karşı antibiyotiklere güçlü alternatifler olarak değerlendirilebilir. *Bacillus* spp. metabolitlerinin, bunların gümüş nanopartiküllerinin (SNP) ve MDR *Salmonella* spp'ye karşı bazı antibiyotiklerin antibakteriyel potansiyelleri değerlendirildi.

Gereç ve Yöntemler: *Bacillus* spp.'den biyosentezlenen metabolitlerin ve SNP'lerin antimikrobiyal etki potansiyelleri, fizikokimyasal parametrelerin SNP biyosentezine etkileri, SNP'lerin antimikrobiyal aktivitesi ve SNP'ler ile kombine edilen antibiyotiklerin MDR *Salmonella* suşlarına karşı etkileri değerlendirildi.

Bulgular: *Bacillus* türlerinin biyoaktif metabolitleri test edilen MDR *Salmonella* spp.'ye karşı değişken antimikrobiyal aktivite gösterdiler. Metabolitler, SNP biyosentezi için gümüş nitratı ($AgNO_3$) Ag+'ya biyolojik olarak indirgeyebilmiştir. Beyazımsıdan koyu kahverengiye renk değişimi ve yüzey

*Correspondence: E-mail: bukola.tayo@gmail.com, Phone: +234 8035522409 ORCID-ID: orcid.org/0000-0003-2404-1686
Received: 08.07.2019, Accepted: 05.09.2019

plazmon rezonans spektroskopisinde 600-800 nm'de bir pik gözlendi. Agrege olan SNP'lerin, çubuk ve kristal şeklinde oldukları; boyutlarının 15 µm, 16 µm ve 13 µm olduğu tespit edilmiştir. Karboksilik asit, amino asit, alkol, ester ve aldehit, biyosentezlenmiş SNP'lerde bulunan fonksiyonel gruplardır. BAC1-SNP'lerin, BAC7-SNP'lerin ve BAC20-SNP'lerin MDRSA9 ve MDRSA18'e karşı gösterdikleri antibakteriyel aktivite sırasıyla 6,0-22 mm ve 11-20 mm aralığındaydı. pH 7 ve 10 mM $AgNO_3$'te biyosentezlenen SNP'lerin en yüksek antagonistik aktiviteye sahip olduğu bulundu. En iyi antagonistik potansiyel SNP'lerin ve antibiyotiklerin kombinasyonu ile elde edildi.

Sonuç: *Bacillus* spp.'den biyosentezlenen metabolitlerin ve SNP'lerin MDR *Salmonella* spp'ye karşı antagonistik etkileri olduğu bulundu. SNP'ler ile kombine antibiyotiklerin daha iyi antimikrobiyal aktiviteye sahip olduğu tespit edildi.

Anahtar kelimeler: *Bacillus* suşları, metabolitler, antimikrobiyal, gümüş nanopartiküller, MDR *Salmonella* türleri, sinerjistik etki

INTRODUCTION

Infections caused by harmful microorganisms affect many people globally and they are an important cause of morbidity and mortality with adverse effects on the healthcare economy.[1,2] The treatment of these infections is of public health concern as a result of development of resistance to antibiotics by these etiological agents.[3,4]

Salmonella, the most commonly isolated food-borne pathogens associated with fresh fruits and vegetables, are Gram-negative flagellated rod-shaped facultative anaerobe bacteria.[5,6] *Salmonella* are a group of bacteria that cause typhoid fever, food poisoning, gastroenteritis, enteric fever, and other illnesses. *Salmonella* infections, or salmonellosis, are bacterial diseases of the intestinal tract.

The occurrence of enteric fever has been a major health problem in spite of the use of antibiotics and the development of newer antimicrobials. Resistance of *Salmonella* spp. to previously efficacious drugs like ciprofloxacin, ampicillin, ceftriaxone, and cotrimoxazole has been reported.[7] Adabara et al.[8] reported the prevalence and antibiotic susceptibility pattern of *Salmonella typhi* among patients in a military hospital in Minna, Nigeria. The isolates were resistant to all the antibiotics tested, which are the drugs of choice routinely used in the study area for the treatment of typhoid fever.

Multidrug resistant (MDR) *Salmonella* strains are very common and are the causative agent of endemic and epidemic typhoid fever infections in many communities. MDR *Salmonella typhi* poses a serious threat because it has developed resistance to available antibiotics, resulting in an increase in the death rate and high capability for epidemic outbreaks of typhoid that may be difficult to manage.

The consequence of typhoid fever outbreaks may be highly destructive most especially in developing countries where health facilities are very poor. *Salmonella* has been reported as the most common cause of bacterial food-borne illness in the US and is estimated to annually cause over 1 million cases, 19,000 hospitalizations, 350 deaths, and $2.6 billion in social costs.[9,10] *Salmonella enterica* serovar *typhimurium* is one of the most common salmonellae in humans and livestock, and most of these strains are resistant to multiple antibiotics.

Bacillus species are Gram-positive, endospore-forming, chemoheterotrophic rod-shaped bacteria that are usually motile with peritrichous flagella; they are aerobic or facultative anaerobic and catalase positive and part of the phylum *Firmicutes.* Many *Bacillus* species are of remarkable importance because they are antibiotic producers. *B. subtilis*, *B. polymyxa*, *B. brevis*, *B. licheniformis*, *B. circulans*, and *B. cereus* have been reported as antibiotic producers. Antibiotics such as bacitracin, gramycidin S, polymyxin, and tyrotricidin produced by *Bacillus* spp. have found application in medical treatments.[11-14] A wide range of antimicrobial, antiviral, anti-ameobocytic, and antimycoplasma activities of *Bacillus* species have been reported.[15-17]

The ability of *Bacillus* species to produce different metabolites with antimicrobial activity has been extensively used in medicine and the pharmaceutical industry; one of its potentials is its application as a biocontrol agent for animal, human, and plant diseases.[18]

Silver and silver-containing products are among the most popular and efficient antimicrobial agents commonly used against pathogenic bacteria.[19] Since ancient times silver has been in used as an antimicrobial agent but with the development of antibiotics there has been a reduction in the medical applications of silver as an antimicrobial.[20]

Nanolevel manipulation and physicochemical changes of silver can lead to production of silver nanoparticles (SNPs) with an increase in antimicrobial potential. SNPs are characterized by high surface-area-to-volume ratio and the unique chemical and physical properties that confer on them better antimicrobial properties.[21]

SNPs 0-100 nm in size showed strong bactericidal potential against both Gram-positive and Gram-negative bacteria.[22] Silver in the form of SNPs is known to exhibit strong biocidal effects on different bacterial strains, including MDR bacteria.[23,24] SNPs have little chance of drug resistance, which provides a solution to multidrug resistance problems.[25] Drug resistance has been reported as one of the most serious threatening and widespread problems in all developing countries.[26] Hence, diverse medical applications of AgNPs are necessary to avoid the effect of these drug-resistant pathogenic microorganisms by various methods, ranging from silver-based dressings and silver-coated medical devices, such as nanogels and nanolotions, to dental materials, sunscreen lotions, biological labeling, water treatment, in optical devices, and as an antibactericidal.[27-29] Microbial resistance to antimicrobials is highly prevalent worldwide, particularly in developing countries, and this has made therapeutic options appear more limited than ever. As a result of the emergence of MDR pathogens, research interest has been geared towards the development of efficient and safe antimicrobials. For these reasons, the aim of the present research was to investigate the

antimicrobial potential of metabolites from *Bacillus* spp., their SNPs, and combination of SNPs with some antibiotics against some selected MDR *Salmonella* spp.

MATERIALS AND METHODS

Microorganisms

Cultures of *Bacillus* spp. and 10 MDR *Salmonella* spp. were obtained from the culture collection of our previous work in the Microbial Physiology and Biotechnology Unit, Department of Microbiology, University of Ibadan. The isolates were kept on nutrient agar slants in a refrigerator. Constant subculturing was carried out to ensure the viability of the isolates.

Production of bioactive metabolites from Bacillus strains

Three *Bacillus* strains were used for the production of bioactive metabolites using sterile nutrient broth. The supernatant from the sterile inoculated nutrient broth was incubated at 35 °C for 48 h and used as bioactive metabolites.

Antagonistic potential of the bioactive metabolites produced by Bacillus spp. against some MDR Salmonella spp.

The antagonistic potential of the bioactive metabolites against some MDR *Salmonella* spp. was investigated using agar well diffusion.[30] Inoculum suspensions of 24-h-old culture of the *Salmonella* spp. were spread plated on Mueller-Hinton agar. Uniform wells of 6 mm were bored in the agar. Each well was filled with 60 µL of the bioactive metabolites from the *Bacillus* isolates. The plates were incubated at 37 °C for 24 h. The incubated plates were observed for a zone of inhibition (ZOI) around the well. The formation of a clear zone around the well is an indication of antibacterial activity.[31] Results were considered positive if the diameter (mm) of the ZOI around the well was greater than 1 mm. The bioactive metabolites of the best three *Bacillus* spp. were used for further studies.

Production of SNPs using the selected Bacillus strains

The bioactive metabolites of the best three *Bacillus* spp. were used for the production of SNPs. First 30 mL of the bioactive metabolites was added to 70 mL of 10 mM silver nitrate ($AgNO_3$) solution. The mixture was stored at room temperature (35 °C) in a dark place for 24-72 h. After 12 h of incubation, the whitish solution turned brownish, which confirmed the formation of SNPs.

Characterization of the synthesized SNPs

The SNPs were characterized using visual detection for change in color. Ultraviolet (UV)-Visabsorption (Vis) spectra of the SNPs were analyzed at room temperature using a UV-Vis spectrophotometer (Lambda 25, PerkinElmer, Waltham, MA, USA) with a resolution of 0.5 nm at the wavelengths of 200-800 nm. The fourier transform infrared (FTIR) spectra of the nanoparticles were analyzed using FTIR spectroscopy (Shimadzu) at a resolution of 4 cm^{-1}. The size, shape, and morphology of the biosynthesized SNPs were determined using scanning electron microscopy (SEM).

Antibacterial activity of the SNPs against some selected (MDR) Salmonella spp. and their synergetic effect with some selected antibiotics

The antibacterial activity of the biosynthesized SNPs and the synergistic effect of SNPs along with some selected antibiotics (ciprofloxacin, Zinacef, amoxicillin, Rocephin, streptomycin, Ampiclox, and gentamycin) were tested using agar well diffusion[30] against the selected MDR *Salmonella* spp. as previously described.

Determination of minimum inhibitory concentration (MIC) of the biosynthesized SNPs

MIC was determined using different concentrations (100%, 50%, 25%, 12.5%, 6.25%, and 3.125%) of the SNPs against the isolates.[30] The lowest dilution of the SNPs at which ZOIs were observed against the *Salmonella* sp. is regarded as the MIC for the SNPs. Ciprofloxacin was used as a positive control.

Effect of physiochemical parameters on SNP biosynthesis

The effects of temperature (25 °C, 35 °C, and 40 °C), pH (4, 7, and 9), and different concentrations of $AgNO_3$ (2-10 mM) on the biosynthesized SNPs were evaluated.

Statistical analysis

The results were subjected to One-Way ANOVA using Minitab student Release 12 (Minitab Inc., State College, PA, USA). Statistically significant means were separated using Duncan's multiple range test and Fisher pairwise comparisons. A significance level of $p \leq 0.05$ was used for the rejection of the null hypothesis.

RESULTS AND DISCUSSION

The antimicrobial activity of the bioactive metabolites of the *Bacillus* spp. against some MDR *Salmonella* spp. is shown in Table 1. The antimicrobial activity of *Bacillus subtilis* BAC1, *B. licheniformis* BAC7, and *Bacillus subtilis* BAC20 bioactive metabolites against the 10 MDR *Salmonella* strains was 3.0-17.0 mm, 4-14 mm, and 14-2.0 mm. MDR *Staphylococcus aureus* 9 (MDRSA9) and MDRSA20 had the highest susceptibility.

The ability of the *Bacillus* spp. metabolites to inhibit the test pathogens may be as a result of the production of some bioactive metabolites. Several antimicrobial activities of *Bacillus* spp. against pathogens have been reported. Antagonistic activity of *Bacillus subtilis* and *Bacillus cereus* against *Staphylococcus* spp. has been reported by Perez et al.[13] and Riley and Wertz.[32]

Biosynthesis of SNPs using Bacilli spp. broth

The 3 bioactive metabolites were able to bioreduce the $AgNO_3$ to produce SNPs by the evident change in color from a whitish reaction mixture to darkish brown, which indicates the formation of SNPs.

The biosynthesis of SNPs was done using the bioactive metabolites of *Bacillus* spp. with the highest antagonistic potential from the previous screening. This is in accordance with the work by Kalishwaralal et al.[33] who biosynthesized SNPs from culture supernatant of *Bacillus licheniformis*. The culture supernatant was able to bioreduce Ag^+ to Ag^o. Kanmani

and Lim[34] reported the bioreduction of Ag^{+} to Ag^{o} using exopolysaccharides.

Changes in color from white to brown indicate SNP biosynthesis. A visible color change from whitish yellow to brown was also reported by El-Batal et al.[35] Changes in color may be attributed to the surface plasmon resonance (SPR).[34]

Spectrophotometric analysis of the biosynthesized SNPs

The biosynthesized SNPs were characterized by UV-Vis spectroscopy. UV-absorption measurements in the range of 200-1000 nm were observed (Figures 1A-1C).

The UV spectra of the biosynthesized SNPs using BAC1 metabolites incubated for 24, 48, and 72 h had the highest SPR peak at 600 nm (Figure 1c). SNPs from BAC7 metabolites had the highest SPR peak at 800 nm, 600 nm, and 400 nm (Figure 1b). SNPs from BAC20 metabolites had the highest SPR peak at 600 nm, 600 nm, and 800 nm after 24, 48, and 72 h of incubation (Figure 1C), which corresponds to plasmon excitation of the SNPs. All the peaks obtained were in the range of 400-800 nm. There was variation in the SPR peaks of the SNPs incubated for different time intervals.

Primary confirmation of SNP biosynthesis was carried out by UV-Vis spectroscopy in the range of 200-1000 nm. A strong SPR peak was observed at 600 nm for the SNPs biosynthesized by the *Bacillus subtilis* BAC1 and BAC20 after 24 h of incubation, indicating the formation of SNPs that varied in shape and size. Kanmani and Lim[34] reported a strong SPR peak at 400-550 nm with a broad band. El-Batal et al.[35] reported an SPR band at 431 nm of SNPs synthesized with *Bacillus stearothermophilus*, indicating the presence of spherical or roughly spherical SNPs. Valencia et al.[36] reported that solutions containing SNPs changed to yellow from an initial whitish color and presented SPR peaks between 411 and 414 nm.

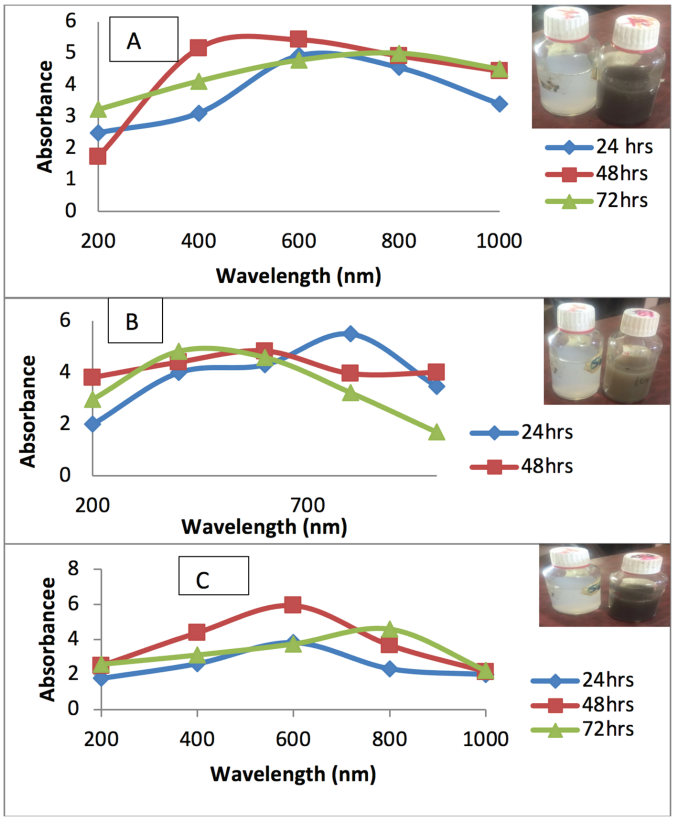

Figure 1A-C. UV-Visible spectra of the SNPs biosynthesized using metabolites of *Bacillus* spp. A) BAC1-SNPs, B) BAC7-SNPs, and C) BAC20-SNPs at different incubation times

UV: Ultraviolet, SNPs: Silver nanoparticles, BAC1: *Bacillus subtilis*, BAC7: B. licheniformis, BAC20: *Bacillus subtilis*

Scanning electron microscopy

The biosynthesized SNPs were characterized by SEM. Figures 2a-2c show the micrographs of the SNPs. The SEM images show that SNPs from BAC1, BAC7, and BAC20 were of varying shape and size. BAC1-SNPs were aggregated, BAC7-SNPs were aggregated rods, and BAC20-SNPs were crystalline in shape (Figures 2A-2C). Their sizes were 15 µm, 13 µm, and 10 µm, respectively.

SEM is used for morphological characterization at the nanometer to micrometer scale and can provide morphological information on the submicron scale and elemental information at the micron scale as reported by Schaffer et al.[37]

SEM studies revealed that the biologically synthesized SNPs were different in size and shape and they showed that they were aggregated, rod shaped, and crystalline. The aggregation observed may have been due to the drying process. This observation agrees with the work by Sadowski et al.[38] who observed aggregated SNPs biosynthesized using *Penicillium* strains isolated from soil. They concluded that the drying can affect the shape and size of SNPs.

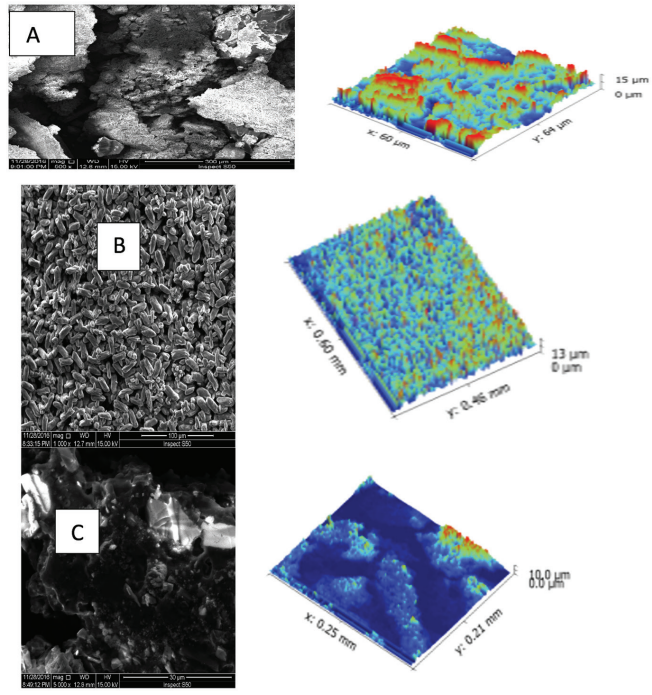

Figure 2A-C. SEM micrograph of SNPs biosynthesized using metabolites of *Bacillus* spp. (A), BAC1-SNPs, B) BAC7-SNPs, and C) BAC20-SNPs

SEM: Scanning electron microscope, SNPs: Silver nanoparticles, BAC1: *Bacillus* subtilis, BAC7: *B. licheniformis*, BAC20: *Bacillus subtilis*

The rod shape observed in BAC7-SNPs is in accordance with the work by Gardea-Torresday et al.[39] who reported a rod shape from the SEM characterization of biosynthesis of gold nanoparticles from *Triticum aestivum* leaves.

The crystalline SNPs observed in the present work agree with the report by Vithiya et al.[40] who stated that the extracellular biosynthesized SNPs from *Bacillus* spp. were monodispersed.

FTIR spectra of the SNPs

FTIR analysis of the SNPs was carried out to identify interactions between silver salts and protein molecules, which could account for the reduction of silver ions and stabilization of the SNPs formed.

The BAC1-SNPs characterized using FTIR show 7 bands with transmission peaks at 3448.00, 2937.14, 1638.92, 1552.59, 1404.40, 1103.65, and 607.24 cm^{-1} (Figure 3A). The bands corresponded to O-H stretch of alcohol, C-H symmetrical stretch, presence of amide, NH bend, C=O stretch, C-O stretch of alcohol, and acetylenic CH of alkynes, respectively. The functional groups generally observed indicated the presence of amino acids, alcohol, aldehydes, and carboxylic acid in the sample and this may have been responsible for the reduction of $AgNO_3$ to SNPs.

The FTIR analysis of BAC7-SNPs shows 9 bands and the peaks' spectrum ranged from 3423.00 cm^{-1} to 352.84 cm^{-1} (Figure 3B). The peaks were attributed to O-H stretch vibration of alcohol, symmetrical C-H, C=O stretch of carboxylates and NH stretch of secondary amides, presence of O-H bends of esters, phenol and tertiary alcohol or C-C bend of aldehyde, C-O stretching vibration of carboxylic esters, C-O stretching vibration of secondary alcohol, and presence of acetylenic CH of alkynes and aromatic benzene ring. From the FTIR spectrum, it was observed that the SNPs were surrounded by carboxylic acid, aldehyde, esters, protein, and amino acids, which may have been responsible for the biosynthesis and stability of the SNPs (Figure 3B).

The FTIR analysis of BAC20-SNPs revealed 12 absorption peaks that ranged between 3760.00 cm^{-1} and 361.39 cm^{-1}. The peak indicated the presence of an O-H stretch free, strong alcohol, O-H stretch vibration of alcohol, C-H symmetrical stretching, carbonyl stretching of transition metals, NH bend of amide, NH stretch of secondary amides, C-O stretch of esters, carboxylic acids, acetylenic CH of alkynes, and weak aromatic benzene. The functional groups that corresponded to the FTIR spectrum generally indicated the presence of amino acids, alcohol, aldehydes, and carboxylic acid, which may have been responsible for the reduction of $AgNO_3$ to SNPs (Figure 3c). The presence of the intense peak in C=O stretching mode indicates the presence of carboxylic groups in the material bound to SNPs.

The FTIR measurements were obtained to identify possible interactions between silver salts and protein molecules. FTIR is very useful for SNP characterization as reported by Kanmani and Lim.[34] El-Batal et al.[35] reported that the release of extracellular protein molecules from bacteria could possibly perform the function of formation and stabilization of SNPs in aqueous medium. Balashanmugam et al.[30] also suggested that from FTIR spectrum analysis SNPs were surrounded by proteins and amino acids, which may be responsible for the stability of the SNPs.

The functional groups such as carboxylic acid, amino acid, alcohol, esters, and aldehydes present in the SNPs biosynthesized using the *Bacillus* metabolites were responsible for reduction, capping, and stabilization of the nanoparticles. El-Batal et al.[35] reported functional groups as the reducing agents responsible for SNP formation and stabilization in their work.

Antibacterial activity of the biosynthesized SNPs from the Bacillus strains against MDR Salmonella spp.

The antibacterial activity of the biosynthesized SNPs from the *Bacillus* spp. against the selected MDR *Salmonella* spp. is shown in Figure 4.

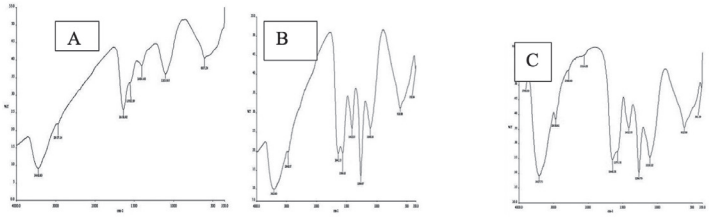

Figure 3A-C. FTIR spectra of the SNPs from *Bacillus* spp. A) BAC1-SNPs, B) BAC7-SNPs, and C) BAC20-SNPs
FTIR: Fourier transform infrared, SNPs: Silver nanoparticles, BAC1: *Bacillus subtilis*, BAC7: *B. licheniformis*, BAC20: *Bacillus subtilis*

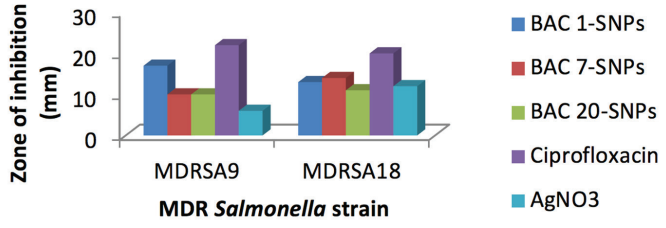

Figure 4. Antibacterial activity of the synthesized SNPs against the selected (MDR) *Salmonella* spp.
MDR: Multidrug resistant, SNPs: Silver nanoparticles, $AgNO_3$: Silver nitrate, MDRSA: Multidrug resistant *Staphylococcus aureus*, BAC1: *Bacillus subtilis*, BAC7: *B. licheniformis*, BAC20: *Bacillus subtilis*

The antibacterial activity of BAC1-SNPs, BAC7-SNPs, and BAC20-SNPs against MDRSA9 ranged from 6.0 to 22 nm. MDRSA9 had the highest susceptibility to BAC1-SNPs. BAC7-SNPs and BAC20-SNPs exhibited higher activity against the MDRSA9 compared to $AgNO_3$. Ciprofloxacin exhibited higher activity against MDRSA9 compared to the SNPs.

The antibacterial activity of BAC1-SNPs, BAC7-SNPs, and BAC20-SNPs against MDRSA18 ranged from 11 to 20 nm. All the biosynthesized SNPs had antagonistic activity against MDRSA18. BAC7-SNPs exhibited higher antagonistic activity against MDRSA18 than BAC1-SNPs and BAC20-SNPs.

BAC1-SNPs had the highest antagonistic potential against MDRSA9 while BAC7-SNPs and BAC20-SNPs had the highest antagonistic potential against MDRSA18. Ciprofloxacin exhibited higher activity against MDRS18 compared to the SNPs.

Guzman et al.[41] reported the possibility of SNPs acting similarly to the antimicrobial agents used for the treatment of bacterial infections, which show four different mechanisms of action, including interference with cell wall synthesis, inhibition of protein synthesis, interference with nucleic acid synthesis, and inhibition of metabolic pathway. Sharma et al.[42] also noted that SNPs not only interact with the surface of the membrane, but can also penetrate inside the bacteria. It is reported that the bactericidal effect of SNPs decreases as the size increases and is also affected by the shape of the particles. Dhanalakshmi and Rajendran[43] reported the interaction of nanoparticles with the DNA inside a bacterium thus losing its ability to replicate, which may lead to cell death.

The antibacterial activities of the SNPs produced from *Bacillus* spp. metabolites against MDR *Salmonella* spp. are in agreement with the work by Natarajan and Selvaraj[44] who reported the antibacterial activity of SNPs produced from *Bacillus subtilis* against pathogens like *Escherichia coli*, *Staphylococcus epidermidis*, *Staphylococcus coagulase* positive, *Serratia* spp., and *Salmonella typhi*. They also stated that the SNPs showed the most activity against *Salmonella typhi*. This is not in accordance with Kanmani and Lim[34] who reported that Gram-negative bacteria were more susceptible to SNPs than Gram-positive bacteria.

MIC of the SNPs against the MDR Salmnella spp.

The MIC of the SNPs against the MDR *Salmonella* spp. is shown in Table 2. BAC1- SNPs had an MIC of 3.25% on SA9 and 6.25% on SA18. BAC7-SNPs had an MIC of 3.25% on SA9 and of 6.25% on SA18. The BAC20-SNPs had an MIC of 6.25% on SA9 and 3.25% on SA18. *Salmonella* spp. SA9 was resistant to BAC20-SNPs at a concentration of 3.25%, while *Salmonella* sp. SA18 was resistant to BAC1-SNPs and BAC7-SNPs at a 3.25% concentration.

The MIC was defined as the lowest concentration of the SNPs that can have an antimicrobial effect on the test organisms; 10 mM was used to prepare the different concentrations of the SNPs for the MIC evaluation and different MICs were recorded for the two (MDR) *Salmonella* spp. Balashanmugam et al.[30] also reported the MIC of their SNPs after testing on some pathogens, with *Escherichia coli* and *Bacillus subtilis* having the highest values.

Effect of temperature on SNP biosynthesis

The effect of temperature (25-40 ˚C), pH (4-9), and different concentrations of $AgNO_3$ (2-10 mM) on the biosynthesis of SNPs was evaluated and the SNPs were characterized.

The UV-Vis spectra of BAC1-SNPs had a sharp SPR peak at 400 and 800 at 25 ˚C and 35 ˚C. At 40 ˚C, a sharp SPR peak was observed at 600 nm. SNPs synthesized at 35 ˚C had the highest SPR peak (Figure 5A). For BAC7- SNPs biosynthesized at 25 ˚C, 35 ˚C, and 40 ˚C, the sharp SPR peak was observed at 400 nm and 800 nm (Figure 5B). For BAC20-SNP at 25 ˚C and 40 ˚C, the UV-Vis spectra showed a sharp SPR peak at 400 nm and 800 nm, while at 35 ˚C, the sharp SPR peak was observed at 600 nm (Figure 5C). The highest absorbance values were obtained at 35 ˚C followed by 40 ˚C for all the SNPs. The optimum temperature for the production of SNPs was 35 ˚C.

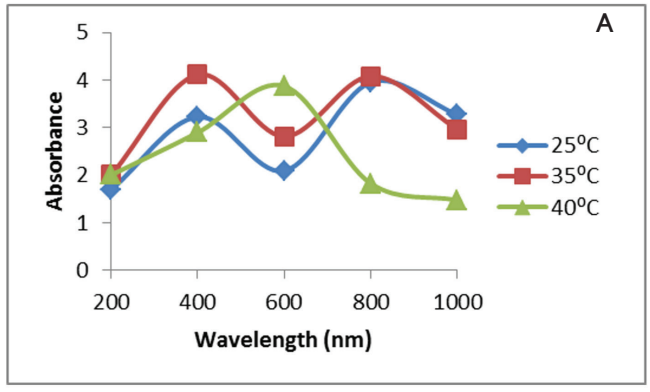

Figure 5A. UV-Visible spectra of BAC1 SNPs at different temperature
UV: Ultraviolet, SNPs: Silver nanoparticles, BAC1: *Bacillus subtilis*

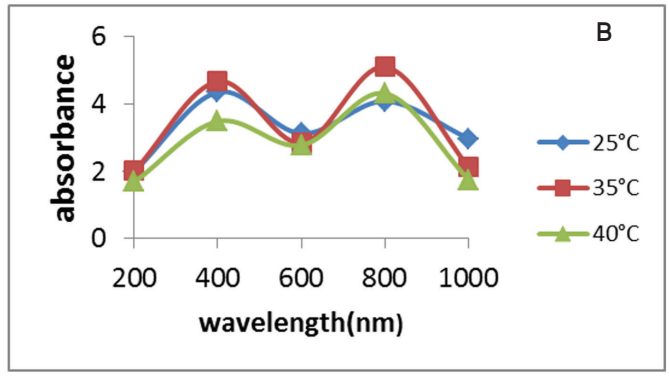

Figure 5B. UV-Visible spectra of BAC7 SNPs at different temperature
UV: Ultraviolet, SNPs: Silver nanoparticles, BAC7: *B. licheniformis*

Table 1. Antimicrobial activity (mm) of the bioactive metabolites of *Bacillus* spp. against some multidrug resistant *Salmonella* spp.

Bioactive *Bacillus* spp. metabolites	MDR *Salmonella* strains/Zone of inhibition (mm)									
	SA23	SA15	SA32	SA20	SA32b	SA9	SA7	SA18	SA21	SA8
BSM (BAC1)	7.0±0.5^{e}	11.0±1.0^{b}	8.0±0.5^{d}	5.0±1.00^{f}	4.0±1.0^{fg}	17.0±0.5^{a}	4.0±1.0^{fg}	10.0±1.0^{c}	0.0±0.0^{h}	3.0±0.5^{g}
BLM (BAC7)	0.0±0.0^{g}	10.0±0.5^{d}	6.0±0.5^{e}	4.0±1.0^{f}	10.0±0.0^{d}	14.0±1.0^{a}	0.0±0.0^{g}	12.0±0.5^{b}	10.0±0.0^{d}	11.0±1.0^{c}
BMM (BAC20)	2.0±0.0^{f}	0.0±0.0^{g}	0.0±0.0^{g}	14.0±1.0^{a}	12.0±0.0^{c}	6.0±1.0^{e}	2.0±0.0^{f}	11.0±0.0^{d}	6.0±0.0^{e}	13.0±0.5^{b}

Values are means ± standard deviations of triplicate observations. Means with different letters across the row are statistically significant at p≤0.05. MDR: Multidrug resistant, BSM (BAC1): Bioactive metabolites from *Bacillus subtilis*, BLM (BAC7): Bioactive metabolites from *B. licheniformis*, BMM (BAC20): Bioactive metabolites from *Bacillus subtilis*, BAC20, $^{a, b, c, d, e, f, g}$: Are statistically significant letters from Duncan multiple range test

The effect of temperature on SNP synthesis was evaluated and the best temperature was 35 ˚C. This is not in accordance with the work by Amin et al.[45] who observed that with an increase in temperature from 25 ˚C to 45 ˚C the SPR peaks became sharper and an absorption band at 406 nm was obtained, which suggested the formation of SNPs.

Annadurai et al.[46] also reported that the synthesis of SNPs from leaf extract of *Coleus aromaticus* increased when the reaction temperature was increased and they concluded that a higher temperature (70 ˚C) was best for nanoparticle synthesis. Amin et al.[45] observed that the best temperature required for the completion of the reaction was 45 ˚C.

Effect of pH on SNP biosynthesis

The UV spectra of the effect of different pH values (4, 7, and 9) on SNP biosynthesis are shown in Figures 6A-6C. The UV-Vis spectra of BAC1-SNPs produced at different pH values are shown in Figure 6A. At pH 4 and 7 a sharp peak was observed at 600 nm, while at pH 9 a sharp SPR peak was observed at 400 nm. The highest absorbance was observed at pH 7. The UV-Vis spectra of BAC7-SNPs at pH 4, pH 7, and pH 9 had a broad spectrum between 400 nm and 800 nm. BAC7-SNPs at pH 7 had a sharp peak at 200 nm (Figure 6B). The UV-Vis spectra of BAC20-SNPs biosynthesized at different pH values are shown in Figure 5C. BAC20-SNPs had the highest sharp SPR peak at 600 nm. The SNPs biosynthesized at pH 4 and 7 had a broad band between 600 nm and 800 nm.

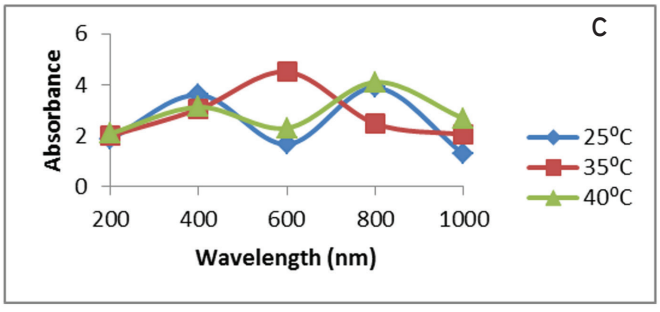

Figure 5c. UV-Visible spectra of BAC20 SNPs at different temperature

UV: Ultraviolet, SNPs: Silver nanoparticles, BAC20: *Bacillus subtilis*

The optimum pH for the production of SNPs by *Bacillus* spp. fermentation broth was 7. Goldie et al.[47] reported that the optimum pH for extracellular fabrication of SNPs using *Pseudomonas aeruginosa* was 10. Annadurai et al.[47] reported

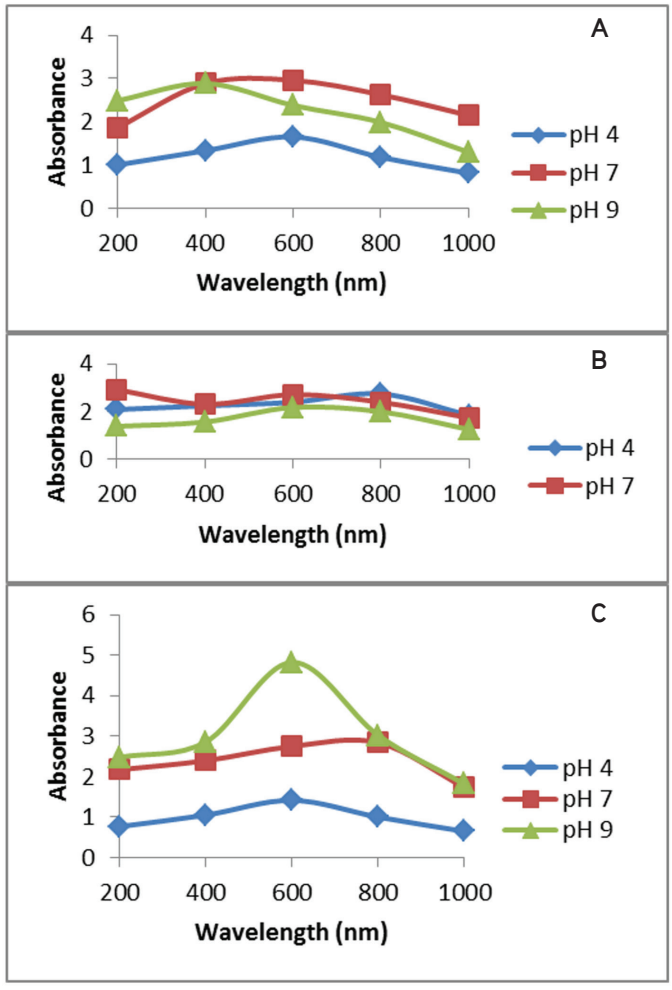

Figure 6A-C. UV-Visible spectra of SNPs biosynthesized at different pH by Bacillus spp. A), BAC1-SNPs, B) BAC7-SNPs and C) BAC20 SNPs

UV: Ultraviolet, SNPs: Silver nanoparticles, BAC1: *Bacillus subtilis*, BAC7: *B. licheniformis*, BAC20: *Bacillus subtilis*

Table 2. Determination of minimum inhibitory concentration of *Bacillus* spp. silver nanoparticles on the selected multidrug resistant *Salmonella* spp.

MIC concentration (%)	Zones of inhibition (mm)					
	MDRSA9			MDRSA18		
	BAC1-SNPs	BAC7-SNPs	BAC20-SNPs	BAC1-SNPs	BAC7-SNPs	BAC20-SNPs
50	13±0.0^{ab}	14.0±0.2^{a}	12.0±0.7^{b}	10.0±0.0^{b}	12.0±1.0^{a}	8.0±0.5^{c}
25	12±0.4^{b}	14.0±0.5^{a}	10.0±1.0^{c}	12.0±0.2^{a}	10.0±0.0^{b}	10.0±0.3^{b}
12.5	9.0±1.0^{b}	12.0±0.6^{a}	12.0±0.0^{a}	9.0±0.6^{a}	8.0±1.0^{b}	6.0±1.0^{c}
6.25	6.0±1.0^{b}	8.0±0.0^{a}	5.0±0.3^{c}	5.0±1.0^{a}	4.0±0.1^{b}	4.0±0.15^{b}
3.25	4.0±0.2^{b}	5.0±0.5^{a}	0.0±0.0^{c}	0.0±0.0^{b}	0.0±0.0^{b}	2.0±1.0^{a}
Ciprofloxacin	12.0±0.5^{b}	14.0±0.0^{a}	4.0±0.2^{c}	10.0±0.8^{a}	10.0±0.0^{a}	1.0±0.5^{b}

Values are means ± standard deviations of triplicate observations. Means with different letters across the row are statistically significant at p≤0.05. MIC: Minimum inhibitory concentration, SNPs: Silver nanoparticles, MDRSA: Multidrug resistant *Staphylococcus aureus*, BAC1: *Bacillus subtilis*, BAC7: *B. licheniformis* , BAC20: *Bacillus subtilis*, $^{a, b, c}$: Are statistically significant letters from Duncan multiple range test

that alkaline pH was more suitable for SNP synthesis by *Coleus aromaticus*. Amin et al.[45] reported more SNPs biosynthesized under basic conditions, while the formation of SNPs was repressed by acidic conditions and at lower pH (pH 5) larger nanoparticles were formed, whereas at higher pH (pH 9) smaller and highly dispersed nanoparticles were formed.

Antimicrobial potential of $AgNO_3$ and SNPs biosynthesized at different pH values against MDR-Salmonella spp.

The antimicrobial activity of the SNPs biosynthesized at different pH values against MDR-SA9 is shown in Table 3a. All the $AgNO_3$ and the SNPs had antimicrobial activity against MDR-SA9.

The antibacterial activity of BAC1-SNPs, BAC7-SNPs, and BAC20-SNPs at pH 4, pH 7, and pH 9 against MDR-SA9 was 8-16 mm, 4-14 mm, and 4-14 mm, respectively. BAC1-SNPs produced at pH 9 and BAC7-SNPs and BAC20-SNPs produced at pH 7 exhibited the highest antagonistic activity against MDR-SA9.

The antimicrobial activity of SNPs biosynthesized at different pH values by *Bacillus* spp. against MDR-SA18 is shown in Table 3b. The SNPs had antimicrobial activity against MDR-SA18 at different pH values. The antimicrobial activity of BAC1-SNPs, BAC7-SNPs, and BAC20-SNPs against MDR-SA18 was 4.0-9.0 mm, 4.0-9.0 mm, and 3.0-10 mm, respectively. The highest activity was recorded at pH 7. There was no ZOI at pH 9 by BAC1-SNPs or BAC7-SNPs against MDR-SA18 after 24 h of incubation.

Effect of different concentrations of $AgNO_3$ on SNP biosynthesis

The effect of different concentrations (2-10 mM) of $AgNO_3$ solutions on the biosynthesis of SNPs was evaluated and was monitored by UV-Visible spectrophotometer. Figure 7A shows the spectra of BAC1-SNPs produced at different concentrations of silver nitrate. The SPR peak was observed at 400 nm for *Bacillus* sp. BAC1 SNPs produced with 8 mM. The SNPs produced with 2 mM and 4 mM of $AgNO_3$ had a broad band between 400 nm and 800 nm. The SNPs produced with 10 mM $AgNO_3$ had a strong SPR peak at 600 nm.

The spectra obtained for BAC7 SNPs produced with different concentrations of $AgNO_3$ are shown in Figure 7B. A broad band spectrum between 400 nm and 600 nm was observed for the SNPs synthesized with 2 mM, 6 mM, and 8 mM concentrations of $AgNO_3$. The SNPs produced with the 10 mM $AgNO_3$ has a strong peak at 600 nm. The 10 mM $AgNO_3$ concentration had the highest OD.

The effect of concentration on the biosynthesis of *Bacillus* sp. BAC20 SNPs is presented in Figure 7c. The SNPs produced with 2 mM to 10 mM $AgNO_3$ concentration all had a broad band spectrum between 400 nm and 800 nm. A SPR peak of 600 nm was observed for 2 mM, 4 mM, and 6 mM. The highest OD was shown by the SNPs produced with 10 mM at 500 nm.

Antimicrobial potential of SNPs biosynthesized using different concentrations of $AgNO_3$

The antimicrobial activity of the SNPs biosynthesized by *Bacillus* spp. using different concentrations of $AgNO_3$ is shown in Tables 4a and 4b.

All the SNPs produced by *Bacillus* spp. using different concentrations of $AgNO_3$ had antagonistic activity against the isolates. The antimicrobial activity of BAC1-SNPs, BAC7-SNPs, and BAC20-SNPs against MDR-SA9 was 6-24 mm, 2-25 mm, and 2-20 mm at 24, 48, and 72 h of incubation, respectively. The highest antagonistic activity (15 mm) against SA9 was shown by 10 mM $AgNO_3$.

Table 3a. The antimicrobial potential of silver nitrate and silver nanoparticles biosynthesized at different pH values against multidrug resistant-SA9

Samples	Antimicrobial activity (mm)					
	BAC1-SNPs SA9		BAC7-SNPs		BAC20-SNPs	
	24 h	48 h	24 h	48 h	24 h	48 h
SNPs pH 4	10.0±1.0^{a}	8.0±1.0^{b}	4.0±0.0^{d}	4.0±0.0^{d}	7.0±0.3^{c}	4.0±1.0^{d}
SNPs pH 7	12.0±0.5^{b}	10.0±0.0^{b}	14.0±1.0^{a}	12.0±0.5^{b}	14.0±0.5^{a}	11.0±0.0^{bc}
SNPs pH 9	14.0±0.2^{b}	16.0±0.2^{a}	12.0±0.3^{c}	9.0±0.4^{d}	6.0±0.0^{f}	8.0±0.5^{e}

Values are means ± standard deviations of triplicate observations. Means with different letters across the row are statistically significant at p≤0.05. SNPs: *Silver nanoparticles*, SA: *Staphylococcus aureus*, BAC1: *Bacillus subtilis*, BAC7: *B. licheniformis*, BAC20: *Bacillus subtilis*, $^{a, b, c, d, e}$: Are statistically significant letters from Duncan multiple range test

Table 3b. The antimicrobial potential of silver nitrate and silver nanoparticles biosynthesized at different pH values against multidrug resistant-SA18

Samples	Antimicrobial activity (mm)					
	BAC1-SNPs		BAC7-SNPs		BAC20-SNPs	
	24 h	48 h	24 h	48 h	24 h	48 h
SNPs pH 4	4.0±0.0^{c}	6.0±0.5^{b}	7.0±0.2^{a}	4.0±0.^{c}	2.0±0.2^{d}	6.0±0.2^{b}
SNPs pH 7	9.0±0.4^{b}	8.0±0.00^{c}	6.0±0.0^{d}	9.0±0.2^{b}	6.0±0.50^{d}	10.0±0.4^{a}
SNPs pH 9	0.0±0.0^{d}	3.0±0.2^{c}	0.0±0.0^{d}	4.0±0.0^{b}	5.0±0.2^{a}	3.0±0.27^{c}

Values are means±standard deviations of triplicate observations. Means with different letters across the row are statistically significant at p≤0.05. SNPs: Silver nanoparticles, SA: *Staphylococcus aureus* BAC1: *Bacillus subtilis*, BAC7: *B. licheniformis*, BAC20: *Bacillus subtilis*, $^{a, b, c, d}$: Are statistically significant letters from Duncan multiple range test

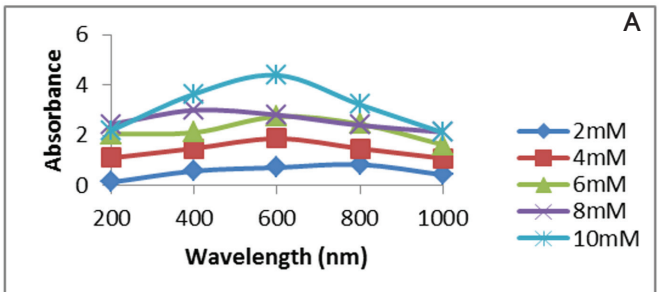

Figure 7A. UV-Visible spectra of BAC1 SNPs at different concentrations of $AgNO_3$

UV: Ultraviolet, SNPs: Silver nanoparticles, $AgNO_3$: Silver nitrate, BAC1: *Bacillus subtilis*

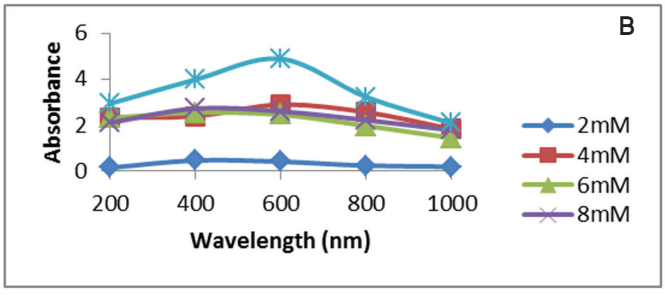

Figure 7B. UV-Visible spectra of BAC7 SNPs at different concentrations of $AgNO_3$

UV: Ultraviolet, SNPs: Silver nanoparticles, $AgNO_3$: Silver nitrate, BAC1: *Bacillus subtilis*

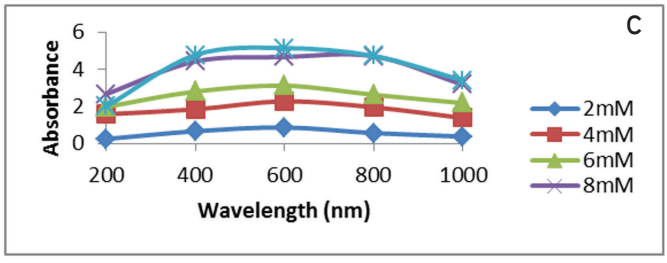

Figure 7C. UV-Visible spectra of BAC20 SNPs at different concentrations of $AgNO_3$

UV: Ultraviolet, SNPs: Silver nanoparticles, $AgNO_3$: Silver nitrate, BAC20: *Bacillus subtilis*

The antimicrobial activity of BAC1-SNPs, BAC7-SNPs, and BAC20-SNPs against MDR-SA18 was 2.0-15 mm, 2.0-17 mm, and 2.0-21 mm, respectively. The SNPs from the *Bacillus* spp. had the highest activity against MDR-SA18 at 10 mM concentration of $AgNO_3$.

Synergistic effect of the biosynthesized SNPs and some antibiotics against MDR Salmonella spp.

The synergetic effect of the biosynthesized SNPs and some antibiotics against MDR *Salmonella* sp. SA9 and MDR *Salmonella* sp. SA18 is shown in Figures 8A and 8B.

The MDR-SA9 showed susceptibility to antibiotics with antagonistic potential ranging between 3.0 and 20 mm. Colistin had the lowest antagonistic activity while chlortetracycline had the highest activity.

The synergetic effect of the biosynthesized SNPs and some antibiotics against MDR-SA9 is shown in Figure 8a. The antagonistic potential of BAC1 SNPs + the antibiotics ranged from 10 to 33 mm. BAC1 SNPs + erythromycin had the highest antagonistic activity against MDR-SA9, while BAC1 SNPs + oxytetracycline had the lowest activity.

The antagonistic potential of BAC7-SNPs + antibiotics against MDR-SA9 ranged from 6.0 to 30 mm. BAC7-SNPs + gentamicin had the highest activity, while BAC7 SNPs + colistin had the lowest antagonistic activity. The antagonistic activity of BAC20-SNPs + antibiotics against MDR-SA9 ranged from 5.0 to 31 mm. BAC20 + chlortetracycline had the highest antagonistic potential, while BAC20-SNPs + colistin had the lowest activity.

The synergistic effect of the SNPs and the antibiotics against the MDRSA18 is shown in Figure 8B. The antagonistic activity against MDR-SA18 ranged from 2.0 to 18 mm. Colistin had the lowest activity, while gentamicin had the highest activity against MDR-SA18.

The antagonistic activity of BAC1 SNPs + the antibiotics against MDR-SA18 ranged from 9.0 to 20 mm, showing a high susceptibility. MDR-SA18 had the highest susceptibility to BAC1 SNPs + ciprofloxacin, while the least susceptibility was to BAC1 SNPs + colistin.

BAC7 SNPs + antibiotics had antibacterial activity ranging from 10 to 24 mm against MDR-SA18. BAC7 SNPs + gentamicin have

Table 4a. Antimicrobial potential of silver nanoparticles biosynthesized using different concentrations of silver nitrate against multidrug resistant-SA9 at different incubation times

Concentrations of $AgNO_3$	Zone of inhibition (mm)/Incubation time (h) against MDRSA9								
	BAC1-SNPs			BAC7-SNPs			BAC20-SNPs		
	24 h	48 h	72 h	24 h	48 h	72 h	24 h	48 h	72 h
2 mM	6.0±0.5^{e}	8.0±0.0^{d}	8.0±0.1^{d}	4.0±0.2^{f}	8.0±0.0^{d}	14.0±0.0^{a}	12.0±0.3^{b}	6.0±0.0^{e}	10.0±1.0^{c}
4 mM	8.0±0.0^{f}	20.0±1.0^{a}	12.0±0.0^{d}	14.0±0.45^{c}	10.0±1.0^{e}	12.0±1.0^{d}	18.0±0.0^{b}	10.0±0.0^{e}	8.0±0.0^{f}
6 mM	12±0.53^{d}	17.0±0.3^{b}	16.0±1.0^{c}	2.0±0.0^{g}	10.0±0.5^{e}	16.0±0.5^{c}	4.0±0.10^{f}	10.0±0.0^{e}	18.0±0.5^{a}
8 mM	6.0±0.6^{f}	16.0±0.0^{c}	18.0±0.53^{b}	6.0±0.2^{f}	12.0±0.2^{e}	14.0±0.3^{d}	2.0±0.0^{g}	20.0±1.0^{a}	12.0±1.0^{e}
10 mM	10.0±0.0^{g}	20.0±1.0^{d}	24.0±0.25^{b}	6.0±0.0^{h}	22.0±1.0^{c}	25.0±0.0^{a}	17.0±0.6^{e}	15.0±0.6^{f}	20.0±1.0^{d}

Values are means ± standard deviations of triplicate observations. Means with different letters across the row are statistically significant at p≤0.05. $AgNO_3$: Silver nitrate, SNPs: *Silver nanoparticles*, SA: *Staphylococcus aureus*, MDRSA: Multidrug resistant *Staphylococcus aureus*, BAC1: *Bacillus subtilis*, BAC7: *B. licheniformis*, BAC20: *Bacillus subtilis*, $^{a, b, c, d, e, f, g, h}$: Are statistically significant letters from Duncan multiple range test

the highest activity against MDR-SA9. The antagonistic activity of BAC20 SNPs + antibiotics against MDR-SA18 ranged from 6.0 to 26 mm. BAC20 + erythromycin had the highest antagonistic potential, while BAC20 SNPs + colistin had the lowest.

The antagonistic potential of the combined BAC1- SNPs and the antibiotics against MRDSA9 and MDRS18 is shown in Tables 4a and 4b. The antagonistic activity against MRDSA9 and MRDSA18 was 3.0-33 mm and 2.0-20 mm, respectively. MRDSA9 was highly susceptible to BAC1-SNPs + erythromycin.

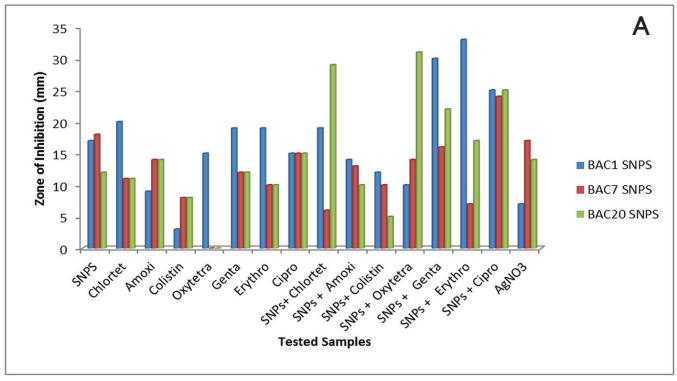

Figure 8A. Diameter of zones of inhibition in (mm) of the of the SNPs, antibiotic and combination of SNPs + antibiotics against the MDR-SA9

SNPs: Silver nanoparticles, MDR: Multidrug resistant, $AgNO_3$: Silver nitrate, BAC1: Bacillus subtilis, BAC7: B. licheniformis, BAC20: Bacillus subtilis

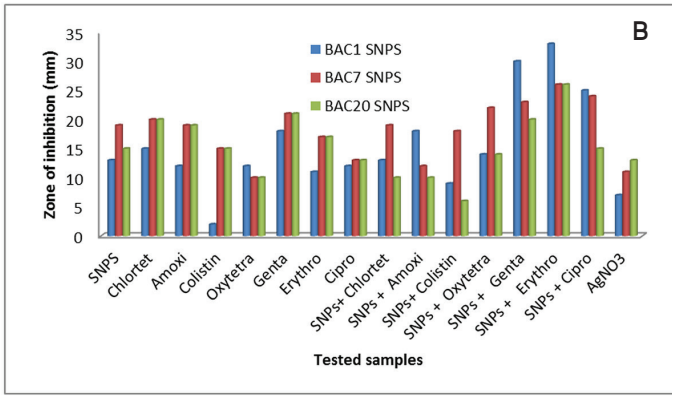

Figure 8B. Diameter of zones of inhibition (mm) of the SNPs, antibiotic and combination of SNPs + antibiotics against the MDR-SA18

SNPs: Silver nanoparticles, MDR: Multidrug resistant, $AgNO_3$: Silver nitrate, BAC1: Bacillus subtilis, BAC7: B. licheniformis, BAC20: Bacillus subtilis

It was found that the SNPs produced from *Bacillus* spp. enhanced the reaction rates of the antibiotics in a synergistic mode as well as in its own way on these pathogens. In the cases of both *Salmonella* spp. (SA9) and *Salmonella enterica* subsp. *enterica* (SA18) the highest ZOI was produced by the combination of antibiotics + SNPs. This result is in agreement with the findings reported by Krishna et al.[48] who mentioned increasing efficacies (percentage) of antibiotics like streptomycin and ceftriaxone when used in combination with SNPs against *Bacillus subtilis*, *S. aureus*, *E. coli*, and *Proteus vulgaris*.

Shahnaz et al.[49] reported that *in vitro* antibacterial activity of SNPs synthesized from *Penicillium* species was obtained in combination with the antibiotics sparfloxacin and ofloxacin against the clinically isolated pathogens *Staphylococcus aureus*, *Bacillus cereus*, *E. coli*, and *Proteus vulgaris*. It was found that the SNPs produced by *Penicillium* species enhanced the reaction rates of the antibiotics in a synergistic mode on the clinically isolated pathogens.

The MIC was defined as the lowest concentration of the SNPs that can have an antimicrobial effect on the test organisms. For the MIC evaluation 10 mM was used to prepare different concentrations of the SNPs and different MICs were recorded for the two (MDR) *Salmonella* spp. Balashanmugam et al.[30] also reported the MIC of SNPs after testing on some pathogens, with *Escherichia coli* and *Bacillus subtilis* having the highest values.

CONCLUSION

The bioactive metabolites from *Bacillus* spp. had antibacterial activity against the selected MDR *Salmonella* spp. The bioactive metabolites were able to bioreduce $AgNO_3$ for SNP biosynthesis. These biologically synthesized SNPs exhibited good antibacterial activity and the combination of SNPs with some antibiotics equally enhanced the antibacterial potential of the antibiotics against the tested isolates. Thus, these nanoparticles can be used as antibacterial agents alone or in *combination with antibiotics to improve their antibacterial potential.*

Table 4b. Antimicrobial potential of silver nanoparticles biosynthesized using different concentrations of silver nitrate against multidrug resistant-SA18 at different incubation times

Concentrations of $AgNO_3$	Zone of inhibition (mm)/Incubation time (h) against MDRSA18								
	BAC1-SNPs			BAC7-SNPs			BAC20-SNPs		
	24 h	48 h	72 h	24 h	48 h	72 h	24 h	48 h	72 h
2 mM	3.0±0.0^{d}	4.0±0.3^{c}	0.0±0.0^{e}	4.0±1.0^{c}	4.0±1.0^{c}	7.0±0.2^{a}	0.0±0.0^{e}	6.0±0.0^{b}	0.0±0.0^{e}
4 mM	5.0±0.5^{c}	0.0±0.0^{f}	5.0±0.0^{c}	2.0±0.6^{e}	3.0±0.0^{d}	9.0±0.4^{b}	10.0±0.0^{a}	10.0±0.2^{a}	9.0±0.0^{b}
6 mM	0.0±0.0^{e}	10.0±1.0^{b}	12.0±1.0^{a}	0.0±0.0^{e}	8.0±0.5^{c}	10.0±0.5^{b}	2.0±1.0^{d}	0.0±0.0^{e}	0.0±0.0^{e}
8 mM	7.0±0.10^{e}	12.0±0.2^{a}	9.0±0.45^{c}	8.0±1.0^{d}	4.0±0.1^{f}	4.0±0.1^{e}	8.0±0.3^{d}	12.0±0.0^{a}	10.0±1.0^{b}
10 mM	13.0±0.6^{e}	15.0±0.0^{c}	14.0±1.0^{d}	3.0±0.0^{h}	12.0±1.0^{f}	17.0±0.0^{b}	8.0±1.0^{g}	12.0±0.0^{f}	21.0±0.3^{a}

Values are means±standard deviations of triplicate observations. Means with different letters across the row are statistically significant at p≤0.05. SNPs: *Silver nanoparticles*, $AgNO_3$: *Silver nitrate,* SA: *Staphylococcus aureus*, MDRSA: Multidrug resistant *Staphylococcus aureus*, BAC1: *Bacillus subtilis*, BAC7: *B. licheniformis*, BAC20: *Bacillus subtilis*, $^{a, b, c, d, e, f, g}$: Are statistically significant letters from Duncan multiple range test

Conflicts of interest: No conflict of interest was declared by the authors. The authors alone are responsible for the content and writing of the paper.

REFERENCES

1. Oveisi H, Rahighi S, Jiang X, Agawa Y, Beitollahi A, Soichi W, Yusuke Y. Improved inactivation effect of bacteria: Fabrication of mesoporous anatase films with fine Ag nanoparticles prepared by coaxial vacuum Arc deposition. Chem Lett. 2001;40:420-422.
2. Thabit A, Crandon J, Nicolau D. Antimicrobial resistance: impact on clinical and economic outcomes and the need for new antimicrobials. Exp Opin Pharmacother. 2015;16:159-177.
3. Maisonneuve E, Gerdes K. Molecular mechanisms underlying bacterial persisters. Cell. 2014;157:539-548.
4. Ferri M, Ranucci E, Romagnoli P, Giaccone V. Antimicrobial resistance: A global emerging threat to public health systems. Crit Rev Fd Sci Nutr. 2015;2857-2876.
5. Montville TJ, Matthews KR. Food microbiology: an introduction. 2nd ed. Washington; United States of America: ASM Press; 2008.
6. Pui CF, Wong WC, Chai LC, Nillian E, Ghazali FM, Cheah YK, Nakaguchi Y, Nishibuchi M, Radu S. Simultaneous detection of *Salmonella* spp., *Salmonella* typhi and *Salmonella* typhimurium in sliced fruits using multiplex PCR. Fd Contr. 2011;22:337-342.
7. Butt T, Ahmad RN, Mahmood A, Zaidi S. Ciprofloxacin treatment failure in typhoid fever case, Pakistan. Emerg Infectious Dis. 2003;9:1621-1622.
8. Adabara N, Ezugwu BU, Momojimoh A, Madzu A, Hashiimu Z, Damisa D. The prevalence and antibiotic susceptibility pattern of *Salmonella* typhi among Patients Attending a Military Hospital in Minna, Nigeria. Adv Prev Med. 2012;2012:875419.
9. Schaffer B, Hohenester U, Trugler A, Hofer F. High-resolution surface plasmon imaging of gold nanoparticles by energy-filtered transmission electron microscopy. Physical Rev. 2009;79:1-10.
10. Service ER. Foodborne Illness Cost Calculator: *Salmonella*. Washington, D.C; United States Department of Agriculture; 2009.
11. Morikawa M, Ito M, Imanaka T. Isolation of a new surfactin producer *Bacillus pumilus* A-1, and cloning and nucleotide sequence of the regulator gene, psf-1. J Ferment Bioeng. 1992;74:255-261.
12. Perez C, Suarez C, Castro GR. Production of antimicrobials by *Bacillus subtilis* MIR 15. J Biotechnol. 1992;26:331-336.
13. Perez C, Suarez C, Castro GR. Antimicrobial activity determined in strains of *Bacillus circulans* cluster. Folia Microbiol. 1993;38:25-28.
14. Drablos F, Nicholson D, Ronning M. EXAFS study of zinc coordination in Bacitracin A. Biochim Biophys Acta. 1999;1431:433-442.
15. Milner JL, Raffel SJ, Lethbridge BJ, Handelsman J. Culture conditions that influence accumulation of zwittermicin a by *Bacillus cereus* UW85. Appl Microbiol Biotechnol. 1995;43:685-691.
16. Steller S, Vollenbroich D, Leenders F, Stein T, Conrad B, Hofemeisterr J, Jaques P, Thonart P, Vater J. Structural and functional organization of the fengycin synthease multienzyme system from *Bacillus subtilis* b213 and A1/3. Chem Biol. 1999;6:31-41.
17. Galvez A, Maqueda M, Cordovilla P, Martinez-Bueno M, Lebbadi M, Valdivia E. Characterization and biological activitiy against Naegleria fowleri of amonebicins produced by *Bacillus licheniformis* D-13. Antimicrob. Agents Chemother. 1994;38:1314-1319.
18. Leifert C, Li H, Chidburee S, Hampson S, Workman S, Sigee D. Antibiotic production and biocontrol activity by *Bacillus subtilis* CL27 and *Bacillus pumilus* CL45. J Appl Bacteriol. 1995;78:97-108.
19. Paulraj K, Seung Taik L. Synthesis and structural characterization of silver nanoparticles using bacterial exopolysaccharide and its antimicrobial activity against food and multi-drug resistant pathogens. Process Biochem. 2013;48:1099-1106.
20. Castellano JJ, Shafii SM, Ko F, Donate G, Wright TE, Mannari RJ, Payne WG, Smith DJ. Comparative evaluation of silver-containing antimicrobial dressings and drugs. Intern Wound J. 2007;4:14-22.
21. Kim JS, Kuk E, Yu KN, Kim J, Park SJ, Lee HJ, Kim SH, Park YK, Park YH, Hwang C, Kim Y, Lee Y, Jeong DH, Cho M. Antimicrobial effects of silver nanoparticles. Nanomed. Nanotechnol. Biol Med. 2007;3:95-101.
22. Morone JR, Elechiguerra JL, Camacho A, Holt K, Kouri JB, Ramirez JT. The bactericidal characterization of silver nanoparticles. Nanotechnol. 2005;16:2340-2353.
23. Sondi I, Salopek-Sondi B. Silver nanoparticles as antimicrobial agent: a case study on E. coli as a model for Gram-negative bacteria. J Colloid Interface Sci. 2004;275:177-182.
24. Rai M, Yadav A, Gade A. Silver nanoparticles as a new generation of antimicrobials. Biotechnol. Adv. 2009;27:76-83.
25. Lim HK, Asharani PV, Hande MP. Enhanced genotoxi- city of silver nanoparticles in DNA repair deficient mammalian cells. Front Genet. 2012;3:1-13.
26. Stevanovic MM, Skapin SD, Bracko I, Milenkovic M, Petkovic J, Filipic M. Poly (lactide-co-glycolide)/silver nanoparticles: synthesis, characterization, antimicrobial activity, cytotoxicity assessment and ROS-inducingpotential. Polymer. 2012;53:2818-2828.
27. Karthik R, Nanasivayam S, Gnanendra KE, Reepika R. Synthesis of silver nanoparticles by *L. acidophilus* 01 strain and evaluation of its in vitro genomic DNA toxicity. Nano-micro Let. 2010;2:160-163.
28. Mandal D, Bolander ME, Mukhopadhyay D, Sarkar G, Mukherjee P. Appl Microbiol Biotechnol. 2006;69:485.
29. Singh D, Rathod V, Ninganagouda S, Herimath J, Kulkarni P. Biosynthesis of silver nanoparticle by endophytic fungi *Penicillium* sp. isolated from *Curcuma longa* (turmeric) and its antibacterial activity against pathogenic gram negative bacteria. J Pharm Res. 2013;7:448-453.
30. Balashanmugam P, Santhosh S, Giyaullah H, Balakumaran MD, Kalaichelvan PT. Mycosynthesis, characterization and antibacterial activity of silver nanoparticles from Microporus xanthopus: a macro mushroom. International J Innova Res Sci Engr Technol. 2013;2:1-9.
31. Cappuccino JG, Sherman N. A Laboratory Manual in General Microbiology, 3th ed. California; Benjamin Commius Publication Company Inc; 1996.
32. Riley MA, Wertz JE. Bacteriocins: evolution, ecology, and application. Annu Rev Microbiol. 2002;56:117-137.
33. Kalishwaralal K, Deepak V, Ram Kumar Pandian S, Gurunathan S. Biosynthesis of gold nanocubes from *Bacillus lichemiformis*. Biores Technol. 2009;100:5356-5358.
34. Kanmani P, Lim ST. Synthesis and structural characterization of silver nanoparticles using bacterial exopolysaccharide and its antimicrobial activity against food and multidrug resistant pathogens. Process Biochem. 2013;48: 1099-1106.
35. El-Batal A, Amin M, Shehata M, Hallol M. Synthesis of silver nanoparticles by *Bacillus stearothermophilus* using gamma radiation and their antimicrobial activity. World Appl Sci J. 2012;22:1-16.

Turk J Pharm Sci 2020;17(5): 523-527
DOI: 10.4274/tjps.galenos.2019.76094

ORIGINAL ARTICLE

Simultaneous Determination of Hydrochlorothiazide and Irbesartan from Pharmaceutical Dosage Forms with RP-HPLC

Farmasötik Dozaj Formlarında TF-YPSK ile Hidroklorotiyazid ve İrbesartanın Eş Zamanlı Tayini

Sevinç KURBANOĞLU[1]*, Aysu YARMAN[2]

[1]Ankara University Faculty of Pharmacy, Department of Analytical Chemistry, Ankara, Turkey
[2]University of Potsdam, Institute of Biochemistry and Biology, Potsdam, Germany

ABSTRACT

Objectives: In this work, a simple and rapid liquid chromatographic method for the simultaneous determination of irbesartan (IRBE) and hydrochlorothiazide (HCT) was developed and validated by reverse phase high performance liquid chromatography (RP-HPLC).

Materials and Methods: Experimental conditions such as different buffer solutions, various pH values, temperature, composition of the mobile phase, and the effect of flow rate were optimized.

Results: The developed RP-HPLC method for these antihypertensive agents was wholly validated and IRBE was detected in the linear range of 0.1-25 μg mL^{-1} and HCT was detected in the linear range of 0.25-25 μg mL^{-1}. Moreover, the suggested chromatographic technique was successfully applied for the determination of the drugs in human serum and pharmaceutical dosage forms with limit of detection values of 0.008 μg mL^{-1} for IRBE and 0.012 μg mL^{-1} for HCT.

Conclusion: The proposed rapid analysis method of these antihypertensive drugs can be easily used and applied by pharmaceutical companies for which the analysis time is important.

Key words: HPLC, irbesartan, hydrochlorothiazide, pharmaceutical dosage forms

ÖZ

Amaç: Bu çalışmada, irbesartan (IRBE) ve hidroklorotiyazidin (HCT) eşzamanlı tayini için basit ve hızlı bir ters fazlı yüksek performanslı sıvı kromatografisi (TF-YPSK) yöntemi geliştirilmiş ve validasyon çalışmaları yapılmıştır.

Gereç ve Yöntemler: Deneysel koşullar; farklı tampon çözeltileri, çeşitli pH değerleri, sıcaklık, mobil fazın bileşimi, akış hızının etkisi gibi parametrelerin üzerinden optimize edildi.

Bulgular: Bu antihipertansif ajanlar için geliştirilen TF-YPSK yönteminin tüm validasyon parametrelerine ilişkin çalışmalar yapılmış, ve IRBE 0,1-25 μg mL^{-1} doğrusal aralığında ve HCT 0,25-25 μg mL^{-1} doğrusal aralığında tespit edilmiştir. Ayrıca önerilen TF-YPSK yöntemi ile IRBE için 0,008 μg mL^{-1} ve HCT için 0,012 μg mL^{-1} tayin alt sınır değerleri bulunmuştur. Geliştirilen yöntem, insan serumunda ve farmasötik dozaj formlarında bulunan IRBE ve HCT'nin belirlenmesi için başarıyla uygulanmıştır.

Sonuç: Bu antihipertansif ilaçların miktar tayininde önerilen YPSK analiz yönteminin, analiz süresinin önemli olduğu ilaç firmalarında rahatlıkla kullanılabileceği ve uygulanabileceği düşünülmektedir.

Anahtar kelimeler: YPSK, irbesartan, hidroklorotiyazit, farmasötik dozaj formları

***Correspondence: E-mail:** skurbanoglu@gmail.com, **Phone:** +90 505 316 22 86 **ORCID-ID:** orcid.org/0000-0002-7079-7604
Received: 19.03.2019, **Accepted:** 05.09.2019

36. Valencia GA, Vercik LC, Ferrari R, Vercik A. Synthesis and characterization of silver nanoparticles using water-soluble starch and its antibacterial activity on *Staphylococcus aureus*. Starch/Stärke, 2013;65:1-7.

37. Schaffer B, Hohenester U, Trugler A, Hofer F. High-resolution surface plasmon imaging of gold nanoparticles by energy-filtered transmission electron microscopy. Physical Rev. 2009;79:1-10.

38. Sadowski Z, Maliszewska IH, Grochowalska B, Polowczyk I, Koźlecki T. Synthesis of silver nanoparticles using microorganisms. Mater Sci Poland. 2008; 26:419-424.

39. Gardea-Torresday LJ, Gomez E, Peratta-Videa RJ, Persons GJ, Troiani H, Jose- Yacaman M. Alfalfa sprouts: a natural source for synthesis of silver nanoparticles. Langmuir. 2003;19:1357-1361.

40. Vithiya K, Kumar R, Sen S. *Bacillus* spp. Mediated extracellular synthesis of silver nanoparticles. Inter J Pharm Pharmaceut Sci. 2014;6:3.

41. Guzman M, Dille J, Godet S. Synthesis and antibacterial activity of silver nanoparticles against Gram-positive and Gram-negative bacteria. Nanomed Nanotechnol Biol Med. 2012;8:35-45.

42. Sharma VK, Yngard RA, Lin Y. Silver nanoparticles: Green synthesis and their antimicrobial activities. Adv Colloid Interf Sci. 2009;145:83-96.

43. Dhanalakshmi T, Rajendran S. Synthesis of silver nanoparticles using Tridax procumbens and its antimicrobial activity. Arch Appl Sci Res. 2012;4:1289-1293.

44. Natarajan K, Selvaraj S. Green synthesis of silver nanoparticles using *Bacillus subtilis* 1A751 and its antimicrobial activity. Res J Nanosci Nanotechnol. 2011;10:1-8.

45. Amin M, Anwar F, Janjua MR, Iqbal MA, Rashid U. Green Synthesis of Silver Nanoparticles through Reduction with Solanum xanthocarpum L. Berry Extract: Characterization, Antimicrobial and Urease Inhibitory Activities against Helicobacter pylori. Intern J Molecu Sci. 2012;13:9923-9941.

46. Annadurai G, Vanaja M. Coleus aromaticus leaf extract mediated synthesis of silver nanoparticles and its bactericidal activity. Appl Nanosci. 2013;3:217-223.

47. Goldie O, Sunil P, Ashmi M, Golap K, Madhuri S. Facile biosynthesis of gold nanoparticles exploiting optimum pH and temperature of fresh water algae Chlorella pyrenoidusa. Adv Appl Sci. 2012;3:1405-1412.

48. Krishna G, Kumar SS, Pranitha V, Alha M, Charaya S. Biogenic Synthesis of Silver Nanoparticles and their Synergistic Effect with Antibiotics: A Study against *Salmonella* Sp. International J Pharmaceu Sci. 2015;7:1-5.

49. Shahnaz M, Anima N, Kathirvel T. Evaluation of antimicrobial activity of biologically synthesized silver nanoparticles from filamentous fungi. Intern. J Pharm Tech Res. 2014;6:1049-1053.

INTRODUCTION

Cardiovascular disease causes the death of 17.9 million people annually, which represents nearly 30% of all global deaths.[1] Hypertension is responsible for at least 45% of deaths due to heart disease. A variety of pharmaceuticals, such as angiotensin converting enzyme inhibitors, angiotensin-receptor blockers, beta-blockers, diuretics, and calcium channel blockers, have been applied for the management of hypertension.[2]

Irbesartan (IRBE) (2-butyl-3-[p-(o-1 H-tetrazol-5-yl phenyl) benzyl]-1,3-diazospiro[4,4]non-1-en-4-one) is an angiotensin II receptor antagonist that selectively and noncompetitively binds to the angiotensin II receptor subtype I (Figure 1). It has no affinity for the receptor subtype 2 or α1- and α2-adrenoceptor and serotonergic receptors.[3-6] IRBE is mainly used for the treatment of hypertension. Furthermore, it may also play roles in postponement of the progression of diabetic nephropathy. It also has a role in the indication for the reduction of renal disease progression in patients with type 2 diabetes, hypertension, and microalbuminuria or proteinuria.[3-6] Hydrochlorothiazide (HCT), 6-chloro-1,1-dioxo3,4-dihydro-2H-1,2,4-benzothiadiazine-7-sulfonamide, is one of the oldest members of the thiazide class of diuretics (Figure 1). Thiazides decrease peripheral resistance by an unknown mechanism and thereby lower blood pressure. HCT is widely used in the form of a combination pill with other antihypertensive agents including IRBE.[7-9]

Combined cardiovascular therapy is beneficial, since most of these therapies exploit complementary mechanisms of differently acting antihypertensive agents to maximize blood pressure-lowering effects.[10] In the literature several methods have been described concerning simultaneous determination of IRBE and HCT in pharmaceutical dosage and biological samples using spectrophotometric,[11-13] spectrofluorometric,[14] capillary electrophoretic,[15] and chromatographic methods.[16,17]

In the present work, a liquid chromatographic method for the simultaneous determination of IRBE and HCT was developed using reverse phase high performance liquid chromatography (RP-HPLC). Experimental conditions such as different buffer solutions, various pH values, temperature, additives, and the effect of flow rate were optimized. Moreover, the developed chromatographic technique was successfully applied for the determination of IRBE and HCT in pharmaceutical dosage forms.

MATERIALS AND METHODS

Chemicals and instruments

IRBE and HCT in their dosage forms Karvezide® and Co-Irda® were obtained from pharmaceutical companies. All reagents were of analytical grade and were prepared using doubly distilled water. All experiments were performed at room temperature; all solutions were protected from light and used within 24 h to avoid decomposition. Chromatographic grade acetonitrile, methanol, hydrogen peroxide, and phosphoric acid were used. All other reagents were of analytical grade.

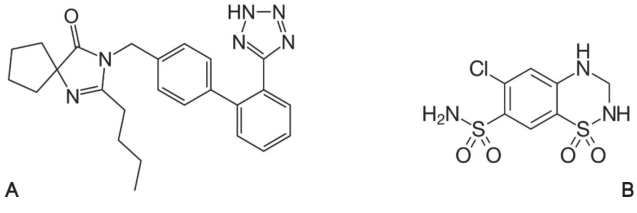

Figure 1. Chemical structures of A) irbesartan and B) hydrochlorothiazide

The analyses were performed with the Agilent Technologies HP 1100 series (Wilmington, DE, USA) LC system equipped with a G1379A degasser, G1311A quaternary pump, 61313 auto injector, and G1315B diode array detector. Chromatographic separation was achieved using 60:40 (V/V) ACN: pH 3 phosphate buffer (from H_3PO_4) as a mobile phase, with an X Terra RP® (250x5 mm I.D.: 3 µm) column at a flow rate of 0.8 mL min^{-1} and an injection value of 10 µL. The separation was carried out at 30 °C and the diode array detector was adjusted to 226 nm. Before using the mobile phase, the pH was adjusted with 5 M NaOH, and the mobile phase filtered through 0.45-µm polytetrafluoroethylene membranes using a vacuum pump and degassed. For the pH measurements, a pH meter Model 538 (WTW, Weilheim, Germany) was used with a combined electrode with an accuracy of ±0.05 pH.

Preparation of stock solutions

Stock solutions of IRBE and HCT (100 µg mL^{-1}) were prepared by dissolving 5 mg of each compound in 50 mL of methanol by ultrasonication for 10 min in an ultrasonic bath. The required concentration for the analysis was diluted with the mobile phase.

Analysis of pharmaceutical dosage form

For both binary mixtures, 10 tablets of Karvezide® and Co-Irda® were accurately weighed, crushed, and finely powdered, separately. From these powders, desired solutions were prepared, sonicated, and filtered. The analyzed solutions were obtained by diluting with mobile phase. The contents of IRBE and HCT were calculated from the related calibration curves.

Statistical Analysis

System suitability test studies and validation of the analytical method

The system suitability test parameters such as retention time, symmetry factor, theoretical plate number, selectivity, resolution, and tailing were calculated and compared with the recommended values in the United States Pharmacopeia (USP) criteria.[18-20] Validation of the proposed method was performed according to International Council on Harmonisation (ICH) Guidelines and USP criteria in terms of precision, accuracy, linear range, limit of detection (LOD), and quantification values and reported.

Degradation studies

It is recommended in the ICH Guidelines to perform degradation studies for the developed assays to show that the method is stability indicating.[21,22] In order to assess the capacity of the proposed method to separate IRBE and HCT from their degradation products, mild and harsh conditions like heating in an oven (75 °C, 3 h and 24 h), treating the samples with acidic

(0.5 N HCl and 1 N HCl) or alkaline (0.5 N NaOH and 1 N NaOH) solutions or oxidants (3% and 30% H_2O_2), and exposing to ultraviolet (UV) (254 nm, 3 h and 24 h) were applied.

RESULTS AND DISCUSSION

System suitability test parameters

Prior to the validation of the proposed method, system suitability tests such as tailing factor, selectivity, resolution, tailing, and theoretical number of plates were calculated and reported. The retention factor values for IRBE and HCT were calculated as 2.08 for HCT and 3.35 for IRBE; the other system suitability test parameters are summarized in Table 1. Those results show that the proposed method for the determination of IRBE and HCT conformed to the ICH guidelines.[21]

Method validation

Linearity

The linearity of the detector for IRBE and HCT was evaluated by the relation between the peak areas under the corresponding peaks and concentrations of each drug with a correlation coefficient of 0.997 and 0.998, respectively (Table 2). Repeated injections were performed at each concentration level. The linear range was in good agreement and wide linear range values were obtained. For HCT the linear range obtained was between 0.25 and 25 µg mL^{-1} and for IRBE it was between 0.1 and 25 µg mL^{-1} (Figure 2).

Limit of detection and limit of quantification

The ICH guidelines propose several approaches for the determination of LOD and limit of quantification (LOQ). In the present work the LOD and LOQ values were calculated as LOD=3.3 s/m and LOQ=10 s/m using the standard deviation of response (s) and the slope (m) of the calibration curve.[19,22-24] The LOD and LOQ values are also reported in Table 2, where a statistical evaluation of the calibration data is presented. HCT was detected with an LOD value of 0.012 µg mL^{-1} and an LOQ value of 0.036 µg mL^{-1} with the proposed RP-HPLC method. IRBE was detected with an LOD value of 0.008 µg mL^{-1} and an LOQ value of 0.023 µg mL^{-1} with the proposed RP-HPLC method.

Table 1. System suitability tests parameters

	Mobile phase	
Compounds	HCT	IRBE
Retention time (min)	1.85	2.61
Linearity range (µg mL^{-1})	0.25-25	0.1-25
Slope (mAU $µg^{-1}$ mL)	7.925	37.913
Intercept (mAU)	0.313	9.438
Correlation coefficient	0.997	0.998
LOD (µg mL^{-1})	0.012	0.008
LOQ (µg mL^{-1})	0.036	0.023
Within-day repeatability [a] (RSD %)	0.775	0.265
Between-day repeatability [a] (RSD %)	0.848	0.430

HCT: Hydrochlorothiazide, IRBE: Irbesartan, LOD: Limit of detection, LOQ: Limit of quantification, RSD: Relative standard deviation

Precision

The precision of the proposed method was evaluated by repeatability studies. Within-day and between-day repeatability were determined by the injection of three different levels of calibration solutions (n=5) on the same day and on three consecutive days, respectively. The results are expressed by the percentage of relative standard deviation (RSD %) and shown in Table 2, where a statistical evaluation of the calibration data is presented. As seen, there is no significant difference between the values within the within-day and between-day measurements in the mobile phase.

Accuracy

Accuracy is an important parameter for the analysis of pharmaceuticals. Real sample applications and recovery studies were performed to show the accuracy of the purposed method. Acceptable results were obtained for Karvezide® and

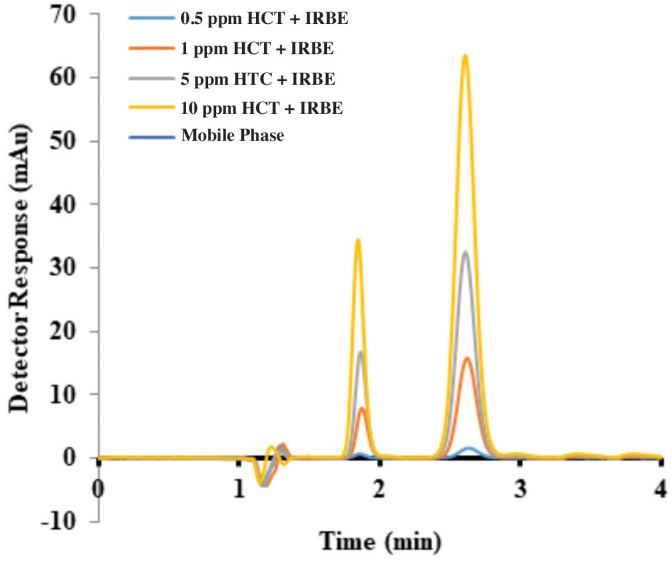

Figure 2. Chromatograms of increasing concentrations of hydrochlorothiazide and irbesartan
HCT: Hydrochlorothiazide, IRBE: Irbesartan

Table 2. Statistical evaluation of the calibration data

Parameters			Recommended values[20]
Compounds	HCT	IRBE	-
Retention time (min)	1.85	2.61	-
Selectivity	-	2.05	>1
Resolution	-	2.03	>2
Tailing	1.18	1.20	<2
Theoretical number of plates	4581	5402	>2000

HCT: Hydrochlorothiazide, IRBE: Irbesartan, Min: Minute

Co-Irda®, which contain 150 mg of IRBE and 12.5 mg of HCT (Table 3). For the accuracy test, recovery of the method was studied using the spiking method. Solutions were prepared by adding 50%, 100%, and 150% level standard solutions of the drugs to the pharmaceutical Karvezide® sample (Table 4). The experiment was performed in triplicate and recovery %, RSD %, and (BIAS %) spiked drugs were calculated. It can be concluded that, using the suggested HPLC method, acceptable recoveries can be obtained with RSD % values lower than 1 and recovery values between 98% and 102%.

Specificity (degradation studies)

Specificity is another essential parameter in pharmaceutical analysis.[19,21-23] Specificity studies were performed by means of degradation studies. Degradation of drugs under mild and drastic stress conditions is shown in Table 5, as degradation %. It can be seen that the hard acidic and alkaline conditions hardly affect these drugs. In UV and heat degradation these drugs can be affected within 3 h (Table 5).

CONCLUSION

In the present work, an RP-HPLC method was developed and validated for the simultaneous separation and determination of IRBE and HCT. The studies were performed for the analyses of IRBE and HCT from the mobile phase. Compared to already published papers we suggest an environmentally friendly, green chemistry method for application to combined drug technology. It is thought that the proposed rapid analysis method of these antihypertensive drugs can be easily used and applied by pharmaceutical companies for which the analysis time is important. Moreover, in studies with real samples or in bioequivalence studies this method may be used.

Table 3. Results of tablet analysis from Karvezide® and Co-Irda®

	HCT	IRBE
Label claimed (Karvezide® mg)	150.00	12.5
Found [a] (mg)	150.59	12.42
RSD (%)	0.20	0.11
Bias (%)	-0.39	0.63
Label claimed (Co-Irda® mg)	150	12.5
Found[a] (mg)	149.72	12.45
RSD (%)	0.71	0.19
BIAS (%)	0.18	0.37

[a]Each value is the mean of five experiments. HCT: Hydrochlorothiazide, IRBE: Irbesartan, RSD: Relative standard deviation

Table 4. Results of analysis from pharmaceutical dosage form Karvezide®

	50% accuracy		100% accuracy		150% accuracy	
	HCT	IRBE	HCT	IRBE	HCT	IRBE
Added (mg)	5.00	5.00	10.00	10.00	15.00	15.00
Found[a] (mg)	5.10	4.98	10.02	10.32	14.95	14.97
Recovery (%)	102.07	99.73	100.16	100.33	99.64	99.81
RSD (%)	0.19	0.25	0.51	0.18	0.85	0.15
BIAS (%)	-2.07	0.26	-0.16	-0.33	0.36	0.19

[a]Each value is the mean of five experiments, HCT: Hydrochlorothiazide, IRBE: Irbesartan, RSD: Relative standard deviation

Table 5. Results of stress conditions by reverse phase liquid chromatography in terms of degradation %

	Conditions	HCT	IRBE
Mild conditions	HCl (0.5 M)	43.97	77.10
	NaOH (0.5 M)	33.16	25.15
	H_2O_2 (3%)	12.16	84.49
	UV light exposure (3 h at 254 nm)	90.18	90.98
	Oven (3 h at 75 °C)	95.11	72.56
Harsh conditions	HCl (1 M)	49.98	79.69
	NaOH (1 M)	37.23	59.95
	H_2O_2 (30%)	25.21	93.91
	UV light exposure (24 h at 254 nm)	97.48	78.46
	Oven (24 h at 75 °C)	96.97	87.87

HCT: Hydrochlorothiazide, IRBE: Irbesartan, UV: Ultraviolet

Conflicts of interest: No conflict of interest was declared by the authors. The authors alone are responsible for the content and writing of the paper.

REFERENCES

1. Foley RN, Parfrey PS, Sarnak MJ. Clinical epidemiology of cardiovascular disease in chronic renal disease. Am J Kidney Dis. 1998:S16-S23.
2. Nguyen Q, Dominguez J, Nguyen L, Gullapalli N. Hypertension management: an update. Am Heal Drug Benefits. 2010;3:47-56.
3. Adams MA, Trudeau L. Irbesartan: review of pharmacology and comparative properties. Can J Clin Pharmacol. 2000;7:22-31.
4. Ohlstein EH, Brooks DP, Feuerstein GZ, Ruffolo RR. Inhibition of sympathetic outflow by the angiotensin ii receptor antagonist, eprosartan, but not by losartan, valsartan or irbesartan: relationship to differences in prejunctional angiotensin ii receptor blockade. Pharmacology. 1997;55:244-251.
5. Vachharajani NN, Shyu WC, Smith RA, Greene DS. The effects of age and gender on the pharmacokinetics of irbesartan. Br J Clin Pharmacol. 1998;46:611-613.
6. Li P, Fukuhara M, Diz DI, Ferrario CM, Brosnihan KB. Novel angiotensin II AT(1) receptor antagonist irbesartan prevents thromboxane A(5)-induced vasoconstriction in canine coronary arteries and human platelet aggregation. J Pharmacol Exp Ther. 2000;292:238-246.
7. Ford RV. The clinical pharmacology of hydrochlorothiazide. South Med J. 1959;52:40-45.
8. Kurbanoğlu S, Gümüştaş M, Özkan SA. Simultaneous estimation and validation of some binary mixtures of antihypertensive drugs by RP-LC methods using two new generation silica columns. J Pharm Biomed Anal. 2013;72:198-201.
9. Nezhadali A, Mojarrab M. Computational study and multivariate optimization of hydrochlorothiazide analysis using molecularly imprinted

polymer electrochemical sensor based on carbon nanotube/polypyrrole film. Sensors Actuators B Chem. 2014;190:829-837.

10. Vongpatanasin W. Hydrochlorothiazide is not the most useful nor versatile thiazide diuretic. Curr Opin Cardiol. 2015;30:361-365.
11. Albero I, Ródenas V, García S, Sánchez-Pedreño C. Determination of irbesartan in the presence of hydrochlorothiazide by derivative spectrophotometry. J Pharm Biomed Anal. 2002;29:299-305.
12. Joseph-Charles J, Brault S, Boyer C, Langlois M-H, Cabrero L, Dubost JP. Simultaneous determination of irbesartan and hydrochlorothiazide in tablets by derivative spectrophotometry. Anal Lett. 2003;36:2485-2495.
13. Chakravarthy KK, Darak V, Arshad MD, Bharath SA. Development and validation of simultaneous spectrophotometric estimation of Doxycycline and Tinidazole in tablet dosage forms. Pharma Sci Monit. 2010;1:534-539.
14. El-Shaboury SR, Hussein SA, Mohamed NA, El-Sutohy MM. Spectrofluorimetric method for determination of some angiotensin II receptor antagonists. J Pharm Anal. 2012;2:12-18.
15. Hillaert S, Van Den Bossche W. Simultaneous determination of hydrochlorothiazide and several angiotensin-II-receptor antagonists by capillary electrophoresis. J Pharm Biomed Anal. 2003;31:329-339.
16. Coudoré F, Harvard L, Lefeuvre S, Billaud EM, Beaune P, Bobrie G, Azizi M, Prognon P, Laurent S. HPLC-DAD analysis of hydrochlorothiazide and irbesartan in hypertensive patients on fixed-dose combination therapy. Chromatographia. 2011;74:559-565.
17. Vujić Z, Mulavdić N, Smajić M, Brborić J, Stankovic P. Simultaneous analysis of irbesartan and hydrochlorothiazide: an improved HPLC method with the aid of a chemometric protocol. Molecules. 2012;17:3461-3474.
18. The USP 40. The United States Pharmacopeia, The Official Compendia of Standards. MD, Rockville, USA; 2017.
19. Swartz ME, Krull IS. Analytical Method development and validation (1st ed). Boca raton; Imprint CRC Press;1997:53-67.
20. Center for Drug Evaluation and Research (CDER), Reviewer Guidance Validation of Chromatographic Methods, 1994.
21. ICH Guidelines T. Validation of Analytical Procedures, Methodology International Council on Harmonization. Brussels, Belgium; 1995.
22. Chan CC, Lam H, Lee YC, Zhang XM. Analytical Method Validation and Instrument Performance Verification. John Wiley and Sons. 2004:105-130.
23. Green JM. Peer Reviewed: a practical guide to analytical method validation. Anal Chem. 1996;68:305A-309A.
24. Ozkan CK, Kurbanoglu S, Esim O, Savaser A, Ozkan SA, Ozkan Y. Simultaneous Determination and Drug Dissolution Testing of Combined Amlodipine Tablet Formulations Using RP-LC. Chromatographia. 2016;79:1143-1151.

Turk J Pharm Sci 2020;17(5):528-534
DOI: 10.4274/tjps.galenos.2019.71598

ORIGINAL ARTICLE

Cholinesterase and Tyrosinase Inhibitory Potential and Antioxidant Capacity of *Lysimachia verticillaris* L. and Isolation of the Major Compounds

Lysimachia verticillaris L.'nin Kolinesteraz ve Tirozinaz İnhibitör Etki Potansiyeli ve Antioksidan Kapasitesi ile Ana Bileşiklerinin İzolasyonu

Ufuk ÖZGEN[1]*, Sıla Özlem ŞENER[1], Karel ŠMEJKAL[2], Jiri VACLAVIK[2], Fatma Sezer ŞENOL DENİZ[3], İlkay ERDOĞAN ORHAN[3], Emil SVAJDLENKA[2], Ahmet C. GÖREN[4], Milan ŽEMLIČKA[2]

[1]Karadeniz Technical University Faculty of Pharmacy, Department of Pharmacognosy, Trabzon, Turkey
[2]University of Veterinary and Pharmaceutical Sciences Brno, Faculty of Pharmacy, Department of Natural Drugs, Brno, Czechia
[3]Gazi University Faculty of Pharmacy, Department of Pharmacognosy, Ankara, Turkey
[4]Bezmialem Vakıf University Faculty of Pharmacy, Department of Chemistry, İstanbul, Turkey

ABSTRACT

Objectives: The scope of the present study was to specify the therapeutic potential for neurodegenerative diseases through evaluating cholinesterase and tyrosinase (TYR) inhibitory and antioxidant activity of *Lysimachia verticillaris* (LV), and to isolate the major compounds considering the most active fraction.

Materials and Methods: The methanol extract (ME) of LV and the chloroform, ethyl acetate (EtOAC), and aqueous fractions obtained from it were used for biological activity and isolation studies. The ME and all fractions were tested for their acetylcholinesterase (AChE), butyrylcholinesterase (BChE), and TYR inhibitory and antioxidant potentials using ELISA microtiter assays. Seven major compounds were isolated from the active EtOAC fraction by semi-preparative high performance liquid chromatography. The structures of the compounds were elucidated by several spectroscopic methods.

Results: Marked AChE inhibitory activity was observed in the EtOAC fraction (6337±1.74%), BChE inhibitory activity in the ME and EtOAC fraction (85.84±3.01% and 83.82±3.93%), total phenol content in the EtOAC fraction (261.59±3.95 mg equivalent of gallic acid/1 g of extract) and total flavonoid contents in the EtOAC fraction (515.54±2.80 mg equivalent of quercetin/1 g of extract), and 2,2-diphenyl-1-picrylhydrazyl radical scavenging activity and ferric-reducing antioxidant power values in the aqueous and EtOAC fractions (92.54±0.67%, 92.11±0.30%; 2.318±0.054, 2.224±0.091, respectively). Accordingly, the isolation studies were carried out on the EtOAC fractions. Compounds 1-7 (gallic acid, (+)-catechin, myricetin 3-O-arabinofuranoside, myricetin 3-O-α-rhamnopyranoside, quercetin 3-O-β-glucopyranoside, quercetin 3-O-arabinofuranoside, and quercetin 3-O-α-rhamnopyranoside, respectively) were isolated from the active EtOAC fraction.

Conclusion: LV may be a potential herbal source for treatment of neurodegenerative diseases based on its strong antioxidant activity and significant cholinesterase inhibition similar to that of the reference.

Key words: Anticholinesterase, HPLC, isolation, *Lysimachia*, tyrosinase

ÖZ

Amaç: Bu çalışmanın amacı, *Lysimachia verticillaris*'in (LV) kolinesteraz, tirozinaz inhibitör etkisini ve antioksidan aktivitesini değerlendirerek nörodejeneratif hastalıklar için terapötik potansiyelini belirlemek ve en etkili fraksiyondan hareketle ana bileşiklerini izole etmektir.

Gereç ve Yöntemler: Biyolojik aktivite ve izolasyon çalışmaları için LV'nin metanol ekstresinden hareketle kloroform, EtOAC ve sulu fraksiyonları elde edilmiştir. Etkili EtOAC fraksiyonundan, yarı preparatif yüksek performanslı sıvı kromatografisi (YBSK) yöntemi ile 7 ana bileşik izole edilmiştir. İzole edilen bileşiklerin yapıları çeşitli spektroskopik yöntemler kullanılarak aydınlatılmıştır. Metanol ekstresi (ME) ve tüm fraksiyonların asetilkolinesteraz (AChE), butirilkolinesteraz (BChE), tirozinaz inhibitor etkileri ve antioksidan potansiyelleri ELISA yöntemleri kullanılarak belirlenmiştir.

Bulgular: En yüksek AChE inhibitor etki EtOAc fraksiyonunda (%63,37±1,74), en yüksek BChE inhibitör etki ME'de ve etil asetat fraksiyonunda

*Correspondence: E-mail: uozgen@ktu.edu.tr, Phone: +90 462 377 88 28 ORCID-ID: orcid.org/0000-0001-9839-6717
Received: 15.05.2019, Accepted: 05.09.2019

(%85,84±3,01 ve %83,82±3,93), en yüksek total fenolik içeriği etil asetat fraksiyonunda (261,59±3,95 mg gallik asit eşdeğeri/g ekstre), en yüksek total flavonoit içeriği etil asetat fraksiyonunda (515,54±2,80 mg kersetin eşdeğeri/1 g ekstre) gözlenmiştir. En yüksek 2,2-difenil-1-pikrilhidrazil radikal süpürücü etki ve demir azaltıcı antioksidan güç değerleri ise su ve EtOAC fraksiyonlarında sırasıyla %92,54±0.67, %92,11±0,30 ve 2,318±0,054 2,224±0,091 olarak belirlenmiştir. Aktivite sonuçlarına dayanarak izolasyon çalışmalarının etil asetat fraksiyonunda yürütülmesine karar verilmiştir. Etil asetat fraksiyonundan, gallik asit (1), (+) kateşin (2), mirsetin 3-O-arabinofuranozit (3), mirsetin 3-O-α-ramnopiranozit (4), kersetin 3-O-β-glukopiranozit (5), kersetin 3-O-arabinofuranozit (6) ve kersetin 3-O-α-ramnopiranozit (7) ana bileşikleri izole edilmiştir.

Sonuç: LV, güçlü antioksidan aktivitesiye sahip olması ve referans bileşiklerle karşılaştırıldığında benzer kolinesteraz inhibitor etki göstermesi nedeniyle nörodejeneratif hastalıkların tedavisi için potansiyel bir bitkisel ilaç kaynağı olabilir.

Anahtar kelimeler: Antikolinesteraz, YBSK, izolasyon, *Lysimachia*, tirozinaz

INTRODUCTION

Neurodegenerative diseases such as Alzheimer's disease (AD) and Parkinson's disease (PD), common in the elderly population over the age of 65, have become serious health problems especially in industrialized countries. Hence, a huge amount of research is being conducted to find new drugs and treatment strategies for these diseases. In this sense, natural products and medicinal herb extracts are attractive sources in the search for novel anti-AD and anti-PD drug candidates. Deficiency in acetylcholine, hydrolyzed by acetylcholinesterase (AChE) and butyrylcholinesterase (BChE), has been proved in the brains of AD patients.[1] On the other hand, the function of tyrosinase (TYR) is to catalyze the oxidation reaction of tyrosine to melanin, which is linked to hyperpigmentation of skin, occurrence of melanoma, unwanted browning of fruits and vegetables, and dopamine toxicity in PD.[2]

The genus *Lysimachia* (Primulaceae) is represented by 8 taxa in the Turkish flora.[3] *Lysimachia* species, locally known as "*karga otu*", "*adi karga otu*", and "*altın kamış*" in Turkey, have been recorded to be used for expectorant, antipyretic, and wound healing purposes as well as against cough and bronchitis in Anatolian folk medicine.[4] *Lysimachia* species contain assorted secondary metabolites including flavonoids, triterpenes, phenolic acids, etc.[5-7] Moreover, several *Lysimachia* species have many desirable biological activities such as cytotoxic, hepatoprotective, and vasorelaxant.[8-10]

Based on the information that *Lysimachia monnieri* is a synonym of *Bacopa monnieri*, the reputed plant called "brahmi" in Ayurvedic medicine for its strong memory-enhancing effect, we aimed to study the memory-enhancing effect of another species, *L. verticillaris*. For this purpose, in the current study, AChE, BChE, and TYR inhibitory activity and antioxidant potential including 2,2-diphenyl-1-picrylhydrazyl (DPPH) radical scavenging activity and ferric-reducing antioxidant power (FRAP) were studied in the methanol extract (ME) and all fractions. The EtOAC fraction that showed remarkable anticholinesterase and antioxidant effect was subjected to various chromatographic methods, which gave seven pure compounds (1-7). The structures of the compounds were identified by means of ^{1}H-NMR and ^{13}C-NMR. In addition, the total phenol and flavonoid quantities in the samples were measured spectrophotometrically.

MATERIALS AND METHODS

Instruments and chemicals

NMR spectra were obtained on a Varian-600 spectrometer at 600 MHz for ^{1}H-NMR and 150 MHz for ^{13}C-NMR using CD_3OD as solvent. An Agilent-1100 series was used for high-performance liquid chromatography (HPLC) studies (Germany). A Unico 4802 ultraviolet (UV)-visible spectrophotometer (USA) was used for antioxidant activity, total phenol, and flavonoid contents studies. A Supelco Ascentis® RP-amide (250x10 mm, 5 µm) column, HPLC grade acetonitrile and methanol (Scharlau Chemie S.A., Spain), formic acid (Lachema, Brno, CZ), Sephadex LH-20 (Sigma-Aldrich), silica gel 60 (Merck 7734 and Merck 9385), LiChroprep RP-18 (Merck 9303), and silica gel 60 F254 (Merck 5554) were used for the isolation and chromatographic studies.

To measure the enzyme inhibition assays, a 96-well microplate reader (VersaMax Molecular Devices, USA), electric eel AChE (Type-VI-S, EC 3.1.1.7, Sigma), horse serum BChE (EC 3.1.1.8, Sigma), acetylthiocholine iodide and butyrylthiocholine chloride (Sigma, USA), 5,5'-dithio-bis (2-nitrobenzoic acid) (DTNB, Sigma, USA), galantamine (Sigma, USA), TYR (EC 1.14.1.8.1, 30 U, mushroom tyrosinase, Sigma), and L-DOPA were used.

Plant material

The aerial parts of *Lysimachia verticillaris* (LV) were gathered in the vicinity of Kafkasör at an altitude of 1300 m (Artvin Province, Turkey). The identification of the plant was performed by Dr. Ufuk Özgen. A voucher specimen (AEF 26311) is deposited at the Herbarium of the Faculty of Pharmacy.

Extraction

Air-dried and finely powdered samples (500 g) were extracted with MeOH (2 Lx8 h, three times). The combined extracts were evaporated to obtain 74 g of the crude residue. The ME (73 g) was suspended in an H_2O:MeOH (9:1) mixture and then partitioned with chloroform (300 mLx2) and EtOAc (300 mLx2) successively. The chloroform and EtOAc fractions were evaporated at reduced pressure at 40 °C and were 15.6 g and 6.6 g, respectively. The aqueous phase was evaporated to give a residue (46.3 g). The ME and all fractions obtained from it were employed in the activity assays performed herein.

AChE and BChE inhibitory activities

The enzyme inhibitory activities were evaluated by a modified version of the method developed by Ellman et al.[11,12]

Tyrosinase inhibitory activity

The modified dopachrome method was used by measuring at 475 nm.[13] The results were compared with a control consisting of 50% dimethyl sulfoxide in place of sample.

DPPH radical scavenging activity

The activities of the samples were detected by Blois' method.[14] Absorbance was measured at 520 nm.

Ferric-reducing antioxidant power assay

The FRAP values were determined by the assay described by Oyaizu.[15] The absorbance was monitored at 700 nm.

Total phenol and flavonoid contents

Phenolic content of the samples was determined using the Folin-Ciocalteu method.[16] Absorbance was read at 760 nm.

The total flavonoid content of the samples was measured by aluminum chloride colorimetric method.[17]

Statistical analysis

The statistical analysis of the enzyme inhibition and antioxidant capacity assays was conducted using Softmax PRO 4.3.2.LS software. The data were expressed as mean ± scanning electron microscopy. Statistical differences between groups were evaluated by ANOVA (One-Way). Dunnett's multiple comparison tests were used as *post hoc* tests. $p<0.05$ was considered to be significant (*$p<0.05$; **$p<0.01$; ***$p<0.001$, ****$p<0.0001$).

Isolation of the major compounds from LV by combined open column chromatography and semi-preparative HPLC

The EtOAC fraction was applied to column chromatography using a silica gel 60 and $CHCl_3$: MeOH (80:20→50:50) solvent system. The subfractions 5-14 combined were subjected to a semi-preparative HPLC column, which yielded seven compounds (1-7) (Figure 1). The flow rate of the solvent was adjusted to 4.0 mL/min. The mobile phase composition was linear gradient; 0 min: 40% MeOH +60% formic acid (0.2% in aqueous solution); 36 min: 65% MeOH +35% formic acid (0.2% in aqueous solution). UV-DAD detection was performed at 280 nm. The column temperature was 50 °C.

Structure elucidation of the isolated compounds

Structure elucidation of the compounds was performed by ^{1}H-NMR, ^{13}C-NMR, and ESI/MS, which was confirmed finally by comparison of the results with the reported data.

RESULTS

AChE, BChE, and TYR inhibitory activity

The ME and all fractions were tested for their enzyme inhibitory activity against AChE, BChE, and TYR. The aqueous fraction was inactive against both AChE and BChE, while the ME and EtOAc and chloroform fractions of LV showed high degrees of inhibition against AChE, having 58.21±3.36%, 63.37±1.74%, and 41.63±0.45% inhibition, respectively. Although the ME (85.84±3.01%) and EtOAC fraction of LV (83.82±3.93%) exhibited very high BChE inhibitory activity, similar to galantamine (86.66±2.72%), the chloroform fraction exhibited lower BChE inhibition (54.65±0.23%). All of the fractions and the ME displayed weak inhibition toward TYR, ranging between 14.11±1.00% and 16.10±2.14% (Table 1).

Antioxidant activity

In the DPPH radical quenching activity test, the chloroform fraction of LV had moderate activity (63.66±0.57%), whereas high activity against DPPH radical was observed in the aqueous

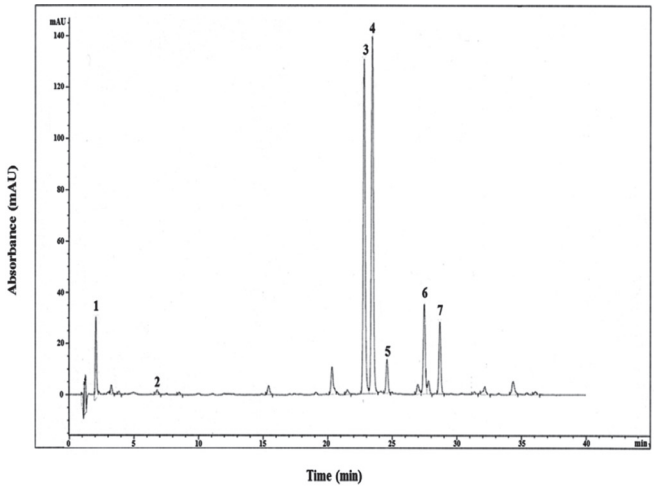

Figure 1. HPLC chromatogram of the EtOAc fraction
HPLC: High-performance liquid chromatography, EtOAc: Ethyl acetate, Min: Minute

Table 1. TYR, AChE, and BChE inhibitory activity of the methanol extract and EtOAC, chloroform, and aqueous fractions

Samples	Inhibitory level (% ± SEM[a]) at 100 µg/mL		
	TYR	AChE	BChE
MeOH Extract	14.11±1.00****	58.21±3.36**	85.84±3.01
EtOAc Fr.	16.10±2.14****	63.37±1.74**	83.82±3.93
Chloroform Fr.	15.33±0.97****	41.63±0.45****	54.65±0.23***
Aqueous Fr.	14.31±0.98****	-[b]	-[b]
Galantamine[c]		94.48±3.81	86.66±2.72
Kojic acid[d]	85.44±0.14		

[a]Standard error mean, [b]No inhibition, [c]Reference for inhibitory activity against AChE and BChE, [d]Reference for inhibitory activity against tyrosinase, (*$p<0.05$, **$p<0.01$, ***$p<0.001$, ****$p<0.0001$), TYR: Tyrosinase, AChE: Acetylcholinesterase, BChE: Butyrylcholinesterase, EtOAc: Ethyl acetate, SEM: Scanning electron microscopy

(92.54±0.67%) and EtOAc fractions (92.11±0.30%). On the other hand, the aqueous and EtOAc fractions possessed the highest FRAP values, which are higher than that of quercetin used as the reference (Table 2).

Total phenol and flavonoid contents

The total phenol contents of the chloroform, EtOAC, and aqueous fractions and ME were stated as gallic acid equivalent (GAE, mg/g extract), while their total flavonoid contents were stated as quercetin equivalent (QUE, mg/g extract). The richest total phenol content belonged to the EtOAC fraction (261.59±3.95 mg/g extract). Similarly, the EtOAc fraction was also found to have the most abundant total flavonoid content (515.54±2.80 mg/g extract) (Table 3).

Identification of the compounds isolated from the active EtOAC fraction

Compounds 1-7 were isolated from the active EtOAC fraction (Figure 2); they were isolated from LV for the first time. The NMR data for all compounds are given as ^{1}H-NMR (600 MHz, CD_3OD) and ^{13}C-NMR (150 MHz, CD_3OD):

Compound 1

Grayish powder. ^{1}H-NMR: δ 6.94 (*s*, 2H, H-2 and H-6). ^{13}C-NMR: δ 169.45 (-COOH), 144.91 (2C, C-3 and C-5), 137.90 (C-4), 121.25 (C-1), 108.84 (2C, C-2 and C-6). NMR data are in total agreement with the data for gallic acid.[18]

Compound 2

Grayish powder. ^{1}H-NMR: δ 6,73 (*d*, 1H, *J*=2.0 Hz, H-2′), 6.65 (*d*, 1H, *J*=8.1 Hz, H-5′), 6.62 (*dd*, 1H, J_1=2.0, J_2=8.1 Hz, H-6′), 5.82 (*d*, 1H, *J*=2.4 Hz, H-8), 5.75 (*d*, 1H, *J*=2.4 Hz, H-6), 4.46 (*d*, 1H, *J*=7.6 Hz, H-2), 3.87 (*td*, 1H, H-3), 2.75 (*dd*, 1H, J_1=5.3, J_2=15.9 Hz, H-4a), 2.40 (*dd*, 1H, J_1=8.2, J_2=15.8 Hz, H-4b). ^{13}C-NMR: δ 156.42 (C-7), 156.16 (C-5), 155.49 (C-9), 144.83 (C-3′ or C-4′), 144.80 (C-3′ or C-4′), 130.79 (C-1′), 118.59 (C-6′), 114.63 (C-5′), 113.82 (C-2′), 99.37 (C-10), 94.83 (C-8), 94.05 (C-6), 81.43 (C-2), 67.39 (C-3), 27.10 (C-4). NMR data are in total agreement with the data for (+)-catechin.[19]

Compound 3

Yellow powder. ^{1}H-NMR: δ 7.08 (*s*, 2H, H-2′ and H-6′), 6.38 (*d*, 1H, *J*=1.0 Hz, H-8), 6.19 (*d*, 1H, *J*=1.0 Hz, H-6), 5.54 (*d*, 1H, *J*=1.1 Hz, H-1′′), 4.18-3.32 (sugar protons, 5H, *m*, H-2′′, H-3′′, H-4′′, H-5′′). ^{13}C-NMR: δ 177.71 (C-4), 164.64 (C-7), 161.19 (C-5), 157.15 (C-9), 156.38 (C-2), 145.71 (2C, C3′ and C-5′), 136.58 (C-4′), 133.23 (C-3), 119.82 (C-1′), 108.03 (2C, C-2′ and C-6′), 107.57 (C-10), 103.85 (C-1′′), 98.74 (C-6), 93.52 (C-8), 85.33 (C-4′′), 82.00 (C-3′′), 76.74 (C-2′′), 60.40 (C-5′′). NMR data are in total agreement with the data for myricetin 3-*O*-α-arabinofuranoside.[20]

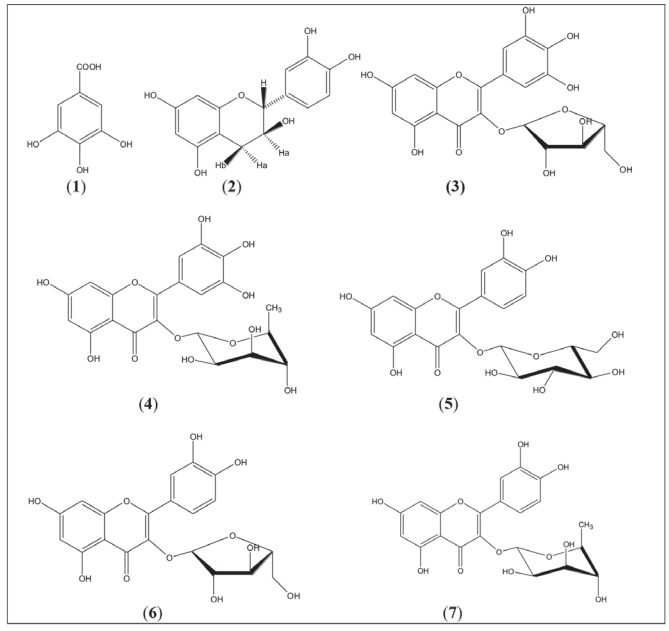

Figure 2. Compounds (1-7) isolated from the EtOAc fraction
EtOAc: Ethyl acetate

Table 2. DPPH radical scavenging activity and FRAP of the methanol extract and EtOAc, chloroform, and aqueous fractions at 1000 µg/mL

Samples	DPPH radical scavenging activity (% ± SEM[a])	FRAP[b]
MeOH Extract	82.20±2.82	0.917±0.030*
EtOAC Fr.	92.11±0.30	2.224±0.091
Chloroform Fr.	63.66±0.57**	0.650±0.007*
Aqueous Fr.	92.54±0.67	2.318±0.054
Quercetin[c]	92.75±0.05	2.090±0.032

[a]Standard error mean, [b]Absorbance at 700 nm ± SEM (greater absorbance indicates greater antioxidant power), [c]Reference, (*p<0.01, **p<0.001), DPPH: 2,2-diphenyl-1-picrylhydrazyl, FRAP: Ferric-reducing antioxidant power, EtOAC: Ethyl acetate, SEM: Scanning electron microscopy

Table 3. Total phenol and total flavonoid contents of the methanol extract and EtOAC, chloroform, and aqueous fractions

Sample	Total phenol content[a] ± SEM[b]	Total flavonoid content[c] ± SEM
MeOH Extract	64.41±2.26	229.45±2.80
EtOAC Fr.	261.59±3.95	515.54±2.80
Chloroform Fr.	20.73±5.53	136.54±2.52
Aqueous Fr.	ND[d]	ND

[a]Data expressed in mg equivalent of gallic acid (GAE) to 1 g of extract, [b]Standard error of the mean, [c]Data expressed in mg equivalent of quercetin (QUE) to 1 g of extract, [d]Not determined due to very low solubility, EtOAC: Ethyl acetate, SEM: Scanning electron microscopy

Compound 4

Yellow powder. ^{1}H-NMR: δ 6.94 (*s*, 2H, H-2' and H-6'), 6.35 (*d*, 1H, *J*=2.1 Hz, H-8), 6.18 (*d*, 1H, *J*=2.1 Hz, H-6), 5.30 (*d*, 1H, *J*=1.1 Hz, H-1''), 4.21 (*t*, 1H, *J*=1.5 Hz, H-2''), 3.77 (*dd*, 1H, J_1=3.3, J_2=9.4 Hz, H-3''), 3.50 (*m*, 1H, H-5''), 3.32 (*t*, 1H, *J*=9.6 Hz, H-4''), 0.95 (*d*, 3H, *J*=6.1 Hz, H-6''). ^{13}C-NMR: δ 178.23 (C-4), 164.47 (C-7), 161.77 (C-5), 158.00 (C-2), 157.07 (C-9), 145.42 (2C, C-3' and C-5'), 136.45 (C-4'), 134.87 (C-3), 120.47 (C-1'), 108.12 (2C, C-6' and C-2'), 104.42 (C-10), 102.18 (C-1''), 98.36 (C-6), 93.24 (C-8), 71.91 (C-4''), 70.67 (C-2''), 70.60 (C-3''), 70.44 (C-5''), 16.23 (C-6''). NMR data are in total agreement with the data for myricetin 3-*O*-α-rhamnopyranoside.[21]

Compound 5

Yellow powder. ^{1}H-NMR: δ 7.60 (*d*, 1H, *J*=2.3 Hz, H-2'), 7.49 (*dd*, 1H, *J*=2.3, 8.8 Hz, H-6'), 6.77 (*d,* 1H, *J*=8.8 Hz, H-5'), 6.29 (*d*, 1H, *J*=1.7 Hz, H-8), 6.10 (*d*, 1H, *J*=2.3 Hz), H-6, 5.15 (*d*, 1H, *J*=7.7 Hz, H-1''), 3.61 (*dd*, 1H, J_1=2.4, J_2=11.7 Hz, H-6a''), 3.48 (*dd*, 1H, J_1=5.3, J_2 =11.7 Hz, H-6b''), 3.38 (*dd*, 1H, J_1=7.7, J_2 =8.8 Hz, H-2''), 3.32 (*t*, 1H, *J*=8.8 Hz, H-3''), 3.25 (*dd*, 1H, J_1=8.8, J_2=9.9 Hz, H-4''), 3.12 (*m*, 1H, H-5''). ^{13}C-NMR: δ 178.01 (C-4), 165.11 (C-7), 161.61 (C-5), 157.51 (C-9), 157.08 (C-2), 148.44 (C-3'), 144.49 (C-4'), 134.15 (C-3), 121.73 (C-1'), 121.63 (C-6'), 116.07 (C-2'), 114.56 (C-5'), 104.11 (C-10), 102.87 (C-1''), 98.67 (C-6), 93.42 (C-8), 76.96 (C-5''), 76.69 (C-3''), 74.28 (C-2''), 69.77 (C-4''), 61.12 (C-6''). NMR data are in agreement with the data for quercetin 3-*O*-β-glucopyranoside.[22]

Compound 6

Yellow powder. ^{1}H-NMR: δ 7.43 (*d*, 1H, *J*=1.8 Hz, H-2'), 7.40 (*dd*, 1H, J_1= 2.1, J_2= 8.5 Hz, H-6'), 6.80 (*d*, 1H, *J*=8.3 Hz, H-5'), 6.30 (*s*, 1H, H-8), 6.10 (*d*, 1H, *J*=2.4 Hz, H-6), 5.37 (*s*, 1H, H-1''), 4.23 (*d*, 1H, *J*=2.3 Hz, H-2''), 3.81 (*m,* 1H, H-3''), 3.77 (*m*, 1H, H-4''), 3.40 (*m*, 2H, H-5''). ^{13}C-NMR: δ 178.54 (C-4), 164.80 (C-7), 161.64 (C-5), 157.89 (C-2), 157.15 (C-9), 148.43 (C-4'), 144.94 (C-3'), 133.45 (C-3), 121.65 (C-1'), 121.52 (C-6'), 115.38 (C-2'), 114.99 (C-5'), 108.07(C-1''), 104.12 (C-10), 98.49 (C-6), 93.36 (C-8), 86.57 (C-4''), 81.87 (C-2''), 77.24 (C-3''), 61.09 (C-5''). NMR data are in total agreement with the data for quercetin 3-*O*-α-arabinofuranoside.[20]

Compound 7

Yellow powder. ^{1}H-NMR: δ 7.24 (*d*, 1H, *J*=1.8 Hz, H-2'), 7.21 (*dd*, 1H, J_1=1.8, J_2=8.2 Hz, H-6'), 6.82 (*d*, 1H, *J*=8.2 Hz, H-5'), 6.28 (*s*, 1H, H-8), 6.11 (*d*, 1H, *J*=1.2 Hz, H-6), 5.25 (*d*, 1H, *J*=1.2 Hz, H-1''), 4.12 (*d*, 1H, *J*=1.1 Hz, H-2''), 3.65 (*dd*, 1H, J_1=2.9, J_2=9.4 Hz, H-3''), 3.32 (*m*, 1H, H-5''), 3.24 (*d*, 1H, *J*=9.4 Hz, H-4''), 0.84 (*d*, 3H, *J*=6.4 Hz, H-6''). ^{13}C-NMR: δ 178.21 (C-4), 164.65 (C-7), 161.76 (C-5), 157.89 (C-2), 157.11 (C-9), 148.39 (C-4'), 144.99 (C-3'), 134.78 (C-3), 121.52 (C-1'), 121.42 (C-6'), 115.50 (C-5'), 114.95 (C-2'), 104.41 (C-10), 102.11 (C-1''), 98.45 (C-6), 93.33 (C-8), 71.82 (C-4''), 70.67 (C-3''), 70.61 (C-2''), 70.47 (C-5''), 16.21 (C-6''). NMR data are in total agreement with the data for quercetin 3-*O*-α-rhamnopyranoside.[18-21]

DISCUSSION

Since ancient times, plants have served as one of the most important sources of medicines. Approximately 500 species are known to be used as folk medicine in Anatolia.

Many desirable biological activities such as analgesic, anticholecystitis, cholagogic, cytotoxic, hepatoprotective, and vasorelaxant activity of *Lysimachia* species used traditionally for expectorant, antipyretic, and wound healing purposes in Turkey are reported.[4-10]

Taking the folkloric and modern use of *L. monnieri* for memory enhancement into account, we designed the current study, which was the first on the neuroprotective effect of any *Lysimachia* species. Confirming its folkloric use, the ME as well as the EtOAC and chloroform fractions of LV inhibited AChE and BChE effectively. Among them, we chose the EtOAc fraction for further study due to its high cholinesterase inhibitory and antioxidant effects. Our phytochemical studies in order to identify substances found in the fraction led to the isolation of seven phenolic compounds (1-7) from the plant for the first time. The compounds were characterized as gallic acid (1), (+)-catechin (2), myricetin 3-*O*-α-arabinofuranoside (3), myricetin 3-*O*-α-rhamnopyranoside (4), quercetin 3-*O*-β-glucopyranoside (5), quercetin 3-*O*-α-arabinofuranoside (6), and quercetin 3-*O*-α-rhamnopyranoside (7).

Previous phytochemical studies on other *Lysimachia* species showed the presence of secondary metabolites including flavonoids, triterpenes, phenolic acids, etc.[5-7] According to these studies, *Lysimachia* species have rich phenolic compounds such as gentisic acid, caffeic acid, chlorogenic acid, *p*-coumaric acid, apigenin, luteolin, myricetin, quercetin, kaempferol, isorhamnetin, quercetin 3-*O*-glucoside, quercetin 3-*O*-rutinoside, myricetin 3-*O*-glucoside, myricetin 3-*O*-rhamnoside, eriodictyol 7-*O*-glucoside, vitexin, and isovitexin.[5-7] Phenolic compounds are known to be generally responsible for the antioxidant capacity of plant extract. For instance, among them, gallic acid, (+) -catechin, myricetin-3-*O*-arabinofuranoside, and myricetin-3-*O*-rhamnoside have been demonstrated to be well-known compounds with remarkable antioxidant potential.[23-25] The antioxidant activity, anti-inflammatory, antinociceptive, and antipyretic activities of quercetin 3-*O*-β-arabinopyranoside and quercetin 3-*O*-α-L-rhamnopyranoside have been proven by Ramzi et al.[26] The DPPH assay, which determines the scavenging ability of antioxidants against stable radical DPPH·, is applied as a valid and practical assay, while the FRAP assay is based on the determination of the antioxidant capacity of foods, beverages, and other nutritional supplements rich in polyphenols via their ferric reducing ability.[27,28] It is a simple, automated test to measure antioxidant capacity. It should be noted that the high antioxidant activity of the EtOAC fraction is strongly correlated with its richest total phenol and flavonoid content and the isolated compounds (1-7) are the major contributors to the marked antioxidant activity of the plant.

On the other hand, flavonoid derivatives have been known to exert strong cholinesterase inhibitory effects.[29] Many

researchers have so far pointed out various flavonoids to be responsible for the potent cholinesterase inhibitory capacity of plant extracts. For example, the flavonoid fraction obtained from the fern *Dryopteris erythrosora* that contained gliricidin 7-*O*-hexoside, apigenin7-*O*-glucoside, quercetin 7-*O*-rutinoside, quercetin 7-*O*-galactoside, kaempferol 7-*O*-gentiobioside, kaempferol 3-*O*-rutinoside, myricetin 3-*O*-rhamnoside, and quercitrin exhibited strong AChE inhibition over 90% in dose-dependent manner.[30]

Some studies showed that the isolated compounds (+)-catechin, myricetin 3-*O*-arabinofuranoside, quercetin 3-*O*-β-glucopyranoside, quercetin 3-*O*-arabinofuranoside, and quercetin 3-*O*-α-rhamnopyranoside exhibited an active inhibitory effect against the AChE enzyme as well as strong antioxidative activity.[31,32] Moreover, gallic acid is well known as a powerful antioxidant to remedy DNA damage due to oxidative stress.[33]

In our previous study,[17] we reported quercetin with a significant AChE and BChE inhibitory effect in a competitive manner, which was shown to bind with hydrogen bonds to important amino acid residues at the anionic site of AChE. Recently, Ado et al.[34] demonstrated the presence of many flavonoid derivatives, i.e. catechin, quercetin pentoside, quercetin hexoside, etc. in the AChE-inhibiting fraction of *Cynometra cauliflora* leaves. In fact, an AChE inhibitory effect of (+)-catechin isolated from *Canarium patentinervium* was described at low level (>100 µg/mL).[35] Nevertheless, other flavonoid derivatives isolated from LV herein could be suggested to contribute to some extent to the cholinesterase inhibitory effect of the plant as Russo et al.[35] demonstrated a strong correlation between flavonoids and cholinesterase inhibition through calculation of Pearson correlation.

Actually, it should be also noted that the occurrence of marked cholinesterase inhibitory activity as well as antioxidant activity might also be due to a synergistic action of the flavonoids present in the extract, because in many cases flavonoids have been shown to exert synergistic or additive effects, whereas sometimes antagonism occurs.[36-38] This is because the antioxidant activity of green tea, grape seed, and lettuce extracts was shown to increase after the addition of quercetin via acting synergistically, while catechins were proven to be responsible for synergism in green tea regarding its antioxidant activity, which might the case in the present study as well.[37,38]

According to previous bioactivity studies, various *Lysimachia* species such as *Lysimachia laka*, *Lysimachia punctata*, *Lysimachia foenum-graecum*, *Lysimachia clethroides*, and *Lysimachia vulgaris* have potent antioxidant capacity.[39-43] There are limited studies about the cholinesterase inhibitory activity of *Lysimachia* species. One study showed that *Lysimachia christinae* was inactive on AChE.[44]

The results of the present study showed that the EtOAc fraction had the highest total phenol and flavonoid content. This may explain why the highest enzyme inhibitor effect was observed on the EtOAC fraction. The total flavonoid content of ME extract was high. The high flavonoid content and other minor compounds of ME extract may be responsible for the similar enzyme inhibitor effect compared with the EtOAc fraction. Although the aqueous fraction has high antioxidant activity, no enzyme inhibitor effect of the aqueous fraction was observed. Furthermore, no total phenol or flavonoid content of the aqueous fraction was detected. The high antioxidant activity of the aqueous fraction may be based on the other compounds, which have no cholinesterase inhibitory effect.

CONCLUSION

The results obtained from the present study demonstrated that the ME and EtOAc fraction of the aerial parts of LV have strong AChE and BChE inhibitory effects, providing scientific justification for its use in folk medicine. The compounds mentioned herein have been isolated from LV for the first time. The current study is the very first on phytochemistry and neuroprotective effects through the cholinesterase and TYR inhibitory activity of LV. The phenolic compounds we isolated (1-7) may be responsible for the anticholinesterase and antioxidant activities.

ACKNOWLEDGEMENT

F. Sezer Şenol and Sıla Özlem Şener would like to acknowledge the scholarship during their postgraduate program provided by the Scientific and Technological Research Council of Turkey (TÜBİTAK). Also, Prof. Dr. Ufuk Özgen and Sıla Özlem Şener would like to acknowledge the financial support provided by the Council of Higher Education.

Conflicts of interest: No conflict of interest was declared by the authors. The authors alone are responsible for the content and writing of the paper.

REFERENCES

1. Orhan IE. Current concepts on selected plant secondary metabolites with promising inhibitory effects against enzymes linked to Alzheimer's disease. Curr Med Chem. 2012;19:2252-2261.
2. Mendes E, Perry MJ, Francisco AP. Design and discovery of mushroom tyrosinase inhibitors and their therapeutic applications. Expert Opin Drug Disc. 2014;9:533-554.
3. Terzioglu S, Karaer F. An Alien Species New to the Flora of Turkey. *Lysimachia japonica* Thunb. (Primulaceae) Turk J Bot. 2009;33:123-126.
4. Kızılarslan Ç, Özhatay N. Wild plants used as medicinal purpose in the south part of İzmit (Northwest Turkey). Turk J Med Sci. 2012;9:199-218.
5. Tóth A, Riethmüller E, Alberti Á, Végh K, Kéry Á. Comparative phytochemical screening of phenoloids in *Lysimachia* species. Eur Chem Bull. 2012;1:27-30.
6. Marr KL, Bohm BA, Cooke C, Gunning P. Flavonoids of Hawaiian endemic *Lysimachia* in honour of professor GH Neil Towers 75th birthday. Phytochemistry. 1998;49:553-557.
7. Hanganu D, Olah NK, Mocan A, Vlase L, Benedec D, Raita O, Toma CC. Comparative polyphenolic content and antioxidant activities of two Romanian *Lysimachia* species. Studies. Rev Chim. 2016;67:227-231.
8. Podolak I, Koczurkiewicz P, Michalik M, Galanty A, Zajdel P, Janeczko Z. A new cytotoxic triterpene saponin from *Lysimachia nummularia* L. Carbohydrate Res. 2013;375:16-20.

9. Wang J, Zhang Y, Zhang Y, Cui Y, Liu J, Zhang B. Protective effect of *Lysimachia christinae* against acute alcohol-induced liver injury in mice. Biosci Trends. 2012; 6:89-97.
10. Lee JO, Chang K, Kim CY, Jung SH, Lee SW, Oak MH. *Lysimachia clethroides* extract promote vascular relaxation via endothelium-dependent mechanism. J Cardiovasc Pharmacol. 2010;55:481-488.
11. Ellman GL, Courtney KD, Andres V, Featherstone RM. A new and rapidcolorimetric determination of acetylcholinesterase activity. Biochem Pharmacol. 1961;7:88-95.
12. Khan MTH, Orhan I, Senol FS, Kartal M, Sener B, Dvorská M, Smejkal K, Slapetová T. Cholinesterase inhibitory activities of some flavonoid derivatives and chosen xanthone and their molecular docking studies. Chem-Biol Interact. 2009;181:383-389.
13. Masuda T, Yamashita D, Takeda Y, Yonemori S. Screening for tyrosinase inhibitors among extracts of seashore plants and identification of potent inhibitors from *Garcinia subelliptica*. Biosci Biotechnol Biochem. 2005;69:197-201.
14. Blois MS. Antioxidant determinations by the use of a stable free radical. Nature. 1958;181:1199-1200.
15. Oyaizu M. Studies on products of browning reactions-antioxidative activities of products of browning reaction prepared from glucosamine. Jpn J Nutr. 1986;44:307-315.
16. Singleton VL, Rossi Jr. JA. Colorimetry of total phenolics withphosphomolibdic-phosphotungtic acid reagents. Am J Enol Viticult. 1965;16:144-158.
17. Woisky R, Salatino A. Analysis of propolis: some parameters and procedures for chemical quality control. J Apicol Res. 1998;37:99-105.
18. Eldashan OA. Isolation and structure elucidation of phenolic compounds of carob leaves grown in Egypt. Curr Res J Biol Sci. 2011;3:52-55.
19. Adrienne LD, Ya C, Alan PD, Lewis JR. ^{1}H and ^{13}C NMR assignments of some green tea polyphenols. Magnetic Res Chem. 1996;34:887-890.
20. Ek S, Kartimo H, Mattila S, Tolonen A. Characterization of phenolic compounds from Lingonberry (*Vaccinium vitis-idaeae*). J Agric Food Chem. 2006;54:9834-9842.
21. Aderogba MA, Ndhlala AR, Rengasamy KRR, Van Staden J. Antimicrobial and selected *in vitro* enzyme inhibitory effects of leaf extracts, flavonols and indole alkaloids isolated from *Croton menyharthii*. Molecules. 2013;18:12633-12644.
22. Ko JH, Kim BG, Kim JH, Kim H, Lim CE, Lim J, Lee C, Lim Y, Ahn, JH. Four glucosyltransferases from rice: cDNA cloning, expression, and characterization. J Plant Physiology. 2008;165:435-444.
23. Mansouri A, Embarek G, Kokkalou E, Kefalas P. Phenolic profile and antioxidant activity of the Algerian ripe date palm fruit (*Phoenix dactylifera*). Food Chem. 2005;89:411-420.
24. Verma AK, Rajkumar V, Banerjee R, Biswas S, Das AK. Guava (*Psidium guajava* L.) Powder as an Antioxidant Dietary Fibre in Sheep Meat Nuggets. Asian-Australas J Anim Sci. 2013;26:886-895.
25. Okoth DA, Chenia HY, Koorbanally NA. Antibacterial and antioxidant activities of flavonoids from *Lannea alata* (Engl.) Engl. (Anacardiaceae). Phytochem Lett. 2013;6:476-481.
26. Ramzi AA, Mothana MS, Al-Said AJ, Al-Rehaily TM, Thabet NA, Awad M, Lalk UL. Anti-inflammatory, antinociceptive, antipyretic and antioxidant activities and phenolic constituents from *Loranthus regularis* Steud. ex Sprague. Food Chem. 2012;130:344-349.
27. Sun LJ, Zhang JB, Lu XY, Zhang, LY, Zhang YL. Evaluation to the antioxidant activity of total flavonoids extract from persimmon (*Diospyros kaki* L.) leaves. Food Chem Toxicol. 2011;49:2689-2696.
28. Cao J, Xia X, Chen X, Xiao J, Wang Q. Characterization of flavonoids from *Dryopteris erythrosora* and evaluation of their antioxidant, anticancer and acetylcholinesterase inhibition activities. Food Chem Toxicol. 2013;51:242-250.
29. Orhan IE. Implications of some selected flavonoids towards Alzheimer's disease with the emphasis on cholinesterase inhibition and their bioproduction by metabolic engineering. Curr Pharm Biotechnol. 2014;15:352-361.
30. Anand P, Singh B. Flavonoids as lead compounds modulating the enzyme targets in Alzheimer's disease. Med Chem Res. 2013;22:3061-3075.
31. Odontuya G. Anti-oxidative, acetylcholinesterase and pancreatic lipase inhibitory activities of compounds from *Dasiphora fruticosa, Myricaria alopecuroides* and *Sedum hybridum*. Mongolian Journal of Chemistry. 2017;43:42-49.
32. Gasca CA, Castillo WO, Takahashi CS, Fagg CW, Magalhães PO, Fonseca-Bazzo YM, Silveira D. Assessment of anti-cholinesterase activity and cytotoxicity of cagaita (*Eugenia dysenterica*) leaves. Food and Chemical Toxicology. 2017;109:996-1002.
33. Farhoosh R, Nyströmm L. Antioxidant potency of gallic acid, methyl gallate and their combinations in sunflower oil triacylglycerols at high temperature. Food Chem. 2018;244:29-35.
34. Ado MA, Abas F, Ismail IS, Ghazali HM, Shaari K. Chemical profile and antiacetylcholinesterase, antityrosinase, antioxidant and α-glucosidase inhibitory activity of *Cynometra cauliflora* L. leaves. J Sci Food Agric. 2015;95:635-642.
35. Russo D, Valentão P, Andrade PB, Fernandez EC, Milella L. Evaluation of antioxidant, antidiabetic and anticholinesterase activities of *Smallanthus sonchifolius* landraces and correlation with their phytochemical profiles. Int J Mol Sci. 2015;16:17696-71718.
36. Wang S, Wang D, Liu Z. Synergistic, additive and antagonistic effects of *Potentilla fruticosa* combined with EGb761 on antioxidant capacities and the possible mechanism. Ind Crops Prods. 2015;67:227-238.
37. Altunkaya A, Gökmen V, Skibsted LH. PH dependent antioxidant activity of lettuce (*L. sativa*) and synergism with added phenolic antioxidants. Food Chem. 2016;190:25-32.
38. Colon M, Nerín C. Synergistic, antagonistic and additive interactions of green tea polyphenols. Eur Food Res Technol. 2015;242:211-220.
39. Gupta S, Sarma S, Mao AA, Seal T. Antioxidant activity of different parts of *Lysimachia laxa* and *Gymnocladus assamicus*, a comparison using three different solvent extraction systems. J Chem Pharm Res. 2013;5:33-40.
40. Toth A, Toth G, Kery A. Polyphenol composition and antioxidant capacity of three *Lysimachia* species. Nat Prod Commun. 2014;9:1473-1478.
41. Li HY, Hao ZB, Wang XL, Huang L, Li JP. Antioxidant activities of extracts and fractions from *Lysimachia foenum-graecum* Hance. Bioresour Technol. 2009;100:970-974.
42. Wei JF, Zhang ZJ, Cui LL, Kang WY. Flavonoids in different parts of *Lysimachia clethroides* duby extracted by ionic liquid: analysis by HPLC and antioxidant activity assay. J Chem. 2017;2017:1-10.
43. Yildirim AB, Guner B, Karakas FP, Turker AU. Evaluation of antibacterial, antitumor, antioxidant activities and phenolic constituents of field-grown and *in vitro*-grown *Lysimachia vulgaris* L. Afr J Tradit Complement Altern Med. 2017;14:177-187.
44. Kaufmann D, Kaur Dogra A, Tahrani A, Herrmann F, Wink M. Extracts from traditional Chinese medicinal plants inhibit acetylcholinesterase, a known Alzheimer's disease target. Molecules. 2016; 21:1161-1177.

Turk J Pharm Sci 2020;17(5):535-541
DOI: 10.4274/tjps.galenos.2019.82335

ORIGINAL ARTICLE

Determination of the Physicochemical Properties of Piroxicam

Piroksikamın Fizikokimyasal Özelliklerinin Belirlenmesi

Mustafa ÇELEBİER[1]*, Merve NENNİ[2], Ozan KAPLAN[1], Emrah AKGEYİK[3], Mustafa Sinan KAYNAK[4], Selma ŞAHİN[5]

[1]Hacettepe University Faculty of Pharmacy, Department of Analytical Chemistry, Ankara, Turkey
[2]Çukurova University Faculty of Pharmacy, Department of Analytical Chemistry, Adana, Turkey
[3]İnönü University Faculty of Pharmacy, Department of Analytical Chemistry, Malatya, Turkey
[4]Anadolu University Yunus Emre Vocational School, Department of Pharmacy, Program in Pharmacy Services, Eskişehir, Turkey
[5]Hacettepe University Faculty of Pharmacy, Department of Pharmaceutical Technology, Ankara, Turkey

ABSTRACT

Objectives: The aim of this study was to determine the acid dissociation constant (pKa) of piroxicam using high performance liquid chromatography (HPLC) and ultraviolet-visible (UV-Vis) spectrophotometry, and to determine the partition coefficient (Log P), distribution coefficient (Log D), and "Log kw" values of piroxicam using HPLC.

Materials and Methods: The HPLC studies were performed on a reversed-phase ACE C18 (150x4.6 mm ID, 5 µm) column at a flow rate of 1.0 mL min^{-1}. The detector was set to 360 nm. Log D at different pH values (3.0-6.5) was examined with a phosphate buffer (20 mM) and acetonitrile (30:70 v/v) mixture as the mobile phase. For pKa determination, HPLC studies were performed with a mixture of phosphate buffer (20 mM) and methanol within the pH range of 3.50-6.00. Log kw measurements were performed with phosphate buffer (20 mM) and MeOH (from 20:80 v/v to 10:90 v/v) mixtures within the pH range of 3.50-6.00. UV-Vis spectrophotometric pKa measurements were performed at 285 nm wavelength.

Results: The pKa value of piroxicam was found to be 5.3 by HPLC and 5.7 by UV-Vis spectrophotometry. Log P of piroxicam was determined as 1.58 in our experimental conditions. Log D values were 1.57, 1.57, 1.44, 1.13, and 0.46 for pH values of 3.17, 3.79, 4.44, 5.42, and 6.56, respectively.

Conclusion: In the literature, different Log P (3.1, 2.2, and 0.6) and pKa (6.3 and 4.8) values were reported for piroxicam. The Log P (1.58) and pKa (5.3 and 5.7) values obtained for piroxicam in our study were within the range of the literature values. All these results indicate that different experimental approaches used for the determination of physicochemical properties could provide different values. Although UV spectrophotometry is easy to apply, HPLC is a unique technique for simultaneous determination of pKa, Log D, and Log P values of compounds.

Key words: Piroxicam, physicochemical properties, pKa, Log P, Log D, Log kw

ÖZ

Amaç: Bu çalışmanın amacı, yüksek performanslı sıvı kromatografisi (HPLC) ve ultraviyole-görünür bölge (UV-GB) spektrofotometresi kullanılarak piroksikamın asit ayrışma sabitinin (pKa) bulunması; HPLC kullanılarak partisyon katsayısı (Log P), dağılım katsayısı (Log D) ve "Log kw" değerlerininin belirlenmesidir.

Gereç ve Yöntemler: HPLC çalışmaları, 1,0 mL min^{-1} akış hızında ters faz kromatografisinde ACE C18 (150x4,6 mm ID, 5 µm) kolon kullanılarak gerçekleştirildi. Detektör 360 nm'ye ayarlandı. Farklı pH değerlerinde (3,0-6,5) Log D değeri, hareketli faz olarak fosfat tamponu (20 mM): asetonitril (30:70 h/h) karışımı ile incelendi. pKa'nın belirlenmesi için HPLC çalışmaları, 3,50 ve 6,00 pH aralığında fosfat tamponu (20 mM): metanol karışımı ile gerçekleştirildi. Log kw ölçümleri, pH 3,50 ila 6,00 arasında bir pH aralığında fosfat tamponu (20 mM): MeOH (20:80 h/h ile 10:90 h/h) karışımları ile yapıldı. UV-GB spektrofotometrik pKa ölçümleri 285 nm dalga boyunda gerçekleştirildi.

Bulgular: Piroksikamın pKa değeri sırasıyla HPLC ile 5,3 ve UV-GB spektrofotometresi ile 5,7 olarak bulundu. Deney şartlarımızda piroksikamın Log P değeri 1,58 olarak bulundu. Log D değerleri, sırasıyla 3,17, 3,79, 4,44, 5,42 ve 6,56 pH değerleri için 1,57, 1,57, 1,44, 1,13 ve 0,46 olarak bulundu.

Sonuç: Literatürde, piroksikam için farklı Log P (3,1, 2,2 ve 0,6) ve pKa (6,3 ve 4,8) değerleri bildirilmiştir. Çalışmamızda piroksikam için elde edilen Log P (1,58) ve pKa (5,3 ve 5,7) değerleri literatür değerleri arasındaydı. Tüm bu sonuçlar, fizikokimyasal özelliklerin belirlenmesinde kullanılan farklı deneysel yaklaşımların farklı değerler verebileceğini göstermektedir. UV spektrofotometresinin uygulanması kolay olsa da, HPLC, bileşiklerin pKa, Log D ve Log P değerlerinin eşzamanlı olarak belirlenmesi için eşsiz tekniklerden biridir.

Anahtar kelimeler: Piroksikam, fizikokimyasal özellikler, pKa, Log P, Log D, Log kw

*Correspondence: **E-mail:** celebier@hacettepe.edu.tr, **Phone:** +90 (312) 305 14 99 **ORCID-ID:** orcid.org/0000-0001-7712-5512
Received: 25.02.2019, **Accepted:** 05.09.2019

INTRODUCTION

Dissolution from the dosage form is one of the factors limiting the absorption of drugs from the gastrointestinal (GI) tract. According to the Noyes-Whitney dissolution model,[1] the *in vivo* dissolution rate is influenced by drug diffusivity, drug solubility in GI contents, the wetted surface area of solid by biological fluids, and GI hydrodynamics.[2]

Non-steroidal anti-inflammatory drugs (NSAIDs) are chronically used as anti-inflammatory, analgesic, and antipyretic agents[3] to reduce pain, decrease stiffness, and improve function in patients suffering from all forms of arthritis. They are also used for the acute treatment of pain associated with headaches, dysmenorrhea, and postoperative pain.[4] Recent studies have focused on the usage of NSAIDs for cancer treatment and prevention.[5] Pharmacologic treatment of cancer pain using NSAIDs has also been investigated for a long time,[6] although their use is limited due to their side effects.[7] The relationship between some GI tract diseases and NSAIDs usage is also discussed.[8] Drug-drug interactions related with the usage of NSAIDs are still an issue to be investigated.[9] Because of all these aspects, the physicochemical properties of drugs are one of the key points in understanding their behavior inside the body. Therefore, to understand the drug's behavior in the GI tract, it is important to know the lipophilicity and pKa of drugs.[10]

Piroxicam is a NSAID of the oxicam class and is used to alleviate the symptoms of painful and inflammatory conditions such as arthritis.[3] They are also used for the treatment of headaches, dysmenorrhea, and postoperative pain.[4]

In the literature, it is easy to find various studies on the determination of the pKa values of pharmaceuticals using high performance liquid chromatography (HPLC),[11-14] ultraviolet (UV) spectrophotometry,[15-17] capillary electrophoresis,[18,19] and potentiometric titrations.[20-22] Identical analytical techniques have also been applied over a long period for calculation of partition coefficient (Log P) and distribution coefficient (Log D) values.[23-30] For piroxicam, the reported Log P values differ from 0.6 to 3.6 and the reported pKa values differ from 4.76 to 6.30 according to DrugBank. Variable results in such basic physicochemical parameters motivated us to investigate these parameters in our conditions. In the present study, a simple experimental procedure based on HPLC and UV-visible (Vis) spectrophotometry was applied for the determination of the physicochemical properties (pKa, Log P, and Log D) of piroxicam (Figure 1). A comparison of HPLC and UV-Vis spectrophotometry used for the determination of pKa values was also carried out. A chromatographic approach based on Log kw is suggested in the literature[31,32] to determine the lipophilicity of drugs. This technique is relatively new compared to the classical shake-flask method,[33] and, to the best of our knowledge, there is no report available in the literature to correlate the shake-flask method and Log kw measurements with each other. Therefore, this is the only study to compare the Log P and Log kw measurements for an active pharmaceutical ingredient.

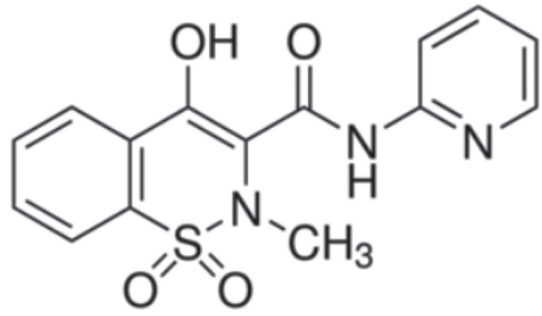

Figure 1. Chemical structure of piroxicam

MATERIALS AND METHODS

Chemicals

Piroxicam was supplied by Sigma Aldrich (St. Louis, MO, USA). Sodium dihydrogen phosphate ($NaHPO_4 \bullet 2H_2O$) and NaOH were purchased from Merck (Darmstadt, Germany). Disodium hydrogen phosphate ($Na_2HPO_4 \bullet 2H_2O$), potassium chloride (KCl), acetonitrile (ACN), methanol (MeOH), and 1-octanol were obtained from Sigma Aldrich. Water was obtained from the Milli-Q water system (Barnstead, USA) and used for the preparation of all standard solutions and buffers.

Instrumentation

The HPLC system used was equipped with a gradient pump (Spectra System P2000), a degasser (Spectra System SCM 1000), a manual injector with a 20-µL injection loop (Rheodyne), and a detector (Spectra System UV2000, Thermo Separation Products, USA). The detector was adjusted to 360 nm, and retention times were determined automatically by an online computer equipped with ChromQuest software. The separations were performed using a reversed-phase (RP) ACE C18 (125x4.6 mm ID, 5 µm) HPLC column (Aberdeen, Scotland) at a flow rate of 1 mL min^{-1}. The spectrophotometric measurements were carried out using a Varian Cary 50 UV-Vis wavelength spectrophotometer with a xenon lamp (200-800 nm). The UV spectra of reference and sample solutions were determined in 1-cm quartz cells at wavelengths from 200 to 800 nm.

Solutions

Standard stock solution of piroxicam (1000 µg mL^{-1} in MeOH)

Piroxicam standard stock solution was prepared by dissolving piroxicam (50 mg) in MeOH in a volumetric flask (50 mL).

Phosphate buffer (20 mM) with potassium chloride (100 mM) solution (between pH 3.00 and 7.50) for UV-Vis spectrophotometric pKa determination

A phosphate buffer (20.0 mM) and 100 mM KCl mixture were prepared by dissolving 3.56 g of sodium dihydrogen phosphate ($NaH_2PO_4 \bullet 2H_2O$) and 7.45 g of KCl in about 800 mL of water and then making up the volume to 1000 mL with water. The pH of the solutions was adjusted with 1 M NaOH and 0.1 M KCl mixture solution.

Phosphate buffer (20 mM):MeOH (50:50 v/v) solutions (between pH 3.50 and 6.00) for HPLC pKa determination

Phosphate buffer (20.0 mM) was prepared by dissolving 3.12 g of sodium dihydrogen phosphate ($NaH_2PO_4 \bullet 2H_2O$) in about 800 mL of water and then making up the volume to 1000 mL with water. The mobile phase was prepared as 500 mL of a mixture of phosphate buffer/MeOH (50:50 v/v) and the pH was adjusted with o-phosphoric acid/MeOH (50:50 v/v) or 20 mM disodium hydrogen phosphate (Na_2HPO_4)/MeOH (50:50 v/v) mixtures for different pH values in the range of 3.64-5.94.

Phosphate buffer (20 mM) solutions (between pH 3.00 and 6.60) for Log D determination

Phosphate buffer (20.0 mM) was prepared by dissolving 3.56 g of disodium hydrogen phosphate ($Na_2HPO_4 \bullet 2H_2O$) in about 800 mL of water and then making up the volume to 1000 mL with water, and adjusting the pH with o-phosphoric acid to different pH values in the range of 3.17-6.56.

Phosphate buffer (20 mM, pH 3.0):ACN (30:70 v/v) solutions as the HPLC mobile phase for Log D determination

Phosphate buffer (20.0 mM) was prepared by dissolving 3.56 g of disodium hydrogen phosphate ($Na_2HPO_4 \bullet 2H_2O$) in about 800 mL of water, adjusting the pH with o-phosphoric acid to 3.0, and then making up the volume to 1000 mL with water. The mobile phases were prepared as 500 mL of a mixture of phosphate buffer (20 mM, pH 3.0) and ACN (30:70 v/v).

Phosphate buffer (20 mM):MeOH (from 20:80 v/v to 10:90 v/v) solutions for Log kw determination (between pH 3.00 and 6.00)

Phosphate buffer (20.0 mM) was prepared by dissolving 3.56 g of disodium hydrogen phosphate ($Na_2HPO_4 \bullet 2H_2O$) in about 800 mL of water and then making up the volume to 1000 mL with water. The mobile phases were prepared as 500 mL of a mixture of phosphate buffer (20 mM)/MeOH in the range of 20:80-10:90, v/v. The pH of the mobile phases was adjusted with o-phosphoric acid/MeOH (20:80-10:90, v/v) or 20 mM disodium hydrogen phosphate (Na_2HPO_4)/MeOH (20:80-10:90, v/v) mixtures for different pH values (3.00 and 6.00) and different mobile phase compositions (phosphate buffer (20 mM)/MeOH in the range of 20:80-10:90, v/v).

Procedures

UV-Vis spectrophotometric pKa determination

The standard stock solution of piroxicam was diluted to 20.0 µg mL^{-1} by using phosphate buffer (20 mM): KCl (100 mM) solutions for UV-Vis spectrophotometric pKa determination (pH 3.09-7.48). The spectra were recorded at wavelengths from 200 to 400 nm. The shifts in absorption were considered. A sigmoidal curve was constructed between pH of the solutions and absorption at 285 nm. The pKa of piroxicam was determined according to the sigmoidal relationship given by Microsoft Excel between pH 3.09 and 7.48.

HPLC pKa determination

The standard stock solution of piroxicam was diluted to 5.0 µg mL^{-1} with phosphate buffer (20 mM):MeOH (50:50 v/v) solutions for HPLC pKa determination (pH 3.64-5.94). These solutions were injected into the HPLC system with the mobile phases in which they were dissolved. A sigmoidal curve was constructed between the pH of the mobile phases and the capacity factor (k') of piroxicam. The pKa of piroxicam was determined according to the sigmoidal relationship between pH 3.64 and 5.94.

Log D determination

The experimental system was a modified shake-flask method to meet the requirements of the OECD guideline for the testing of chemicals.[33] For this purpose, the standard stock solution of piroxicam was diluted to 250 µg mL^{-1} with MeOH. Then 50.0 µL of this solution was added to aqueous biphasic systems containing phosphate buffer (20 mM) solutions for Log D determination (pH 3.17-6.56) and 1-octanol (50:50 v/v, 950 µL). After extraction at ambient temperature, the amount of piroxicam remaining in the buffer was determined by HPLC. A phosphate buffer (20 mM, pH 3.0):ACN (30:70 v/v) mixture was used as a mobile phase and the buffer phase of the extracted sample was diluted 5-fold with the mobile phase before injection into the HPLC system. Peak areas were compared with 5.0 µg mL^{-1} piroxicam solution to determine the piroxicam amount that partitioned into the octanol phase.

Log P determination

The lipophilicity of a compound can be expressed by its Log P, which is the concentration ratio of a nonionized compound in a mixture of two immiscible phases (aqueous and organic phases) at equilibrium. For measurement of the Log P value of a weakly basic drug, piroxicam, the equation given below is used for different pH values. The average of the obtained results was calculated to find the Log P value.

$$LogD=LogP-Log(1+10^{pKa-pH}) \qquad \text{Equation 1}$$

Log kw determination

For determination of Log kw values, piroxicam was diluted to 5.0 µg mL^{-1} using phosphate buffer (20 mM):MeOH (from 20:80 v/v to 10:90 v/v) solutions (pH 3.00 and 6.00). The relationship between Log k' and MeOH concentration in the mobile phase is described by $Log\ k'=Log\ kw-S\phi$.[31,34] In this equation, kw is the k' value for a compound when the aqueous phase is used as the eluent, S is the slope of the regression line, and ϕ is the volume percentage of MeOH in the mobile phase. If ϕ is zero (no MeOH in the mobile phase), the mobile phase is composed of only the phosphate buffer and the Log k' will be equal to the Log kw.

Measurements on sigmoidal curves

The data measured from the sigmoidal curve for pKa determination were found using two different approaches. The first one was to print the whole graph on A4 paper and find the pKa values by drawing tangents. The second one was to use the derivative of the actual graph.

Statistical analysis

Measurements were performed as three replicates and the results were statistically evaluated to obtain standard deviation and standard error for the calculations. The mean values were used to present the data.

RESULTS AND DISCUSSION

In the present study, we focused on the pKa, Log P, and Log D values of piroxicam because the reported values are very different from each other. The Log kw values of piroxicam were also evaluated and the values were compared with the Log D values. Based on the statistical evaluation, mean values were used to present the results.

UV-Vis spectrophotometric pKa determination

Absorption of organic compounds including most of the drugs is based on transitions of n or π electrons to the π* excited state. The absorption peaks for these transitions fall in the 200-700 nm range, which is the experimentally convenient region of the spectrum. The transitions referred to require an unsaturated group in the molecule to provide π electrons. The solvent in which the absorbing species are dissolved may have serious effects on the spectrum.[35] In the present study, the spectra of piroxicam in the phosphate buffers having identical ionic strengths (adjusted with 0.1 M KCl) but at different pH values from 3.09 to 7.48 were recorded. The values between 3.09 and 7.48 were used to construct the sigmoidal curve at 285 nm wavelength. The characteristic of the absorption spectrum for piroxicam was changed by changing the pH of the buffered aqueous media (Figure 2). The changes in the absorbance values are usually followed by overlaid plots of recorded spectra, and the greatest change occurs when the acidity of the aqueous solution is equal to the pKa of the studied compound. The sigmoidal curve was constructed and the pKa value of piroxicam was estimated as 5.7 (Figure 3).

HPLC pKa determination

The capacity factor of a drug in a RP-HPLC system is related to its lipophilicity.[36,37] Since weak acidic drugs like piroxicam are ionized at basic pH, they tend to be eluted rapidly from a lipophilic C_{18} stationary phase with basic mobile phases. The situation is the opposite for acidic mobile phases. Our results are in good agreement with this statement. Piroxicam was eluted at 7.44 min at acidic pH (pH 3.64) and eluted at 4.34

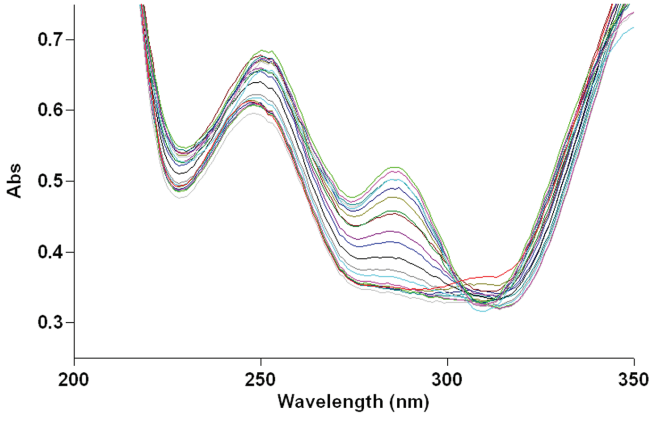

Figure 2. Representative overlaid spectra (200-400 nm) of piroxicam under optimum conditions at various pH values (pH 3.09-7.48)

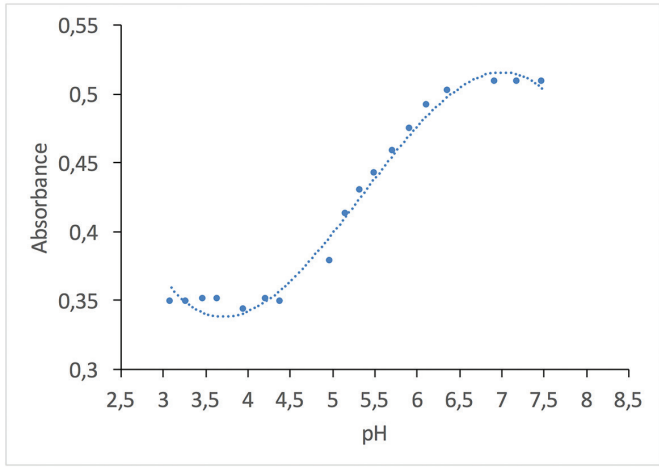

Figure 3. The plot of the absorbance values of piroxicam at 285 nm obtained as a function of pH (3.09-7.48)

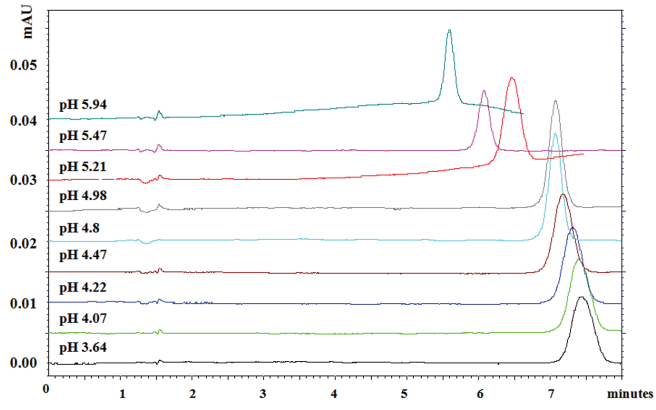

Figure 4. Representative overlaid chromatograms of piroxicam taken under optimum conditions at various pH (3.64-5.94) values. pH values are given on the top of each chromatogram peak

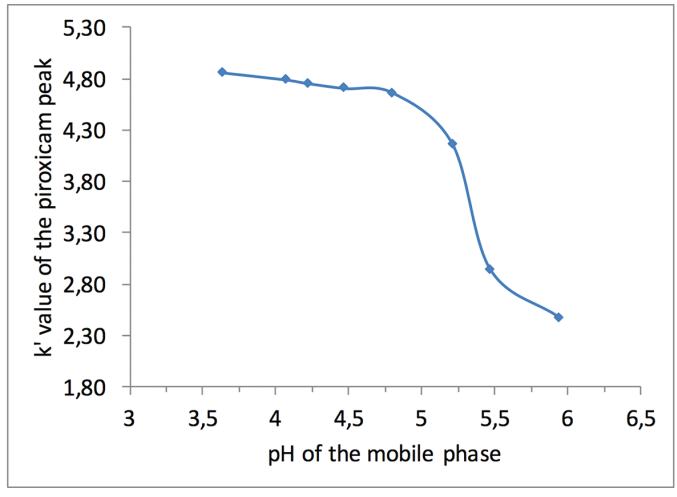

Figure 5. Sigmoidal relationship between pH (3.64-6.22) and k' of the piroxicam peak

min at relatively basic pH (pH 5.94) values (Figure 4). When the pH value of the mobile phase was plotted against k' values, a sigmoidal relationship was obtained between pH and capacity factor (Figure 5). The pKa value of piroxicam was calculated as 5.3 from this relationship.

Log D and Log P determination

In drug discovery and development, the lipophilicity of a compound is usually expressed by its partition between water and 1-octanol. The concentration of a nonionized compound in the organic and aqueous phases refers to Log P. The Log P of any ionizable solution can be measured in the aqueous phase in which the pH is adjusted to the nonionized form. The concentration ratio of nonionized solute in the solvents is calculated according to the Log P value, which is a measure of lipophilicity and is not pH dependent (Equation 2).

$$LogP_{oct/wat} = Log\left(\frac{[solute]_{octanol}}{[solute](nonionized\ water}\right) \quad \text{Equation 2}$$

As described above, piroxicam is a weak base, and it is partially ionized when dissolved in water. Log D is the ratio of the sum of the concentrations of all forms of the compound (ionized plus nonionized) in each phase and is pH dependent. The distribution coefficient is defined as a function of the ratio of the total concentration of the solute species in each phase (Equation 3).[38]

$$LogD_{(oct/wat)} = Log\left(\frac{[solute]_{octanol}}{[solute](nonionized\ water + [solute]\ neutral\ water}\right)$$

Equation 3

For a non-ionized drug, Log P is equal to Log D at any pH value, but the effective lipophilicity at any specific pH value is directly related to its pKa value for any ionized drug. In our experimental conditions, Log D of piroxicam was investigated at pH 3.17, 3.79, 4.44, 5.42, and 6.56. Table 1 summarizes the Log D values of piroxicam at the investigated pH values. The Log P values given in Table 1 were calculated according to Equation 1, in which the pKa of piroxicam was accepted as 5.7 and 5.3 based on the UV spectrophotometric and HPLC measurements, respectively.

Since piroxicam is an acidic drug, it is ionized at basic pH values and tends to be dissolved in aqueous phases. As expected, the solubility of piroxicam in the aqueous phase (phosphate buffer) was increased about 13-fold by the changes in pH from 6.56 to 3.17. This situation was in harmony with the capacity factor of piroxicam on HPLC for different mobile phase pH values. Although Log D values differ with pH values, calculated Log P values should be identical according to the theory. When the mean and standard error of Log P values were calculated it was found that Log P was 1.58±0.04 if pKa was taken as 5.3 and 1.46±0.05 if pKa was taken as 5.7. This shows us that the pKa value of 5.3 determined by HPLC provides a lower standard error for the calculated Log P values. Therefore, the Log P value for piroxicam was accepted as 1.58 in our experimental conditions.

Log kw determination

Since the retention time of an analyte in RP-HPLC is directly related to its lipophilicity, this relationship can be used to show how the lipophilicity of an analyte will be affected by pH changes. In our study, initially we calculated the Log k' values for all mobile phase compositions (80:20, 85:15, 90:10 MeOH:phosphate buffer (20 mM); (v/v) for pH values below (3.0) and above (6.0) the calculated pKa (5.3). The Log k' values were calculated for the mobile phase not containing any organic phase (0% MeOH). Figure 5 shows an example of this application for pH 6.0. When there was no MeOH in the mobile phase, the kw' values were calculated for pH 3.0 and 6.0 and found to be 37.5 and 7247.7, respectively.

CONCLUSION

In this study, spectrophotometric and chromatographic analytical approaches were examined to determine the physicochemical properties of piroxicam. Since piroxicam is a well-known compound, the results were easily compared with those in DrugBank (https://www.drugbank.ca/drugs/DB00554). According to our experimental results, the pKa value was found to be 5.7 and 5.3 for the spectrophotometric and HPLC experiments, respectively. The value found by UV-Vis spectrophotometry is close to the experimental value of 6.3 given in DrugBank. However, the predicted value of 4.76 given in DrugBank is close to the one calculated by the results of HPLC analysis. The experimental Log P value in DrugBank for piroxicam is 3.06, where the predicted values are 0.6 and 2.2. Our experiments show that piroxicam's Log P value is 1.58. This value is between the predicted and experimental values

Table 1. Experimental Log D and calculated Log P values of piroxicam

pH	Log D	Log D	Log P (pKa is accepted as 5.3)	Log P (pKa is accepted as 5.7)
3.17	37.17	1.57	1.57	1.57
3.79	37.38	1.57	1.58	1.58
4.44	27.65	1.44	1.50	1.46
5.42	13.58	1.13	1.50	1.32
6.56	2.89	0.46	1.74	1.38

Log D: Distribution coefficient, Log P: Partition coefficient, pKa: Dissociation constant

reported in DrugBank. The differences for pKa and Log P between the experimental and predicted values in DrugBank indicate that the experimental data found in the present study are novel for piroxicam. Based on all these results, we can conclude that the use of different experimental approaches for the determination of physicochemical properties can clearly provide different values for drugs.

Conflicts of interest: No conflict of interest was declared by the authors. The authors alone are responsible for the content and writing of the paper.

REFERENCES

1. Costa P, Lobo JMS. Modeling and comparison of dissolution profiles. Eur J Pharm Sci. 2001;13:123-133.
2. Hörter D, Dressman J. Influence of physicochemical properties on dissolution of drugs in the gastrointestinal tract. Adv Drug Deliv Rev. 2001;46:75-87.
3. Crofford LJ. Use of NSAIDs in treating patients with arthritis. Arthritis Res Ther. 2013;15(Suppl 3):S2.
4. Simon LS. Nonsteroidal anti-inflammatory drugs and their risk: a story still in development. Arthritis Res Ther. 2013;15(Suppl 3):S1.
5. Cha YI, DuBois RN. NSAIDs and cancer prevention: targets downstream of COX-2. Annu Rev Med. 2007;58:239-252.
6. Portenoy RK, Lesage P. Management of cancer pain. The Lancet. 1999;353:1695-1700.
7. Carr DB, Goudas LC, Balk EM, Bloch R, Ioannidis J, Lau J. Evidence report on the treatment of pain in cancer patients. JNCI Monographs. 2004;32:23-31.
8. Rainsford KD, Velo GP. Side-effects of anti-inflammatory drugs: part two studies in major organ systems: Springer Science & Business Media; 2012.
9. Franz CC, Egger S, Born C, Bravo AER, Krähenbühl S. Potential drug-drug interactions and adverse drug reactions in patients with liver cirrhosis. Eur J Clin Pharmacol. 2012;68:179-188.
10. Dressman J, Vertzoni M, Goumas K, Reppas C. Estimating drug solubility in the gastrointestinal tract. Eur J Clin Pharmacol. 2007;59:591-602.
11. Uhrova M, Miksik I, Deyl Z, Bellini S. Determination of dissociation constants by separation methods (HPLC and CE). Theoretical background and guidelines for application. Process Contr Qual. 1997;10:151-167.
12. Oumada FZ, Rafols C, Roses M, Bosch E. Chromatographic determination of aqueous dissociation constants of some water-insoluble nonsteroidal antiinflammatory drugs. J Pharm Sci. 2002;91:991-999.
13. Demiralay EC, Koc D, Daldal YD, Çakır C. Determination of chromatographic and spectrophotometric dissociation constants of some beta lactam antibiotics. J Pharmaceut Biomed. 2012;71:139-143.
14. Canbay HS, Demiralay EC, Alsancak G, Ozkan SA. Chromatographic Determination of pK(a) Values of Some Water-Insoluble Arylpropionic Acids and Arylacetic Acids in Acetonitrile plus Water Media. J Chem Eng Data. 2011;56:2071-2076.
15. Santos E, Rosillo I, Delcastillo B, Avendano C. Determination of Pka Values for Hydantoins by Spectrophotometry. J Chem Res-S. 1982:131.
16. Rosenberg LS, Simons J, Schulman SG. Determination of Pka Values of N-Heterocyclic Bases by Fluorescence Spectrophotometry. Talanta. 1979;26:867-871.
17. Pereira AV, Garabeli AA, Schunemann GD, Borck PC. Determination of Dissociation Constant (K-a) of Captopril and Nimesulide - Analytical Chemistry Experiments for Undergraduate Pharmacy. Quim Nova. 2011;34:1656-1660.
18. Fu XF, Liu Y, Li W, Bai Y, Liao YP, Liu HW. Determination of dissociation constants of aristolochic acid I and II by capillary electrophoresis with carboxymethyl chitosan-coated capillary. Talanta. 2011;85:813-815.
19. Ehala S, Misek J, Stara IG, Stary I, Kasicka V. Determination of acid-base dissociation constants of azahelicenes by capillary zone electrophoresis. J Sep Sci. 2008;31:2686-2893.
20. Schurman H, Thun H, Verbeek F. Potentiometric Determination of Dissociation Constants of Itaconic Acid. J Electroanal Chem. 1970;26:299-305.
21. Qiang ZM, Adams C. Potentiometric determination of acid dissociation constants (pK(a)) for human and veterinary antibiotics. Water Res. 2004;38:2874-2890.
22. Roda G, Dallanoce C, Grazioso G, Liberti V, De Amici M. Determination of Acid Dissociation Constants of Compounds Active at Neuronal Nicotinic Acetylcholine Receptors by Means of Electrophoretic and Potentiometric Techniques. Anal Sci. 2010;26:51-54.
23. Mirrlees MS, Moulton SJ, Murphy CT, Taylor PJ. Direct measurement of octanol-water partition coefficients by high-pressure liquid chromatography. J Med Chem. 1976;19:615-619.
24. Haky JE, Young AM. Evaluation of a simple HPLC correlation method for the estimation of the octanol-water partition coefficients of organic compounds. J Liq Chromatogr. 1984;7:675-689.
25. Kaliszan R, Haber P, Baczek T, Siluk D. Gradient HPLC in the determination of drug lipophilicity and acidity. Pure Appl Chem. 2001;73:1465-1475.
26. Yamana T, Tsuji A, Miyamoto E, Kubo O. Novel method for determination of partition coefficients of penicillins and cephalosporins by high pressure liquid chromatography. J Pharm Sci. 1977;66:747-749.
27. Wiczling P, Kawczak P, Nasal A, Kaliszan R. Simultaneous determination of p K a and lipophilicity by gradient RP HPLC. Anal Chem. 2006;78:239-249.
28. Singh S, Sharda N, Mahajan L. Spectrophotometric determination of nimesulide through ion-pair complex formation with hexadecyltrimethylammonium bromide. Int J Pharm. 1999;176:261-264.
29. Völgyi G, Ruiz R, Box K, Comer J, Bosch E, Takács-Novák K. Potentiometric and spectrophotometric pKa determination of water-insoluble compounds: validation study in a new cosolvent system. Anal Chim Acta. 2007;583:418-428.
30. Cleveland Jr J, Benko M, Gluck S, Walbroehl Y. Automated p< i> K</ i>< sub> a</sub> determination at low solute concentrations by capillary electrophoresis. J Chromatogr A. 1993;652:301-308.
31. Hong H, Wang L, Zou G. Retention in RP-HPLC: Lipophilicity determination of substituted biphenyls by reversed-phase high performance liquid chromatography. J Liq Chromatogr Relat Technol. 1997;20:3029-3037.
32. Markuszewski MJ, Wiczling P, Kaliszan R. High-throughput evaluation of lipophilicity and acidity by new gradient HPLC methods. Comb Chem High Throughput Screen. 2004;7:281-289.
33. Kocak E, Celebier M, Altinoz S. Validation of spectrophotometric method to quantify varenicline content in tablets. Asian J Chem. 2013;25:1845-1848.
34. Braumann T. Determination of hydrophobic parameters by reversed-phase liquid chromatography: theory, experimental techniques, and

application in studies on quantitative structure-activity relationships. J Chromatogr A. 1986;373:191-225.

35. Celik H, Buyukaga M, Celebier M, Turkoz Acar E, Baymak MS, Gokhan-Kelekci N, Palaska E, Erdoğan H. Determination of pKa values of some benzoxazoline derivatives and the structure-activity relationship. J Chem Eng Data. 2013;58:1589-1596.
36. Demiralay EC, Alsancak G, Ozkan SA. Determination of pKa values of nonsteroidal antiinflammatory drug-oxicams by RP-HPLC and their analysis in pharmaceutical dosage forms. J Sep Sci. 2009;32:2928-2936.
37. Wiczling P, Kawczak P, Nasal A, Kaliszan R. Simultaneous determination of pKa and lipophilicity by gradient RP HPLC. Anal Chem. 2006;78:239-249.
38. Royal Society of Chemistry, Learn Chemistry, Partition and distribution coefficients Available from: http://www.rsc.org/learn-chemistry/resource/

Turk J Pharm Sci 2020;17(5):542-548
DOI: 10.4274/tjps.galenos.2019.99896

ORIGINAL ARTICLE

Investigation of Pectin-Hydroxypropyl Methylcellulose-Coated Floating Beads for Pulsatile Release of Piroxicam

Pektin-Hidroksipropil Metilselüloz Kaplı Yüzer Mikro Küreciklerin Piroksikamın Pulsatil Salımı Açısından Araştırılması

Dipali KAMBLE, Dilesh SINGHAVI*, Shrikant TAPADIA, Shagufta KHAN

Borgaon (Meghe) Institute of Pharmaceutical Education and Research, Wardha, Maharashtra, India

ABSTRACT

Objectives: The aim of the present study was to prepare pectin-hydroxypropyl methylcellulose-coated floating beads for pulsatile release of piroxicam in the treatment of early morning inflammation.

Materials and Methods: Piroxicam-loaded beads were prepared from sodium alginate and hydroxypropyl methylcellulose (HPMC) in different concentrations of calcium carbonate using the ionotropic gelation method. In order to avoid drug release in the upper part of the gastrointestinal tract, the beads were coated with a pectin-HPMC layer using the dip coating method. Size analysis and encapsulation efficiency, drug loading, *in vitro* release, swelling behavior, and surface morphology studies of the beads were carried out.

Results: The *in vitro* release study revealed that the pectin-HPMC coating of the beads prevented the release of the drug in an acidic medium and provided pulsed release of the drug after a lag time. Formulation CF4 (containing calcium carbonate in the ratio 3:4 with respect to sodium alginate) exhibited pulsed release of 95.55% at the end of 7 h in phosphate buffer, which was after the desired lag time of 6 h.

Conclusion: The study revealed that optimized floating pulsatile beads coated with pectin-HPMC can efficiently retain piroxicam in an acidic medium and that there is pulsed release in an alkaline medium after a lag time. It also showed that the beads prepared can potentially be used for chronotherapeutic treatment of the disease associated with early morning inflammation.

Key words: Beads, floating, hydroxypropyl methylcellulose, pectin, pulsatile

ÖZ

Amaç: Bu çalışmanın amacı, sabah erken enflamasyonun tedavisinde kullanılmak üzere pulsatil piroksikam salımı yapan pektin-hidroksipropil metilselüloz kaplı yüzer mikro küreciklerin hazırlanmasıdır.

Gereç ve Yöntemler: Piroksikam yüklü mikroküreler, iyonotropik jelleştirme yöntemi kullanılarak kalsiyum karbonatın farklı konsantrasyonları içinde sodyum aljinat ve hidroksipropil metilselülozdan (HPMC) hazırlandı. Gastrointestinal sistemin üst kısmında ilaç salımını önlemek için mikro küreler daldırmalı kaplama yöntemi kullanılarak pektin-HPMC tabakası ile kaplandı. Mikrokürelerin boyut analizi ve enkapsülasyon verimi, ilaç yükleme, *in vitro* salım, şişme davranışı ve yüzey morfolojisi çalışmaları yapılmıştır.

Bulgular: *İn vitro* salım çalışması, mikrokürelerin pektin-HPMC kaplamasının ilacın asidik ortamda salınmasını önlediğini ve bir gecikme süresinden sonra ilacın pulsatil salımını sağladığını ortaya koymuştur. Formülasyon CF4 (sodyum alginata göre 3:4 oranında kalsiyum karbonat içerir), istenen 6 saatlik gecikme süresinden sonra fosfat tamponunda 7 saatin sonunda%95,55'lik pulsatil salım sergilediği bulunmuştur.

Sonuç: Çalışma, pektin-HPMC ile kaplanmış, optimize edilmiş yüzen pulsatil mikrokürelerin, piroksikam etken maddesinin asidik ortamda koruyarak tutabildiğini ve bir gecikme süresinden sonra alkali ortamda pulsatil salım yaptığını ortaya koymuştur. Ayrıca, hazırlanan boncukların potansiyel olarak sabah erken iltihaplanma ile bağlantılı hastalığın kronoterapötik tedavisi için kullanılabileceğini gösterdi.

Anahtar kelimeler: Mikroküreler, hidroksipropil metilselüloz, pektin, pulsatil

*Correspondence: **E-mail:** dileshsinghavi@rediffmail.com, **Phone:** 07152240284 **ORCID-ID:** orcid.org/0000-0002-2544-7226
Received: 03.06.2019, **Accepted:** 05.09.2019

INTRODUCTION

Drug delivery systems based on circadian variations are gaining much attention.[1] Several diseases treated by chronotherapeutics, such as asthma, hypertension, arthritis, and peptic ulcers, require an instantaneous and complete release of a drug after a scheduled time for effective action. Pulsatile drug delivery systems are developed to deliver drugs at the right time, in the right amount, and at the right site of action and thus improve patient compliance.[2] Time-controlled and site-specific drug delivery systems must be programmed such that they can be administered at bedtime and the drugs are released rapidly when the symptoms worsen. Pulsatile drug delivery systems have a short residence time in the stomach although they release drugs after a certain lag time. Different approaches have been developed to improve the retention time and bioavailability of drugs in the gastrointestinal tract (GIT), such as intragastric floating formulations, magnetic formulations, extensible or swellable formulations, and superporous hydrogel gel formulations.[3] Multiple-unit dosage forms have various advantages over monolithic-type dosage forms in reducing intersubject and intrasubject variabilities of transit due to the all-or-nothing emptying process. Various approaches have been used to impart buoyancy to multiple-unit dosage forms. These involve effervescent or noneffervescent systems.[4,5] Jagdale et al.[6] developed press-coated floating pulsatile tablets of lisinopril for the treatment of hypertension. Gadad et al.[7] formulated hollow multiparticulate floating formulations using low-methoxy pectin (LM-PC) and gellan gum as polymers for site- and time-specific delivery of antihypertensive drugs.

The aim of the present investigation was to design and evaluate floating pulsatile beads of piroxicam (PX). LM-PC can be used as a coating material to avoid drug release in an acidic medium. LM-PC has a strong coating film-forming property, but it is highly soluble in water. Due to this water solubility, it cannot be used to prevent the release of PX to a great extent in the upper GIT. Absorption of water may lead to weakening of the rigid gel structure of an LM-PC coating. The use of hydroxylpropyl methylcellulose (HPMC) E50 LV along with LM-PC not only maintains the gel structure but also gives strength and better coating properties.[8,9] PX was incorporated in sodium alginate (SA) and HPMC E50 LV polymeric membrane along with a gas-forming agent (calcium carbonate) so that the beads would remain buoyant in the stomach for a longer duration. The addition of LM-PC to the HPMC E50 LV coating layer to reduce the release of PX from floating pulsatile beads in an acidic medium is reported for the first time in the present work. The prepared beads were coated with LM-PC-HPMC E50 LV to prevent drug release in the upper portion of the GIT. The prepared beads were analyzed in terms of size, swelling and erosion, drug loading, encapsulation efficiency, floating properties, and *in vitro* drug release. Fourier transform infrared spectroscopy was carried out and their surface morphology was studied.

MATERIALS AND METHODS

Materials

PX was a gift sample from Apex Health Care Ltd (Gujarat). SA, HPMC K15M, LM-PC, HPMC E50 LV, and calcium chloride were obtained from LOBA Chemical Pvt Ltd (Mumbai). All other chemicals were of analytical grade.

Selection of polymer combinations

Nine formulations were made using the ionotropic gelation method with SA and different polymers (xanthan gum, HPMC K100 M, and HPMC K15 M) in different ratios, keeping total polymer weight constant. The concentrations of the drug, crosslinking agent (2% w/v calcium chloride solution in 1% v/v acetic acid aqueous solution), and floating agent were maintained constant, as shown in Table 1. The beads were observed and a promising polymer ratio was selected visually.

Effect of concentration of calcium chloride on formation of beads

The polymers selected from a previous study, HPMC K15 M and SA, were weighed accurately in the ratio 9.3:0.7. The HPMC

Table 1. Preliminary selection of polymer combinations and ratios for preparation of beads

Serial number	Polymer	Concentration	Crosslinking solution	Observation
1	Sodium alginate:xanthan gum	8:2	3% w/v calcium chloride solution in 1% v/v acetic acid	Formation of highly viscous solution
		9:1		Less viscous but not passable through needle
		9.5:0.5		Non-spherical beads and does not float more than 20 min
2	Sodium alginate:HPMC K100 M	9:1		Highly viscous solution
		9.5:0.5		Not passable through needle
		7:1		Irregular shaped beads
		7.5:0.5		Spherical beads but does not have desired floating time
3	Sodium alginate:HPMC K15 M	8:2		Highly viscous solution
		9:1		Formation of rigid beads
		9.3:0.7		Spherical beads with desired floating time

HPMC: Hydroxpropyl methylcellulose

K15 M was soaked overnight in deionized water and the SA was dissolved in it. A syringe with a 23G needle was used to extrude the resultant solution into 50 mL of a crosslinking solution containing different concentrations of calcium chloride (2%, 3%, and 4% w/v). The effect of concentration of calcium chloride on the formation of beads was observed visually. The polymer combination of SA:HPMC K15 M in the ratio 9.3:0.7 and a 3% calcium chloride crosslinking solution were selected for further studies.

Preparation of PX-loaded floating pulsatile beads[10]

PX-loaded beads were prepared using the ionotropic gelation method. An aqueous polymeric solution (10% w/v) of SA and HPMC K15 M (in the ratio 9.3:0.7) was prepared using deionized water. PX was dispersed uniformly using a magnetic stirrer running at a speed of 150 rpm. Calcium carbonate at different concentrations was added to this mixture as shown in Table 2, and the resulting dispersion was sonicated for 15 min in a sonicator to remove any air bubbles that formed during the mixing process. The prepared dispersion was extruded using a 23G needle and syringed into a crosslinking solution (3% w/v calcium chloride solution in deionized water containing 1% v/v acetic acid). The loosely formed beads were cured by stirring at 150±5 rpm for 15 min. The prepared beads were separated by filtration, washed three times with deionized water, and subsequently dried at room temperature.

Coating of floating pulsatile beads

Film-forming study[10,11]

The solvent casting method was used to prepare films. LM-PC (2% w/v) and HPMC E50 LV (0.1% w/v) were dissolved in deionized water and allowed to stand and swell. A plasticizer (polyethylene glycol 600/0.1% v/v) was added dropwise so that a homogeneous solution was achieved. The solution was kept undisturbed for some time to allow air bubbles to escape. The solution was poured into a petri dish. The petri dish was maintained at 40 °C for 24 h to achieve evaporation in a controlled manner. The film-forming ability, physical appearance, and texture of the coating solution were evaluated visually.

Procedure for coating beads

PX-loaded uncoated beads were dip coated uniformly in coating solution containing LM-PC (2% w/v) and HPMC E50 LV (0.1% w/v) for 3 min. The coated beads were dried at room temperature and kept in an airtight container for further use.

Encapsulation efficiency and drug-loading efficiency[12-14]

Accurately weighed PX-loaded beads (50 g) from each batch were crushed by mortar and pestle. The crushed beads were added to 50 mL of phosphate buffer (pH 7.4). The resulting solution was stirred using a magnetic stirrer for 24 h and filtered through Whatman filter paper 42. The filtered solution was diluted sufficiently, and the absorbance was read at 353.80 nm with phosphate buffer (pH 7.4) as the blank solution. The percent encapsulation efficiency and drug loading were determined using the following equations:

$$\% \text{ encapsulation efficiency} = \frac{\text{Actual drug content}}{\text{Theoretical drug content}} \times 100 \quad (1)$$

$$\% \text{ drug loading} = \frac{\text{Weight of drug in beads}}{\text{Weight of drug-loaded beads}} \times 100 \quad (2)$$

Floating property study[12,13,15]

Floating properties of the beads, such as the total floating time and floating lag time, were determined by placing them (n=50) in a USP type II Dissolution Apparatus (model no. DA-3, Veego Scientific Devices, Mumbai, India) filled with 500 mL of

Table 2. Composition, encapsulation efficiency, percent drug loading, particle size, and floating properties of different batches of beads

Formulation	Composition of drug polymer dispersion (10 mL)				Crosslinking solution (50 mL)		Encapsulation efficiency* (% w/w)	Percent drug loading* (% w/w)	Particle size** (mm)	Floating study	
	Drug (mg)	SA (mg)	HPMC k15 M (mg)	Calcium carbonate (mg)	$CaCl_2$ (% w/v)	Acetic acid (% v/v)				Floating property	Floating duration* (hours)
F1	20	465	35	0	3	1	98.56±0.12	28.15±0.15	1.348±0.012	+ -	3.20±0.30
F2	20	465	35	116.25	3	1	96.73±0.13	23.70±0.22	1.413±0.014	+ -	4.30±0.07
F3	20	465	35	232.5	3	1	95.84±0.11	20.48±0.18	1.521±0.018	+ +	5.18±0.03
F4	20	465	35	348	3	1	95.03±0.28	18.05±0.15	1.542±0.015	+ +	6.15±0.06
F5	20	465	35	465	3	1	90.12±0.23	15.30±0.13	1.576±0.011	+ +	12

*Mean ± SD (n=3), **Mean ± SD (n=20), + + indicates better floating property (45-50 beads floated), + - moderate floating property (20-25 beads floated)
SA: Sodium alginate, HPMC: Hydroxypropyl methylcellulose, SD: Standard deviation

pH 1.2 buffer. The paddle speed was kept at 100 rpm and the temperature was maintained at 37±0.5 °C. The buoyancy of the beads was observed by visual inspection.

Particle size analysis[12-14]

An imaging system (Biowizard Software 4.1) was used to determine the particle size of the beads. The diameters of 20 beads were determined.

In vitro drug release[13-15]

The release profiles of the PX from the different formulations were obtained using a USP type I Dissolution Apparatus operated at 100 rpm. Prepared beads equivalent to 20 mg of PX were kept in a basket that was inserted in 500 mL of the dissolution medium at 37±0.5 °C. A release study was carried out with a pH 1.2 buffer for the first 2 h and then with a phosphate buffer (pH 7.4) for 10 h. Samples were withdrawn at predetermined time periods and passed through Whatman filter paper. The samples were then diluted sufficiently and analyzed spectrophotometrically at 335 nm and 353.8 nm in a pH 1.2 buffer and pH 7.4 phosphate buffer, respectively. The amount of drug release was determined from the standard calibration curve of PX in both media. The calibration curve in both media obeyed Beer-Lambert's law within the concentration range of 0-20 (µg/mL) with a correlation coefficient (R^2) of 0.999.

Swelling study[16]

Accurately weighed beads (40 mg) were placed in the basket of a USP type I Dissolution Apparatus containing 500 mL of a buffer solution. Considering the floating characteristics of the beads, the swelling study was carried out in a pH 1.2 buffer solution and then in a pH 7.4 phosphate buffer maintained at 37±0.5 °C with the basket being rotated at 100 rpm. The baskets were withdrawn at predetermined intervals, blotted to remove excess water, and immediately weighed. The swelling index of the beads was calculated as the relative weight gain/loss of the beads according to the following equation:

% swelling index = (3)

where

Ws = weight of swollen beads

Wd = weight of dried beads

The change in swelling with time was noted.

Scanning electron microscopy[17]

The external morphology of the prepared beads (size, shape, and surface) was studied using scanning electron microscopy. The beads of the optimized batch (CF4) were kept on double-sided copper conductive tape (NEM Nisshin EM Co Ltd) fixed on aluminum stubs. The beads were then coated by sputtering with a thin layer of gold in a vacuum for 45 s at I=20 mA using a coating unit (Cressington 108 auto sputter coater, UK) to make them electrically conductive. They were then analyzed using a scanning electron microscope (Supra 5 Carl Zeiss, Germany) operated at 5 kV.

Stability study[18,19]

Stability was studied by maintaining the optimized formulation at 40±0.5 °C and 75±5% RH for 90 days. The samples were tested for drug content after 0, 30, 60, and 90 days. The formulation was analyzed for percent drug loading and floating ability. The physical appearance of the formulation was noted and an *in vitro* release study was carried out.

Statistical analysis[20]

All the data were represented as the mean ± standard deviation. The drug entrapment efficiency, floating duration, and mean particle size were compared using One-Way ANOVA, and the difference between the means for significance was observed using Tukey's HSD post-hoc test (GraphPad Prism InStat software).

RESULTS AND DISCUSSION

Crosslinking of the alginate with the divalent calcium ion is responsible for the formation of beads.[21] Carbon dioxide is liberated as gas bubbles in the chemical reaction between calcium carbonate and acetic acid.[12] This was responsible for the floating of the beads.

The percent encapsulation efficiency of the PX-loaded uncoated formulations was in the range from 98.56±0.12% to 90.12±0.23% w/w (Table 2). The percent drug loading of the uncoated formulations F1-F5 was in the range from 28.15±0.15% to 15.30±0.13% w/w. The percent drug loading of the coated formulations CF1-CF5 was in the range from 28.15±0.15% to 14.20±0.13% w/w. A reduction in percent encapsulation efficiency and percent drug loading was observed due to an increase in the proportion of the gas-forming agent. The increased formation of gas led to a reduction in extent of the rigid structure of the beads due to increased pore density and diameter. This results in the leaching of the drug during the formation of the beads, which leads to reduced entrapment of drug molecules.[1,12-15] No significant difference was observed ($p>0.05$) in the percent drug loading between the coated and uncoated formulations.

Carbon dioxide gas was generated due to the reaction between the gas-forming agent, i.e. calcium carbonate, and the acidic medium. The generated gas was entrapped in a polymeric network of SA and HPMC K15M and imparted buoyancy to the beads. The floating properties of the uncoated beads and coated beads are shown in Tables 2 and 3. As the amount of gas-forming agent present in the formulation during the formation of beads was increased, the floating duration increased. The increased porosity of the beads might be due to the generation of greater amounts of gases, which led to a reduction in the density of beads, resulting in the improved floating duration. The reduced proportion of the high-density SA in the beads also led to the formation of lighter beads. The paddle speed does not affect the floating properties of the beads. The beads were able to float until disintegration occurred. Thus, in both the coated and uncoated formulations, as the concentration of the gas-forming agent was increased, the porosity was increased, causing them to remain buoyant for a longer duration.[12-15,22] The differences between the floating duration of the coated and uncoated formulations were insignificant ($p>0.05$).

Table 3. Percent drug loading, particle size, and floating properties of different batches of coated beads

Formulation	Percent drug loading (% w/w)	Particle size** (mm)	Floating study	
			Floating property	Floating duration* (hours)
CF1	28.15±0.15	1.431±0.014	+ -	3.31±0.03
CF2	22.80±0.22	1.587±0.047	+ -	4.42±0.02
CF3	19.60±0.18	1.611±0.033	+ +	5.19±0.01
CF4	18.01±0.15	1.640±0.042	+ +	6.12±0.01
CF5	14.20±0.13	1.661±0.061	+ +	12.19±0.01

*Mean ± SD (n=3), **Mean ± SD (n=20), + + indicates better floating property (45-50 beads floated), + - moderate floating property (20-25 beads floated)
SD: Standard deviation

The mean particle size of the formulations F1-F5 was in the range from 1.348±0.012 mm to 1.576±0.011 mm, while that of the coated formulations was in the range from 1.431±0.014 mm to 1.661±0.061 mm. From the results (Table 2), it may be seen that increasing the amount of gas-forming agent led to an increase in the bead diameter due to increases in the number and size of pores. Again, the formation of more gas resulted in a less dense bead structure of greater size. The beads of batch F5, with a higher concentration of gas-forming agent, were not spherical, in contrast to those of batch F1, containing no gas-forming agent. This was due to expansion of carbon dioxide, which led to a rapid bursting of walls before they had hardened sufficiently.[1,12-14] A significant difference ($p<0.05$) was observed in particle size between the uncoated and coated formulations.

It was observed that there was an appreciably high drug release from uncoated beads in an acidic medium (Figure 1), which is not desirable. This might be because a lower concentration of SA and a higher concentration of the gas-forming agent led to pore formation and faster release of drug. The increased floating duration also led to an increase in the duration over which the drug was released in an acidic medium. Beads were dip coated with a layer of LM-PC and HPMC E50 LV to reduce the release of the drug in acidic media. Formulation CF4 gave the desired lag time of 6 h in acidic medium and rapid release (95.55% at the end of 7 h) in the phosphate buffer. In contrast, formulations CF1 (lag time 3 h), CF2 (lag time 4 h), CF3 (lag time 5 h), and CF5 (lag time 12 h) gave cumulative releases of 88.54% in 4 h, 93.15% in 5 h, 93.75% in 6 h, and 5% in 12 h, respectively (Figure 2). It was observed that the release of drug from the coated beads in acidic medium was significantly reduced compared with uncoated beads. The rigid gel structure of the PC and HPMC E50 LV coating led to a reduction in the diffusion of molecules from the inner core of the beads to an acidic medium. When the beads were transferred to the phosphate buffer of pH 7.4 after the lag time, pulsed release was observed because of rapid swelling and gel relaxation of pectin in the alkaline pH.[1,13-15,21] As the floating duration of formulations F5 and CF5 was more than 12 h, their lag time of release was also more than 12 h. Formulations F5 and CF5 remained in acidic medium throughout the dissolution study, leading to very slow release rates.

The percent swelling study showed that formulations CF1-CF5 showed less swelling in the pH 1.2 HCl buffer compared with a pH 7.4 phosphate buffer (Figure 3). In an acidic pH, pectin remains protonated in an insoluble form, with reduced swelling. The concentration of the gas-forming agent also acts as a barrier to the absorption of water. From the floating characteristics, formulation CF1, with no gas-forming agent, was found to have the maximum swelling. The swelling decreased with increasing concentration of gas-forming agent due to the formation of void spaces in the beads that retained the maximum volume of solvent. Thus, formulation CF5 showed the minimum floating-dependent swelling because of the high concentration of the gas-forming agent.

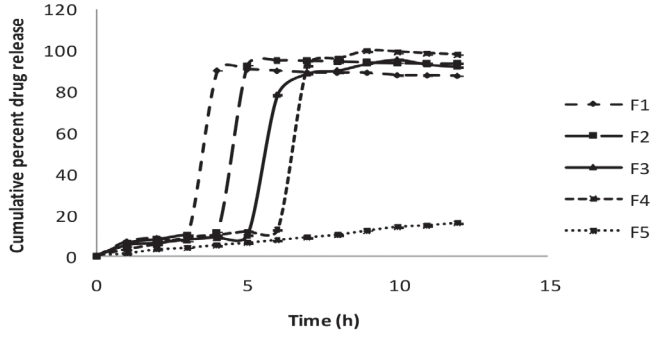

Figure 1. Cumulative amounts of PX released from beads of formulations F1, F2, F3, F4, and F5 (mean ± SD, n=3)

SD: Standard deviation, PX: Piroxicam

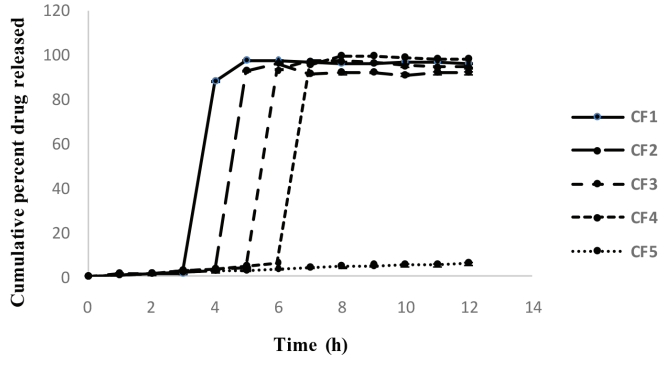

Figure 2. Cumulative amounts of PX released from beads of formulations CF1, CF2, CF3, CF4, and CF5 (mean ± SD, n=3)

SD: Standard deviation, PX: Piroxicam

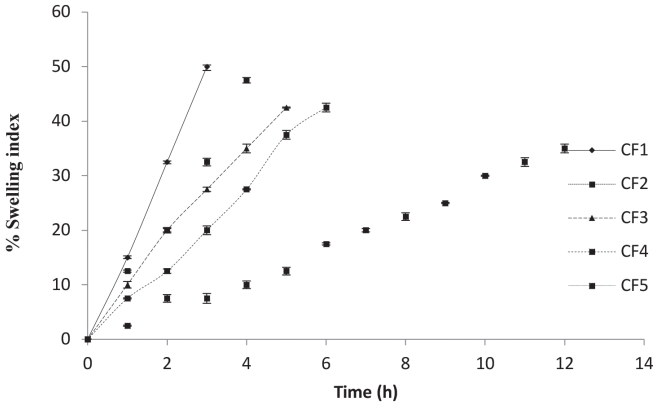

Figure 3. Percent swelling index of beads of formulations CF1, CF2, CF3, CF4, and CF5 (mean ± SD, n=3)

SD: Standard deviation

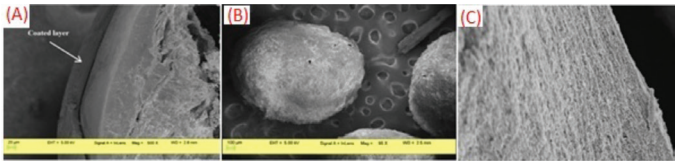

Figure 4. Morphological characterization of formulation CF4 using scanning electron microscopy A) showing coating layer, B) showing the roundness, and C) surface morphology

The uncoated beads of all the optimized formulations were seen to be almost spherical in the scanning electron photomicrographs (Figure 4). The beads with higher concentrations of the gas-forming agent were porous, rough, and spherical. The high porosity of the beads was due to the rapid evolution of carbon dioxide during bead formation as the number of pores formed is directly related to the concentration of the gas-forming agent present.[15]

After exposure to extreme conditions, formulation CF4 was analyzed for physical appearance, percent drug loading, floating ability, and *in vitro* drug release at an interval of 1 month. No significant changes ($p>0.01$) were observed in the physical appearance, percent drug loading, floating ability, or *in vitro* drug release.

CONCLUSION

PX-loaded beads of SA and HPMC K15M were prepared using the ionotropic gelation method, and their performance was analyzed through *in vitro* experiments. The release of PX from uncoated beads in the acidic medium due to entry of the GI fluid through the unprotected polymeric matrix was observed. Therefore, the beads were coated with a polymeric film of LM-PC and HPMC E50 LV. Addition of HPMC E15 LV decreased the rupturing of the film and reduced the extent of premature drug release in the upper GI tract. Overall, the buoyant beads exhibited gastroretention and provided a lag phase, followed by pulsatile drug release. These would be beneficial for treating the inflammation associated with chronotherapeutic diseases. Addition of HPMC E50 LV increased the flexibility, gelation, transparency, and mechanical properties of the LM PC films. From the results it can be concluded that the PC: HPMC E50 LV-coated floating pulsatile beads can be used to treat the early morning inflammatory conditions in rheumatoid arthritis.

Conflicts of interest: No conflict of interest was declared by the authors. The authors alone are responsible for the content and writing of the paper.

REFERENCES

1. Badve S, Sher P, Korde A, Pawar A. Development of hollow/porous calcium pectinate beads for floating pulsatile drug delivery. Eur J Pharm Biopharm. 2007;65:85-93.
2. Nief RA, Sulaiman HT, Jabir SA. Pulsatile drug delivery system-A review article. J Pharm Res. 2018;12:764-770.
3. Yao H, Yao H, Zhu J, Yu J, Zhang L. Preparation and evaluation of a novel gastric floating alginate/poloxamer inner-porous beads using foam solution. Int J Pharm. 2012;422:211-219.
4. Hamadani J, Moes AJ, Amighi K. Development and *in vitro* evaluation of a novel floating multiple unit dosage form obtained by melt pelletization. Int J Pharm. 2006;322:96-103.
5. Sungthongjeen S, Paeratakul O, Limmatvapirat S, Puttipipatkhachorn S. Preparation and *in vitro* evaluation of a multiple-unit floating drug delivery system based on gas formation technique. Int J Pharm. 2006;324:136-143.
6. Jagdale S, Suryawanshi V, Pandya S, Kuchekar B, Chabukswar A. Development of press-coated, floating-pulsatile drug delivery of lisinopril. Sci Pharm. 2014;82:423-440.
7. Gadad AP, Reddy AD, Dandagi PM, Masthiholimath VS. Design and characterization of hollow/porous floating beads of captopril for pulsatile drug delivery. Asian J Pharm. 2014;6:137-143.
8. Sureshkumar R, Munikumar, Ganesh GNK, Jawahar N, Nagasamyvenkatesh D, Senthil V, Raju L, Samantha MK. Formulation and evaluation of pectin-hydroxypropyl methylcellulose coated curcumin pellets for colon delivery. Asian J Pharm. 2009;138-142.
9. Turkoglu M, Ugurlu T. *In vitro* evaluation of pectin-HPMC compression coated 5-aminosalicylic acid tablets for colonic delivery. Eur J Pharm Biopharm. 2002; 53:65-73.
10. Newton AMJ, Prabakaran L, Jayaveera KN. Pectin-HPMC E15 LV Vs pH sensitive polymer coating film for delayed drug delivery to the colon-A comparison of two dissolution models to assess colonic targeting performance *in-vitro.* Int J Appl Res Nat Prod. 2012;5:1-16.
11. Hirpara F, Debnath SK, Saisivam S. Optimization and screening of different film forming polymers and plasticizers in fast dissolving sublingual film. Int J Pharm Pharm Sci. 2014;6:41-42.
12. Shishu, Gupta N, Aggrawal N. Stomach specific drug delivery of %-flurouracil using floating alginate beads. AAPS Pharm Sci Tech. 2007;8:E143-E149.
13. Somani VG, Shahi SR, Udavant YK, Atram SC, Satpute R, Shinde NM. A floating pulsatile drug delivery system based on hollow calcium pectinate beads. Asian J Pharmacol. 2009;120-124.
14. Gadad AP, Reddy AD, Dandagi PM, Masthiholimath VS. Design and characterization of hollow/porous floating beads of captopril for pulsatile drug delivery. Asian J Pharmacol. 2012:6:137-143.
15. Gadad A, Patil M, Naduvinamani S, Mastiholimath V, Dandagi P, Kulkarni A. Sodium alginate polymeric floating beads for the delivery of

cefpodoxime proxetil. J Appl Polym Sci. 2009;114:1921-1926.

16. Lamoudi L, Chaumeil JC, Daoud K. Swelling, erosion and drug release characteristics of sodium diclofenac from heterogenous matrix tablet. J Drug Deliv Sci Technol. 2016;31:93-100.
17. Patel N, Lalwani D, Gollmer S, Injeti E, Sari Y, Nesamony J. Development and evaluation of calcium alginate based oral cefitriaxone sodium formulation. Prog Biomatter. 2016;:117-133.
18. Gadad AP, Reddy AD, Dandagi PM, Masthiholimath VS. Design and characterization of hollow/porous floating beads of captopril for pulsatile drug delivery. Asian J Pharm. 2012;6:137-143.
19. Rathnanand M, Pannalal S. Formulation and *in vitro* evaluation of floating pulsatile tablets of nizatidine for chronotherapy of ulcers. J Pharm Res. 2011;4:1388-1390.
20. Patel MA, Aboughaly MH, Schryer-Praga JV, Chadwick K. The effect of ionotropic gelation residence time on alginate cross-linking and properties. Carbohyd Polym. 2017;155:362-371.
21. Bhattarai RS, Dhandapani NV, Shrestha A. Drug delivery using alginate and chitosan beads-An overview. Chron Young Sci. 2011;2:192-196.
22. Bajpai SK, Tankhiwale R. Preparation, characterization and preliminary calcium release study of floating sodium alginate/dextran-based hydrogel. Part I. Polym Int. 2008;57:57-65.

Turk J Pharm Sci 2020;17(5):549-554
DOI: 10.4274/tjps.galenos.2019.71602

ORIGINAL ARTICLE

Citral Protects Human Endothelial Cells Against Hydrogen Peroxide-induced Oxidative Stress

Sitral, İnsan Endotel Hücrelerini Hidrojen Peroksitin Neden Olduğu Oksidatif Strese Karşı Korur

Leila SAFAEIAN[1]*, Seyed Ebrahim SAJJADI[2], Hossein MONTAZERI[1], Farzaneh OHADI[3], Shaghayegh JAVANMARD[4]

[1]Isfahan University of Medical Sciences, School of Pharmacy and Pharmaceutical Sciences, Department of Pharmacology and Toxicology, Isfahan Pharmaceutical Sciences Research Center, Isfahan, Iran
[2]Isfahan University of Medical Sciences, School of Pharmacy and Pharmaceutical Sciences, Department of Pharmacognosy, Isfahan, Iran
[3]Isfahan University of Medical Sciences, Vice Chancellery for Food and Drugs, Office for Drug, Food, Cosmetics and hygienic Product's QC Laboratory, Isfahan, Iran
[4]Isfahan University of Medical Sciences, Cardiovascular Research Institute, Applied Physiology Research Center, Isfahan, Iran

ABSTRACT

Objectives: Oxidative stress plays a major role in endothelial dysfunction. Citral is a monoterpene aldehyde with antioxidant properties. This study aimed to investigate the effect of citral on human umbilical vein endothelial cells (HUVECs) under hydrogen peroxide (H_2O_2)-induced oxidative stress.

Materials and Methods: The cells were treated with citral (0.625-10 µg/mL) for 24 h before exposure to H_2O_2 (0.5 mM, 2 h). Cell viability was evaluated by 3-(4,5-dimethylthiazol-2-yl)-2,5-diphenyl-tetrazolium bromide (MTT) assay. The hydroperoxide concentrations and ferric reducing ability of plasma (FRAP) were measured in intra- and extracellular fluids.

Results: Pretreatment of HUVECs with citral at concentrations of 5 and 10 µg/mL significantly enhanced the cell viability in H_2O_2-induced cytotoxicity. It reduced intracellular hydroperoxide levels at the concentrations of 5 and 10 µg/mL and extracellular hydroperoxide levels at the concentrations of 2.5-10 µg/mL. Pretreatment with citral significantly increased the FRAP value in intra- and extracellular fluids at the concentration range of 1.25-10 µg/mL.

Conclusion: Antioxidant and cytoprotective effects were found for citral against oxidative damage induced by H_2O_2 in human endothelial cells. However, more studies in this area are needed to assess its clinical value for prevention and treatment of cardiovascular diseases.

Key words: Citral, HUVECs, oxidative stress, antioxidant, hydrogen peroxide

ÖZ

Amaç: Oksidatif stres endotel disfonksiyonda önemli bir rol oynamaktadır. Sitral, antioksidan özelliklere sahip olan monoterpen bir aldehittir. Bu çalışma, sitralin, hidrojen peroksit (H_2O_2) kaynaklı oksidatif stres altındaki insan göbek kordonu ven endotel hücreleri (HUVEC) üzerindeki etkisini araştırmak amacı ile gerçekleştirilmiştir.

Gereç ve Yöntemler: Hücreler, H_2O_2'ye (0,5 mM, 2 saat) maruz kalmadan önce 24 saat boyunca sitral (0,625-10 µg/mL) ile muamele edildi. Hücre canlılığı, 3-(4, 5-dimetiltiazol-2-yl)-2, 5-difenil-tetrazolyum bromür deneyi ile belirlendi. Hidroperoksit yoğunluğu ve plazmadaki ferrik demir iyonu indirgeme kapasitesi (FRAP) hücre içi ve dışı sıvılarda ölçüldü.

Bulgular: HUVEC'lerin önceden sitral ile 5 ve 10 µg/mL yoğunluğunda maruz kalması, H_2O_2 kaynaklı sitotoksisitede hücre canlılığını önemli ölçüde artırdı. Bu hücre içi hidroperoksit seviyesini 5 ve 10 µg/mL yoğunluğuna ve hücre dışı hidroperoksit seviyesini ise 2,5-10 µg/mL yoğunluğuna düşürdü. Sitrale önceden maruz kalmaları, 1,25-10 µg/mL yoğunluk aralığında hücre içi ve hücre dışı sıvılarda FRAP değerini önemli ölçüde artırdı.

Sonuç: İnsan endotel hücrelerinde H_2O_2'nin neden olduğu oksidatif hasara karşı sitralin antioksidan ve sitoprotektif etkili olduğu bulundu. Ancak, kardiyovasküler hastalıkların önlenmesi ve tedavisinde klinik değeri ve yerini tespit edebilmek için bu alanda daha fazla çalışma ve deneye ihtiyaç vardır.

Anahtar kelimeler: Sitral, HUVEC'ler, oksidatif hasar, antioksidan, hidrojen peroksit

*Correspondence: **E-mail:** leila_safaeian@pharm.mui.ac.ir, **Phone:** +98 313 792 7087 **ORCID-ID:** orcid.org/0000-0002-7811-3406
Received: 24.12.2018, **Accepted:** 14.02.2019

INTRODUCTION

Cardiovascular diseases (CVDs) are the most prominent causes of death worldwide.[1] Many studies have confirmed the pivotal role of oxidative stress in the pathogenesis and progression of CVDs. Oxidative stress is a state of overproduction of free radicals and an imbalance between oxidants and antioxidants. Cellular damage and endothelial dysfunction resulting from excessive generation of reactive oxygen species (ROS) have been reported to be involved in various CVDs.[2] Superoxide anion, hydroxyl radicals, lipid radicals, and hydrogen peroxide (H_2O_2) are examples of ROS in the vascular system. ROS have a physiological role in controlling cardiovascular homeostasis by mediating diverse biological responses such as induction of host defense genes, activation of transcription factors, phosphorylation of kinases, and mobilization of ion transport systems.[3,4] Besides their physiological role, ROS also play an important pathophysiological role in inflammation, hypertrophy, proliferation, apoptosis, migration, fibrosis, angiogenesis, vascular remodeling, and endothelial dysfunction.[5,6]

Natural antioxidants are widely distributed in fruits, vegetables, and medicinal plants, produced via the secondary metabolisms and possessing various biological activities.[7,8] In many investigations, herbal antioxidants and bioactive plant constituents have been associated with beneficial therapeutic effects and a reduction in the risk of CVDs.[9]

Citral (3,7-dimethyl-2,6-octadienal) is one of the most important natural flavoring compounds, widely used in the food, pharmaceutical, and cosmetic industries.[10] This monoterpene aldehyde also called lemonal and is a mixture of geranial (trans-citral or citral A) and neral (cis-citral or citral B).[11] Citral is present in several plants with lemon aroma such as lemongrass (*Cymbopogon citratus*) and lemon balm (*Melissa officinalis*).[12,13] This essential oil has exhibited antifungal, bactericidal, insecticidal, anticancer, analgesic, anti-inflammatory, anticonvulsant, and spasmolytic activities in pharmacological studies.[10,14] Moreover, some beneficial cardiovascular effects have been reported for citral due to its antioxidant, radical scavenging, anti-inflammatory, and vasodilatory properties.[15,16] The present study aimed to investigate the possible protective effects of citral against oxidative damage induced by H_2O_2 in human umbilical vein endothelial cells (HUVECs).

MATERIALS AND METHODS

Cell culture

HUVECs were maintained in Dulbecco's Modified Eagle's Medium in a humidified atmosphere of 5% CO_2 at 37 °C. The medium was supplemented with 10% fetal bovine serum, 100 µ/mL penicillin, and 100 µg/mL streptomycin. Citral (Sigma, Germany) was dissolved in dimethyl sulfoxide 0.8% and diluted with cell culture medium to get different concentrations as required.

Cell viability assay

The viability of HUVECs was determined by 3-(4,5-dimethylthiazol-2-yl)-2,5-diphenyl- tetrazolium bromide (MTT) assay (Bioidea Co., Tehran, Iran) for evaluation of the potential cytotoxicity of citral under normal conditions and its possible cytoprotective effect against oxidative stress.[17] In brief, the cell monolayer in exponential growth was harvested and $1.5x10^5$ cells/mL were seeded in each well of the 96-well plates. Twenty-four hours after plating, the HUVECs were treated with 0.625 to 100 µg/mL citral and incubated for an additional 24 h for assessment of the effect of citral on HUVEC proliferation under normal conditions. After washing out with butylene succinate (PBS), MTT reagent was added to each well, followed by further incubation for 3 h. Then dimethyl sulfoxide was used and the absorbance was measured at 570 nm by a microplate reader.

For evaluation of the cytoprotective effect of citral on HUVECs against H_2O_2-induced oxidative stress, the cells were pre-incubated with 0.625 to 10 µg/mL citral for 24 h and then the citral was removed from the media and the wells were washed out with PBS. After that the cells were exposed to 0.5 mM H_2O_2 for 2 h. The rest of the experiment was performed as above. The cells without any exposure to the extract or H_2O_2 were considered the negative control. The viability of treated samples was measured according to the following formula and each experiment was tested in triplicate:

Cell viability (%) = (OD test - OD blank/OD negative control - OD blank) × 100

Hydroperoxide assay

A ferrous ion oxidation by xylenol orange (FOX-1) kit (Hakiman Shargh Research Co., Isfahan, Iran) was used for evaluation of the effects of pretreatment with citral on intra- and extracellular hydroperoxide levels. In this method, hydroperoxides are detected based upon oxidation of reagent Fe^{+2} to Fe^{+3} by oxidizing agents and formation of a color complex through its binding to xylenol orange in an aqueous medium containing sorbitol.[18] Ten milliliters of supernatant of the cells or the cell lysates after being pretreated with different concentrations of citral and then exposed to H_2O_2 was mixed with 190 µL of FOX-1 reagent. After incubation for 30 min at 40 °C, the absorbance was measured at 540 nm using a microplate reader/spectrophotometer. The hydroperoxide content of the samples was estimated as H_2O_2 equivalents using a H_2O_2 standard curve.

Ferric reducing ability of plasma assay (FRAP)

The effects of citral on the intra- and extracellular FRAP was determined by a commercial kit (Hakiman Shargh Research Co., Isfahan, Iran).[19] In this assay, the total antioxidant capacity is estimated based on the reduction of ferric-tripyridyltriazine complex to ferrous form. Briefly, after pretreatment of HUVECs with different concentrations of citral and then exposure to H_2O_2, 10 µL of the supernatant of the cells or the cell lysates was added to 200 µL of FRAP reagent containing tripyridyltriazine/ferric chloride/acetate buffer. The reaction mixture was incubated for 40 min at 40 °C and absorbance was read at 570 nm using a microplate reader/spectrophotometer. The FRAP values of the samples were calculated using a standard curve of $FeSO_4x7H_2O$ concentrations and were expressed as FeII equivalents.

Statistical analysis

The data were presented as mean ± standard error of the mean. For statistical analysis, One-Way ANOVA followed by Tukey's post-hoc test was performed using SPSS version 18.0. A p value <0.05 was considered significant.

RESULTS

Effect of citral on HUVEC viability

The potential cytotoxicity of citral on HUVECs was evaluated by MTT assay. There was an inhibitory effect on HUVEC proliferation after 24 h exposure to the concentrations of 20-100 µg/mL of citral ($p<0.001$ compared with control cells) (Figure 1). Therefore, citral was used at the concentration range of 0.625-10 µg/mL for further studies.

Effect of citral on H_2O_2-induced oxidative stress

Figure 2 shows the cytoprotective effect of citral against oxidative cell death induced by H_2O_2 using an MTT assay. H_2O_2 (0.5 mM) produced a significant reduction in HUVEC viability compared with the control cells ($p<0.001$). Pretreatment with citral at the concentrations of 5 and 10 µg/mL significantly enhanced cell viability in H_2O_2-induced cytotoxicity ($p=0.005$ and $p<0.001$, respectively).

Effects of citral on hydroperoxide levels

The FOX-1 assay was performed to detect the effects of citral on intra- and extracellular hydroperoxide concentrations in HUVECs after exposure to the oxidative stress induced by H_2O_2. A significant increase in hydroperoxide production was observed in the presence of 0.5 mM H_2O_2 as compared to the untreated normal control ($p<0.001$). Incubation of HUVECs with citral significantly decreased the intracellular hydroperoxide levels at the concentrations of 5 µg/mL ($p=0.35$) and 10 µg/mL ($p=0.001$) compared to the cells treated with H_2O_2 alone (Figure 3A). Citral also caused a significant reduction in the extracellular hydroperoxide levels at the concentrations of 2.5, 5, and 10 µg/mL ($p=0.003$, $p<0.001$, and $p<0.001$, respectively) (Figure 3B).

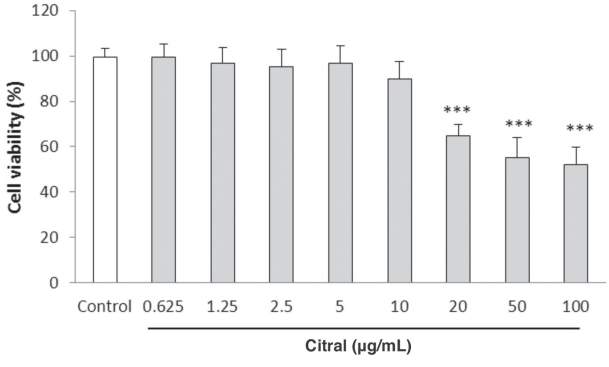

Figure 1. Effect of citral on HUVEC viability determined by MTT assay. Cells were incubated with different concentrations of citral (0.625-100 µg/mL) for 24 h. Values are means ± SEM from three independent experiments in triplicate. ***$p<0.001$ versus control (untreated cells)

HUVEC: Human umbilical vein endothelial cell, MTT: 3-(4,5-dimethylthiazol-2-yl)-2,5-diphenyl-tetrazolium bromide, SEM: Standard error of the mean

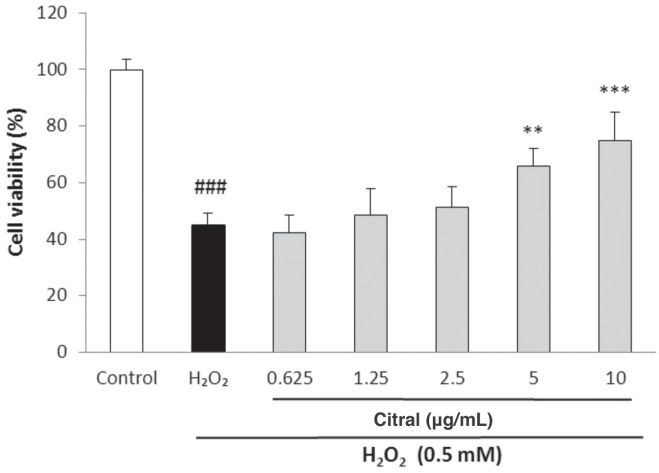

Figure 2. Effect of citral on HUVEC viability in H_2O_2-induced oxidative stress determined by MTT assay. Cells were incubated with H_2O_2 (0.5 mM, 2 h) after pretreatment with different concentrations of citral (0.625-10 µg/mL). Values are means ± SEM from three independent experiments in triplicate. ###$p<0.001$ versus control (untreated cells), **$p<0.01$ and ***$p<0.001$ versus H_2O_2 stimulated cells

HUVEC: Human umbilical vein endothelial cell, MTT: 3-(4,5-dimethylthiazol-2-yl)-2,5-diphenyl-tetrazolium bromide, SEM: Standard error of the mean

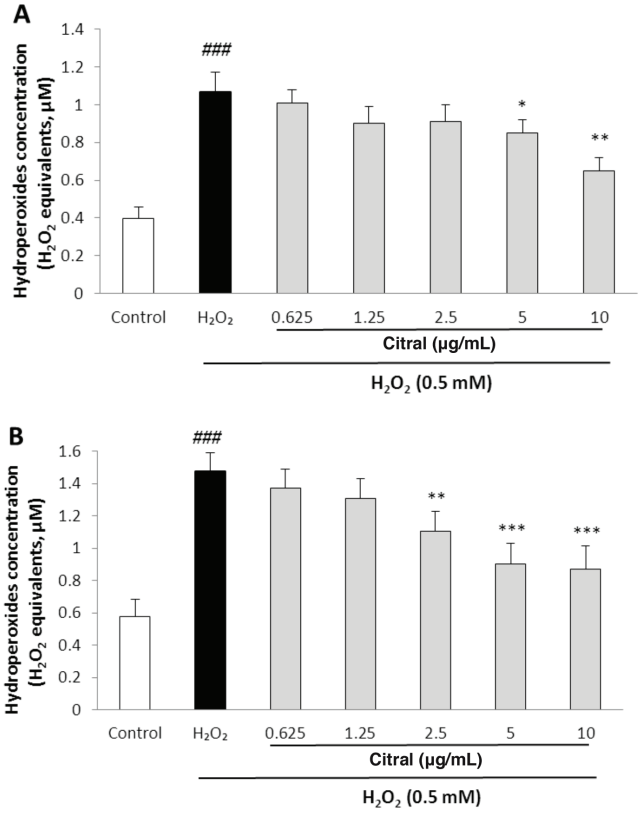

Figure 3. Effect of citral on intra- A) and extracellular B) hydroperoxide concentration in HUVECs as H_2O_2 equivalents determined by FOX-1 method. Cells were incubated with H2O2 (0.5 mM, 2 h) after pretreatment with different concentrations of citral (0.625-10 µg/mL). Values are means ± SEM from three independent experiments in triplicate. ###$p<0.001$ versus control (untreated cells), *$p<0.05$, **$p<0.01$, and ***$p<0.001$ versus H_2O_2 stimulated cells

HUVEC: Human umbilical vein endothelial cell, FOX-1: Ferrous ion oxidation by xylenol orange, SEM: Standard error of the mean

Effects of citral on FRAP value

The effect of citral on total antioxidant capacity was evaluated by FRAP assay. Exposure of HUVECs to H_2O_2 resulted in a significant decrease in the FRAP value (p=0.007). Pretreatment with citral significantly increased the FRAP value in intracellular fluids at the concentrations of 1.25, 2.5, 5, and 10 µg/mL (p=0.025, p=0.004, p=0.002, and p=0.003, respectively) (Figure 4A). It also improved the FRAP value in extracellular fluids at the concentrations of 1.25, 2.5, 5, and 10 µg/mL (p=0.016, p=0.001, p<0.001, and p<0.001, respectively) (Figure 4B).

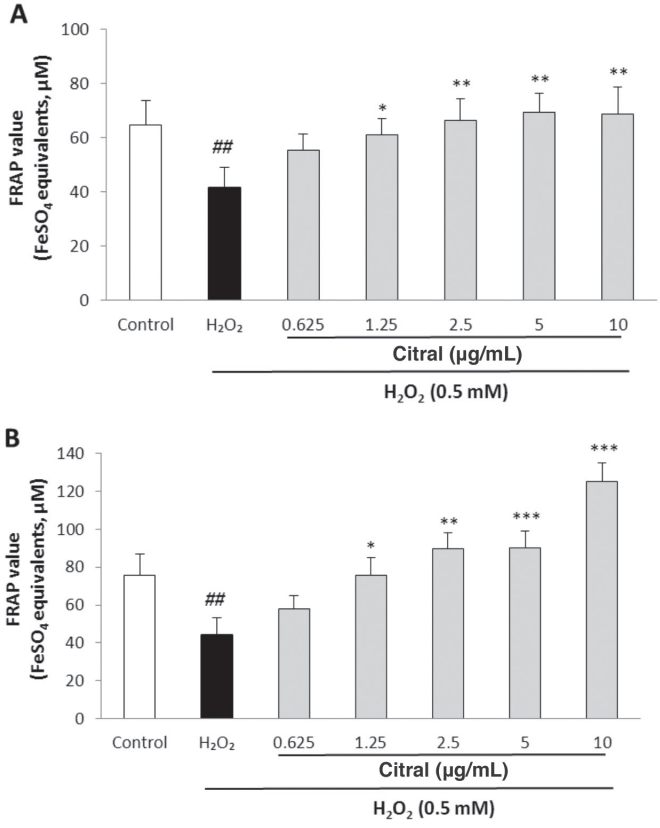

Figure 4. Effect of citral on intra- A) and extracellular B) FRAP value in HUVECs determined as ferrous sulfate equivalents. Cells were incubated with H2O2 (0.5 mM, 2 h) after pretreatment with different concentrations of citral (0.625-10 µg/mL). Values are means ± SEM from three independent experiments in triplicate. ##p<0.01 versus control (untreated cells), *p<0.05, **p<0.01, and ***p<0.001 versus H2O2 stimulated cells

FRAP: Ferric reducing ability of plasma, HUVECs: Human umbilical vein endothelial cells

DISCUSSION

The findings of the present study showed cytoprotective and antioxidant effects of citral against oxidative stress induced by H_2O_2 in HUVECs. Citral protected the cells against oxidative cell death at the concentrations of 5 and 10 µg/mL. It reduced hydroperoxide levels and increased the FRAP value in both intra- and extracellular fluid at different concentration ranges.

H_2O_2 is a stable ROS with capability of readily diffusing through the cellular membrane and plays a significant role in vascular cell signaling such as proliferation, apoptosis, and inflammation.[20] H_2O_2 as a trigger of oxidative stress in human endothelial cells has been used in many studies to provide insight into the mechanisms of CVD development. In the present study, the exposure of HUVECs to H_2O_2 caused significant reductions in cell viability and the FRAP value and an increase in hydroperoxide levels.

Citral, the major constituent of the essential oil of lemon-scented plants, has been reported to possess several pharmacological activities.[11] Studies have shown that citral dose- and time-dependently protects some normal cells against distressing stimuli. At higher concentrations, it may show a cell growth inhibitory effect.[21] Our results showed the cytoprotective activity of citral at concentrations less than 20 µg/mL. Nordin et al.[22] reported similar results for the effect of citral on the proliferation of normal spleen cells.

In the present investigation, citral also exhibited antioxidant effects through reducing hydroperoxides level and elevating the FRAP value in intra- and extracellular fluids. Measurement of ROS provides important data to study the effects of oxidative stress inducers and antioxidant remedies. FOX-1 is a sensitive assay for detection of hydroperoxides in biological samples.[18] This assessment was performed to detect the effects of citral on intra- and extracellular hydroperoxide concentrations in HUVECs after exposure to oxidative stress induced by H_2O_2. The effect of citral on total antioxidant capacity was evaluated by FRAP assay. Antioxidants are enzymes or nonenzymatic compounds involved in the defense mechanisms against oxidative injuries induced by free radicals through preventing ROS creation and scavenging or eliminating ROS.[23] FRAP is a simple and rapid colorimetric measurement widely used for screening of nonenzymatic antioxidants.[19] Several studies have reported the antioxidant properties of the phytochemicals *in citrus* plants.[24] Radical scavenging activity and induction of enzymatic and nonenzymatic cellular antioxidants have been presented for monoterpenes.[14] Cytoprotective and antioxidant effects have been described for *Melissa officinalis* extract as a plant containing a high level of citral against H_2O_2-induced oxidative stress in endothelial cells.[25] Vimal et al.[16] showed the *in vitro* antioxidant effects of some essential oil compounds including citral through evaluation of free radical scavenging, lipid peroxidation, and antioxidant enzymes activities. Bouzenna et al.[26] reported a protective effect of citral against aspirin-induced oxidative stress through attenuation of mitogen-activated protein kinases, reduction of malondialdehyde level, and modulation of superoxide dismutase and glutathione activities. Protection against high glucose-induced oxidative stress has also been found for citral through inhibiting the ROS activated protein kinases signaling pathway in HepG2 cells.[27]

Besides antioxidant properties, some studies have revealed anti-inflammatory effects of citral by suppression of pro-inflammatory cytokines such as tumor necrosis factor-α and interleukins (IL-6 and IL-8), inhibition of inducible endothelial nitric oxide synthase transcription, reduction of p50 nuclear factor-κB levels, and suppression of vascular cell adhesion molecule 1, intercellular adhesion molecule 1, and *cyclooxygenase*-2 expression.[28-31]

Moreover, the helpful vascular effects including vasodilatory effect likely through affecting the intracellular calcium concentration and nitric oxide pathway have been found for citral in isolated aorta.[15] Regarding the beneficial cardiovascular activities such as antioxidant, cytoprotective, anti-inflammatory, and vasorelaxant effects, citral as a natural component could be suggested for prevention of vascular oxidative stress and endothelial dysfunction and consequently prevention of CVDs.

CONCLUSION

Citral was found to protect HUVECs against oxidative damage induced by H_2O_2 by enhancing total antioxidant capacity and reducing hydroperoxide production. However, more studies in this area are required to evaluate its clinical value for prevention and treatment of CVDs.

ACKNOWLEDGMENTS

This study was financially supported by the Vice-Chancellery for Research and Technology of Isfahan University of Medical Sciences (research projects no. 393659).

Conflicts of interest: No conflict of interest was declared by the authors. The authors alone are responsible for the content and writing of the paper.

REFERENCES

1. Mendis S, Puska P, Norrving B. Global atlas on cardiovascular disease prevention and control. Geneva: WHO, World Heart Federation, World Stroke Organization. 2011:155.
2. Cervantes Gracia K, Llanas-Cornejo D, Husi H. CVD and oxidative stress. J Clin Med. 2017;6:22.
3. Droge W. Free radicals in the physiological control of cell function. Physiol Rev. 2002;82:47-95.
4. Fujino G, Noguchi T, Matsuzawa A, Yamauchi S, Saitoh M, Takeda K, Ichijo H. Thioredoxin and TRAF family proteins regulate reactive oxygen species-dependent activation of ASK1 through reciprocal modulation of the N-terminal homophilic interaction of ASK1. Mol Cell Biol. 2007;27:8152-8163.
5. Touyz RM, Briones AM. Reactive oxygen species and vascular biology: implications in human hypertension. Hypertens Res. 2011;34:5.
6. Schulz E, Anter E, Keaney J, John F. Oxidative stress, antioxidants, and endothelial function. Curr Med Chem. 2004;11:1093-1104.
7. Yegdaneh A, Ghannadi A, Dayani L. Chemical constituents and biological activities of two Iranian *Cystoseira species*. Res Pharm Sci. 2016;11:311-317.
8. Mesripour A, Moghimi F, Rafieian-Kopaie M. The effect of *Cinnamomum zeylanicum* bark water extract on memory performance in alloxan-induced diabetic mice. Res Pharm Sci. 2016;11:318-323.
9. Kris-Etherton PM, Keen CL. Evidence that the antioxidant flavonoids in tea and cocoa are beneficial for cardiovascular health. Curr Opin Lipidol. 2002;13:41-49.
10. Lu WC, Huang DW, Wang CC, Yeh CH, Tsai JC, Huang YT, Li P-H. Preparation, characterization, and antimicrobial activity of nanoemulsions incorporating citral essential oil. J Food Drug Anal. 2018;26:82-89.
11. Devi RC, Sim SM, Ismail R. Spasmolytic effect of citral and extracts of *Cymbopogon citratus* on isolated rabbit ileum. J Smooth Muscle Res. 2011;47:143-156.
12. Wilson ND, Ivanova MS, Watt RA, Moffat AC. The quantification of citral in lemongrass and lemon oils by near-infrared spectroscopy. J Pharm Pharmacol. 2002;54:1257-1263.
13. Sadraei H, Ghannadi A, Malekshahi K. Relaxant effect of essential oil of *Melissa officinalis* and citral on rat ileum contractions. Fitoterapia. 2003;74:445-452.
14. Porto MdeP, da Silva GN, Luperini BC, Bachiega TF, de Castro Marcondes JP, Sforcin JM, Salvadori DMF. Citral and eugenol modulate DNA damage and pro-inflammatory mediator genes in murine peritoneal macrophages. Mol Biol Rep. 2014;41:7043-7051.
15. da Silva R, de Morais L, Silva A, Bastos CMS, Pereira-Gonçalves Á, Kerntopf MR, Menezes IRA, Leal-Cardoso JH, Barbosa R. Vasorelaxant effect of the *Lippia alba* essential oil and its major constituent, citral, on the contractility of isolated rat aorta. Biomed Pharmacother. 2018;108:792-798.
16. Vimal M, Vijaya P, Mumtaz P, Farhath M. Free radical scavenging activity of essential oil compounds citral, limonene, menthone and thymol by using different methods. J Pharm Res. 2013;6:410.
17. Ma ZC, Hong Q, Wang YG, Tan HL, Xiao CR, Liang QD, Wang D-G, Gao Y. Ferulic acid protects lymphocytes from radiation-predisposed oxidative stress through extracellular regulated kinase. Int J Radiat Biol. 2011;87:130-140.
18. Wolf SP. Ferrous ion oxidation in presence of ferric ion indicator xylenol orange for measurement of hydroperoxides. Methods Enzymol. 1994;233:182-189.
19. Benzie IF, Strain JJ. The ferric reducing ability of plasma (FRAP) as a measure of "antioxidant power": the FRAP assay. Anal Biochem. 1996;239:70-76.
20. Cai H. Hydrogen peroxide regulation of endothelial function: origins, mechanisms, and consequences. Cardiovasc Res. 2005;68:26-36.
21. Patel PB, Thakkar VR. Addition of citral controls ROS and reduces toxicity in 5-fluorouracil treated *Schizosaccharomyces pombe* cells. Indian J Exp Biol. 2015;53:152-157.
22. Nordin N, Yeap SK, Zamberi NR, Abu N, Mohamad NE, Rahman HS, How CW, Masarudin MJ, Abdullah R, Alitheen NB. Characterization and toxicity of citral incorporated with nanostructured lipid carrier. PeerJ. 2018;6:e3916.
23. Pellegrini N, Serafini M, Colombi B, Del Rio D, Salvatore S, Bianchi M, Brighenti F. Total antioxidant capacity of plant foods, beverages and oils consumed in Italy assessed by three different *in vitro* assays. J Nutr. 2003;133:2812-2819.
24. Zou Z, Xi W, Hu Y, Nie C, Zhou Z. Antioxidant activity of Citrus fruits. Food Chem. 2016;196:885-896.
25. Safaeian L, Sajjadi SE, Javanmard SH, Montazeri H, Samani F. Protective effect of *Melissa officinalis* extract against H_2O_2-induced oxidative stress in human vascular endothelial cells. Res Pharm Sci. 2016;11:383-389.
26. Bouzenna H, Hfaiedh N, Giroux-Metges MA, Elfeki A, Talarmin H. Biological properties of citral and its potential protective effects against cytotoxicity caused by aspirin in the IEC-6 cells. Biomed Pharmacother. 2017;87:653-660.
27. Subramaniyan SD, Kumar AN. Citral, A monoterpene protect against high glucose induced oxidative injury in HepG2 cell *in vitro*-an experimental study. J Clin Diagn Res. 2017;11:BC10-BC15.

28. Sforcin J, Amaral J, Fernandes Jr A, Sousa J, Bastos J. Lemongrass effects on IL-1β and IL-6 production by macrophages. Nat Prod Res. 2009;23:1151-1159.

29. Lin CT, Chen CJ, Lin TY, Tung JC, Wang SY. Anti-inflammation activity of fruit essential oil from *Cinnamomum insularimontanum* Hayata. Bioresour Technol. 2008;99:8783-8787.

30. Katsukawa M, Nakata R, Takizawa Y, Hori K, Takahashi S, Inoue H. Citral, a component of lemongrass oil, activates PPARα and γ and suppresses COX-2 expression. Biochim Biophys Acta Mol Cell Biol Lipids. 2010;1801:1214-1220.

31. Song Y, Zhao H, Liu J, Fang C, Miao R. Effects of citral on lipopolysaccharide-induced inflammation in human umbilical vein endothelial cells. Inflammation. 2016;39:663-671.

Turk J Pharm Sci 2020;17(5):555-564
DOI: 10.4274/tjps.galenos.2019.32704

ORIGINAL ARTICLE

Tualang Honey Ameliorates Hypoxia-induced Memory Deficits by Reducing Neuronal Damage in the Hippocampus of Adult Male Sprague Dawley Rats

Tualang Balı, Yetişkin Erkek Sprague Dawley Sıçanlarının Hipokampusundaki Nöronal Hasarı Azaltarak Hipoksiye Bağlı Bellek Kayıplarını İyileştiriyor

Entesar Yaseen Abdo QAID[1], Rahimah ZAKARIA[1]*, Nurul Aiman MOHD YUSOF[2], Shaida Fariza SULAIMAN[3], Nazlahshaniza SHAFIN[1], Zahiruddin OTHMAN[4], Asma Hayati AHMAD[1], Che Badariah ABD AZIZ[1], Sangu MUTHURAJU[5]

[1]Universiti Sains Malaysia, School of Medical Sciences, Department of Physiology, Kubang Kerian, Malaysia
[2]Universiti Sains Malaysia, School of Medical Sciences, Department of Anatomy, Kubang Kerian, Malaysia
[3]Universiti Sains Malaysia, School of Biological Sciences, Penang, Malaysia
[4]Universiti Sains Malaysia, School of Medical Sciences, Department of Psychiatry, Kubang Kerian, Malaysia
[5]Universiti Sains Malaysia, School of Medical Sciences, Department of Neuroscience, Kubang Kerian, Malaysia

ABSTRACT

Objectives: A growing body of evidence indicates that hypoxia exposure causes learning and memory deficits. An effective natural therapeutic approach has, however, not been explored widely. Our previous studies found that Tualang honey administration protected learning and memory functions in ovariectomized rats. Therefore, the present study investigated its efficacy in ameliorating hypoxia-induced memory deficits in adult male Sprague Dawley rats.

Materials and Methods: The rats were divided into four groups: i) Normoxia treated with sucrose (n=12), ii) Normoxia treated with Tualang honey (n=12), iii) Hypoxia treated with sucrose (n=12), and iv) Hypoxia treated with Tualang honey (n=12). Tualang honey (0.2 g/kg/BW) and sucrose (1 mL of 7.9%) supplementations were administered orally to the rats daily for 14 days. Then the hypoxia groups were exposed to hypoxia (~11%) for 7 days, while the normoxia groups were kept in normal conditions. Following exposure to hypoxia, the rats' memories were analyzed using a novel object recognition task and T-maze test.

Results: The data revealed that rats exposed to hypoxia showed significant impairment in short-term memory (STM), spatial memory ($p<0.01$), and long-term memory (LTM) when compared to the normoxia group. Hypoxia rats treated with Tualang honey showed significant improvement in STM, LTM, and spatial memory ($p<0.05$) compared with those treated with sucrose ($p<0.05$). Tualang honey also reduced neuronal damage in the hippocampus of adult male Sprague Dawley rats exposed to hypoxia.

Conclusion: It is suggested that Tualang honey pretreatment has protective effects against hypoxia-induced memory deficits, possibly through its antioxidant contents.

Key words: Hypoxia, Tualang honey, sucrose, memory performance, novel object recognition task, T-maze

ÖZ

Amaç: Giderek artan sayıda kanıt, hipoksiye maruz kalmanın öğrenme ve hafıza eksikliklerine neden olduğunu göstermektedir. Bununla birlikte, etkili doğal kaynaklı terapötik yaklaşım detaylı araştırılmamıştır. Önceki çalışmalarımız, Tualang bal uygulamasının ovarektomi yapılmış sıçanlarda öğrenme ve hafıza işlevlerini koruduğunu bulmuştur. Bu nedenle, bu çalışmada Tualang balının yetişkin erkek Sprague Dawley sıçanlarında hipoksinin neden olduğu hafıza kayıplarını gidermedeki etkinliği araştırıldı.

*Correspondence: E-mail: rahimah@usm.my, Phone: +6097676156 ORCID-ID: orcid.org/0000-0002-2459-3213
Received: 16.10.2018, Accepted: 07.03.2019

Gereç ve Yöntemler: Sıçanlar dört gruba ayrıldı: i) sükroz ile muamele edilmiş Normoksi (n=12), ii) Tualang balı ile muamele edilmiş normoksi (n=12), iii) sükroz ile muamele edilmiş hipoksi (n=12) ve iv) Tualang balı ile tedavi edilen hipoksi (n=12). Tualang balı (0,2 g/kg/BW) ve sükroz (1 mL %7,9) takviyeleri 14 gün boyunca her gün farelere ağızdan uygulandı. Daha sonra hipoksi grupları 7 gün süreyle hipoksiye (~%11) maruz bırakılırken, normoksi grupları normal koşullarda tutuldu. Hipoksiye maruz kalmanın ardından, farelerin bellek analizleri yeni bir nesne tanıma görevi ve T-labirent testi kullanılarak yapıldı.

Bulgular: Veriler, hipoksiye maruz kalan sıçanların normoksi grubuna kıyasla kısa süreli belleğinde (STM), uzamsal belleğinde ($p<0,01$) ve uzun süreli belleğinde (LTM) anlamlı kayıp olduğunu ortaya koydu. Tualang balı ile tedavi edilen hipoksi sıçanları, sükroz ile tedavi edilenlere kıyasla ($p<0,05$) STM, LTM ve uzamsal hafızada önemli gelişme gösterdi ($p<0,05$). Tualang balı, hipoksiye maruz kalan yetişkin erkek Sprague Dawley sıçanlarının hipokampusundaki nöronal hasarı da azalttı.

Sonuç: Tualang balı ön tedavisinin, muhtemelen antioksidan içeriği yoluyla, hipoksiye bağlı hafıza kayıplarına karşı koruyucu etkilere sahip olduğu ileri sürülmektedir.

Anahtar kelimeler: Hipoksi, Tualang balı, sükroz, bellek performansı, yeni nesne tanıma görevi, T-labirenti

INTRODUCTION

High altitude is considered one of the most adverse environments, where hypoxia causes many physiological and psychological changes in humans as well as in animals.[1,2] The challenge to regulate homeostasis of oxygen at high altitude is important for the survival of all species of vertebrates. Failure to maintain homeostasis of oxygen leads to damage to both the peripheral nervous system and central nervous system (CNS). The CNS is responsible for cognitive functions including learning and memory. In previous studies, findings suggest that the hippocampus involved in spatial learning and memory is also vulnerable to hypoxia.[3] Hypoxia exposure has been shown to affect the hippocampus, causing memory impairment.[4,5] Although previous findings strongly indicated that exposure to hypoxia induced memory loss, few studies have evaluated the protective effects of natural products and their compounds on memory loss after exposure to hypoxia.

Administration of exogenous antioxidants such as polyphenols and vitamin E has been reported to be a potential way to combat the adverse effects of oxidative stress-induced hypoxia.[6-16] In animal models and patients with impaired cognition, antioxidant-rich diets or treatments prevent memory and learning deficits.[17] Several approaches have been used to target oxidative stress including supplements such as blueberry extracts,[18] melatonin,[13,19] and vitamin E.[20] Despite promising results from both rodent and human studies, much is still being studied regarding the benefit and role of specific nutritional supplements in the treatment of various hypoxic conditions.[18,19,21]

Numerous studies have demonstrated the beneficial effects of Tualang honey and its potential therapeutic applications as an antidiabetic, anticancer, and antimicrobial agent as well as its possessing wound healing properties.[22] Moreover, Tualang honey enhances the hippocampal neuronal morphology and minimizes hippocampal neuronal damage.[23] Tualang honey is rich in phenolic acid and contains antioxidant compounds such as quercetin and flavonoids.[24] A recent study reported that Tualang honey improved brain function through the cholinergic system.[25] Our previous studies concluded that Tualang honey improved memory performance in stressed ovariectomized rats,[26] rats subjected to noise stress,[27] and postmenopausal women[28] and decreased depressive-like behavior and increased brain-derived neurotrophic factor (BDNF) level in ovariectomized rats.[29] Correspondingly, another study identified significantly reduced markers of oxidative stress and increased levels of antioxidative enzymes in brain tissue, further supporting the protective effect of Tualang honey against brain oxidative stress.[30] However, to the best of our knowledge, no study has investigated the effect of Tualang honey on learning and memory of rats in hypoxic condition. Therefore, the present study aimed to evaluate the efficacy of Tualang honey in adult male Sprague Dawley rats to alleviate hypoxia-induced memory deficit.

MATERIALS AND METHODS

Forty-eight adult male Sprague Dawley rats were supplied by the Laboratory Animal Research Unit, Universiti Sains Malaysia (USM). The rats were approximately 8 weeks old with body weight of 200±20 g. They were kept in polypropylene cages (32x24x16 cm) and had free access to food and water. The rats were exposed to 12-h light/dark cycles and held at 23 ˚C room temperature. The experimental protocol followed internationally accepted principles for laboratory animal use and care, and was approved by the research and Ethics Committee of this university [USM/Animal Ethics Approval/2015/ (95) (609)].

Experimental animals

The four groups of rats were as follows: normoxia treated with sucrose (n=12), normoxia treated with Tualang honey (n=12), hypoxia treated with sucrose (n=12), and hypoxia treated with Tualang honey (n=12). Tualang honey (1 mL of 0.2 g/kg body weight)[23] and sucrose (1 mL of 7.9%)[31] were freshly prepared and administered via oral gavage to the rats daily for 14 days. The Tualang honey and sucrose used in this study were from single batch honey obtained from Federal Agricultural Marketing Authorities, Malaysia and Sigma-Aldrich, Inc., St. Louis, MO, USA, respectively. The total food intake and body weight of the rats were recorded throughout the experimental period.

Hypoxia exposure

The rats in the hypoxia groups were housed in an acrylic air-tight chamber with ~11% O_2, ~25 ˚C temperature, and ~76% humidity. The O_2 content of ~11% was generated by an HCA HYPO-002 high-altitude simulation system. The rats in the

normoxia groups were kept in room condition. The rats' food intake and body weight change were recorded weekly.

Behavioral tests

The behavioral tests were performed before and after exposure to hypoxia or normoxia for 2 weeks. The experiments were conducted in a ventilated, dimly lit, and soundproof room. The room temperature was maintained at about 23 °C.

Novel object recognition (NOR) test

All rats were habituated to the open arena (60x60x30 cm). They were allowed to freely explore the arena for 10 min per session for 2 days. On the third day, two similar objects were placed and fixed in symmetrical position on the right and the left side of the arena, about 10 cm from the wall. The rats were allowed to freely explore the objects for 10 min.[32,33] The time spent to explore the objects was recorded manually.

The test sessions were carried out after 2 and 24 h for short-term memory (STM) and long-term memory (LTM), respectively. During these sessions, familiar and novel objects were placed in the arena for 10 min and the time spent to explore each object was recorded. In order to avoid discrimination by olfactory cues, all the equipment was cleaned with 70% alcohol between each session. Object position was changed (right and left) to avoid place preference. The objects were made of plastic toys with a height of 5 cm, and had similar textures, colors, and sizes but distinctive shapes. Sniffing or touching the object with the rat's nose was defined as exploration.[34] Sitting on the object was not defined as exploration.[34]

The discrimination index was calculated based on the difference in exploration time between the novel and familiar objects and dividing it by the total exploration time of both objects.[35] The index was used to measure recognition memory.[36] A positive score means a preference for the novel object and indicates successful memory retention for the familiar object, while a negative score means a preference for the familiar object and indicates memory deficit.[37]

T-maze

The T-maze was made of black Perspex, was 30 cm in height, consisted of three arms (start arm: 60x16.5 cm; two goal arms: 50x16.5 cm), and was equipped with three doors. Before the experiment, the rats were placed in a room for at least 30 min to accustom them to it. The test was carried out in a single continuous session. It started with one-forced choice trial followed by 14-free choice trials.[38] During the forced-choice trial, the door was lowered to close the left or right goal arm. The rat was released from the start arm and was allowed to navigate the maze until it entered the open goal arm. Once the rat returned to the start position, it was detained for 5 s by lowering the door of the start arm. During the 14-free choice trials, the rat was released from the start arm and was free to enter either the right or left goal arm. Once the rat entered one goal arm, the other goal arm was closed immediately. After the rat returned to the start arm, it was again detained for 5 s in the start arm.

If the animal did not return to the start arm within 2 min, the door was used to gently push the rat to the start arm. The test session was terminated as soon as 14-free choice trials had been completed or 30 min had elapsed, whichever came first. In order to avoid discrimination by olfactory cues, all the equipment was cleaned with 70% alcohol between each session. The number of correct alternations out of the 14-forced trials was recorded and the rats that passed fewer than 8-free-choice trials within 30 min were excluded from the study.

Morphological changes

Histological analysis

Twenty-four hours after the last behavioral test, the rats were anesthetized using sodium pentobarbital (0.27 mL) (Alfasan, Woerden, Holland). Intracardiac perfusion with 0.1 M phosphate-buffered saline (PBS) (pH 0.7) for 2 min followed by 4% paraformaldehyde (PFA) (pH 7.0) for 3 min (Fisher Scientific, USA) was performed to prefix the tissue. The brain was carefully dissected, postfixed in 4% PFA (Fisher Scientific, USA) and kept at 4 °C in the refrigerator. Then the brain tissues were subjected to paraffin sectioning following the standard protocol.

Cresyl violet staining

The paraffin section was dewaxed by immersion in xylene 1 and 2 solutions for 2 min each. After that, the slides were hydrated in decreasing dilutions of ethanol for 2 min each, immersed in cresyl violet for 3 min, and then cleaned with distilled water to remove excess cresyl violet. Next, the slides were dehydrated in increasing dilutions of ethanol for 2 min each, immersed in xylene 1 and 2 for 2 min each, and finally left to dry for 30 min. The slides were then mounted in DPX mounting medium (BDH Chemicals, UK) and covered using coverslips (HmbG Inc., Germany). Finally, the slides were examined under a light microscope (Olympus Corporation, Japan) attached to an image analyzer (20x objective lens power) by three blinded investigators.

Apoptosis detection by propidium iodide assay

The paraffin sections were dewaxed, hydrated in decreasing dilutions of alcohol, and washed in PBS. The slides were gently dabbed on tissue paper to drain excess PBS. Then the slides were blocked by incubation in the blocking solution for 20 min in the dark. Before incubation in 25 µL of buffer for 10 min, the area around the sample was carefully wiped and washed in PBS. Next, 25 µL of propidium iodide reagent was added to each slide for 30 min and then washed in PBS. The slides were then mounted in fluorescent mounting medium (Thermo Fisher Scientific, USA) and covered with coverslips (HmbG Inc., Germany). Finally, the slides were examined under a fluorescent microscope (Olympus Corporation, Japan) attached to an image analyzer under a green filter (20x objective lens power) by three blinded investigators.

Statistical analysis

Differences in the means of behavioral scores, food intake, and body weight among the experimental groups were analyzed

using One-Way ANOVA with a Bonferroni *post hoc* test. Differences were regarded as significant at $p<0.05$.

RESULTS

Changes in food intake

There were no differences in food intake in normoxia animals, whereas hypoxia animals treated with sucrose and honey showed a significant ($p<0.05$) reduction in food intake (Figure 1).

Changes in body weight

Following exposure to hypoxia, the body weight of the animals was significantly ($p<0.05$) reduced in both the sucrose and honey treated groups (Figure 1).

NOR test

The results suggest that hypoxia adversely affects STM more than LTM. There was a significant improvement in the discrimination indexes of the STM and LTM tests following honey treatment, indicating that honey pretreatment was able to prevent the adverse effects of hypoxia on recognition memory functions, especially STM (Figure 2).

T-maze

The results suggest that hypoxia also affects the number of alterations in the T-maze. Similar to the NOR test, a significant improvement in the mean number of alterations in the T-maze was noted following honey treatment, suggesting the protective effects of honey pretreatment on spatial memory functions (Figure 2).

Morphological changes

Following the behavioral experiments, hippocampal morphology was analyzed using cresyl violet (Figures 3-6) and propidium iodide staining (Figures 7 and 8). The quantity analysis of CA1, CA2, CA3, and DG of the hippocampus showed significant ($p<0.05$) numbers of dead cells in the sucrose-treated hypoxic group, whereas the Tualang honey-treated hypoxic group of animals showed fewer dead cells, indicating that Tualang honey prevented neuronal damage (Figure 7). Cytoplasmic shrinkage and pyknotic nucleus are features indicative of a dead cell. For qualitative analysis to further confirm neuronal damage especially in the hypoxia groups treated with sucrose and honey, PI staining was carried out. The results displayed and reconfirmed that there was considerable neuronal damage in the hypoxia group treated with sucrose but not much in the hypoxia group treated with Tualang honey (Figure 8).

DISCUSSION

We present three important findings in the present study. First, continuous exposure to normobaric hypoxia for 7 days exerted adverse effects on food intake, body weight gain, and memory performance. Second, with regard to memory function, STM, LTM, and spatial memory performance were significantly affected. Third, Tualang honey pretreatment was able to protect against hypoxia-induced memory deficits and hippocampal neuronal damage. Regarding food intake, hypoxic animals treated with sucrose and honey consumed significantly less food than normoxia animals treated with sucrose and honey. Numerous previous studies support the present findings that high altitude exposure is associated with a reduction in food intake.[39] Westerterp-Plantenga et al.[40] demonstrated that high altitude causes hypophagia and reported it as being more specific to carbohydrate[41] and protein.[42] Not only humans subjected to high altitude experience hypophagia but also animals exhibit changes in feeding behavior following exposure to hypobaric hypoxia, whereby reductions in food intake are directly linked to the degree of simulated altitude.[43]

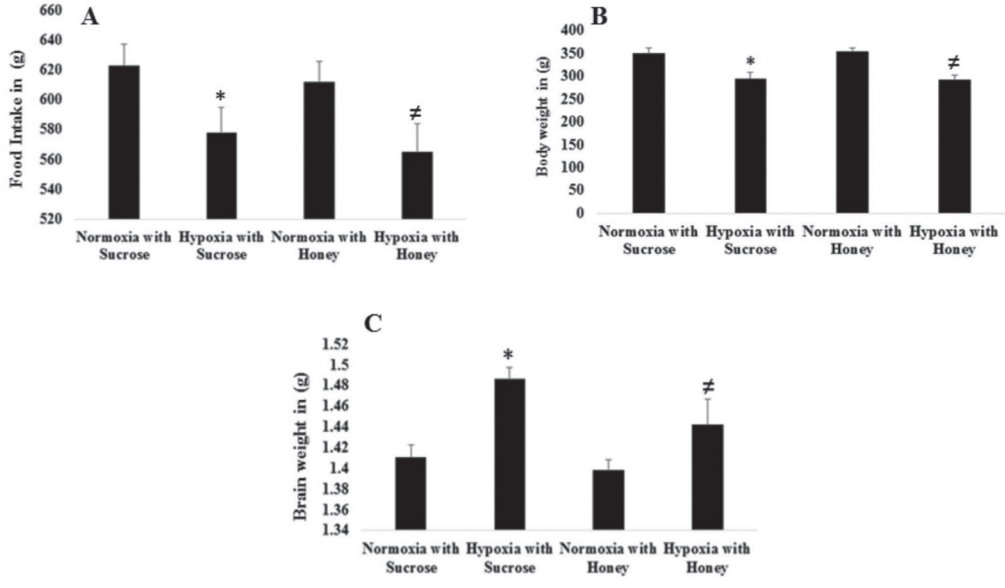

Figure 1. Food intake A), body weight B), and brain weight C) following exposure to hypoxia. The data are displayed as mean (SEM). *$p<0.05$ vs. normoxia with sucrose, ≠ $p<0.05$ vs. normoxia with honey

SEM: Standard error of the mean

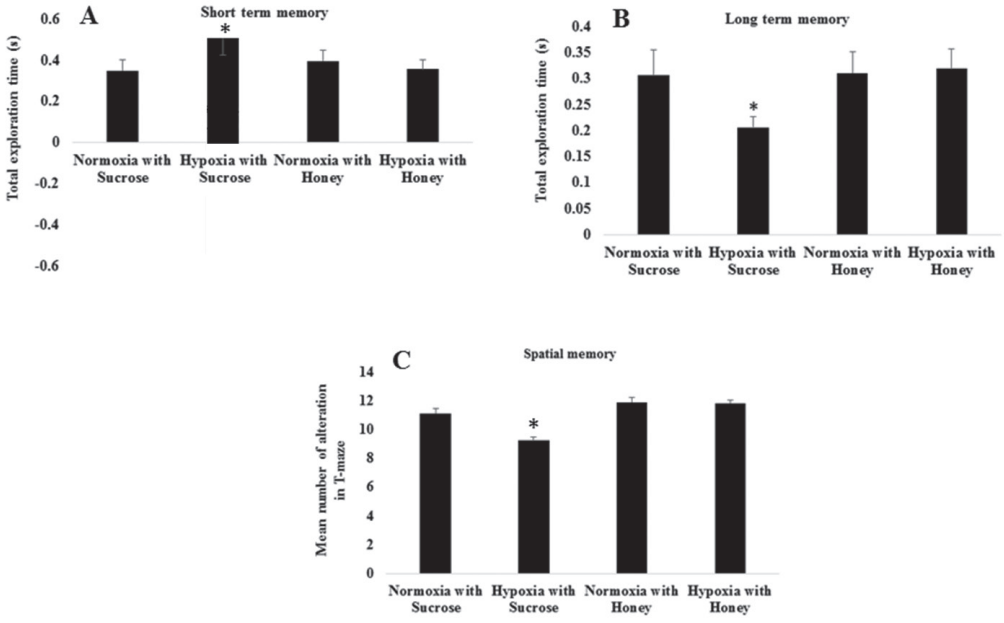

Figure 2. Short-term memory A), long-term memory B), and spatial memory C) following exposure to hypoxia. The data are displayed as mean (SEM). *p<0.05 vs normoxia with sucrose

SEM: Standard error of the mean

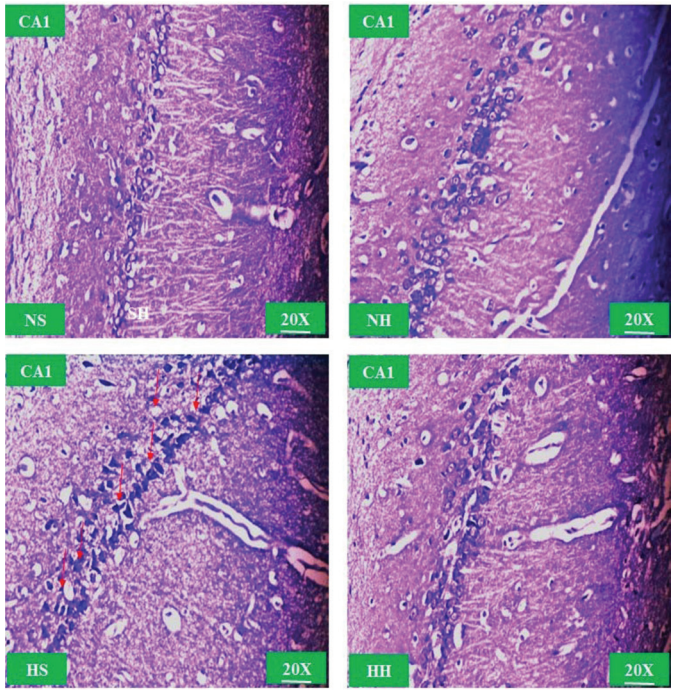

Figure 3. Morphological changes in CA1 of the hippocampus in normoxia sucrose (NS), normoxia honey (NH), hypoxia treated with sucrose (HS), and hypoxia treated with honey (HH). Neuronal damage indicated with red arrow. Cytoplasmic shrinkage and pyknotic nucleus indicate dead cells. Bar scale 200 µm

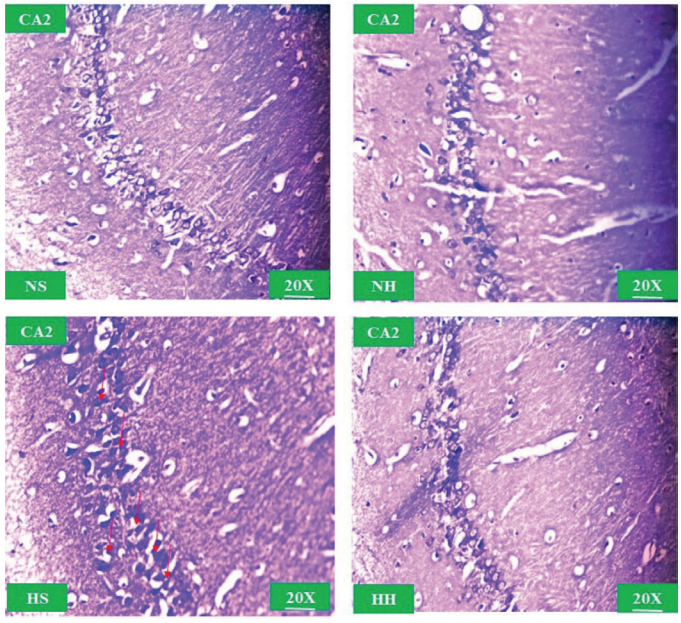

Figure 4. Morphological changes in CA2 of the hippocampus in normoxia sucrose (NS), normoxia honey (NH), hypoxia treated with sucrose (HS), and hypoxia treated with honey (HH). Neuronal damage indicated with red arrow. Cytoplasmic shrinkage and pyknotic nucleus indicate dead cells. Bar scale 200 µm

As a result of the decrease in food intake, animals exposed to hypoxia display a substantial reduction in body weight in both sucrose and honey treated groups. Loss of appetite could be one of the possibilities for the reduction in body weight.[44] Hypoxia also affects body weight regulation as noted in humans as well as in animals.[45] Similar findings were obtained in the present study, in which the food intake and body weight gain were lower in the rats exposed to hypoxia compared to the nonhypoxic rats. The poor appetite and decreased food intake often produce an imbalance in the energy equation that leads to low weight gain and changes in body composition.[46] The proposed mechanisms include changes in leptin, glucagon-like peptide 1,

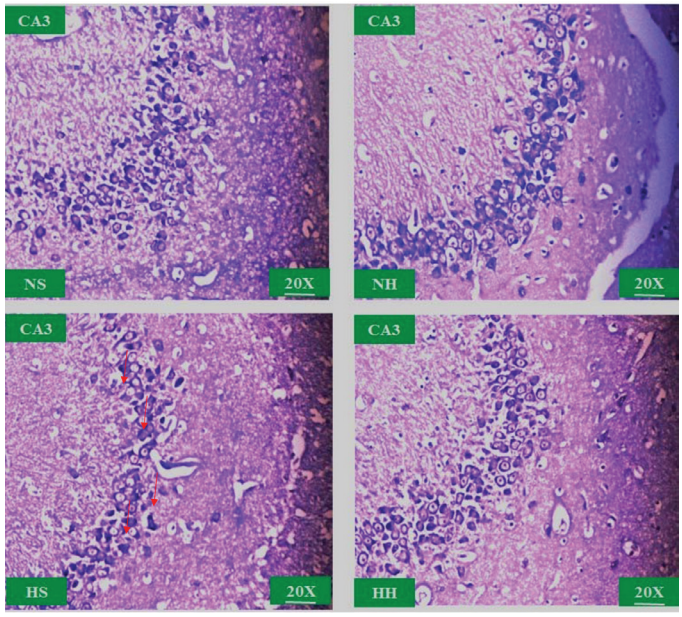

Figure 5. Morphological changes in CA3 of the hippocampus in normoxia sucrose (NS), normoxia honey (NH), hypoxia treated with sucrose (HS), and hypoxia treated with honey (HH). Neuronal damage indicated with red arrow. Cytoplasmic shrinkage and pyknotic nucleus indicate dead cells. Bar scale 200 µm

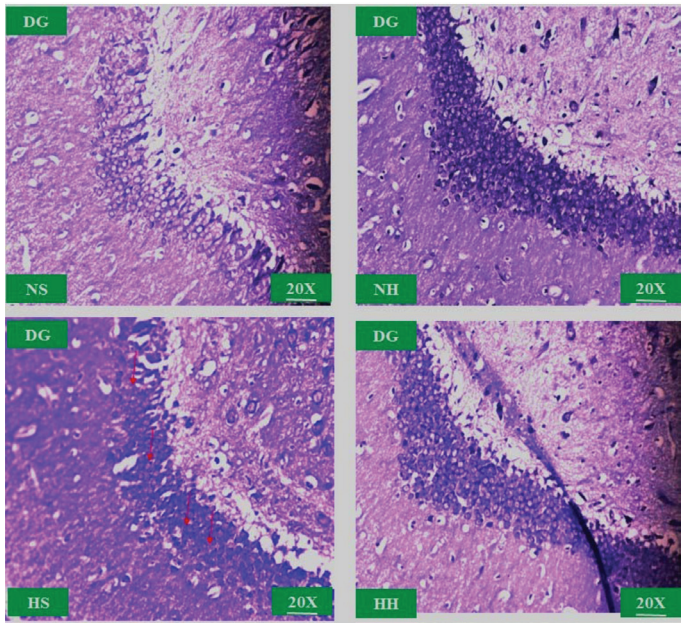

Figure 6. Morphological changes in DG of the hippocampus in normoxia sucrose (NS), normoxia honey (NH), hypoxia treated with sucrose (HS), and hypoxia treated with honey (HH). Neuronal damage indicated with red arrow. Cytoplasmic shrinkage and pyknotic nucleus indicate dead cells. Bar scale 200 µm

protein synthesis, intestinal absorption, and hypoxia-regulated genes.[47] Moreover, previous work suggested leptin as the main candidate for the reduction in food intake following hypoxia.[44] However, the role of leptin and food intake during hypoxia is still a subject of debate and the mechanisms responsible for the decrease in energy intake in hypoxia conditions remain unclear.

Despite the hypoxic groups of animals displaying a reduction in food intake and body weight, these groups did not show any kind of locomotor deficits in the open field test. Hence, the recognition objective memory test was carried out following exposure to hypoxia. Interestingly, the hypoxia group treated with Tualang honey showed improvement in recognition objective memory performance, whereas the hypoxia group treated with sucrose failed to retain memory function. There were no significant changes found in the normoxia rats treated with sucrose and Tualang honey. Many previous studies used a hypoxic chamber set at 6-8% of oxygen content for a shorter time and found significant memory deficit.[47,48] Reducing the oxygen content to 6% impaired acquisition of the avoidance response, and the significant difference between the percentages of avoidance responses of animals placed in normoxic and hypoxic conditions on day 3 were 69.2% and 38.0%, respectively. This finding was in line with an earlier report by Saligaut et al.[47] in which the acquisition of a conditioned avoidance response was impaired under 8% oxygen content (300 torr) of hypobaric hypoxia.

Our results, along with those of previous studies, clearly indicated that both normoxic and hypobaric hypoxia were able to induce memory deficits. Thus, this 'equivalent air altitude model'[49] can also be used to study memory function despite earlier reported physiological differences between acute exposures to normobaric and hypobaric hypoxia.[50] In the present study, two behavioral tests were carried out, i.e. spatial working memory and recognition memory. Rats that were exposed to hypoxia displayed deficits in STM, LTM, and spatial memory. Such findings are consistent with earlier evidence that hypoxic exposure impaired visual memory and spatial memory.[51-58] Interestingly, the present study demonstrated that pretreatment with Tualang honey was able to protect the rats against hypoxia-induced memory deficits as revealed by the behavioral output that was comparable to that of the controls.

Numerous studies have reported that exposure to hypoxia triggers memory deficits through involvement of various mechanisms.[56,59] In particular, neuronal apoptosis in the cortex, striatum, and hippocampal cells;[53] imbalance in oxidative and antioxidative enzymes;[60] and alteration in cholinergic[55] and glutamate neurotransmission[61] might be the root cause of impairment of spatial working memory during exposure to hypoxia. However, the potential therapeutic method to reduce these changes during hypoxia has not been evaluated. The present results suggested that Tualang honey treatment could improve memory following exposure to hypoxia. Hence, Tualang honey could potentially be a way to mitigate deleterious effects following hypoxia.

A broad range of studies have been carried out in Asian countries to analyze the chemical composition of Tualang honey as well as its functional properties.[22,23,62] Tualang honey has been reported to possess high flavonoid content, including quercetin, luteolin, kaempferol, apigenin, chrysin, and galangin.[63] Likewise, honey, in general, contains enzymatic and nonenzymatic antioxidants.[64-66] Based on the present results, memory performance improved after hypoxia exposure in

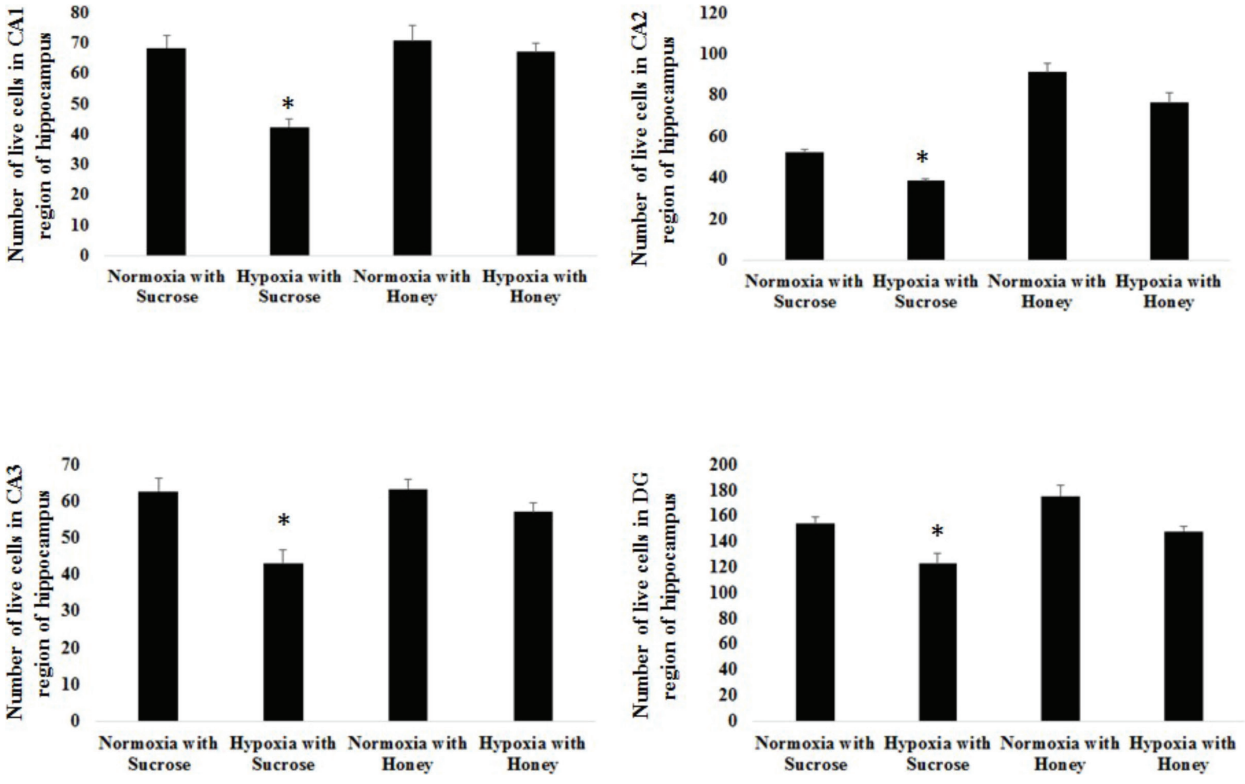

Figure 7. Quantification of neuronal damage in CA1, CA2, CA3 and DG of the hippocampus. The data are displayed as mean (SEM). *p<0.05 vs normoxia with sucrose

SEM: Standard error of the mean

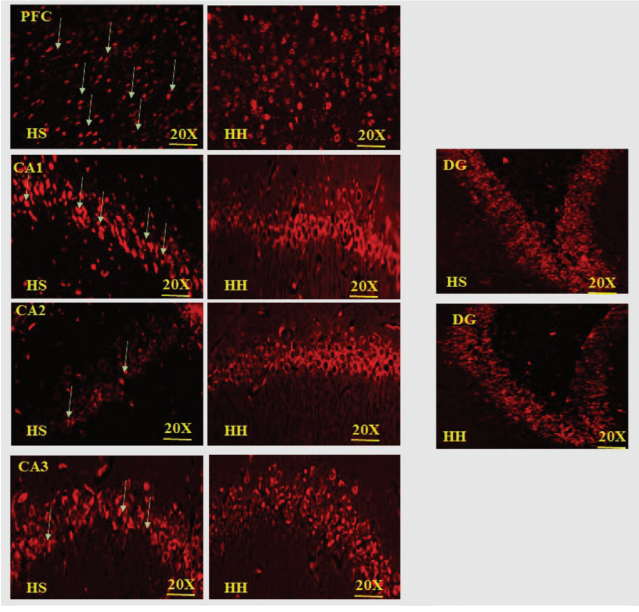

Figure 8. The apoptotic dead cells using PI staining in PFC and CA1, CA2, CA3, and DG of the hippocampus in hypoxia treated with sucrose (HS) and hypoxia treated with honey (HH). Neuronal damage indicated with arrows. Cytoplasmic shrinkage and pyknotic nucleus indicate dead cells. Bar scale 200 μm

Tualang honey treated groups through modulation of oxidative stress. Previous studies reported that Tualang honey decreased oxidative stress caused by kainic acid.[62] It also shows antioxidant properties in streptozotocin-induced diabetic rats.[22] In human subjects, Tualang honey treatment in healthy postmenopausal women resulted in an improvement in memory.[28] Al-Rahbi et al.[23] also reported that Tualang honey treatment improved memory in animals subjected to instability stress. Al-Rahbi et al.[23] reported that Tualang honey supplement improves memory performance and prevents neuronal damage in hippocampal regions. A recent study reported that in female athletes Tualang honey showed antioxidant activity and oxidative stress in a dose-dependent manner.[67] Tualang honey was also found to protect the rat midbrain from oxidative stress.[68] Azman et al.[27,69] demonstrated that Tualang honey prevented memory deficits following noise stress. An *in vitro* study also stated that Tualang honey improved cell migration and resistance against oxidative stress.[70] Not only does Tualang honey control oxidative stress but it also enhances the level of BDNF,[29] which could be one of the mechanisms involved in the improvement of memory during hypoxia. However, this needs further exploration.

Brain weight and morphological changes were also studied following exposure to hypoxia. The results suggested that the weight of the brain following hypoxia significantly increased in the hypoxia group treated with sucrose but not in the hypoxia group treated with Tualang honey. Mórocz et al.[71] reported that brain volume changes occur in patients following exposure to hypoxia due to changes in cerebral blood volume. Another important factor is the occurrence of brain edema due to the

inflammatory process following acute exposure to hypoxia.[72] In the present study, we did not evaluate the factors that could contribute to edema but the increased brain weight indicates this. The hippocampal morphological changes were analyzed in CA1, CA2, CA3, and DG. The hypoxia group treated with sucrose showed a significant number of dead cells as compared to the hypoxia group treated with Tualang honey. It is assumed that Tualang honey prevents neuronal damage through reduction of oxidative stress. It is possible that its antioxidant content contributes to minimizing the neuronal damage and improving memory.[31] It is thought that Tualang honey prevents hippocampal neuronal damage through phenolic acid, which has an antioxidant property.[73] Phenolic antioxidants attenuate the hippocampal neuronal cell damage induced by excitotoxicity.[74] We postulate that the superior therapeutic performance seen in Tualang honey treated rats in hypoxic condition was due to many antioxidant components and other components involved to improve memory through prevention of neuronal damage.

Taking together all findings in the present study, Tualang honey could improve memory and prevent neuronal damage due to hypoxia, possibly through mechanisms involving its antioxidant properties bringing about these effects. To the best of our knowledge, this is the first time that Tualang honey has been evaluated under hypoxic condition using rats. For better understanding regarding the underlying mechanisms whereby Tualang honey improves memory and prevents neuronal damage, further studies are warranted.

CONCLUSION

We propose that Tualang honey pretreatment potentially has protective effects against memory deficits triggered by hypoxia through its antioxidant content.

ACKNOWLEDGEMENTS

This research work was supported by a short-term grant from Universiti Sains Malaysia; 304/PPSP/61313086.

Conflicts of interest: No conflict of interest was declared by the authors. The authors alone are responsible for the content and writing of the paper.

REFERENCES

1. Mórocz IA, Zientara GP, Gudbjartsson H, Muza S, Lyons T, Rock PB, Kikinis R, Jólesz FA. Volumetric quantification of brain swelling after hypobaric hypoxia exposure. Exp Neurol. 2001;168:96-104.
2. Muthuraju S, Maiti P, Solanki P, Sharma AK, Amitabh, Singh SB, Prasad D, Ilavazhagan G. Acetylcholinesterase inhibitors enhance cognitive functions in rats following hypobaric hypoxia. Behav Brain Res. 2009;203:1-14.
3. Maiti P, Singh SB, Mallick B, Muthuraju S, Ilavazhagan G. High altitude memory impairment is due to neuronal apoptosis in hippocampus, cortex and striatum. J Chem Neuroanat. 2008;36:227-238.
4. Malle C, Quinette P, Laisney M, Bourrilhon C, Boissin J, Desgranges B, Eustache F, Piérard C. Working memory impairment in pilots exposed to acute hypobaric hypoxia. Aviat Space Environ Med. 2013;84:773-779.
5. Qaid E, Zakaria R, Sulaiman SF, Yusof NM, Shafin N, Othman Z, Ahmad AH, Aziz CA. Insight into potential mechanisms of hypobaric hypoxia-induced learning and memory deficit - Lessons from rat studies. Hum Exp Toxicol. 2017;36:1315-1325.
6. Kempermann G, Kuhn HG, Gage FH. More hippocampal neurons in adult mice living in an enriched environment. Nature. 1997;386:493-495.
7. Kempermann G, Kuhn HG, Gage FH. Experience-induced neurogenesis in the senescent dentate gyrus. J Neurosci. 1998;18:3206-3212.
8. van Praag H, Christie BR, Sejnowski TJ, Gage FH. Running enhances neurogenesis, learning, and long-term potentiation in mice. Proc Natl Acad Sci USA. 1999;96:13427-13431.
9. van Praag H, Kempermann G, Gage FH. Running increases cell proliferation and neurogenesis in the adult mouse dentate gyrus. Nat Neurosci. 1999;2:266-270.
10. Hartley R, Castro-S´anchez R, Ramos-Gonzalez B, Bustos-Obreg E. Rat spermatogenesis damage in intermittent hypobaric hypoxia and the protective role of melatonin. I Cauda epididymal spermatozoa. Int J Morphol. 2009;27:1275-1284.
11. Radák Z, Lee K, Choi W, Sunoo S, Kizaki T, Oh-ishi S, Suzuki K, Taniguchi N, Ohno H, Asano K. Oxidative stress induced by intermittent exposure at a simulated altitude of 4000 m decreases mitochondrial superoxide dismutase content in soleus muscle of rats. Eur J Appl Physiol Occup Physiol. 1994;69:392-395.
12. Nakanishi K, Tajima F, Nakamura A, Yagura S, Ookawara T, Yamashita H, Suzuki K, Taniguchi N, Ohno H. Effects of hypobaric hypoxia on antioxidant enzymes in rats. J Physiol. 1995;489:869-876.
13. Farías JG, Zepeda AB, Calaf GM. Melatonin protects the heart, lungs and kidneys from oxidative stress under intermittent hypobaric hypoxia in rats. Biol Res. 2012;45:81-85.
14. Farías JG, Puebla M, Acevedo A, Tapia PJ, Gutierrez E, Zepeda A, Calaf G, Juantok C, Reyes JG. Oxidative stress in rat testis and epididymis under intermittent hypobaric hypoxia: protective role of ascorbate supplementation. J Androl. 2010;31:314-321.
15. Kücükakin B, Gögenur I, Rosenberg J. Melatonin against surgical stress. Ugeskr Laeger. 2007;169:1306-1308.
16. Wright VP, Klawitter PF, Iscru DF, Merola AJ, Clanton TL. Superoxide scavengers augment contractile but not energetic responses to hypoxia in rat diaphragm. J Appl Physiol. 2005;98:1753-1760.
17. Vauzour D, Vafeiadou K, Rodriguez-Mateos A, Rendeiro C, Spencer JP. The neuroprotective potential of flavonoids: a multiplicity of effects. Genes Nutr. 2008;3:115-126.
18. Zepeda AB, Aguayo LG, Fuentealba J, Figueroa CA, Salgado PK, Calaf GM, Farías J. Blueberry extracts protect testis from hypobaric hypoxia induced oxidative stress in rats. Oxid Med Cell Longev. 2012;2012:975870.
19. Bustos-Obreg´on E, Castro-S´anchez R, Ramos-Gonz´alez B, Torres-D´ıaz L. Rat spermatogenesis damage in intermittent hypobaric hypoxia and the protective role of melatonin. II: Testicular parameters. Int J Morphol. 2010;28:537-547.
20. Wu A, Ying Z, Gomez-Pinilla F. Dietary omega-3 fatty acids normalize BDNF levels, reduce oxidative damage, and counteract learning disability after traumatic brain injury in rats. J Neurotrauma. 2004;21:1457-1467.
21. Vauzour D, Vafeiadou K, Rodriguez-Mateos A, Rendeiro C, Spencer JP. The neuroprotective potential of flavonoids: a multiplicity of effects. Genes Nutri. 2008;3:115-126.

22. Erejuwa OO, Sulaiman SA, Wahab MS, Sirajudeen KN, Salleh MS, Gurtu S. Antioxidant protection of Malaysian tualang honey in pancreas of normal and streptozotocin-induced diabetic rats. Ann Endocrinol (Paris). 2010;71:291-296.

23. Al-Rahbi B, Zakaria R, Othman Z, Hassan A, Mohd Ismail ZI, Muthuraju S. Tualang honey supplement improves memory performance and hippocampal morphology in stressed ovariectomized rats. Acta Histochem. 2014;116:79-88.

24. Khalil MI, Alam N, Moniruzzaman M, Sulaiman SA, Gan SH. Phenolic acid composition and antioxidant properties of Malaysian honeys. J Food Sci. 2011;76(6):C921-8. doi:10.1111/j.1750-3841.2011.02282.x. PMID: 22417491.

25. Al-Rahbi B, Zakaria R, Othman Z, Hassan A, Ahmad AH. The effects of Tualang Honey Supplement on Medial Prefrontal Cortex Morphology and Cholinergic System in Stressed Ovariectomised Rats. Int. J Appl Res Nat Prod. 2014;7:28-36.

26. Al-Rahbi B, Zakaria R, Othman Z, Hassan A, Muthuraju S, Wan Mohammad WM. Mood and memory function in ovariectomised rats exposed to social instability stress. Biomed Res Int. 2013;2013:493643.

27. Azman KF, Zakaria R, Ab Aziz CB, Othman Z, Al-Rahbi B. Tualang honey improves memory performance and decreases depressive-like behaviours in rats exposed to loud noise stress. Noise Health. 2015;17:83-89.

28. Othman Z, Shafin N, Zakaria R, Hussain NH, Mohammad WM. Improvement in immediate memory after 16 weeks of tualang honey (Agro Mas) supplement in healthy postmenopausal women. Menopause. 2011;18:1219-1224.

29. Al-Rahbi B, Zakaria R, Othman Z, Hassan A, Ahmad AH. Enhancement of BDNF concentration and restoration of the hypothalamic-pituitary-adrenal axis accompany reduced depressive-like behaviour in stressed ovariectomised rats treated with either Tualang honey or estrogen. Scientific World Journal. 2014;2014:310821.

30. Al-Rahbi B, Zakaria R, Othman Z, Hassan A, Ahmad AH. Protective Effects of Tualang Honey against Oxidative Stress and Anxiety-Like Behaviour in Stressed Ovariectomized Rats. Int Sch Res Notices. 2014;2014:521065.

31. Chepulis LM, Starkey NJ, Waas JR, Molan PC. The effects of long-term honey, sucrose or sugar-free diets on memory and anxiety in rats. Physiol Behav. 2009;97:359-368.

32. De Lima MN, Laranja DC, Bromberg E, Roesler R, Schröder N. Pre- or post-training administration of the NMDA receptor blocker MK-801 impairs object recognition memory in rats. Behav Brain Res. 2005;156:139-143.

33. Pieta Dias C, Martins De Lima MN, Presti-Torres J, Dornelles A, Garcia VA, Siciliani Scalco F, Rewsaat Guimarães M, Constantino L, Budni P, Dal-Pizzol F, Schröder N. Memantine reduces oxidative damage and enhances long-term recognition memory in aged rats. Neuroscience. 2007;146:1719-1725.

34. Bowman R, Ferguson D, Luine V. Effects of chronic restraint stress and estradiol on open field activity, spatial memory, and monoaminergic neurotransmitters in ovariectomized rats. Neurosci. 2002;113:401-410.

35. Reneerkens OAH, Rutten K, Akkerman S, Blokland A, Shaffer CL, Menniti FS, Steinbusch HW, Prickaerts J. Phosphodiesterase type 5 (PDE5) inhibition improves object recognition memory: Indications for central and peripheral mechanisms. Neurobiol Learn Mem. 2012;97:370-379.

36. Kamei H, Nagai T, Nakano H, Togan Y, Takayanagi M, Takahashi K, Kobayashi K, Yoshida S, Maeda K, Takuma K, Nabeshima T, Yamada K. Repeated methamphetamine treatment impairs recognition memory through a failure of novelty-induced ERK1/2 activation in the prefrontal cortex of mice. Biol Psychiatry. 2006;59:75-84.

37. Carlini VP, Martini AC, Schiöth HB, Ruiz RD, Fiol de Cuneo M, de Barioglio SR. Decreased memory for novel object recognition in chronically food-restricted mice is reversed by acute ghrelin administration. Neuroscience. 2008;153:929-934.

38. Spowart-Manning L, van der Staay FJ. The T-maze continuous alternation task for assessing the effects of putative cognition enhancers in the mouse. Behav Brain Res. 2004;151:37-46.

39. Tschop M, Strasburger CJ, Hartmann G, Biollaz J, Bartsch P. Raised leptin concentrations at high altitude associated with loss of appetite. Lancet. 1998;352:1119-1120.

40. Westerterp-Plantenga MS, Westerterp KR, Rubbens M, Verwegen CR, Richelet JP, Gardette B. Appetite at "high altitude" [Operation Everest III (Comex-'97)]: a simulated ascent of Mount Everest. J Appl Physiol. 1999;87:391-399.

41. Rose MS, Houston CS, Fulco CS, Coates G, Sutton JR, Cymerman A. Operation Everest. II: Nutrition and body composition. J Appl Physiol. 1988;65:2545-2551.

42. Armellini F, Zamboni M, Robbi R, Todesco T, Bissoli L, Mino A, Angelini G, Micciolo R, Bosello O. The effects of high altitude trekking on body composition and resting metabolic rate. Horm Metab Res. 1997;29:458-461.

43. Elia R, Elgoyhen AB, Bugallo G, Rio ME, Bozzini CE. Effect of exposure to reduced atmospheric pressure on body weight, food intake and body composition of growing rats. Acta Physiol Pharmacol Latinoam. 1985;35:311-318.

44. Norese MF, Lezón CE, Alippi RM, Martínez MP, Conti MI, Bozzini CE. Failure of polycythemia-induced increase in arterial oxygen content to suppress the anorexic effect of simulated high altitude in the adult rat. High Alt Med Biol. 2002;3:49-57.

45. Quintero P, Milagro FI, Campión J, Martínez JA. Impact of oxygen availability on body weight management. Med Hypotheses. 2010;74:901-907.

46. Westerterp KR. Energy and water balance at high altitude. News Physiol Sci. 2001;16:134-137.

47. Saligaut C, Moore N, Boulu R, Plotkine M, Leclerc JL, Prioux-Guyonneau M, Boismare F. Hypobaric hypoxia: Central catecholamine levels and cortical PO_2 and avoidance response in rats treated with apomorphine. Aviat Space Environ Med. 1981;52:166-170.

48. Groo D, Palosi E, Szporny L. Comparison of the effects of vinpocetine, vincamine, and nicergoline on the normal and hypoxia-damaged learning process in spontaneously hypertensive rats. Drug Dev Res. 1988;15:75-85.

49. Bert P. Barometric pressure: researches in experimental physiology. *Bethesda Md, Undersea* and Hyperbaric *Medical Society, Forgotten Books;1978*:362-367

50. Coppel J, Hennis P, Gilbert-Kawai E, Grocott MP. The physiological effects of hypobaric hypoxia versus normobaric hypoxia: a systematic review of crossover trials. Extrem Physiol Med. 2015;4:2.

51. Crow TJ, Kelman GR. Effect of mild acute hypoxia on human short-term memory. Br J Anaesth. 1971;43:548-552.

52. Hota SK, Barhwal K, Baithar I, Prasad D, Singh SB, Ilavazhagan G. Bacopa monniera leaf extract ameliorates hypobaric hypoxia induced spatial memory impairment. Neurobiol. 2009;34:23-39.

53. Maiti P, Muthuraju S, Ilavazhagan G, Singh SB. Hypobaric hypoxia induces dendritic plasticity in cortical and hippocampal pyramidal neurons in rat brain. Behav Brain Res. 2008;189:233-243.

54. Barhwal K, Hota SK, Jain V, Prasad D, Singh SB, Ilavazhagan G. Acetyl-l-carnitine (ALCAR) prevents hypobaric hypoxia-induced spatial memory impairment through extracellular related kinase-mediated nuclear factor erythroid 2-related factor 2 phosphorylation. Neurosci 2009;161:501-514.

55. Muthuraju S, Maiti P, Solanki P, Sharma AK, Amitabh, Singh SB, Prasad D, Ilavazhagan G. Acetylcholinesterase inhibitors enhance cognitive functions in rats following hypobaric hypoxia. Behav Brain Res. 2009;203:1-14.

56. Muthuraju S, Maiti P, Solanki P, Sharma AK, Singh SB, Prasad D, Ilavazhagan G. Cholinesterase inhibitors ameliorate spatial learning deficits in rats following hypobaric hypoxia. Exp Brain Res. 2010;203:583-592.

57. Kauser H, Sahu S, Kumar S, Panjwani U. Guanfacine is an effective countermeasure for hypobaric hypoxia-induced cognitive decline. Neurosci. 2013;254:110-119.

58. Kauser H, Sahu S, Kumar S, Panjwani U. Guanfacine ameliorates hypobaric hypoxia induced spatial working memory deficits. Physiol Behav. 2014;123:187-192.

59. Muthuraju S, Maiti P, Pati S, Solanki P, Sharma AK, Singh SB, Prasad D, Ilavazhagan G. Role of cholinergic markers on memory function of rats exposed to hypobaric hypoxia. Eur J Pharmacol. 2011;672:96-105.

60. Jayalakshmi K, Singh SB, Kalpana B, Sairam M, Muthuraju S, Ilavazhagan G. N-acetyl cysteine supplementation prevents impairment of spatial working memory functions in rats following exposure to hypobaric hypoxia. Physiol Behav. 2007;92:643-650.

61. Hota SK, Barhwal K, Ray K, Singh SB, Ilavazhagan G. Ceftriaxone rescues hippocampal neurons from excitotoxicity and enhances memory retrieval in chronic hypobaric hypoxia. Neurobiol Learn Mem. 2008;89:522-532.

62. Sairazi NSM, Sirajudeen KNS, Asari MA, Mummedy S, Muzaimi M, Sulaiman SA. Effect of tualang honey against KA-induced oxidative stress and neurodegeneration in the cortex of rats. BMC Complement Altern Med. 2017;17:31.

63. Bogdanov S, Jurendic T, Sieber R, Gallmann P. Honey for nutrition and health: A review. J Am Coll Nutr. 2008;27:677-689.

64. Gheldof N, Engeseth NJ. Antioxidant capacity of honeys from various floral sources based on the determination of oxygen radical absorbance capacity and inhibition of *in vitro* lipoprotein oxidation in human serum samples. J Agric Food Chem. 2002;50:3050-3055.

65. Al ML, Daniel D, Moise A, Bobis O, Laslo L, Bogdanov S. Physicochemical and bioactive properties of different floral origin honeys from Romania. Food Chem. 2009;112:863-867.

66. Ferreira IC, Aires E, Barreira JC, Estevinho LM. Antioxidant activity of Portuguese honey samples: Different contributions of the entire honey and phenolic extract. Food Chem. 2009;114:1438-1443.

67. Ahmad NS, Abdul Aziz A, Kong KW, Hamid MSA, Cheong JPG, Hamzah SH. Dose-response effect of tualang honey on postprandial antioxidant activity and oxidative stress in female athletes: A pilot study. J Altern Complement Med. 2017;23:989-995

68. Tang SP, Sirajudeen KNS, Jaafar H, Gan SH, Muzaimi M, Sulaiman SA. Tualang honey protects the rat midbrain and lung against repeated paraquat exposure. Oxid Med Cell Longev. 2017;2017:4605782.

69. Azman KF, Zakaria R, Ab Aziz CB, Othman Z. Tualang honey attenuates noise stress-induced memory deficits in aged rats. Oxid Med Cell Longev. 2016;2016:1549158. doi:10.1155/2016/1549158.

70. Tan JJ, Azmi SM, Yong YK, Cheah HL, Lim V, Sandai D, Shaharuddin B. Tualang honey improves human corneal epithelial progenitor cell migration and cellular resistance to oxidative stress *in vitro*. PLoS One. 2014;9:e96800.

71. Mórocz IA, Zientara GP, Gudbjartsson H, Muza S, Lyons T, Rock PB, Kikinis R, Jólesz FA. Volumetric quantification of brain swelling after hypobaric hypoxia exposure. Exp Neurol. 2001;168:96-104.

72. Zhou Y, Huang X, Zhao T, Qiao M, Zhao X, Zhao M, Xu L, Zhao Y, Wu L, Wu K, Chen R, Fan M, Zhu L. Hypoxia augments LPS-induced inflammation and triggers high altitude cerebral oedema in mice. Brain Behav Immun. 2017;64:266-275.

73. Kishore RK, Halim AS, Syazana MS, Sirajudeen KNS. Tualang honey has higher phenolic content and greater radical scavenging activity compared with other honey sources. Nutr Res. 2011;31:322-325.

74. Parihar MS, Hemnani T. Phenolic antioxidants attenuate hippocampal neuronal cell damage against kainic acid induced excitotoxicity. J Biosci. 2003;28:121-128.

Turk J Pharm Sci 2020;17(5):565-575
DOI: 10.4274/tjps.galenos.2020.90197

REVIEW

Novel Targets for Antimicrobials

Antimikrobiyaller İçin Yeni Hedefler

Suchita GUPTA, Vaishali Ravindra UNDALE*, Kedar LAKHADIVE

Dr. D.Y. Patil Institute of Pharmaceutical Sciences and Research, Pimpri, Pune, Maharashtra

ABSTRACT

Antimicrobial resistance (AMR) is the phenomenon developed by microorganism on exposure to antimicrobial agents, making them unresponsive. Development of microbial confrontation is a severe rising risk to global community well-being as treatment in addition, management of such resistant microbial infections is difficult and challenging. The situation requires action across all government sectors and society. The change in the molecular target on which antimicrobial drugs act is one of the key mechanisms behind AMR. One of the approaches to battle with AMR can be exploring newer molecular targets in microbes and discovering new molecules accordingly. There are various examples of novel targets such as biomolecules involving in biosynthesis of cell wall, biosynthesis of aromatic amino acid, cell disunion, biosynthesis of fatty acid, and isoprenoid biosynthesis and tRNA synthetases. Fatty acid biosynthesis (FAB) and their enzymes among all the above is the more appealing target for the advancement of new antimicrobial agents. Number of promising inhibitors have been developed for bacterial fatty acid synthesis (FAS) and also few of them are clinically used. Some of these potential inhibitors are found to be used in development of new antibacterial as a lead compound and have been discovered from high throughput screening processes like Platencimycin and their analogue, Platencin. The review majorly encompasses bacterial FAB in type II FAS system and potential inhibitors with respective targets of novel antibacterial.

Key words: Drug resistance, antibacterial activities, FAS system, thiolactomycin, platencimycin, platencin

ÖZ

Antimikrobiyal direnç (AMR), mikroorganizmanın antimikrobiyal ajanlara maruz kalması sonucu geliştirdiği ve organizmayı bu ajanlara tepkisiz hale getiren olgudur. Bu antimikrobiyal ajanlara karşı gelişen direnç, küresel toplum refahı için ciddi bir yükselen risktir, bu tür dirençli mikrobik enfeksiyonların yönetimi zordur. Bu durum, tüm hükümet kademelerinde ve toplumda eyleme geçilmesini gerektirir. Antimikrobiyal ilaçların etki ettiği moleküler hedefteki değişiklik, AMR'nin arkasındaki anahtar mekanizmalardan biridir. AMR ile savaşma yaklaşımlarından biri, mikroplarda daha yeni moleküler hedefleri keşfetmek ve buna göre yeni moleküller keşfetmek olabilir. Hücre duvarının biyosentezine, aromatik amino asit biyosentezine, hücre ayrışmasına, yağ asidinin biyosentezine ve izoprenoid biyosentezine ve tRNA sentetazlarına karşı geliştirilen çeşitli yeni ilaç hedefleri vardır. Yukarıdakilerin tümü arasında yağ asidi biyosentezi (FAB) ve bunların enzimleri, yeni antimikrobiyal ajanların geliştirilmesi için daha çekici bir hedeftir. Bakteriyel yağ asidi sentezi için umut verici inhibitörler geliştirilmiştir ve ayrıca bunlardan bir kısmı klinik olarak kullanılmaktadır. Bu potansiyel inhibitörlerden bazılarının, lider bileşik olarak yeni antibakteriyel geliştirmede kullanıldığı bulunmuştur ve platensimisin ve analoğu platensin gibi yüksek verimli tarama süreçlerinde keşfedilmiştir. Bu derleme büyük ölçüde tip II yağ asidi sentezi sistemindeki bakteriyel FAB'yi ve ilgili yeni antibakteriyel hedeflerle, potansiyel inhibitörleri kapsamaktadır.

Anahtar kelimeler: İlaç direnci, antibakteriyel aktiviteler, FAS sistemi, tiyolaktomisin, platensimisin, platensin

INTRODUCTION

The agents which destroy or prevent the growth of microbes are termed as antimicrobials. Antimicrobials are classified by various ways depending on mechanism or type of action as bacteriostatic and or bactericidal.[1] Antimicrobial have various therapeutic implications like endocarditis, gingivitis, prophylactic or suppressive therapy as presurgical antimicrobials, prophylaxis in immunocompromised patients with HIV/AIDS, traumatic injuries, neutropenia etc.[2] Antimicrobial agents like antibacterial mark vital element of microbial breakdown, thus limiting the bacteria. For example, the β-lactams, such as penicillin or cephalosporins, inhibit cell-wall synthesis etc.[3]

Antimicrobial resistance (AMR) is the capability of micro-organisms to inhibit antimicrobial substances from working against it which results that the standard treatment is ineffective; infections may spread and persist for longer period.[4] As we see the current scenario of antibiotic use it will increase steadily in recent years and therefore antibacterial played a crucial part in fatality and mournfulness in the nation.[5] Hence resistance is the major concern now days as resistant organism

*Correspondence: E-mail: vaishali.undale@dypvp.edu.in/vaishaliundale@gmail.com, Phone: +9372435355 ORCID-ID: orcid.org/ 0000-0003-3837-7471
Received: 18.07.2019, Accepted: 21.04.2020

may lead to treatment failure, widespread in the community at increasing rate, undetected low level of resistance, added burden to healthcare cost, selection pressure of right antibiotic, threatening return to pre-antibiotic era.[6]

Amongst various types of molecular mechanisms involved in development of AMR, alteration in the molecular targets on which antimicrobials act is one of key mechanism. The researchers in drug discovery process had tried to develop new antimicrobials by altering the functional molecular groups in parent moiety thereby modulating potency and safety of newly designed molecules. This has helped to overcome the AMR to some extent. But still the problem development of AMR persists as microbes are smart enough to mutate and change the molecular mechanism for survival.

Prevention and control strategies will require overcoming from the situation by feasible way called as the evolution of inhibitors of resistant enzymes. These inhibitors can be delivered as a co-drug with the antibiotics, thereby prevent AMR and sustain the antimicrobial activity of the drugs. Another approach to overcome the resistance is bacterial fatty acid synthesis (FAS), which is a necessary goal for antibacterial discovery. The organizational difference of the conserved enzymes and the existence of multiple forms of enzymes mobilizing the similar reactions during the path and create the bacterial FAS which is active against selected target preferably than the established multiple target. Likewise, bacterial FAS inhibitors are found to be narrow-targeting, rather than broad-targeting like old mono-therapeutic and broad-spectrum antibiotics. The narrow-targeting FAS inhibitors found to be fast-developing; resistance is target-based which made it a significant application for antibiotic development.[7] Despite of advanced antimicrobials with novel targets proceed to be recognized and contributed to the continuing struggle against AMR the intimidation to send back humanity to a circumstance commensurate to the pre-antibiotic era. Examples of definite target in the areas of cell wall biosynthesis, aromatic amino acid biosynthesis, cell division, two component signal transduction, fatty acid biosynthesis, isoprenoid biosynthesis and tRNA synthetases demonstrates according to characteristics of the above effectiveness were strike in drug finding and depiction of new antibacterial targets.[8]

The review discusses about the novel targets for emerging antimicrobial treatments, featuring important research on which potential to continue to successfully treat bacterial infection relies.

ANTIMICROBIAL: CLASSIFICATION AND ITS TARGETS

According to their application and spectrum of activity antimicrobials are classified as microbicides that kill micro-organisms, whereas bacteriostatic agents inhibit the growth of pathogens and allow the leucocytes and other defense mechanism of the host to confront with immobile invader. The microbicides may show selective toxicity depending on their spectrum of activity. They may act as viricides (killing viruses), bacteriocidic (killing bacteria), algicides (killing algae) or fungicides (killing fungi).

Categorizations of antimicrobial agents

They are mainly classified into three categories:

- Antibiotics and chemically derived chemotherapeutic agents:
  Beta lactam antibiotics, nucleoside antibiotics, aminoglycosides
- Non-antibiotic chemotherapeutic agents:
  Disinfectants, antiseptics and preservatives
- Immunological products:
  Vaccines, polyclonal antibodies.

Antimicrobial targets

Antimicrobial drugs interfere chemically with the molecular components of microorganisms that play crucial physiological role in them. They may act as a bactericidal or bacteriostatic. There are discrete ways by which these agents exert their antimicrobial activity such as inhibition protein synthesis, DNA gyrase inhibition, affecting cell wall synthesis or cell membrane function and folic acid synthesis etc. Figure 1 shows the targets with drugs acting on the targets.

Some of the established antimicrobial targets and the drugs with their pathway of action are briefed in Table 1.

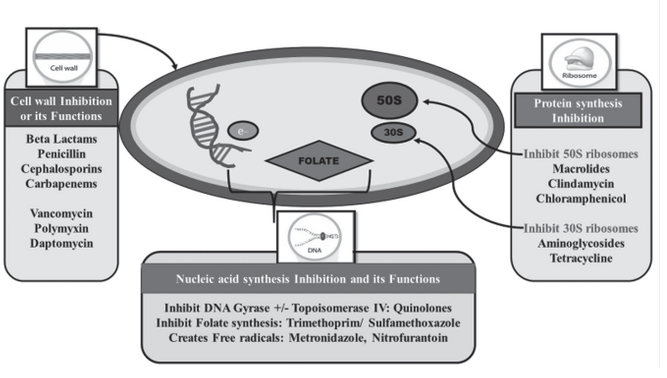

Figure 1. Molecular targets with drugs action on the targets

Development of antibiotics

In 1930s, the first commercially accessible antibacterial prontosil (sulfonamide) was introduced by German biochemist Gerhard Domagk. Before this, Alexander Fleming identified the primary antibiotic, penicillin, in 1928, which is used to control microbial infections. The period after exhibition of penicillin, is called as "golden era" of antibiotics. After this, many antibiotics were introduced commercially and/or are useful as medicine even for activities other than the antibiotic activity. Antibiotics are used as enzyme inhibitors, antitumor, immunosuppressive, hypolipidemic and antiparasitic agents, in addition to their applications as antibiotics.[9]

The research focusses on discovery of new or novel antibiotics and further modifications in existing antibiotics are still in progress. There are several important reasons why the finding and advancement of antibiotics with innovative structural modules are predominantly important, including the expansion of resistant bacteria and other pathogen.[10]

Table 1. Antimicrobial targets with the drugs

Primary target	Drug	Drug type	Origin	Pathway affected
Type 2 topoisomerase (DNA gyrase), type IV topoisomerase	Nalidixic acid, ciprofloxacin, levofloxacin	DNA synthesis inhibitors	Synthetic	Deoxyribonucleic acid (DNA) replication, division of cell, energy generation, citric acid cycle, ROS formation
DNA-dependent RNA polymerase	Rifampicin	RNA synthesis Inhibitor	Natural and semisynthetic	RNA transcription, DNA Replication
Penicillin-binding proteins	Penicillin, cephalosporins	Inhibitors of cell wall synthesis (β-lactams)	Natural and semi-synthetic forms of carbonyl lactam ring-containing azetidinone molecules (from *P. notatum*)	Synthesis of cell wall, cell division, enzyme that breakdown the biological components called as autolysin activity, ROS formation, and envelope
Peptidoglycan units (terminal d-Ala-d-Ala dipeptide)	Vancomycin	Cell wall synthesis inhibitors (Glycopeptides)	amino sugar-linked peptide chains which is natural and semi-synthetic (for glycopeptides)	Cell wall synthesis, trans glycosylation, transpeptidation
Cell membrane	Daptomycin and Polymyxin B	Disruption of cell membrane function	fatty acid-linked with peptide chains which is natural and semi-synthetic obtained from species *S. roseosporus* and *B. polymyxa*)	Cell wall synthesis and envelope two-component systems
30S ribosomes	Tetracycline and aminoglycosides	Protein synthesis inhibitors	It is formed of four-ringed Polyketides and are natural and semi-synthetic originated from species *S. aureofaciens*	Protein translation occurred through inhibition of aminoacyl tRNA binding to ribosome.
50S ribosomes	Erythromycin and azithromycin	Protein synthesis inhibitors	Natural and semi-synthetic forms of 14- and 16-membered lactone rings (from *S. erythraea* and *S. ambofaciens*)	Inhibition of elongation and translocation process protein translation happened and by depletion of free tRNA
Simultaneous binding to bacterial dihydrofolate reductase	Sulfonamide and Trimethoprim	Nucleoside synthesis inhibition	Synthetic	Blocks pathways and inhibit folic acid metabolism

Development void

Today, very fewer novel antibiotics are seemed to be under development. The consequences are seen worldwide as more and more bacterial infections are becoming hard to treat again. This has led to be unavoidable major health problem today. According to Walsh, "no foremost classes of antimicrobials were presented" between 1962 and 2000 which denotes to a modernization gap. Hence due to this innovation gap majority of pharma companies has been pull back their study from this area.[11] The Figure 2 illustrates the Gap in the Antibiotic development.

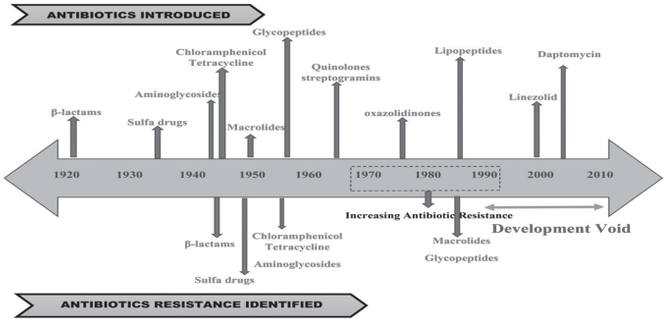

Figure 2. Era of antibiotics development

Newer targets for antimicrobial agents

The fruitful growth of various antimicrobials in the 1930s-1960s[12] established the contented awareness in the therapeutic and methodical societies that microbial infections had been overcome, ensuing in a decreased research in the antimicrobial area. Inappropriately, bacteria altered to their unfavorable novel atmosphere and started surviving even though exposed to the antibiotics. This is a process of gaining resistance that ultimately reduced many of these antimicrobials' noneffective. Presently, communicable diseases are still increasing and may result into one and only major reasons of death globally[13-15] one of the reasons behind it might be firm decrease in development of new antibacterial agents over the last 20 years.[16] To fight against this situation, antimicrobial agents with novel mechanisms of action might be helpful. Though, in the last 7 years out of 11 new antimicrobials that were accepted by the Food and Drug Administration, out of two of them acts through a different mechanism: linezolid, an oxazolidinone, and daptomycin, a cyclic lipopeptide, mutually they are used to cure the Gram-positive bacterial infections only. Hence there is urgent need of identifying and targeting new targets with novel mechanism that drive a crucial part in the growth of antibiotics dynamic against unaffected pathogens.[17-19] Table 2 shows difference in single enzyme and multienzyme targets on which antibiotics may act.

As compared to the sole target approach multi-target concept is thought to provide better resistance inhibition, possibility of generating hybrid molecules that may attack two cellular targets concurrently by fastening distinct inhibitors or pharmacophores together to form a single molecule.[20,21]

Though there are so many targets as described above, in the review focusses upon β-Ketoacyl-acyl carrier protein (ACP)

Table 2. Newer targets

Serial number	Single enzyme target	Multi enzyme target
1.	MurB to MurF enzymes as antibacterial targets	Single pharmacophore, multiple targets a- Dual inhibitors of DNA gyrase and topoisomerase IV b- Dual inhibitors of Gram-positive DNA polymerases c- β-Ketoacyl-ACP synthases of FAS II
2.	Targets of inhibitors discovered by enzyme screening or design a- UppS b- WalK/WalR c- LpxC d- FtsZ	Targeting substrates and cofactors a- Lipid II and other specific cell wall substrates b- A vitamin cofactor as target
3.	Single-enzyme targets of novel inhibitors in clinical trials a- Peptidyl deformylase b- Enoyl-reductases of FAS II c- Leucyl tRNA synthetases of Gram-negative organisms d- RNA polymerase in *C. difficile*	Hybrid molecules: dual pharmacophore, multiple targets

ACP: Acyl carrier protein, FAS: Fatty acid synthesis

synthases of FAS II which plays a role in microbial fatty acid synthesis. The FAS in microbial cells as following.

Fatty acid biosynthesis

Beta-ketoacyl-ACP synthase is an enzyme that participates in FAS. It take part in the establishment of aceto-acetyl ACP and it is briefed in Figure 3.

The hugely conserved enzyme that is established in practically all lifecycle on earth as a domain is fatty acid synthase (FAS) also called as Beta-ketoacyl-ACP synthase.[22] The enzyme plays

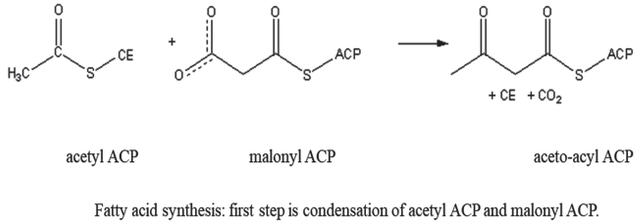

Figure 3. Fatty acid biosynthesis
ACP: Acyl carrier protein

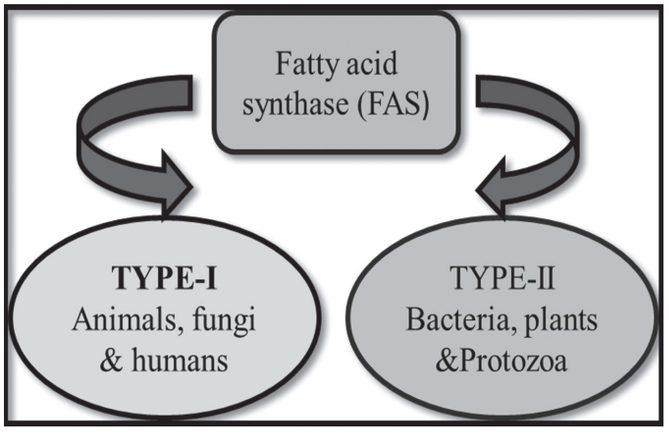

Figure 4. Types of FAS
FAS: Fatty acid synthase

a role in the FA elongation series and is tangled in the feedback regulation of the biosynthetic pathway via product inhibition. Two types of FAS enzymes have been identified yet as type-I and type-II shown in Figure 4.

The type I FAS also called associated form which is present in fungi and animals called as multifunctional protein encrypt by a one gene or two genes. Type II FAS also called dissociated type that is found in prokaryotes and plant plastids consists of separate enzymes.

Structure

Beta-ketoacyl synthase (KAS) consist of two protein domains. Between the N- and C-terminal domains the active site is situated. Most of the structures participating in dimer formation that constitutes the N-terminal domain and also in the active site cysteine. The substrate restraining and catalysis promoted by residues from both domains.[23]

KAS is a domain on type I FAS, which is a wide enzyme compound that has diversified sections to catalyze various distinct reactions.[24] Further experimentation of KAS I and II of *E. coli* disclosed that together are homo-dimeric, but KAS II is somewhat bigger. Still, both are tangled in FA metabolism, they have totally different primary structure.[25] In KAS II, every subunit constitutes a penta-stranded β pleated sheet enclosed by several α helices.

The active positions are almost adjacent, which is around 25 A° away, and comprise of a generally aqua phobic pocket.[26] The occurrence of "fatty acid transport channels" inside the KAS domain that happen into one of many "fatty acid cavities", which basically acts as the active site.[27]

Mechanism

In the reaction sequence the first step is organized by the KAS category of enzymes that is involved in a nucleophilic substitution by the active-site cysteine residue on the substrate carbonyl. The complete reaction is mediated by the KAS and it splits into distinct valuable phases-

a- Beginning with ACP, the acyl moiety is transferred to thioester form [but in situation of KAS III it forms acyl-coenzyme A (CoA)], to the active-site cysteine residue of the KAS.

b- To produce a reactive carbanion, binding and replacement of carboxyl group with hydrogen atom of the chain widen moiety is required and

c- A new C-C bond of the anion in which carbon is trivalent formed by nucleophilic attack on carbonyl carbon of the acyl moiety.[28]

Both type I and II FAS system can essentially prolong the small chain-length pioneers to the 14-carbon form, additionally the extension of C16 to C18 ACP, is effectively mobilized by KAS II or FAS II. Hence miscellaneous forms of KAS were identified specifically and plays a crucial part in deciding the structure of the products formed in the particular multi-step's enzyme catalyzed process.[29] These meaningful characteristics in functioning and arrangement of associated and dissociated form differentiated the type II FAS or dissociated enzymes, as promising goal in the evolution of innovative antibacterial and antiparasitic agents which shows nominal adverse effects in humans. Considering the limitations, words and pages to be published, only KAS III (FabH) are discussed here in detail.[30]

KAS III (FabH)

In cells, fatty acids playing a major role in cell membrane formation and fatty acid biosynthetic pathway indicated important targets in drug discovery. FAS called as multifunctional enzyme complex system that helps in regulating and processing of FAS.[31] KAS III is the functional enzymes which initiates the fatty acid synthesis, thus performed a most prominent part in bacterial fatty acid biosynthesis (FAB) and called as condensing enzyme.[32-35] It is used to mobilize the primary elongation reaction called as Claisen-Schmidt condensation of associated type in microorganisms, plant plastids etc. The FabB and FabF other bacterial condensing enzymes that, work in future in the series, actually showed difference from FabH in a way that they use acyl-ACP in spite of acetyl-CoA as the primer for further condensation reactions shown in Figure 5.

As a result, FabH seems to show a crucial part in the microbial FAB cycle because no additional enzyme in the pathway is found

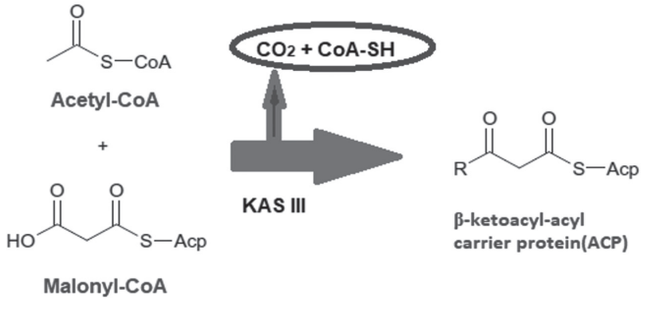

Figure 5. KAS III regulation

The primary condensation step in FAS III regulate by acetoacetyl-ACP synhase (KAS III) KAS: Ketoacyl synthase, FAS: Fatty acid synthase, ACP: Acyl carrier protein, CoA: Coenzyme A

to be capable to carry out valuable reaction.[36] Furthermore, the essential part and 3D assembly of the protein is tremendously protective to the several Gram-positive and Gram-negative bacteria and hence, its inhibitors commit to be dynamic antimicrobials with wide ranging action.[37]

STRUCTURAL EXPLORATION OF β-Ketoacyl-ACP SYNTHASE III

FAB is introduced via KAS.[38,39] By various reduction and dehydration steps, FAS II cycle helps in prolongation of FA. Between the associated FAS II enzymes, the condensing protein, KAS, is an essential target for novel antibacterial drug design.[38,40] The three classes of KAS (I, II, and III) have been established in which KAS I is encrypted by FabB and KAS II by FabF and these are elongation condensing enzymes that prefer acyl-ACP as a primer to abridge with malonyl-ACP.[41] The function and structures of these two enzymes are same, while significant distinct mechanisms are shown by KAS IIII (encrypt by FabH). KAS III regulates primary condensation of acetyl-CoA with malonyl-ACP, and participates as important part of bacterial FAB.[40,42] The crystal structure of KAS I, II and III shows that they all are dimers having α-β-α-β-α pleat and their active sites are distinguished by existence of a Cys-His-His triad, in KAS I and II, and a Cys-His-Asn catalytic triad in KAS III.[40] The concealed active sites of FabH comprised of Cys112, His244 and Asn274. Additionally, Asn343 established near to Asn274, and it was recommended to participate as a major part in the catalysis, Cys112 in the acetyl-CoA/FabH complex structure was found to be acetylated, showing clear proof that, His244 and Asn274 are demanding for decarboxylation and condensation reactions while Cys112 is the catalytical residue.[43]

Type II FAS reaction pathway: activation, elongation and control

FAB takes place in cytosol not in mitochondria. It usually contains a unit called ACP rather than CoA with reducing agent dihydronicotinamide-adenine dinucleotide phosphate (NADPH) instead of NAD/FAD.

It consists of various steps/stages-

- Transport
- Activation and integrating mechanism

(i) Acetyl CoA carboxylase (ACC)

(ii) FAS complex

- Prolongation of palmitate

(i) Condensation

(ii) Reduction

(iii) Dehydration

(iv) Reduction

- Desaturation of FA
- Regulation of FAB

A. From mitochondria to cytosol Passage of acetyl CoA

In the mitochondria the acetyl CoA is synthesized by two ways shown in Figure 6.

- By β-oxidation of FA
- By united action of pyruvate dehydrogenase and dihydrolipoyl transacetylase

Acetyl CoA is moved out from the mitochondria to cytosol and intiate the FAS and this process is takes placed by tricarboxylic carrier protein system in the inner mitochondrial membrane which pushed out the citrate is shown in Figure 7.

Sources of NADPH for Fatty acid synthesis

- For each particle of Acetyl CoA, one fragment of NADPH is generated that is relocated from mitochodria to the cyotosol.

- NADPH molecules come from the pentose phosphate pathway

B. Activation and synthesis mechanism

(i) ACC

ACC mediates the first limiting step of FAB and the enzyme biotin which adds CO_2, a carboxyl group to methyl end of acetyl CoA. The endothermic reaction described in Figure 8.

(ii) FAS complex

The seven different reactions catalyzed by multifunctional enzyme by which 2 carbon moieties are linked together from malonyl-CoA and finally formed the palmitoyl-CoA. During the complete synthesis process the formation of palmitate from acetyl CoA it involves total of 7 ATPs and 14 NADPHs.

C. Elongation of palmitate

The Precursors needed for elongation reaction gets loaded via thioester derivatives and included following steps with their respective enzymes like condensation, reduction, dehydration and reduction shown in Figure 9.

- From malonyl-ACP there is an inclusion of an acetyl group between the thioester bond of the acetyl-ACP molecule and this reaction is takes place by KAS and this enzyme known as condensing enzyme.

- And when there is a reduction of the Beta-keto group to a Beta-hydroxyl group in coordination with NADPH then this step is mobilized by Beta-keto-ACP reductase.

- During third step of dehydration the reaction is catalyzed by Beta-hydroxy acyl-ACP dehydrase and result into dehydration between the alpha and Beta carbons.

- And lastly there is a reduction by NADPH of the trans double bond and reaction is accomplished by enoyl-ACP reductase.

Various other enzymes like elongases that help to elongates the palmitate to produce many other fatty acids along the reaction and the origin of this enzyme in mitochondria and endoplasmic reticulum.

D. Desaturation of fatty acids

Fatty acids get desaturated with the help of enzymes fatty acyl-CoA desaturase which is terminal desaturases that produce unsaturated fatty acids.

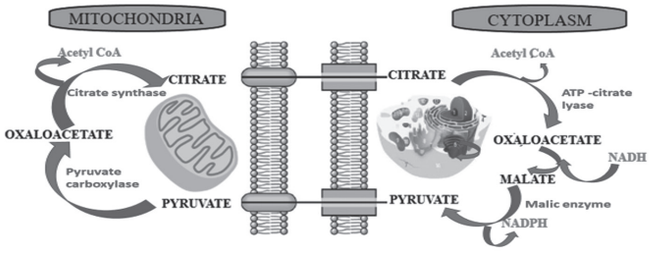

Figure 6. Synthesis of acetyl CoA in mitochondria

CoA: Coenzyme A, NADPH: Dihydronicotinamide-adenine dinucleotide phosphate

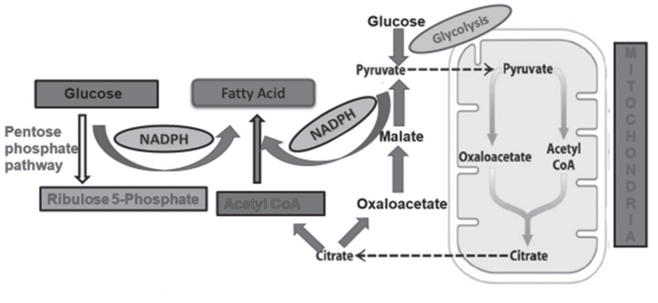

Figure 7. Initiation of fatty acid synthesis in cytosol

CoA: Coenzyme A, NADPH: Dihydronicotinamide-adenine dinucleotide phosphate

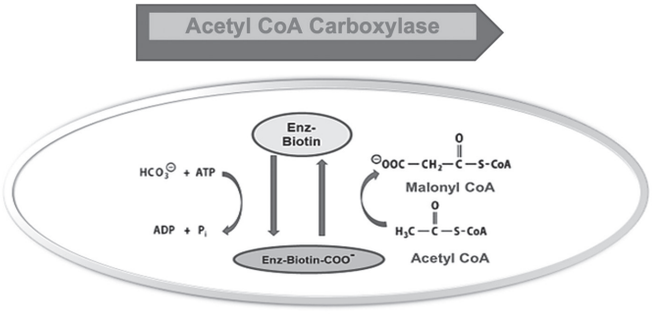

Figure 8. Establishment of malonyl-CoA: most committed steps

CoA: Coenzyme A

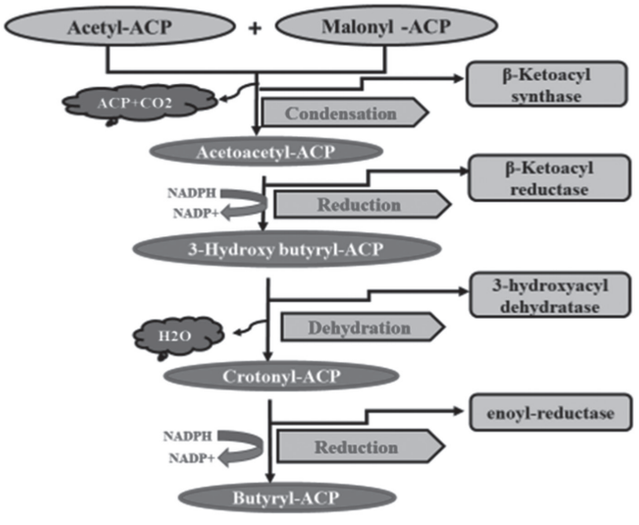

Figure 9. Elongation chain reaction

ACP: Acyl carrier protein, NADPH: Dihydronicotinamide-adenine dinucleotide phosphate

E. Regulator of FAB

During the FA metabolism of cells, like other metabolic pathways there should have an appropriate control mechanism to meet the energy needs. As FAS can be controlled by either of two ways i.e. partly by long-term regulatory mechanism in which governing the rate of reaction by which any protein incorporates or separate and hence controlled the quantity of enzymes responsible for this and partly by short-term regulatory mechanism like enzymes modification.

VARIOUS INHIBITORS OF β-KETOACYL ACP SYNTHASES

The highly conserved, essential and important pathway for survival is type II bacterial FAS.[44] Thus, the enzymes required during this procedure are found to be most fruitful goal to the advancement of innovative therapeutics. Additionally, to this there are various inhibitors which are used to treat various untreatable or resistant infections like FabI inhibitors that are recently in preclinical and clinical development against methicillin-resistant *S. aureus* (MRSA).[45-47] Along with this there is another appropriate target is FAS II β-keto (ACP) synthase enzyme. These enzymes show a foremost part in the beginning and continuation phases of FAS II pathway, by mobilizing a decarboxylative Claisen condensation reaction and bacteria has 3 types of KAS enzymes: FabB, FabF and FabH. As FabB and FabF which is also called as KAS I and KAS II which assemble the condensation of malonyl-ACP and acyl-ACP in the elongation cycle and that consist of Cys-His-His catalytic triad, while FabH (KAS III) contains a Cys-His-Asn triad, and is important for the condensation of malonyl-ACP with acetyl-CoA for beginning of the FASII bacterial cycle.[42,48-50]

Thiolactomycin

Thiolactomycin (TLM) was first originated from soil samples having a *Nocardia* species and it is an actinomycetes product having IUPAC name (4S) (2E,5E)-2-4-6-trimethyl-3-hydroxy-2,5,7-octatriene-4-thiolide.[51,52] TLM showed deprived antibacterial activity and found to be dual inhibitor of FabH and FabF. TLM is a chiral compound with +ve optical rotation and competitive reversible inhibitor that attached with the malonyl-ACP of the KAS enzymes. According to earlier studies TLM was established as an inhibitor of Gram (+) and Gram (-) FAS.[53,54] Additionally, efficacious against *M. tuberculosis*[55] and other unicellular parasites that contain FAS II.[56]

According to previous studies it was found that TLM particularly restrict the KAS and acetyl-CoA: ACP trans acylase actions in *E. coli.* Besides, TLM mimics the malonyl ACP and prevents the synthases from TLM inhibition on KAS. When done with direct binding studies using fluorescence spectroscopy and provides the confirmation against sensitivity in the given order FabF>FabB⋙FabH.[57] Majorly two reasons, that showed TLM poor inhibitor of FabH, primary, histidine 298 and 333 in FabB are recouped by His-244 and Asn-274 in FabH, and our FabB-TLM structure shows that the two-histidine made strong H-bonds with the antibacterial but the inhibition activity of TLM against different species varies. The isoprenoid moiety in TLM makes its advantageous of a particular aqua-phobic gap which exist in the active sites of both FabB and FabF.[58] These TLM analogs in plant and mycobacterial fatty-acid synthase systems would be able to explain the results of inhibition in which the isoprenoid moiety regained by different acyl chains. In these organisms, the congeners with lengthy and pliable chains possessed raised activity against FAS II and the lengthy chains might be more thoroughly filled with the possible spaces.[59] For example, *Mycobacterium tuberculosis* FabH was ~3-time more sensitive to TLM than *E. coli* FabH.[55] TLM and the related thiolactones was found to be efficient inhibitors of fatty acid and mycolic acid synthesis in mycobacteria as well as of chloroplast type II FAB.[58,60] TLM is found to be in toxic in mice and used to treat UTI and intraperitoneal bacterial infections.[61] Strangely, TLM found to stop the evolution of various protozoan parasites including *T. gondii* and *P. falciparum*.[62] Newly, TLM is noted to kill trypanosomes by inhibiting the production of myristate.[63] Myristate is used by the blood-borne form of the parasite to hold the surface glycoproteins that camouflage the parasite from host immune control. This physical awareness shows significant conclusion for the proposal of more effective inhibitors against these enzymes.

Cerulenin (CER)

A natural product CER is originated from *Cephalosporium cerulean*.[64] CER is irreversible inhibitor of FAS of bacteria and eukaryotes or cells[65] and it also shows therapeutic efficacy in various animal models of yeast infections.[66] It shows anticancer activity by inhibiting the FAS in mammals which is highly indicative in neoplastic cells and it also exhibit ability to decrease food intake and body weight in mice.[67] Regardless, of these promising outcomes of CER suggests the root of new therapeutics opportunities, the capability of CER to prevent the mammalian enzymes majorly dabble the interest for further development.

The CER molecule can be differentiate into an aquaphilic head comprising of the functional epoxide ring and a 1,4-diene aqua

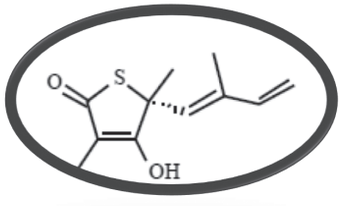

Thiolactomycin (Thiazole derivative)

C11H14O2S

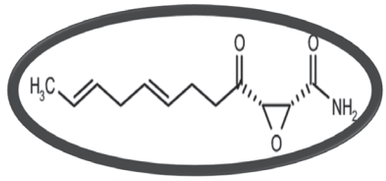

Cerulenin (Aminothiazole derivative)
C12H17NO3

phobic tail.[64] In case of sensitivity of CER the order of inhibition is FabB >FabF »FabH and the reasons of poor inhibition of CER of FabH is because of that, FabH is deficient of the substrate hydrophobic pocket to put up in the acyl chain of the drug. This help our judgement that the His-His active site, is different to the FabH His-Asn active site arrangement, which is critical for optimal CER inhibition. When KAS-CER complexes undergo structural analyses, it proposed that CER effectively mimics the transition state of the condensation reaction and confirm many visible features of the early models of CER enzyme inhibition.[58] The associated type FAS I, of eukaryotes also inhibited by CER by binding to the KAS region of the multi-domain FAS protein.[63,68] Because of this fact of instability and its toxicity and discouraging pharmacological properties, CER has no practicality as a potential wide-spectrum antibiotic.[69]

Platencimycin (PTM) and platencin (PTN)

PTM and PTN were originated from the bacterial soil strain *Streptomyces platensis* with the help of new antisense differential sensitivity screening strategy.[70-72] Fatty acid ACP synthase II (FabF) which is elongation condensing enzyme selectively inhibited by PTM, whereas PTN is a uniformed dual inhibitor of both FabF and fatty acid ACP synthase III (FabH) which is an initiation condensing enzyme.[73] The PTM and PTN shows effective, wide-spectrum Gram (+) *in vitro* activity, including active against antibiotic-resistant bacteria, such as MRSA, vancomycin-resistant *Enterococci* and vancomycin-intermediate *S. aureus*, because of their exclusive antibacterial mechanism.[74] Basically, both PTM and PTN showing no multi drug-resistance to clinically significant pathogens and show *in vivo* efficacy without toxicity.[75] Platensimycin (C24H27NO7, relative molecular mass 441.47), comprises of two distinct structural elements connected by an amide bond. PTM shown to be inhibition selectivity as it does not inhibit DNA, RNA, protein or cell wall biosynthesis at concentrations up to 500 μg/ml. The selectivity of PTM target was first determined within *S. aureus* strains either showing antisense FabF RNA (AS-fabF) or overexpressing FabF protein. PTM exhibited 200-fold greater potency in comparison to CER and similar FabF target selectivity in both assays, reveal that FabF is the major target of PTM for the inhibition of bacterial growth. PTM found to be potent and discriminating inhibitor of mammalian FAS.[74]

PTM and PTN structure shown in Figure 10 having two dissimilar unit attached with a CO-NH bond and both possess an 3-amino-2,4-dihydroxybenzoic acid (ADHBA) moiety. Elastic amide linkage of propanoic acid is common while the aliphatic cages that are linked to ADHBA moiety are dissimilar.[76] The aliphatic moieties are composed of 17 carbons with cyclohexanone ring.[77]

Mechanism of action of PTM and PTN

In FASII, the two classes of decarboxylating condensing enzymes inhibited by PTM and PTN. During the Claisen-Schmidt condensation the chain initiation mediated by condensing enzyme FabH of acetyl-CoA with malonyl-ACP. The chain elongation is mediated by FabB/FabF when the condensation of malonyl-ACP with the growing fatty acyl-ACP takes place.[42] The utilization of two substrates by FabH and FabB/FabF in a three-step double displacement reaction mechanism. The cysteine in the active site is covalently transferred in acetyl-CoA in FabH or acyl-ACP in FabB/FabF that forming an acyl-enzyme intermediate and liberating reduced form of CoA or ACP, respectively. The PTM consists of two moiety that is ADHBA moiety which resides inside the malonate binding pocket of FabF and forms possible interactions with catalytic site residues, and other is ketolide moiety that remains in the opening of the catalytic site, partly showing to solvent.[70] The changes in the organic selectivity's of PTM and PTN must exist in their definite ketolide moieties. The PTM and PTN have similar ADHBA moieties, and have identical catalytic site interactions that is crucial in preventing FA condensation enzymes. In FabF, PTN is still not so much active than PTM, but active as much extent than PTM in FabH.[74] The selectivity of PTM distinguishing lack of the ether ring. In FabF, during the entry of the active site, PTM makes the hydrogen bond to T270 but not with PTN. Vice-versa, in FabH the analogous region is bound with nonpolar residues, allowing PTN, but not PTM, to inhibit FabH[77] described in Figure 11.

Pharmaceutical application

Most promising antibacterial agents are PTN and PTM because of their particular mechanism

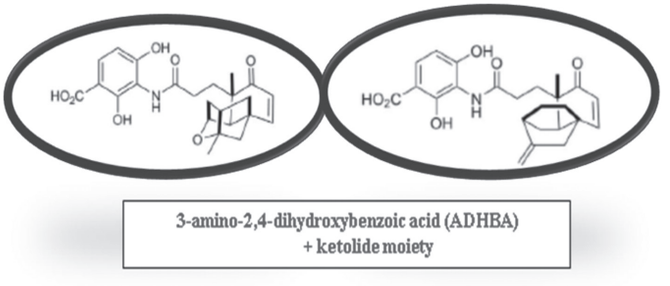

Figure 10. Structure of PTM and PTN

PTM: Platencimycin, PTN: Platencin, ADHBA: 3-amino-2,4-dihydroxybenzoic acid

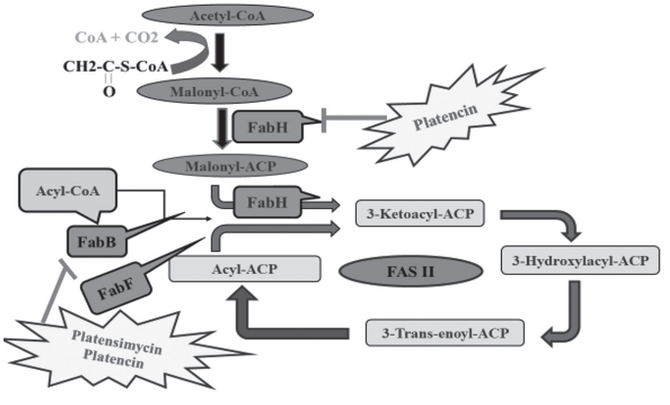

Figure 11. Diagrammatic representation of bacterial fatty acid synthesis cycle (FAS II) red emphasized mark are PTM inhibiting FabF/B and PTN dually inhibiting FabH and FabB

PTM: Platencimycin, PTN: Platencin

of action, efficacious *in vivo* activity and no multi drug-resistance with Gram-negative pathogens. But in spite of these promising utilities there are few roadblocks in pharmaceutical advancement such as poor pharmacokinetics and endless discussion on reasonable target for antibacterial therapies of FAS II.[74,78] Both the natural products found to be unacceptable antibiotics as PTN and PTM both cleared more quickly *in vivo* and hence to maintain the efficacy need of continuous delivery. The better differentiation between mammalian and bacterial FAB promoted FAS II as a most interesting and fruitful goal for the growth of antibacterial.

PTM developed as an anticipated or potential drug for the management of diabetes and different metabolic irregularities. As both these natural products PTM and PTN have motivated start up and development in the field of biology, medicine, study of enzymes and off course synthetic chemistry.

The distinct antibiotic effectiveness of PTM and PTN might be well-known in clinical trials and their usage in humans for managing with cross- resistance may be acceptable in the upcoming future.

CONCLUSION

Increased incidences of AMR and unavailability of potential antimicrobials against these resistant microorganisms is going to be one of the major health challenges in future. A variety of potential targets have been explored, the discovery of molecules targeting them has not yet succeeded. In spite of it, the efforts to explore these targets and their modulators are still in process and the future hopes for potential antimicrobials against resistant species of microorganisms remains.

Though the various novel targets like aromatic amino acids, isoprenoids, tRNA synthetases have been identified, fatty acid biosynthesis and the enzymes involved in their biosynthesis are appealing targets in the discovery of antimicrobial drugs. Though number of the FAS inhibitors have been developed only few have reached to clinical use.

The review here claims that bacterial FAS offers a sequence of rational and fascinating targets for antibacterial drugs however the question of how to approach these targets is not yet answered completely. Yet based on the structures of FAS intermediates presently available and the action of the inhibitors it can be estimated that the accessibility of purified b-ketoacyl-ACP syntheses from a variety of bacteria, along with the combination of techniques involving combinatorial chemistry, high-throughput screening, and rational drug design based on crystal structures, will undoubtedly support in the future discovery and development of much needed potent and broad-spectrum antibacterial agents.

PTM and their analogue PTN have been identified as lead compound during the drug development process. They have been characterized as the new classes of potential antibiotics, and their discovery is a success for natural product drug discovery and for new approaches that develop screening sensitivity and specificity. The fact that they inhibit a new target, fatty acid biosynthesis, increases their significance in the combat to stem multidrug resistance against antibiotics that have been in practice for many years.

Conflicts of interest: No conflict of interest was declared by the authors. The authors alone are responsible for the content and writing of this article.

REFERENCES

1. Mc Dermott PF, Walker RD, White DG. Antimicrobials: modes of action and mechanisms of resistance. Int J Toxicol. 2003;22:135-143.
2. Kang CI, Song JH. Antimicrobial resistance in Asia: current epidemiology and clinical implications. Infection Chemother. 2013;45:22-31.
3. Kochanski MA, Dwyer DJ, Collins JJ. How antibiotics kill bacteria: from targets to networks. Nature Reviews Microbiology. 2010;8:423-435.
4. Ganguly NK, Arora NK, Chandy SJ, Fairoze MN, Gill JP, Gupta U, Hossain S, Joglekar S, Joshi PC, Kakkar M, Kotwani A, Rattan A, Sudarshan H, Thomas K, Wattal C, Easton A, Laxminarayan R; Global Antibiotic Resistance Partnership (GARP) - India Working Group. Rationalizing antibiotic use to limit antibiotic resistance in India. Indian J Med Res. 2011;134:281-294.
5. Leung E, Weil DE, Raviglione M, Nakatani H, World Health Organization World Health Day Antimicrobial Resistance Technical Working Group. The WHO policy package to combat antimicrobial resistance. Bull World Health Organ. 2011;89:390-392.
6. Ventola CL. The antibiotic resistance crisis: part 1: causes and threats. Pharmacy and Therapeutics. 2015 Apr;40:277-283.
7. Yao J, Rock CO. Bacterial fatty acid-metabolism in modern antibiotic discovery. Biochim Biophys Acta Mol Cell Biol Lipids. 2017;1862:1300-1309.
8. Maddocks SE. Novel Targets of Antimicrobial Therapies. Microbiol Spectr. 2016;4.
9. Fair RJ, Tor Y. Antibiotics and bacterial resistance in the 21st century. Perspect Medicin Chem. 2014;6:25-64.
10. Kasanah N, Hamann MT. Development of antibiotics and the future of marine microorganisms to stem the tide of antibiotic resistance. Curr Opin Investig Drugs (London, England:2000). 2004;5:827-837.
11. Silver LL. Challenges of antibacterial discovery. Clin Microbiol Rev. 2011;24:71-109.
12. World Health Organization (WHO) Available from: https://www.who.int/whr/2004/annex/topic/en/annex_2_en.pdf?ua=1
13. Fischbach MA, Walsh CT. Antibiotics for emerging pathogens. Science. 2009;325:1089-1093.
14. Walsh C. Where will new antibiotics come from? Nat. Rev. Microbiol. 2003;1:65-70.
15. Wenzel RP. The antibiotic pipeline-challenges, costs, and values N Engl J Med. 2004;351:523-526.
16. Spielberg M, Powers JH, Brass EP, Miller LG, Edwards JE Jr. Clin Infect Dis. 2004;38:1279-1286.
17. Lee CS, Allwine DA, Barbachyn MR, Grega KC, Dolak LA, Ford CW, Jensen RM, Seest EP, Hamel JC, Schaadt, RD, Stapert D, Yagi BH, Zurenko GE, Genin MJ. Bioorg Med Chem. 2001;9:3243-3253.
18. Singh U, Raju B, Lam S, Zhou J, Gadwood RC, Ford CW, Zurenko GE, Schaadt RD, Morin SE, Adams WJ, Friis JM, Courtney M, Palandra J,

Hackbarth CJ, Lopez S, Wu C, Mortell KH, Trias J, Yuan Z, Patel DV, Gordeev MF. Bioorg Med Chem. 2003;13:4209-4212.

19. Reck F, Zhou F, Girardot M, Kern G, Eyermann CJ, Hales NJ, Ramsay RR, Gravestock MB. J Med Chem. 2005;48:499-506.
20. Barbachyn MR, John EM. Recent advances in the discoveryof hybrid antibacterial agents. Annu Rep Med Chem. 2008;43:281-290.
21. Bremner JB, Ambrus JI, Samosorn S. Dual action-based approaches to antibacterial agents. Curr Med Chem. 2007;14:1459-1477.
22. Christensen CE, Kragelund BB, von Wettstein-Knowles P, Henriksen A. Structure of the human β-ketoacyl [ACP] synthase from the mitochondrial type II fatty acid synthase. Protein Science. 2007;16:261-272.
23. Witkowski A, Joshi AK, Smith S. Mechanism of the β-Ketoacyl synthase reaction catalyzed by the animal fatty acid synthase †. Biochemistry. 2002;41:10877-10887.
24. Beld J, Blatti JL, Behnke C, Mendez MI, Burkart MD. Evolution of acyl-ACP-thioesterases and β-ketoacyl-ACP-synthases revealed by protein-protein interactions. J Appl Phycol. 2014;26:1619-1629.
25. Garwin JL, Klages AL, Cronan JE. Structural, enzymatic, and genetic studies of beta-ketoacyl-acyl carrier protein synthases I and II of Escherichia coli. J Biol Chem. 1980;255:11949-11956.
26. Huang W, Jia J, Edwards P, Dehesh K, Schneider G, Lindqvist Y. Crystal structure of beta-ketoacyl-acyl carrier protein synthase II from E. coli reveals the molecular architecture of condensing enzymes. The EMBO Journal. 1998;17:1183-1191.
27. Cui W, Liang Y, Tian W, Ji M, Ma X. Regulating effect of β-ketoacyl synthase domain of fatty acid synthase on fatty acyl chain length in de novo fatty acid synthesis. Biochim Biophys Acta. 2016;1861:149-155.
28. Witkowski A, Joshi AK, Smith S. Mechanism of the β-ketoacyl synthase reaction catalyzed by the animal fatty acid synthase. Biochemistry. 2002;41:10877-10887.
29. Campbell JW, Cronan Jr JE. Bacterial fatty acid biosynthesis: targets for antibacterial drug discovery. Annual Reviews in Microbiology. 2001;55:305-332.
30. Zhang JH, Li LZ, Zhu LH. Advances in the research of β-ketoacyl-ACP synthase III (FabH) inhibitors. Curr Med Chem. 2012;19:1225-1237.
31. Lai CY, Cronan JE. β-Ketoacyl-acyl carrier protein synthase III (FabH) is essential for bacterial fatty acid synthesis. Journal of Biological Chemistry. 2003;278:51494-503.
32. Khandekar SS, Daines RA, Lonsdale JT. Bacterial β-ketoacyl-acyl carrier protein synthases as targets for antibacterial agents. Curr Protein Pept Sci. 2003;4:21-29.
33. Heath RJ, Rock CO. Inhibition of beta-ketoacyl-acyl carrier protein synthase III (FabH) by acyl-acyl carrier protein in *Escherichia coli*. J Biol Chem. 1996;271:10996-11000.
34. Heath RJ, Rock CO. The Claisen condensation in biology. Nat Prod Rep. 2002;19:581-596.
35. Tsay JT, Oh W, Larson TJ, Jackowski S, Rock CO. Isolation and characterization of the β-ketoacyl-acyl carrier protein synthase III gene (fabH) from *Escherichia coli* K-12. J Biol Chem. 1992;267:6807-6814.
36. Ali A, Seung JC. A combined approach of docking and 3D QSAR studyof β-ketoacyl-acyl carrier protein synthase III (FabH) inhibitors. Bioorg Med Chem. 2006;14:1474-1482.
37. Puupponen-Pimia R, Nohynek L, Meier C, Kahkonen M, Heinonen M. Antimicrobial properties of phenolic compounds from berries. J Appl Microbiol. 2001;4:494-507.
38. Veyron-Churlet R, Guerrini O, Mourey L, Daffe M, Zerbib D. Proteinprotein interactions within the Fatty Acid Synthase-II system of Mycobacterium tuberculosis are essential for mycobacterial viability. Mol Microbiol. 2004;54,.1161-1172.
39. Heath RJ, Rock CO. Inhibition of beta-ketoacyl-acyl carrier protein synthase III (FabH) by acyl-acyl carrier protein in *Escherichia coli*. J Biol Chem. 1996;3:10996-11000.
40. Khandekar SS, Daines RA, Lonsdale JT. Bacterial beta-ketoacyl-acyl carrier protein synthases as targets for antibacterial agents. Curr Protein Pept Sci. 2003;4:21-29.
41. White SW, Zheng J, Zhang YM, Rock CO. The structural biology of type II fatty acid biosynthesis. Annu Rev Biochem. 2005;74:791-831.
42. Heath RJ, Rock CO. The claisen condensation in biology. Nat Prod Rep. 2002;19:581-596.
43. Choi KH, Kremer L, Besra GS, Rock CO. Identification and substrate specificity of β-ketoacyl (acyl carrier protein) synthase III (mtFabH) from *Mycobacterium tuberculosis*. J Biol Chem. 2000;275:28201-28207.
44. Magnuson K, Jackowski S, Rock CO, Cronan JE Jr. Regulation of fatty acid biosynthesis in *Escherichia coli*. Microbiol. Rev. 1993;57:522-542.
45. Escaich S, Prouvensier L, Saccomani M, Durant L, Oxoby M, Gerusz V, Moreau F, Vongsouthi V, Maher K, Morrissey I, Soulama-Mouze C. The MUT056399 inhibitor of FabI is a new antistaphylococcal compound. Antimicrob Agents Chemother. 2011;55:4692-4697.
46. Flamm RK, Rhomberg PR, Kaplan N, Jones RN, Farrell DJ. Activity of Debio1452, a Fabi inhibitor with potent activity against *Staphylococcus aureus* and coagulase-negative *Staphylococcus* spp., including multidrug-resistant strains. Antimicrob Agents Chemother. 2015;59:2583-2587.
47. Park HS, Yoon YM, Jung SJ, Yun IN, Kim CM, Kim JM, Kwak JH. CG400462, a new bacterial enoyl-acyl carrier protein reductase (FabI) inhibitor. Int J Antimicrob Agents. 2007;30:446-451.
48. Campbell JW, Cronan JE Jr. Bacterial fatty acid biosynthesis: targets for antibacterial drug discovery. Annu Rev Microbiol. 2001;55:305-332.
49. Davies C, Heath RJ, White SW, Rock CO. The 1.8 A crystal structure and active-site architecture of β-ketoacyl-acyl carrier protein synthase III (FabH) from *Escherichia coli*. Structure. 2000;8:185-195.
50. Jackowski S, Rock CO. Acetoacetyl-acyl carrier protein synthase, a potential regulator of fatty acid biosynthesis in bacteria. J Biol Chem. 1987;262:7927-7931.
51. Oishi H, Noto T, Sasaki H, Suzuki K, Hayashi T, Okazaki H, Ando K, Sawada M. Thiolactomycin, a new antibiotic. I. Taxonomy of the producing organism, fermentation and biological properties. J. Antibiot (Tokyo). 1982;35:391-395.
52. Sasaki H, Oishi H, Hayashi T, Matsuura I, Ando K, Sawada M. Thiolactomycin, a new antibiotic. II. Structure elucidation. J. Antibiot (Tokyo). 1982;35:396-400.
53. Borgaro, JG, Chang A, Machutta CA, Zhang X, Tonge, PJ. Substrate recognition by β-ketoacyl-ACP synthases. Biochemistry. 2011, 50, 10678-10686.
54. Hamada S, Fujiwara T, Shimauchi H, Ogawa T, Nishihara T, Koga T. Oral Microbiol Immunol. 1990;5:340-345.
55. Choi KH, Kremer L, Besra GS, Rock CO. J Biol Chem. *2000;*275*:* 28201-28207.
56. Morita YS, Paul KS, Englund PT. Specialized fatty acid synthesis in African trypanosomes: Myristate for GPI anchors. Science. 2000;288:140-143.

57. Price AC, Choi KH, Heath RJ, Li Z, White SW, Rock CO. Inhibition of beta-ketoacyl-acyl carrier protein synthases by thiolactomycin and cerulenin. Structure and mechanism. J Biol Chem. 2001;276:6551-6559.

58. Jones AL, Herbert D, Rutter AJ, Dan er JE, Harwood JL. J Biochem 2000;347:205-209.

59. Kremer L, Douglas JD, Baulard AR, Morehouse C, Guy MR, Alland D, Dover LG, Lakey JH, Jacobs WR Jr, Brennan PJ, Minnikin DE, Besra GS. Thiolactomycin and related analogues as novel anti-mycobacterial agents targeting KasA and KasB condensing enzymes in Mycobacterium tuberculosis. J Biol Chem. 2000;275:16857–16864.

60. Slayden RA, Lee RE, Armour JW, Cooper AM, Orme IM, Brennan PJ, Besra GS. Antimycobacterial action of thiolactomycin: an inhibitor of fatty acid and mycolic acid synthesis. Antimicrob Agents Chemother. 1996;40:2813–2819.

61. McFadden JM, Frehywot GL, Townsend CA. A flexible route to (5 R)-thiolactomycin, a naturally occurring inhibitor of fatty acid synthesis. Organic Letters. 2002;4:3859-3862.

62. Waller RF, Keeling PJ, Donald RG, Striepen B, Handman E, Lang-Unnasch N, Cowman AF, Besra GS, Roos DS, McFadden GI. Nuclear-encoded proteins target to the plastid in *Toxoplasma gondii* and *Plasmodium falciparum*. Proc Natl Acad Sci USA. 1998;95:12352–12357.

63. Morisaki N, Funabashi H, Shimazawa R, Furukawa J, Kawaguchi A, Okuda S, Iwasaki S. Effect of side-chain structure on inhibition of yeast fatty-acid synthase by cerulenin analogues. Eur J Biochem. 1993;211:111-115.

64. Omura S, Katagiri M, Nakagawa A, Sano Y, Nomura S. Studies on cerulenin. V. Structure of cerulenin. J Antibiot. 1967;20:349-354.

65. D'Agnolo G, Rosenfeld IS, Awaya J, Omura S, Vagelos PR. Inhibition of fatty acid synthesis by the antibiotic cerulenin. Specific inactivation of beta-ketoacyl-acyl carrier protein synthetase. Biochim Biophys Acta. 1973;326:155-156.

66. Nomura S, Horiuchi T, Omura S, Hata T. The action mechanism of cerulenin. I. Effect of cerulenin on sterol and fatty acid biosynthesis in yeast. J Biochem. 1972;71:783-796.

67. Loftus TM, Jaworsky DE, Frehywot GL, Townsend CA, Ronnett GV, Lane MD, Kuhajda FP. Reduced food intake and body weight in mice treated with fatty acid synthase inhibitors. Science. 2000;288:2379-2381.

68. Kuhajda FP, Pizer ES, Li JN, Mani NS, Frehywot GL,Townsend CA. Synthesis and antitumor activity of an inhibitor of fatty acid synthase. Proc Natl Acad Sci USA. 2000;97:3450-3454.

69. Parrish NM, Kuhajda FP, Heine HS, Bishai WR, Dick, JD. Antimycobacterial activity of cerulenin and its effects on lipid biosynthesis. J Antimicro Chemo. 1999;43:219-226.

70. Wang J, Soisson SM, Young K, Shoop W, Kodali S, Galgoci A, Painter R, Parthasarathy G, Tang Y, Cummings R, Ha S, Dorso K, Moty M, Jayasuriya H, Ondeyka J, Herath K, Zhang C, Hernandez L, Allocco J, Basilio A, Tormo JR, Genilloud O, Vicente F, Pelaez F, Colwell L, Lee SH, Michael B, Felcetto T, Gill C, Silver LL, Hermes JD, Bartizal K, Barrett J, Schmatz D, Becker JW, Cully D, Singh SB. Platensimycin is a selective FabF inhibitor with potent antibiotic properties. Nature. 2006;441:358–361.

71. Young K, Jayasuriya H, Ondeyka JG, Herath K, Zhang C, Kodali S, Galgoci A, Painter R, Brown-Driver V, Yamamoto R, Silver LL, Zheng Y, Ventura JI, Sigmund J, Ha S, Basilio A, Vicente F, Tormo JR, Pelaez F, Youngman P, Cully D, Barrett JF, Schmatz D, Singh SB,Wang J. Discovery of FabH/FabF Inhibitors from Natural Products. Antimicrob Agents Chemother. 2006;50:519–526.

72. Zhang CW, Ondeyka J, Herath K, Jayasuriya H, Guan ZQ, Zink DL, Dietrich L, Burgess B, Ha SN, Wang J, Singh SB. Platensimycin and platencin congeners from Streptomyces platensis. J Nat Prod. 2011;74:329–340.

73. Martens E, Demain AL. Platensimycin and platencin: Promising antibiotics for future application in human medicine. J Antibiot. 2011;64:705–710.

74. Wang J, Kodali S, Lee SH, Galgoci A, Painter R, Dorso K, Racine F, Motyl M, Hernandez L, Tinney E, Colletti SL, Herath K, Cummings R, Salazar O, González I, Basilio A, Vicente F, Genilloud O, Pelaez F, Jayasuriya H, Young K, Cully DF, Singh SB. Discovery of platencin, a dual FabF and FabH inhibitor with *in vivo* antibiotic properties. Proc Natl Acad Sci USA. 2007;104:7612–7616.

75. Peterson RM, Huang T, Rudolf JD, Smanski MJ, Shen B. Mechanisms of self-resistance in the platensimycin-and platencin-producing Streptomyces platensis MA7327 and MA7339 strains. Chem Biol. 2014;21:389-397.

76. Singh SB, Jayasuriya H, Ondeyka JG, Herath KB, Zhang C, Zink DL, Tsou NN, Ball RG, Basilio A, Genilloud O, Diez MT, Vicente F, Pelaez F, Young K, Wang J. Isolation, structure, and absolute stereochemistry of platensimycin, a broad-spectrum antibiotic discovered using an antisense differential sensitivity strategy. J Am Chem Soc. 2006;128:11916-11920.

77. Jayasuriya H, Herath KB, Zhang C, Zink DL, Basilio A, Genilloud O, Diez MT, Vicente F, Gonzalez I, Salazar O, Pelaez F, Cummings R, Ha S, Wang J, Singh SB. Isolation and structure of platencin: a FabH and FabF dual inhibitor with potent broad-spectrum antibiotic activity. Angew Chem Int Ed. 2007;46:4684-4688.

78. Wang J, Soisson SM, Young K, Shoop W, Kodali S, Galgoci A, Painter R, Parthasarathy G, Tang YS, Cummings R, Ha S, Dorso K, Motyl M Jayasuriya H Ondeyka J, Herath K, Zhang C, Hernandez L, Allocco J, Basilio A, Tormo JR, Genilloud O, Vicente F, Pelaez F, Colwell L, Lee SH, Michael B, Felcetto T, Gill C, Silver LL, Hermes JD, Bartizal K, Barrett J, Schmatz D, Becker JW, Cully D, Singh SB. Platensimycin is a selective FabF inhibitor with potent antibiotic properties, Nature. 2006;441:358-361.